



Maria Teresa Terracciano

SEISMIC BEHAVIOUR OF DIAGONAL STRAP BRACED CFS STRUCTURES

*Tesi di Dottorato
XXV ciclo*

*Il Coordinatore
Prof. Ing. Luciano ROSATI*

On the front cover: ...

Maria Teresa Terracciano

SEISMIC BEHAVIOUR OF DIAGONAL STRAP BRACED CFS STRUCTURES

Copyright © 2013 Università degli Studi di Napoli Federico II - P.le Tecchio 80, 80136 Napoli, Italy -
web: www.unina.it

Proprietà letteraria, tutti i diritti riservati. La struttura ed il contenuto del presente volume non possono essere riprodotti, neppure parzialmente, salvo espressa autorizzazione. Non ne è altresì consentita la memorizzazione su qualsiasi supporto (magnetico, magnetico-ottico, ottico, cartaceo, etc.).

Benché l'autore abbia curato con la massima attenzione la preparazione del presente volume, Egli declina ogni responsabilità per possibili errori ed omissioni, nonché per eventuali danni dall'uso delle informazione ivi contenute.

Finito di stampare il 02/04/2013

TABLE OF CONTENTS

Table of Contents.....	i
List of Figures	v
List of Tables	ix
Abstract.....	xi
Acknowledgements	xiii
About the Author.....	xv
1 INTRODUCTION	1
1.1 Motivation.....	1
1.2 Aim of the Study.....	1
1.3 Framing of the Activity.....	2
2 COLD FORMED STEEL STRUCTURES.....	3
2.1 Cold Formed Steel Housing.....	3
2.2 Structural Design of CFS Structures.....	5
2.3 Overview on the Main Research Programs on CFS Diagonal Strap Braced Walls.....	8
2.4 Adham et Al. (1990)	8
2.4.1 Objectives of the research program.....	9
2.4.2 Experimental tests.....	9
2.4.3 Results and conclusions.....	10
2.5 Serrette and Ogunfunmi (1996).....	11
2.5.1 Objectives of the research program.....	11
2.5.2 Experimental tests.....	11
2.5.3 Results and conclusions.....	13
2.6 Gad et Al. (1999)	14
2.6.1 Objectives of the research program.....	15
2.6.2 Experimental tests.....	15
2.6.3 Results and conclusions.....	18
2.7 Fulop and Dubina (2004)	21
2.7.1 Objectives of the research program.....	21
2.7.2 Experimental tests.....	22
2.7.3 Results and conclusions.....	24
2.8 Tian et Al. (2004)	27
2.8.1 Objectives of the research program.....	27

2.8.2	Experimental tests.....	27
2.8.3	Results and conclusions.....	29
2.9	Al Kharat and Rogers (2005)	31
2.9.1	Objectives of the research program	31
2.9.2	Experimental tests.....	32
2.9.3	Results and conclusions.....	34
2.10	Kim et Al. (2006)	35
2.10.1	Objectives of the research program	35
2.10.2	Experimental tests.....	35
2.10.3	Results and conclusions.....	37
2.11	Casafont et Al. (2007)	38
2.11.1	Objectives of the research program	38
2.11.2	Experimental tests.....	39
2.11.3	Results and conclusions.....	40
2.12	Velchev, Comeau and Rogers (2008).....	42
2.12.1	Objectives of the research program	42
2.12.2	Experimental tests.....	42
2.12.3	Results and conclusions.....	43
2.13	Moghimi and Ronagh (2009)	45
2.13.1	Objectives of the research program	45
2.13.2	Experimental tests.....	46
2.13.3	Results and conclusions.....	48
3	CFS STRUCTURES IN SEISMIC CODES	51
3.1	AISI S213-07/S1-09	51
3.1.1	Part A: General.....	52
3.1.2	Part B: General Design Requirements	52
3.1.3	Part C: Walls.....	53
3.2	Discussion and Comparisons.....	54
3.2.1	Behaviour Factor.....	54
3.2.2	Diagonal Brace Verifications.....	58
3.2.3	Overstrength Factor.....	62
4	PLANNING OF THE EXPERIMENTAL ACTIVITY	65
4.1	Basic assumptions and Design actions	65
4.1.1	Definition of dead loads.....	66
4.1.2	Definition of variable actions	67
4.1.3	Definition of seismic actions	68
4.2	Design of Diagonal Strap Braced CFS Walls	71
4.2.1	Design of the Elastic Light Wall	74
4.2.2	Design of the Dissipative Walls	76

4.2.3	Evaluation of stiffness of the walls.....	81
5	EXPERIMENTAL ACTIVITY	85
5.1	General.....	85
5.2	Tests on Materials.....	86
5.2.1	Description of specimens and testing system	87
5.2.2	Test results and discussion.....	90
5.3	Tests on Components: Simple Joints	92
5.3.1	Description of specimens and testing system	92
5.3.2	Test results and discussion.....	93
5.3.3	Comparison and concluding remarks.....	95
5.4	Tests on Components: Connections	96
5.4.1	Description of specimens and testing system	96
5.4.2	Test results and discussion.....	99
5.4.3	Comparison and concluding remarks.....	103
5.5	Tests on Walls	104
5.5.1	Test set-up	105
5.5.2	Monotonic Tests.....	107
5.5.3	Cyclic Tests.....	111
5.5.4	Comparison between monotonic and cyclic tests	115
6	DESIGN CRITERIA.....	117
6.1	Behaviour Factor	117
6.1.1	Evaluation of the behaviour factor of tested walls.....	118
6.2	Diagonal Brace Verifications	122
6.2.1	Diagonal brace verifications in the experimental tests....	123
6.2.2	Local and global collapse mechanisms.....	124
6.3	Overstrength Factor.....	126
6.3.1	Overstrength of fragile elements.....	126
6.3.2	Shear failure of screws	127
7	CONCLUSIONS.....	129
	Appendix A: Tests on Materials and Components	133
A.1	Material	134
A.2	Simple Joints	151
A.3	Connections	159
	Appendix B: Tests on Walls	189
B.1	Monotonic Tests.....	190
B.2	Cyclic Tests.....	196
	REFERENCES	203

LIST OF FIGURES

Figure 2.1 Typical cold formed steel profiles.....	3
Figure 2.2 Typical stick-built cold formed steel construction.	5
Figure 2.3 Design approaches under vertical loads.....	6
Figure 2.4 Design approaches under horizontal loads.....	6
Figure 2.5 Typical configuration of a CFS diagonal strap braced wall.....	7
Figure 2.6 Test set-up.	10
Figure 2.7 Typical connection and hysteretic loops.....	10
Figure 2.8 Configuration of type A, B and C Walls.	12
Figure 2.9 Test set-up: frontal and lateral view.....	13
Figure 2.10 Test results for type A Walls.....	14
Figure 2.11 Test results for type B and C Walls.	14
Figure 2.12 Specimen for single unlined steel wall frame tests.....	16
Figure 2.13 Testing configuration on the shaking table.	17
Figure 2.14 Load–deflection hysteresis loops for tab-in-slot frame.	18
Figure 2.15 Hysteresis loops for one-room-house.....	20
Figure 2.16 External sheeting configuration of wall specimens.....	22
Figure 2.17 Set-up scheme for the experimental tests.	23
Figure 2.18 Force-displacement curves of the experimental results.....	26
Figure 2.19 Frame bracing configurations.....	28
Figure 2.20 Test set-up.	29
Figure 2.21 Racking load vs deflection curves of the tested frames.....	30
Figure 2.22 Testing frame with displaced strap braced wall.	32
Figure 2.23 Light strap braced wall.....	33
Figure 2.24 Medium strap braced wall.	33
Figure 2.25 Heavy strap braced wall.....	33
Figure 2.26 Specimen tested on shaketable.	36
Figure 2.27 Shear vs drift in 100% test.	37
Figure 2.28 Test set-up.	40
Figure 2.29 Shear frame tested.	40
Figure 2.30 Test specimens after loading.....	41
Figure 2.31 Test results: force-displacement curves.....	41
Figure 2.32 Testing frame with test specimen.	43
Figure 2.33 Monotonic and cyclic loading protocols.....	43

Figure 2.34 Monotonic resistance of light and heavy braced walls.....	44
Figure 2.35 Cyclic response of light braced walls.....	44
Figure 2.36 Cyclic response of heavy braced walls.....	44
Figure 2.37 Example of specimen types.	46
Figure 2.38 Test set-up.	47
Figure 2.39 Force-displacement response.	49
Figure 3.1 Table A4-1 of AISI S213.....	55
Figure 3.2 Table 7.5 II of NTC 08.....	58
Figure 3.3 Table C5-1 of AISI S213.....	59
Figure 4.1 Case studies: residential buildings.	65
Figure 4.2 Definition of the seismic actions.....	70
Figure 4.3 Diagonal strap braced walls configurations.	71
Figure 4.4 Lateral resistance of the wall and its components.	74
Figure 4.5 Elastic Light Wall.....	75
Figure 4.6 Dissipative Light Wall.....	79
Figure 4.7 Dissipative Heavy Wall.	80
Figure 4.8 Contributions to deformations of a diagonal braced wall.	81
Figure 4.9 Shear tests on connections (Velchev, 2008).	82
Figure 4.10 Types of tested frame to diagonal connections.	83
Figure 4.11 Contributions in terms of stiffness.....	84
Figure 4.12 Percentage values of stiffness contributions.	84
Figure 5.1 Tests on materials.....	86
Figure 5.2 Shape and size of specimens (EN ISO 6892-1 - Annex B). .	87
Figure 5.3 Dimension of specimen (EN ISO 6892-1 - Annex B).	88
Figure 5.4 Dimension of tested specimen.	88
Figure 5.5 Universal testing machine MTS 810 series.	89
Figure 5.6 Material test results in terms of σ - ϵ	90
Figure 5.7 Influence of test rate on stress-strain values.....	91
Figure 5.8 Specimens properties for tests on mechanical joints.	92
Figure 5.9 Specimens for tests on mechanical joints.	93
Figure 5.10 Collapse mechanisms for tests on mechanical joints.	94
Figure 5.11 Comparison of curves for tests on mechanical joints.....	95
Figure 5.12 Connections distances in EC3 Part 1-3.....	96
Figure 5.13 Tested configurations of connections for WLD.	98
Figure 5.14 Tested configurations of connections for WHD.	98
Figure 5.15 Specimens properties for tests on connections.	99
Figure 5.16 Comparison of the response curves for configuration n.1.....	100
Figure 5.17 Comparison of the response curves for CLD and CHD...101	
Figure 5.18 Comparison of the response curves in terms of test rate...102	

Figure 5.19 Experimental vs theoretical collapse mechanisms.....	104
Figure 5.20 Experimental tests program on walls.	105
Figure 5.21 Testing system for full-scale tests on CFS walls.	105
Figure 5.22 Position of measurement devices.....	106
Figure 5.23 Loading protocol for monotonic tests.	107
Figure 5.24 Force-displacement response curve for monotonic tests..	108
Figure 5.25 Local buckling in the tracks and reinforced tracks.	110
Figure 5.26 Comparison of WHD-M1 and WHD-M2 responses.	111
Figure 5.27 Loading protocol for cyclic tests.	112
Figure 5.28 Force-displacement response curve for cyclic tests.	113
Figure 5.29 Collapse mechanisms for cyclic tests.....	115
Figure 6.1 Behaviour factor for monotonic tests on walls.....	120
Figure 6.2 Behaviour factor for cyclic tests on walls.....	121
Figure 6.3 Experimental curve for S235.	126
Figure 6.4 Failure modes of connections (ECCS, 2009).	128

LIST OF TABLES

Table 2.1 Experimental tests catalogue for X-bracings CFS.	8
Table 2.2 Dynamic characteristics of unlined single frames.	19
Table 2.3 Dynamic characteristics of the one-room-house.	20
Table 2.4 Performance criteria.	27
Table 2.5 Racking test results.	30
Table 3.1 Comparison for Cold Formed Steel grades.	60
Table 3.2 Comparison for Hot Rolled Steel grades.....	60
Table 3.3 Comparison for Cold Formed Steel grades.	61
Table 3.4 Comparison for Hot Rolled Steel grades.....	61
Table 3.5 Comparison for Cold Formed Steel grades.	63
Table 3.6 Comparison for Hot Rolled Steel grades.....	63
Table 4.1 Geometrical characteristics of case studies buildings.	66
Table 4.2 Geographical characteristics.	66
Table 4.3 Dead loads.	67
Table 4.4 Variable actions.	68
Table 4.5 Parameters for the definition of seismic action.	68
Table 4.6 Lateral resistances for the Elastic Light Wall.	74
Table 4.7 Lateral resistances for the Dissipative Light Wall.	78
Table 4.8 Lateral resistances for the Dissipative Heavy Wall.	78
Table 4.9 Displacement and stiffness of designed walls.....	83
Table 5.1 Experimental tests program.	86
Table 5.2 Material test results.	90
Table 5.3 Joint test results.	94
Table 5.4 Connection test results.	100
Table 5.5 Results of monotonic tests on walls.....	109
Table 5.6 Results of cyclic tests on walls.	114
Table 6.1 Behaviour factor for monotonic tests on walls.	120
Table 6.2 Behaviour factor for cyclic tests on walls.	121
Table 6.3 Collapse mechanisms for connections.....	123
Table 6.4 Collapse mechanisms for walls.	124
Table 6.4 Local vs global collapse mechanisms.	125

ABSTRACT

The main scope of this dissertation has been to give a contribution to the evaluation of seismic performance of CFS structures and in particular of diagonal strap braced walls. To this end, two main objectives are pursued in this work: the study of the seismic behaviour of diagonal strap braced walls in terms of global response and the study of local behaviour of connections to understand their influence on the global seismic behaviour of walls.

In the context of ReLUIIS-DPC project, a wide experimental program was planned and carried out. It consists of full-scale experimental tests on walls to investigate the global behaviour and small-scale experimental tests on materials, simple mechanical joints and connections to investigate the influence of the local behaviour on the global seismic behaviour. The experimental tests have been performed at the Dist Laboratory (Department of Structures for Engineering and Architecture, Naples), of the University of Naples Federico II. The obtained results demonstrate a satisfactory experimental response in terms of stiffness, strength and deformation capacity, largely confirming the theoretical predictions.

Since the final scope of the whole study, and in particular of the experimental campaign, is to provide appropriate design criteria for diagonal strap braced CFS structures to be introduced in Italian seismic code, considerations about design criteria were presented, on the basis of the design assumptions and the experimental test results, in comparison with the prescriptions of national and international seismic codes. The attention is focused on the behaviour factor, the diagonal brace verifications and the overstrength of fragile elements.

ACKNOWLEDGEMENTS

Only in the printed version.

ABOUT THE AUTHOR

Maria Teresa Terracciano was born in Nola (NA) on October 15th, 1981. She graduated cum laude in Architecture at the University of Naples “Federico II” in December 2009, with a thesis developed in the field of Structural Engineering, with the title: “Performances and structural potentialities of MPN system: the steel brick between past and future”.

Since February 2010 she is a PhD student in Structural Engineering at the University of Naples “Federico II” (XXV cycle). In these years she has been involved in studies and research activities in the “Department of Structures for Engineering and Architecture” at the University of Naples “Federico II”. In particular her research activity was focussed on the study of aluminium reticular structures and the design principles for cold formed steel structures in seismic areas. She was also involved in the national research project ReLUIS-DPC.

1 INTRODUCTION

1.1 MOTIVATION

In the last years, the use of Cold Formed Steel (CFS) structures became its spreading in Europe and in Italy as a valid alternative to traditional structural systems, because of their capacity to combine high performance to a set of structural characteristics such as lightness, rapidity of implementation and the ability to meet high standards of performance in terms of safety, durability and eco-efficiency.

Previously, this structural systems increased significantly its spreading in North-America, North-Europe and Australia.

The use of cold-formed steel members was initially used for secondary structures of industrial buildings, but now are enough diffused as main structures of residential (housing) and commercial constructions (low-rise buildings), mainly thanks to the economic advantages deriving from the significant reduction of the construction time.

This kind of use is nowadays growing in Europe and in Italy, but obviously this requires an accurate study of the seismic behaviour of CFS systems to be able to compensate for the lack of the Italian seismic code about the requirements for this structural systems. So, the main objective of this dissertation is to give a contribution to the evaluation of seismic performance of CFS structures and in particular of diagonal strap braced walls.

1.2 AIM OF THE STUDY

The main aim of this study is to give a contribution on the knowledge about the seismic behaviour of diagonal strap braced CFS structures. The final scope is to be able to suggest prescriptions for diagonal strap braced CFS structures for Italian seismic code.

Two main objectives are pursued in this work: the study of the seismic behaviour of diagonal strap braced walls, in terms of global response, by

means of full-scale experimental tests on walls; and the study of local behaviour of connections, by means of tests on materials, components and joints, to understand their influence on the global seismic behaviour of walls.

The experimental tests, performed to be able to investigate the seismic behaviour of CFS diagonal strap braced walls, were carried out in the context of the project ReLUIS-DPC 2010-2013, line 1: “Seismic design of new constructions”.

1.3 FRAMING OF THE ACTIVITY

To fulfil the above mentioned aims, this work is divided into 7 chapters. **Chapter 2** provides an introduction on the CFS structures and the main existing structural systems and an overview on the main research programs concerning CFS structures and in particular on the experimental tests performed on CFS diagonal strap braced walls that are nowadays available in scientific literature.

Chapter 3 is devoted to the review and considerations about the principles and the prescriptions of the AISI S213-07/s1-09 seismic code for lateral loads in CFS structures.

Chapter 4 describes the planning of the experimental campaign and in particular the basic assumptions in terms of strategies for elastic design and dissipative design of the diagonal strap braced CFS walls.

Chapter 5 is about the main results of the experimental campaign carried out in the Laboratory of Civil Engineer at the University of Naples in the context of the project ReLUIS-DPC 2010-2013. The experimental tests were focused on the study of global and local behaviour of diagonal strap braced CFS walls under monotonic and cyclic loads.

Chapter 6 is devoted to the definition of seismic design criteria for diagonal strap braced CFS walls that are missing in Italian seismic code.

Chapter 7 contains the conclusions of this work.

2 COLD FORMED STEEL STRUCTURES

This chapter presents a brief introduction on the Cold Formed Steel structures and an overview on the main research programs concerning CFS structures and in particular on the experimental tests performed on CFS braced walls that are nowadays available in scientific literature.

2.1 COLD FORMED STEEL HOUSING

In recent years, cold formed steel structures (CFS) has been growing in popularity all over the world, because it represents a suitable solution to the demand for low-cost high performance houses (Landolfo, 2011).

The CFS members, obtained by cold rolling, are produced pressing or bending steel sheets, with thickness ranging between 0.4 and 7 mm. This construction process provide several advantages such as the lightness of systems, the high quality of end products, thanks to the production in controlled environment, and the flexibility due to the wide variety of shapes and section dimensions that can be obtained by the cold rolling process.

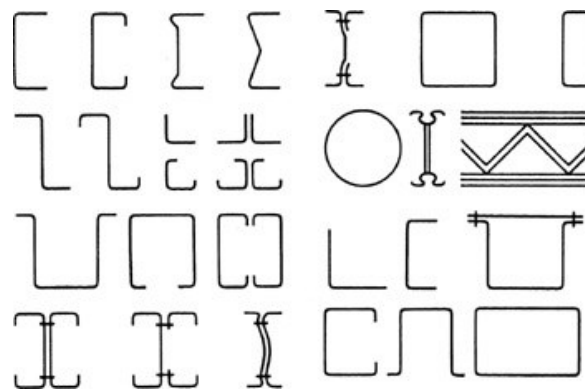


Figure 2.1 Typical cold formed steel profiles.

Moreover the CFS systems, being dry constructions, ensure short execution time. Besides, economy in transportation and handling, the low maintenance along the life time together with the high strength to weight ratio, an essential requirement for a competitive behaviour under seismic actions, represents additional benefits that CFS are able to achieve. In addition, CFS are in line with the requirements of sustainability. Indeed, the use of recyclable and light gauge materials, the flexibility of systems, the dry construction process and the possibility to reuse the elements at the end of the life cycle, contribute to minimize the environmental impacts.

The 3 main structural typologies for CFS structures can be classified in:

- **Stick-built constructions:**

This system is characterized by the lowest prefabrication degree and is the most common method used for CFS structures, because it is the same as the familiar stick-built wood construction method. In fact, in these systems the wood members have been replaced with appropriate CFS members. Similar to wood construction, steel components are fastened together on the floor surface into wall sections and tilted into positions. Once the wall sections are structurally connected together, exterior and interior sheathing materials are applied. The construction time is very short.

Some advantages of stick constructions are the simple constructions techniques, no heavy lifting equipment are necessary, and members can be densely packed for transportation.

- **Panelized constructions:**

In this system walls and floors sub-frames and roof trusses may be prefabricated in the factory. For this reason we can say that it is characterized by an intermediate prefabrication degree. The panels are lifted into their position and fastened together, generally by bolting, to form the required building geometry. This method of construction is particularly efficient when there is repetition of panel types and dimensions. In contrast to stick-built construction, in the panel construction exterior sheathings, thermal insulation and some of the lining and finishing materials may also be applied to the steel sub-frames in the factory.

Some advantages of panel construction are short time of erection, the possibility of quality control during the fabrication of the units;

- **Modular constructions:**

In this system there is the highest prefabrication degree. Structure modules (lightweight steel boxes), for example room units, are completely prefabricated in the factory before being delivered to the construction site. On construction site, the units are stacked side-by-side and up to several storeys high on prepared foundations and service connections made to form the complete structure. Nowadays, many hotels and motels are built in this way.

This chapter is particularly focused on the stick-built construction system that certainly represents the more used structural solution. Besides, this structural solution is also the basic system for the development of more industrialized constructions, like the panelized and modular constructions.

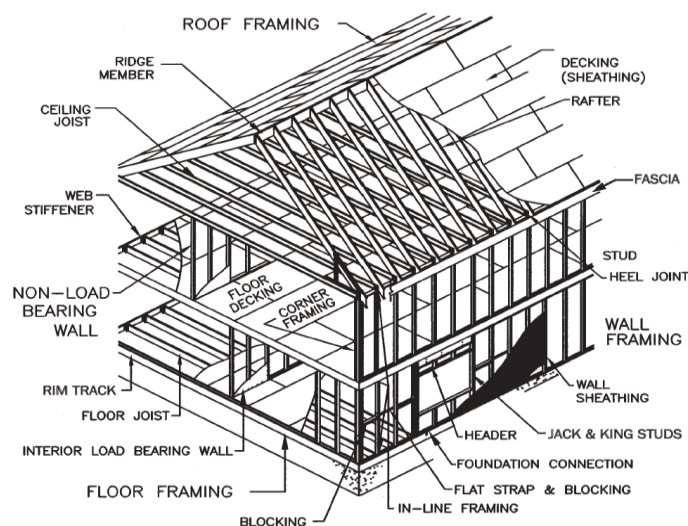


Figure 2.2 Typical stick-built cold formed steel construction.

2.2 STRUCTURAL DESIGN OF CFS STRUCTURES

The design of a CFS structure under vertical and horizontal loads can be carried out using two different approaches: “all-steel design” and “sheathing-braced design”.

The first one considers only steel members as load carrying elements and it does not take into account the influence of sheathing panels, consequently, the design of CFS members can be strongly influenced by local, global and distortional buckling. On the other hand, the “sheathing braced design” considers the sheathing as part of the bearing system. Therefore, in case of horizontal loads the “all steel design” requires the introduction of X or K bracing systems in the lateral resisting walls; while according to the “sheathing-braced design” the system composed by sheathing, frame and fasteners can assure an adequate strength in order to allow the walls to act as in plan diaphragms. In the last case, the shear response of a CFS wall, that represents the main lateral force resisting system, is a quite complex concern and depends on the behaviour of its structural components: sheathings; sheathing-to-frame connections; frame (stud buckling strength); frame-to-foundation connections.

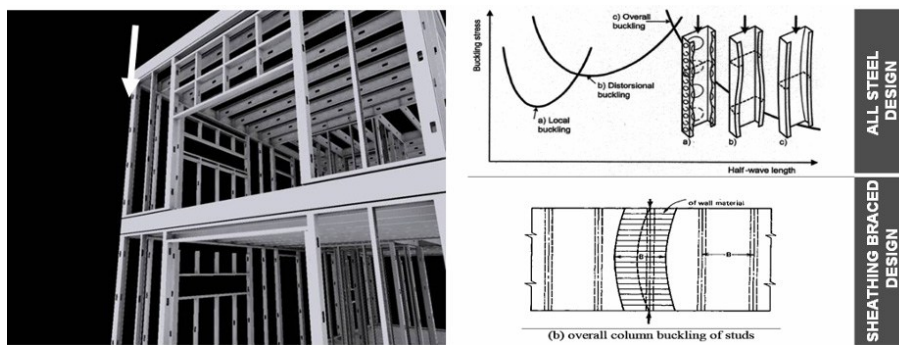


Figure 2.3 Design approaches under vertical loads.

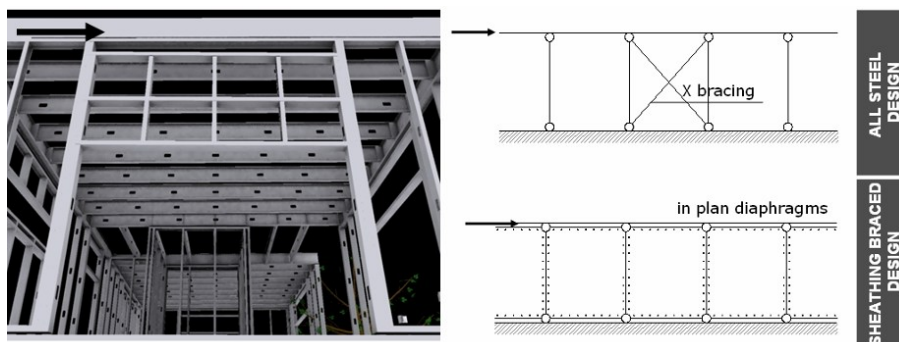


Figure 2.4 Design approaches under horizontal loads.

The typical configuration of a CFS diagonal strap braced wall is showed in fig. 2.5. There is a steel frame, composed by top and bottom tracks, vertical chord studs, diagonal strap braces and their connections, framing studs and hold-down fixtures at the corners.

Tracks are typically U sections, at the ends there are supplementary C profiles reinforced tracks to avoid the local buckling. Mechanic connections (anchors or bolts) are distributed along the tracks to absorb shear force.

Studs are generally C profiles with an inter-axis distance from 300 to 600 mm, chord studs are back-to-back profiles with hold-down devices at the ends to prevent uplift. To improve the stud behaviour, in the middle of the studs are placed flat straps (the buckling length is halved), that are connected by appropriate blocking to the chord stud.

The flat strap bracings can be placed on both sides of the wall or not, and are normally connected to studs and tracks with appropriately dimensioned gusset plates.

All the connections are generally made by self-tapping screws.

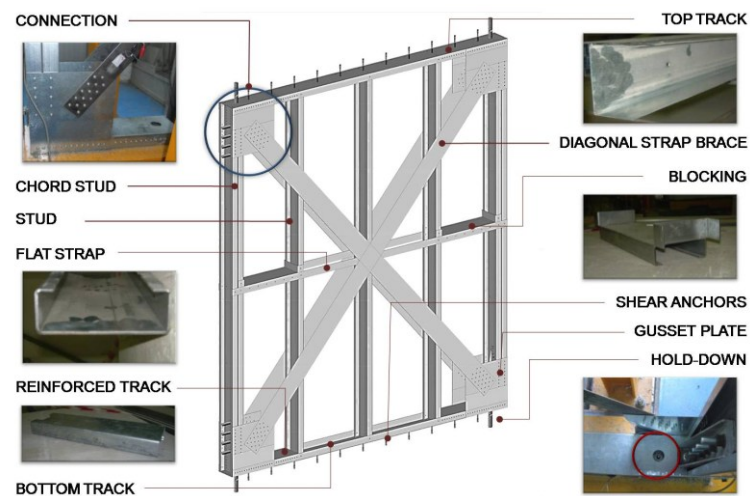


Figure 2.5 Typical configuration of a CFS diagonal strap braced wall.

2.3 OVERVIEW ON THE MAIN RESEARCH PROGRAMS ON CFS DIAGONAL STRAP BRACED WALLS

In the following paragraphs an overview of the main research programs concerning CFS braced walls is organized.

In order to frame and introduce the experimental tests performed in this work, a collection of the experimental tests available in scientific literature performed on CFS braced walls were made (Tab.2.1).

Contribution of different authors were organized chronologically and for each research program objectives, conclusions and details on the experimental tests (specimens, test set-up, loading history, results) are presented.

Table 2.1 Experimental tests catalogue for X-bracings CFS.

Author	Bracing system	Monotonic tests	Cyclic tests
Adham et al. (1990) ^{NA}	X-B+GWB ^(W-1)		6
Serrette and Ogunfunmi (1996) ^{NA}	X-B ^(W-1)	3	
	X-B+GSB+GWB ^(W-1)	5	
Gad et al. (1999) ^A	X-B ^(3D-1)		5
Dubina and Fulop (2004) ^E	X-B ^(W-1)	1	2
Tian et al. (2004) ^E	X-B ^(W-1)	5	
Al-Kharat and Rogers (2005) ^{NA}	X-B ^(W-1)	9	7
Kim et al. (2006) ^{NA}	X-B ^(W-2)		5
Casafont et al. (2007) ^E	X-B ^(W-1)		2
Velchev, Comeau and Rogers (2008) ^{NA}	X-B ^(W-1)	18	17
Moghimi and Ronagh (2009) ^A	X-B ^(W-1)		16
	X-B+GWB ^(W-1)		3

^(W-1): one story wall; ^(W-2): two stories wall; ^(3D1): one story 3D structure.

^{NA}: North American tests; ^A: Australian tests; ^E: European tests

X-B: steel strap X-bracing; GSB: gypsum sheathing board; GWB: gypsum wallboard.

2.4 ADHAM ET AL. (1990)

Details about the experimental tests on cold formed steel walls subjected to lateral cyclic loads developed by S.A. Adham, V. Avanesian, G.C. Hart, R.W. Anderson, J. EIrnlinger, and J. Gregory are showed below (Adham et al. 1990).

2.4.1 Objectives of the research program

The objective of the research was to investigate the in-plane shear wall load/deflection characteristics of lightgage steel stud wall construction when subjected to cyclic lateral loading imposed by wind or earthquakes. The approach combines testing and post-test analysis to investigate the in-plane shear load resistance and response characteristics of this type of wall construction, including the determination of:

- strength and load/deflection characteristics of the lightgage stud walls to in-plane lateral forces;
- strength, energy dissipation and failure mode characteristics under cyclic loading;
- stiffness degradation characteristics resulting from load reversals.

2.4.2 Experimental tests

Experimental investigations were conducted to evaluate the lateral load-deflection characteristics of lightgage steel stud/gypsum wallboard panel combinations subjected to lateral cyclic loads. Six 2.44 m \times 2.44 m cold-formed steel planar frames sheathed with steel straps and gypsum. Straps, 50.8 mm and 76.2 mm in width with three different thicknesses (0.84, 1.09 and 1.37 mm) were screw connected to the framing elements. Most walls were constructed with X straps as well as gypsum panels on both sides. Hold-downs were bolted to each test specimen at the base to limit uplift of the cold-formed steel frame.

The specimens were bolted to the bottom angle, to the top loading beam of the setup, and to the two hold downs. The double acting hydraulic actuator providing the lateral loading of the panel was connected to the loading beam at one end while the dial gage for determining the induced lateral deflection was placed against the face of the exterior stud opposite to the loaded end. To prevent the specimen from sliding horizontally two hold downs, one for each end, were designed and bolted to the test setup.

During the testing, each specimen was subjected to two complete cycles of loading for each designated level of lateral deflection until failure. The lateral load was applied to the specimen at suitable intervals the load and the corresponding induced lateral deflection were recorded.

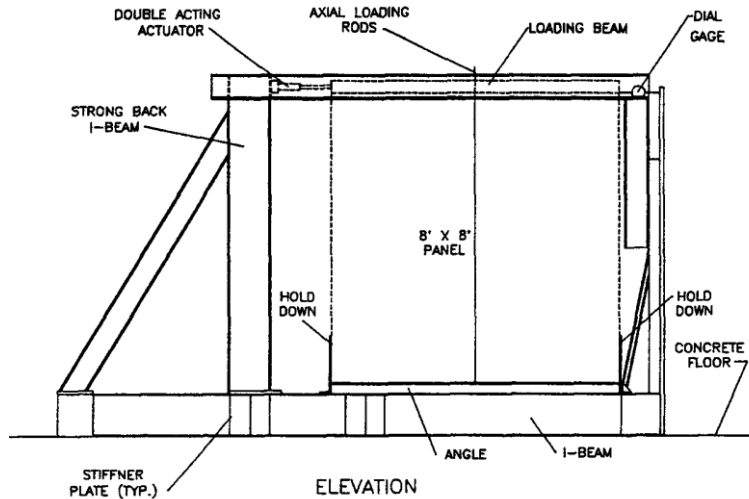


Figure 2.6 Test set-up.

2.4.3 Results and conclusions

The panel response was recorded in terms of lateral deflection of the panel top opposite to the loaded end. All specimens were monitored at their base for possible uplift, however, panel uplift was completely prevented by the hold downs.

Stud buckling will lead to a severe degradation in the shear load that can be applied to the wall; however when this mode is properly addressed in design strap braced systems are effective in dissipating energy under reversed cyclic loading.

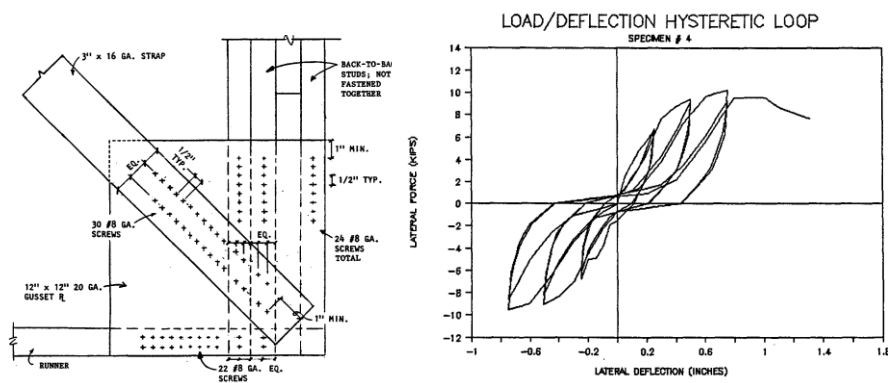


Figure 2.7 Typical connection and hysteretic loops.

In conclusion:

- light-gage steel stud/gypsum wallboard construction has many of the characteristics required of a seismic lateral load resisting system;
- providing diagonal straps on both sides of the panel improves the behavior of the panel by causing the gypsum board to crack at higher load and deflection levels, than with no strap at all or a strap on one side only;
- diagonal straps in compression do not contribute to the load-carrying capacity of the panel;
- degradation of panel stiffness due to cyclic loading is well within the acceptable range;
- hysteretic loops show that this type of system is effective in dissipating energy, especially in its virgin cycle of response.

2.5 SERRETTE AND OGUNFUNMI (1996)

Details about the experimental tests on cold formed steel walls subjected to lateral in-plane loading, performed at the Structures and Materials Testing Lab at Santa Clara University by R.L. Serrette and K. Ogunfunmi, are showed below (Serrette and Ogunfunmi, 1996).

2.5.1 Objectives of the research program

The main objective was to study the contribution of flat strap tension X-bracing; gypsum sheathing board (GSB); gypsum wallboard (GWB); and the combination of X-bracing, GSB, and GWB to the in-plane shear resistance of steel stud walls. Moreover, recommendations for allowable shear values were made based on the observed behavior of the walls.

2.5.2 Experimental tests

A total of 13 walls, 2.44 m x 2.44 m steel frame, were tested in this program. The frame consisted of 150 mm C-shaped, 0.88 mm studs at 0.61 m on center. For the top and bottom plates, 150 mm C-shaped,

0.88 mm tracks were used. At the ends of each wall, double studs (back-to-back) were used to prevent chord buckling. The tracks were attached to the studs using 12.5 mm screws.

The basic difference between the wall types was the shear resisting elements:

- Type A Stud Walls tests were carried out to investigate the contribution of flat strap X-bracing (in tension) to the shear resistance of the wall. A series of 3 walls with 50.8 mm x 0.88 mm flat strap X-bracing on the face were assembled and tested.
- Type B Stud Walls tests were carried out to evaluate the shear capacity provided by the gypsum panels. A series of five tests using this shear wall configuration were tested. On the face of the steel frame, two adjoining, single-layer 1.22 m x 2.44 m GSB panels were attached parallel to the framing.

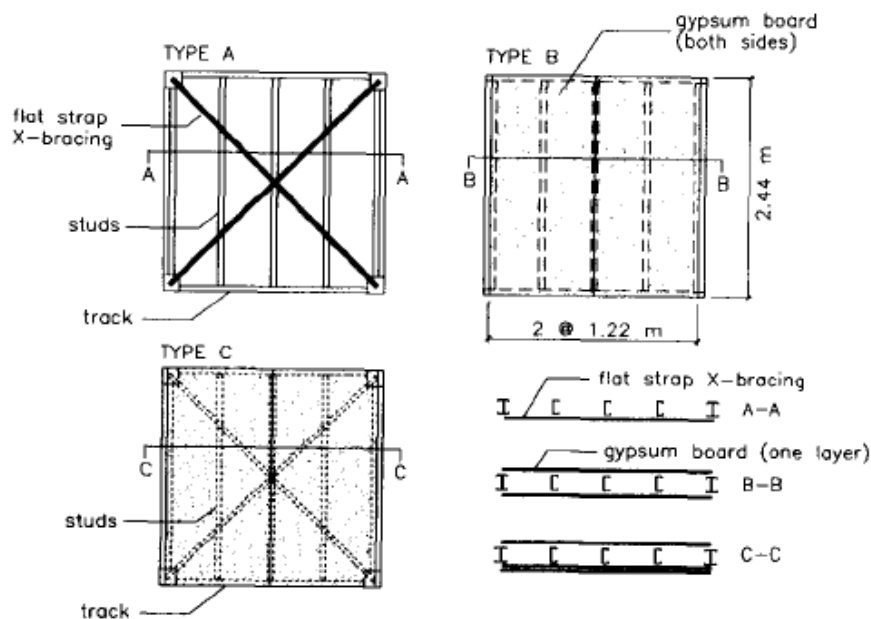


Figure 2.8 Configuration of type A, B and C Walls.

- Type C Stud Walls tests were made to investigate the combined contribution of the flat strap X-bracing and gypsum panels in resisting shear. A series of four specimens consisting of shear walls with 12.5 mm single-layer GSB on the face, 12.5 mm GWB

on the back and 50.8 mm wide flat strap X-bracing on the face (under the GSB) were built and tested. An additional fifth test which was similar to the other four tests, except for flat strap X-bracing on both sides of the wall, was also built and tested.

The overall test setup were based on the recommendation contained in ASTM E 72-80. Once the specimen was secured in the test frame, with guides, lateral braces, and top loading plate in place, the wall was preloaded to 10% of its estimated maximum load to set the connections. After approximately 3 min, the preload was released, all measuring instruments were zeroed and the specimen was then loaded to failure.

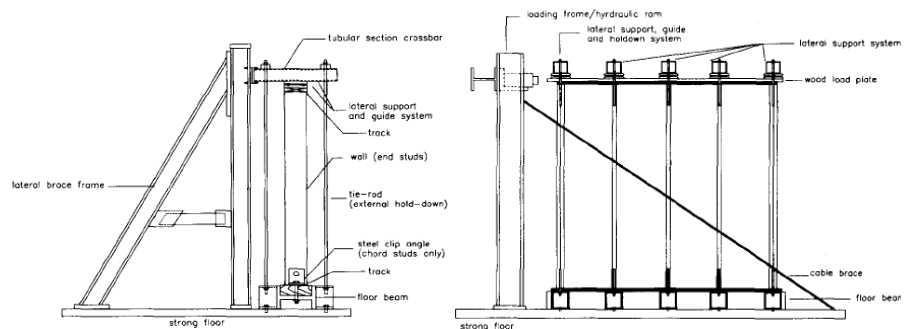


Figure 2.9 Test set-up: frontal and lateral view.

2.5.3 Results and conclusions

In general, failure of the gypsum sheathed walls resulted from breaking/cracking of the paper cover and underlying gypsum. Prior to this behavior, however, rotation of the screws about the flange contact with a subsequent pressing of the screw head into the surface of the panel was observed.

Type A Stud Walls failed as a result of excessive lateral deflection of the wall following yielding in the tension X-bracing. Minor reversed bending in the end studs was also observed.

In Types B and C Stud Walls at approximately half the sustained maximum load, screw rotation at the perimeter edges was observed. Each panel behaved independently during loading and a relative adjoining panel edge displacement in excess of 25 mm was observed.

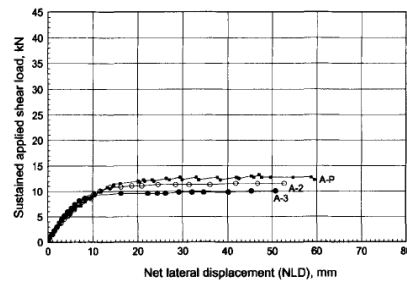


Figure 2.10 Test results for type A Walls.

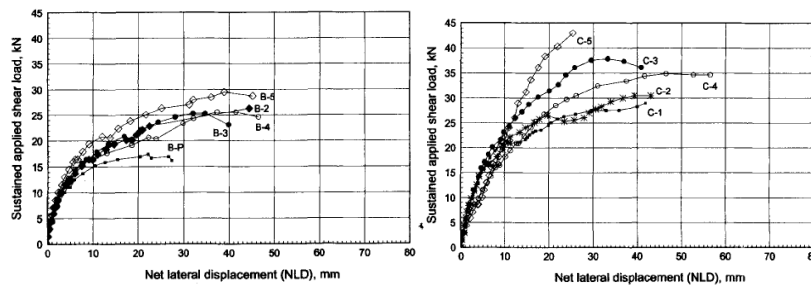


Figure 2.11 Test results for type B and C Walls.

It was shown that walls with bracing on one side alone failed by excessive out-of-plane deformation, which is not a favourable scenario in terms of maintaining lateral stability of the braced frame, nor ductile performance under inelastic shear deformations.

The gypsum board was shown to have significant shear strength, but under seismic loading, the static values should be reduced to compensate for opening of holes around the screw shank.

Although flat strap tension bracing possesses high shear strength, the use of straps plus wall panels (e.g., gypsum board) is not very practical.

It was also noted that in the design of X-braced walls the engineer must be concerned with strap yield strengths in excess of the minimum specified value, which may result in connection or chord stud failure.

2.6 GAD ET AL. (1999)

Details about the experimental tests on domestic structures with cold formed steel frames developed by E.F. Gad, C.F. Duffield, G.L.

Hutchinson, D.S. Mansell and G. Stark of the Department of Civil and Environmental Engineering of the University of Melbourne (Australia) in collaboration with the Port Kembla Laboratories (BHP Research) are showed below (Gad et al. 1999).

2.6.1 Objectives of the research program

The primary objective of the research project was to assess the performance and behaviour of cold formed steel frames domestic structures subjected to earthquake loading.

The research involved an extensive racking and dynamic testing program on both two- and three-dimensional framing configurations. A variety of construction details was tested to identify the critical components and assess the contributions from the non-structural components, particularly the plasterboard lining. The failure mechanisms and the load sharing between the various components are investigated.

In more detail the project aims to:

- improve understanding of the interaction between the different components of a typical wall assemblage;
- quantify the lateral stiffness and strength contributions of plasterboard and determine its reliability under cyclic loads;
- investigate the inertial loading effects of brick veneer walls on the framing assembly;
- develop guidelines that enable prediction of the behaviour of complete domestic structures.

2.6.2 Experimental tests

The experimental program was divided into two main stages. First, preliminary tests on two-dimensional unlined frames with different frame connection types. Second, testing of a one-room-house at various stages of construction.

Tests on unlined single frames were performed to gain an initial appreciation for both the static racking characteristics and the dynamic properties. The frames measured 2.4 x 2.4 m and were constructed from cold-formed steel C sections with steel grade of G300.

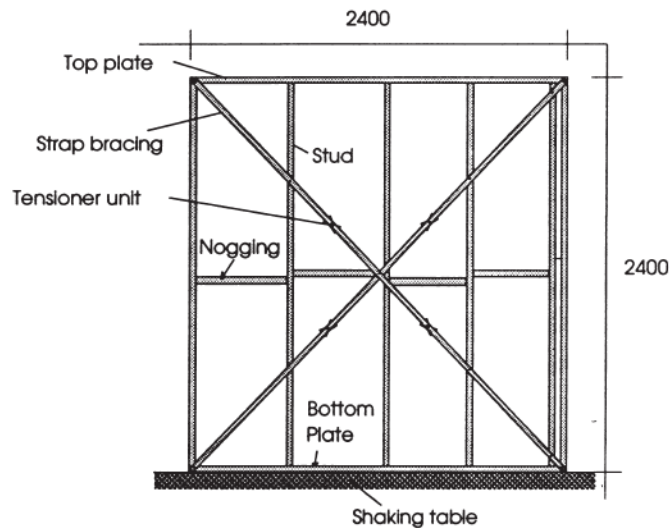


Figure 2.12 Specimen for single unlined steel wall frame tests.

The section of the studs was 75 x 32 x 1.2 mm thick, for the plates the section was 78 x 31 x 1.2 mm thick, and for the noggings was 72 x 34 x 1.2 mm. Each strap brace was 1.0 mm thick and 25 mm wide with steel grade of G250. A tensioner unit was fitted to each brace which is tightened to plumb and square the frame. To simulate the mass of a steel sheet roof, a 350 kg concrete beam was bolted to the top of the frame. This mass was the primary source of earthquake induced loading in the test and, consequently, the dominant dynamic characteristics were similar to that of a single degree-of-freedom system.

The first series of tests was conducted on frames with tab-in-slot connections which are essentially pinned connections. The tests were slow cyclic racking and dynamic. The slow cyclic tests were performed by fixing the top of the panel and slowly cycling the shaking table through increasing amplitudes in plane with the wall panel.

The dynamic characteristics of the wall frames were established through a series of pluck tests (applying a hammer blow on the concrete mass on top of the wall panel) and swept sine wave (SSW) tests. In addition, simulated earthquakes were also used to assess their general performance.

The second series of tests was conducted on identical frames, but with welded connections instead of tab-in-slot connections between the

framing members. Other frame connection types (e.g. clinched and screwed) are expected to fall within these two bounds. The tests conducted on the welded frames were SSW and simulated earthquakes only.

Tests on one-room-house were performed to investigate the effect of lining on frames to take into account the effect of boundary conditions in a realistic manner.

The test house measured 2.3 x 2.4 x 2.4 m high and was constructed from full scale components. It simulated a section of a rectangular house with plan dimensions of 11 x 16 m. The dead load corresponding to a plan area of 11 x 2.4 m was used on the test house. The mass due to roof tiles, battens, insulation, ceiling lining and trusses for that area was found to be 2300 kg. A concrete slab with the same weight was cast and supported on the east-west walls via steel lipped C sections similar to those used for the bottom chord of typical roof trusses. The two walls in the north-south direction were non-load bearing and had standard 900 x 2100 mm door openings. The house was built on the two degree-of-freedom shaking table at the University of Melbourne.

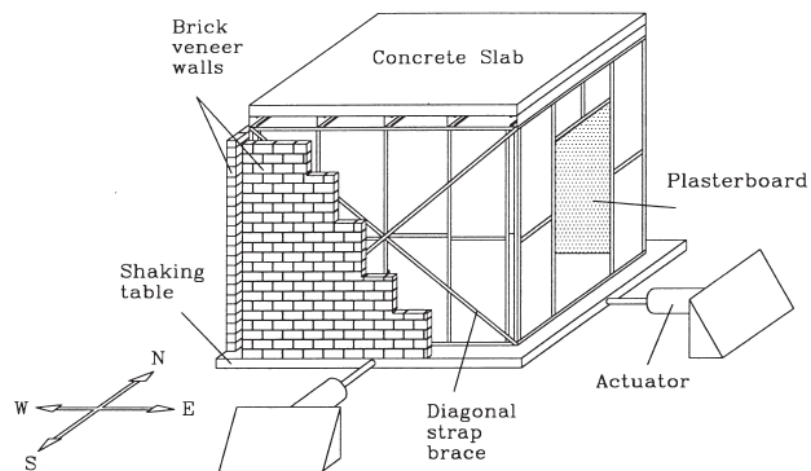


Figure 2.13 Testing configuration on the shaking table.

The house was built from standard components and erected as recommended by the manufacturers, but some details (i.e. hold down) were over designed to eliminate a potential failure mechanism.

All the framing members in the test house were standard C sections, 75 x 35 x 1 mm thick (steel grade of G550). Tab-in-slot connections were used to connect the studs, plates and noggings. Plasterboard lining, 10 mm thick, was used for the ceiling and walls, and connected to the frames with screws.

Screws were spaced at 300 mm centres on the ceiling and 400 mm centres on walls. Along the wall vertical edges the spacing was at 200 mm centres and 600 mm centres along the top and bottom plates. The screws used were 6 gauge, 25 mm long bugle head with a drill point. Skirting-boards, 55 mm ceiling cornices and set corner joints were also used in conjunction with the plasterboard lining.

The house was tested in the east–west (EW) and north–south (NS) directions and at different stages of construction so that the contribution of the various components could be evaluated. After each destructive test the house was rebuilt from identical components and by the same tradesmen to ensure consistency.

The tests conducted were mainly SSW, cyclic racking and simulated earthquakes.

2.6.3 Results and conclusions

Concerning the unlined single frames tests, in the hysteretic load–deflection behaviour of a typical frame, the ‘pinched’ form of the hysteresis curves indicates that a slip zone was present in the bare frame, resulted from a combination of elongation of the straps and deformation in the connections.

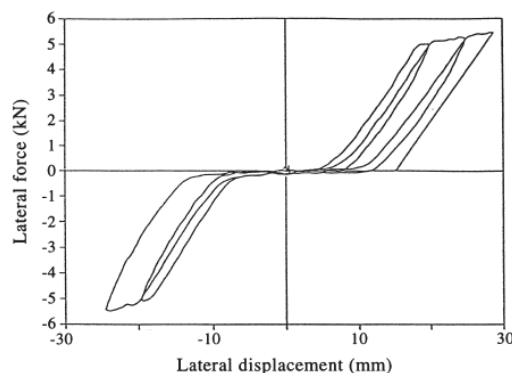


Figure 2.14 Load–deflection hysteresis loops for tab-in-slot frame.

The failure of the frames in the racking tests occurred when the brace sheared one of the two self tapping screws connecting the brace to the bottom corner of the frame. The brace subsequently pulled out from the remaining intact screw.

Results from the pluck tests and the SSW tests on both types of frames are listed in Table 2.2.

Table 2.2 Dynamic characteristics of unlined single frames.

Frame type	Test type	Natural frequency	Damping ratio
	Pluck	7.3 Hz	1.3%
Tab-in-slot	SSW	7.0 Hz	NA
Welded	SSW	6.3 Hz	2.0%

The welded frame had a lower natural frequency than the tab-in-slot frame, conversely from expectation that the welded frame would be stiffer than the frame with the tab-in-slot connections.

It was concluded from this that the stiffness of the frame is governed by the strap bracing, that is considered the critical component, in particular its connection to the frame and its initial tension.

The simulated earthquake tests on the tab-in-slot frame showed that the framing members and bracing performed in a ductile manner, showing that the most important component in unlined single frames is the strap bracing system.

In conclusion for unlined frames:

- the frame behaviour is governed by the strap bracing system;
- the failure load and mechanism is governed by the type of fixity of the strap bracing to the top and bottom plates and the presence of the tensioner unit (as it introduces a hole in the brace);
- the dynamic characteristics of the frames are governed by the initial tension in the straps;
- the type of connections between the framing members does not seem to have an influence on the structural response of the braced frames.

Concerning the one-room-house tests, the SSW tests revealed the natural frequencies, damping ratios and mode shapes. The destructive racking

tests were aimed at finding the failure mechanisms, load–deflection behaviour, level of ductility, energy absorption capacity, and stiffness and strength degradation under repeated cycles. The simulated earthquake tests were adopted to obtain the general performance of the test house. The earthquake tests do not only reveal the maximum response accelerations and drifts, but also confirm and verify the failure mechanisms observed in the racking tests.

Table 2.3 Dynamic characteristics of the one-room-house.

Mode	Description	Natural frequency	Damping ratio
1st	Sway of frame and all brick walls	4.0 Hz	10.0%
2nd	West brick wall vibration	7.0 Hz	2.6%
3rd	East brick wall vibration	7.3 Hz	3.3%

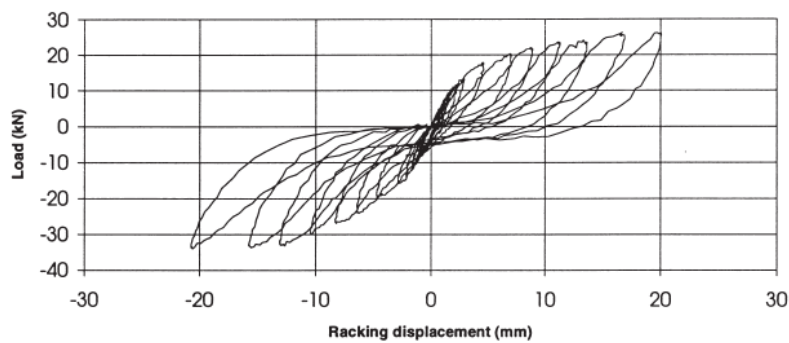


Figure 2.15 Hysteresis loops for one-room-house.

In conclusion for lined frames:

- plasterboard fixed as a non-structural component provides higher stiffness, load carrying capacity and damping than strap braces;
- when plasterboard and strap braces are combined, the overall stiffness and strength of the system is the simple addition of individual contributions from plasterboard and strap braces;
- in the test house, the plasterboard, combined with ceiling cornices, skirting-boards and set corner joints, resisted about 60–70% of the applied racking load whereas the strap braces resisted 30–40%.

For brick veneer walls:

- there was no indication that the in-plane brick veneer walls attached to the frames via clip-on ties contribute to the stiffness of the system;
- differential displacements between the frame and out-of-plane brick veneer walls were mainly accommodated by flexing of the stud flanges rather than deformation of brick ties.

In general, it was concluded that the cold formed steel frames perform very well under earthquake loads and that non-structural components, such as plasterboard lining, make a significant contribution to the lateral bracing of the frames.

2.7 FULOP AND DUBINA (2004)

Details about the experimental tests on full-scale CFS walls developed by L.A. Fulop and D. Dubina at the Department of Steel Structures and Structural Mechanics of the 'Politehnica' University of Timisoara (Romania) are analyzed below (Fulop and Dubina, 2004).

2.7.1 Objectives of the research program

The main objectives of the experimental tests was to clarify certain aspects related to the behavior of shear walls subjected to earthquake, such as strength, stiffness and ductility, as main parameters governing seismic behaviour.

The experimental program was expected to provide information on:

- comparison between monotonic and cyclic behaviour;
- confirmation of earlier findings about the effect of interior gypsum cladding;
- assessment of the effect of openings;
- comparison between wall panels with different cladding materials and cross bracing;
- providing experimental information for the calibration of FE models.

2.7.2 Experimental tests

An experimental program has been undertaken to investigate the shear behaviour of some of the most popular wall panel typologies.

Six series of full-scale wall tests with different cladding arrangements based on common practical solutions in housing and small industrial buildings has been carried out.

Each series consisted of identical wall panels tested statically, both monotonic and cyclic.

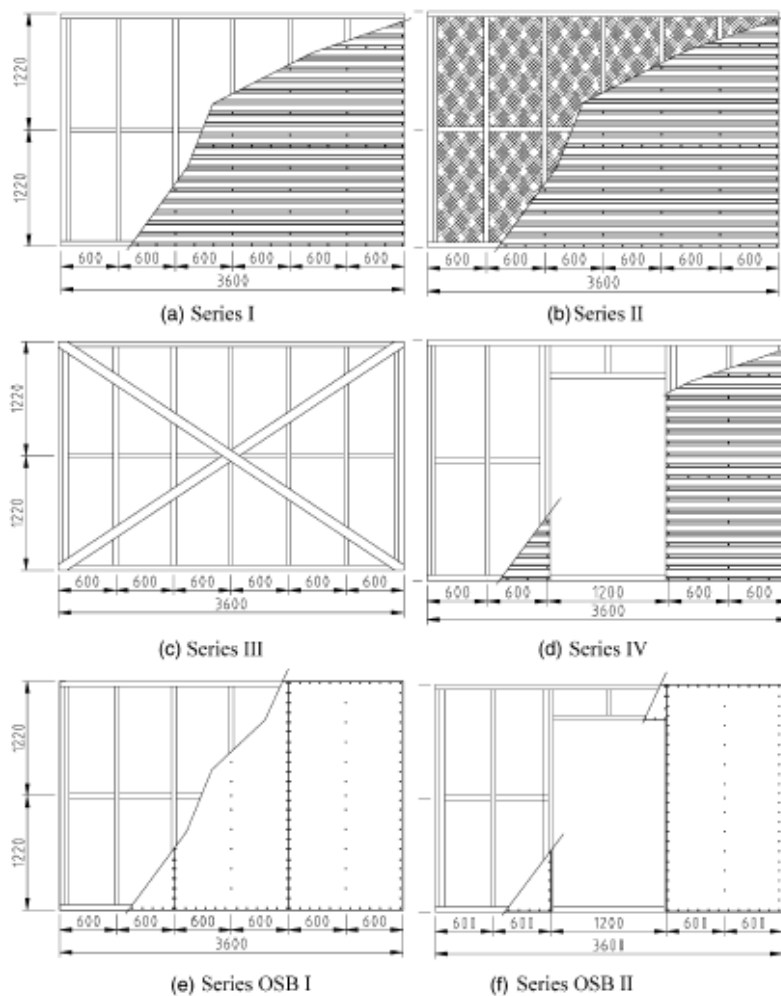


Figure 2.16 External sheeting configuration of wall specimens.

The main frame of the wall panels was made of cold-formed steel elements, top and bottom tracks were U154/1.5, while studs were C150/1.5 profiles, fixed at each end to tracks with two pair of self-drilling self-taping screws ($d=4.8$ mm) (Series I). In specimens using corrugated sheet as cladding the sheets were placed in a horizontal position with a useful width of 1035 mm and one corrugation overlapping and tightened with seam fasteners at 200 mm intervals.

Corrugated sheet was fixed to the wall frame using self-tapping screws ($d=4.8$ mm), sheet ends being fixed in every corrugation, while on intermediate studs at every second corrugation. Additionally on the 'interior' side of specimens in Series II, 12.5 mm thick gypsum panels (1200×2440 mm²) were placed vertically and fixed at 250 mm intervals on each vertical stud.

Bracing was used in three specimens (Series III), by means of 110×1.5 mm² straps on both sides of the frame. Steel straps were fixed to the wall structure using self-drilling screws ($d=4.8$ mm and $d=6.3$ mm), the number of screws being determined to avoid failure at strap end fixings and facilitate yielding.

Ten millimeter OSB panels (1200×2440 mm²) were placed in similar way as the gypsum panels in earlier specimens (Series OSB I and II), only on the 'external' side of the panel and fixed to the frame using bugle head self-drilling screws of $d=4.2$ mm at 105 mm intervals.

The full-scale testing program was completed with tensile tests to determine both material properties for components and behaviour of connections.

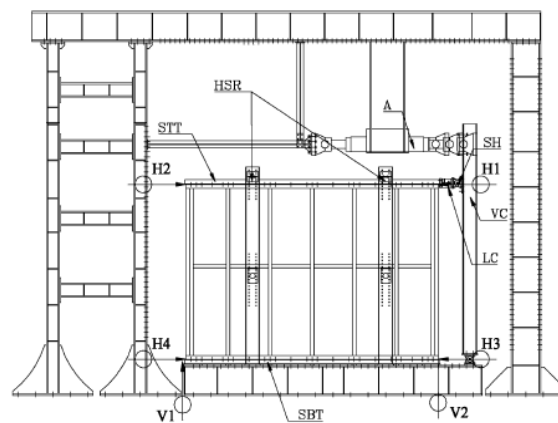


Figure 2.17 Set-up scheme for the experimental tests.

For the set-up scheme, the testing frame at the University of Timisoara, equipped with two actuators of 1000 and 500 kN, was used. Experiments were conducted using displacement control, at the same time measuring the corresponding load with load cell.

Specimens were loaded in shear very similarly like in earthquake or wind conditions, but without taking vertical loads into account. Specimens were restrained against lateral displacement in two points on the upper part, which acted as sliding restraint.

A monotonic test using a loading velocity of 1 cm/min, was performed for each type of panel. Cyclic testing methodology followed ECCS Recommendation until failure or a significant decrease of load bearing capacity. Loading velocity for the cyclic experiments was 6 min/cycle for one specimen and 3 min/cycle for the second.

2.7.3 Results and conclusions

In this work results of a full-scale shear test program on wall panels are presented. In order to evaluate specific properties like the elastic modulus, ultimate force or ductility, curves have been interpreted according to two established procedures: the first based on ECCS Recommendation (1985) and the second based on a method adopted by Kawai et al. (1997). The two methods usually yield similar results, with interesting particularities.

Initial rigidity values are very similar and it is important to realize that, ultimate load and ductility are in direct relationship so if a method yields higher ultimate load this automatically means lower ductility.

Differences between monotonic and cyclic values were observed as follows: initial rigidity is not affected, values of cyclic and monotonic tests range within a difference of less than 20%. The same can be noted for ductility, exception being in case of OSB specimens where ductility is reduced by 10–25% for cyclic results.

One important observation concerns ultimate load, where cyclic results are lower than monotonic ones by 5-10% even if we consider unsterilized envelope curve.

In particular, the comparisons between the bare structure (Series I) and the other Series are important.

- Series I–series II:

Differences can be attributed to the effect of the gypsum board. There is an increase in ultimate load of 16.2 and 17.8%, respectively. As far as initial values are there seem to be no differences, but ductility is improved slightly.

- Series I–series IV:

There is a significant decrease of initial rigidity (60.3; 53.3%), for a lesser degree of ultimate load (16.4; 21.0%), but ductility values are essentially unaffected.

- Series I–series III:

Comparison is more qualitative because of the different sheeting system. There are no differences as far as initial rigidity is concerned; however an increase of ductility had been expected. This was not possible as the failure mode for the strap braced specimens was not the most advantageous one, the damage being concentrated entirely in the lower corners of the panel. Strap-braced wall panels have the advantage of stable hysteretic loops, but also the disadvantage of higher pinching than the sheeted ones.

- Series I–series OSB I:

Comparison is more qualitative, keeping in mind the different wall panel arrangements. Initial rigidity is of similar magnitude, with increase of ultimate load. Failure of OSB specimens under cyclic loading was more sudden than in the case of corrugated sheet specimens where degradation occurs gradually. This is also reflected by the reduced ductility for OSB specimens.

- Series OSB I–series OSB II:

The effect of opening produced similar results as in cases of Series I–Series IV. Initial rigidity decreased (64.6; 59.1%), while ultimate load decreased (32.5; 36.9%). There is also an important decrease of ductility, probably highlighting the different failure modes of the two wall panels.

It can be concluded that the shear-resistance of wall panels is significant both in terms of rigidity and load bearing capacity, and can effectively resist lateral loads.

The hysteretic behaviour is characterized by very significant pinching, and reduced energy dissipation.

Failure starts at the bottom track in the anchor bolt region, therefore strengthening of the corner detail is crucial.

An important aspect of the experiments is to define acceptable damage levels and relate it to the performance objectives for the panels. In the end, the research work suggested a three level set of performance criteria for wall panels clad with corrugated sheeting depending on the storey drift displacement.

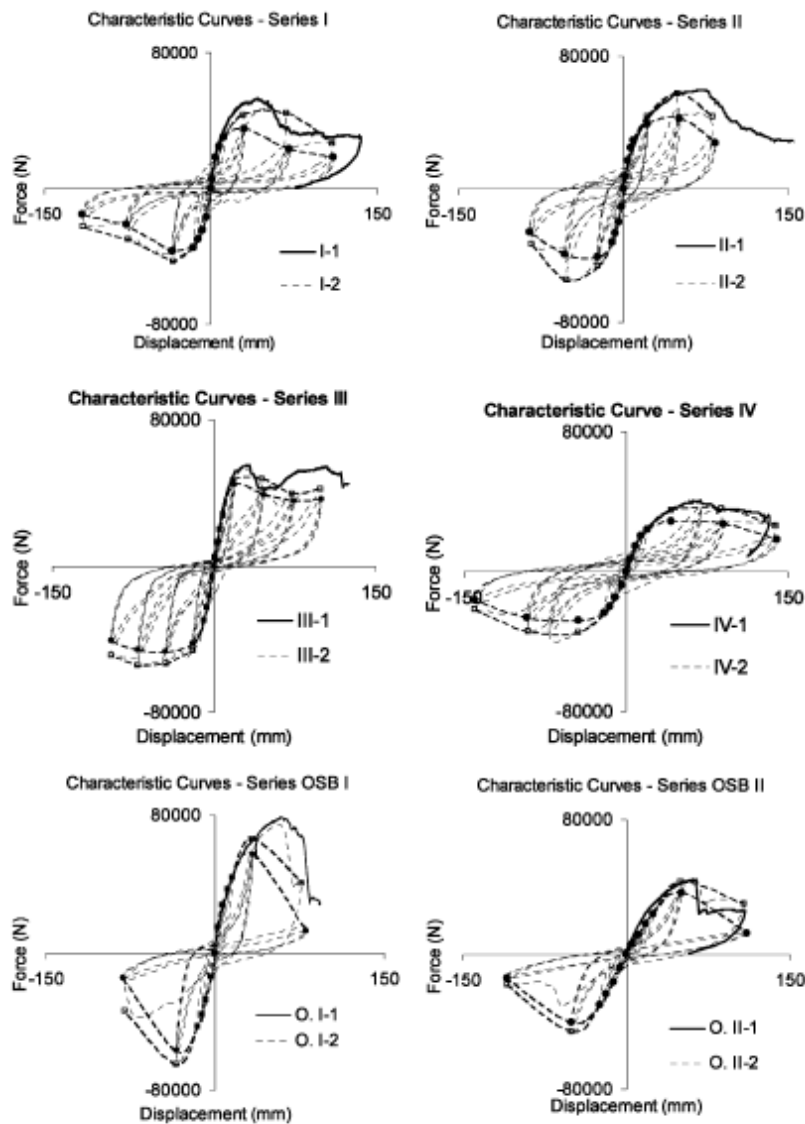


Figure 2.18 Force-displacement curves of the experimental results.

Table 2.4 Performance criteria.

Specimen	Connection deformation (mm)	Force (N)	Panel top displacement (mm)	Drift (%)
I-3	0.197	21423	6.71	0.274
	4.8	43885	29.22	1.197
IV-2	0.197	10106	7.96	0.326
	4.8	35613	44.13	1.808
IV-3	0.197	8849	8.11	0.332
	4.8	26,332	42.22	1.730

2.8 TIAN ET AL. (2004)

Details about the experimental tests on cold-formed steel wall frames developed by Y.S. Tian, J. Wang and T.J. Lu at the Department of Engineering of the University of Cambridge (UK) are summarized below (Tian et al., 2004). The experimental activity were sponsored partly by the UK Engineering and Physical Scientific Research Council.

2.8.1 Objectives of the research program

A combined experimental and analytical study has been carried out to investigate the racking strength and stiffness of cold-formed steel wall frames with and without bracings.

Starting from the consideration that bracing of a frame can significantly increase its capability to carry the vertical as well as lateral load, a variety of bracing methods were investigated.

The main objectives of the research were:

- the observation of deformation behaviour and failure modes of each frame under racking;
- the measurement of the racking strength and stiffness;
- the study of the influence of bracing strap size and bracing method on the racking performance of a frame.

2.8.2 Experimental tests

Racking tests will be carried out on frames braced with different strap configurations, including 1 side X-bracing, 2 side X-bracing, 2 side double X-bracing, and bracing with oriental strand board (OSB) or

cement particle board (CPB). A total number of 10 frames were fabricated for the racking test. Each frame (2450 x 1250 mm) consists of top and bottom tracks, side tracks and middle stud, and is braced with either steel straps or boards (except for frame A-1 which has no bracing). The track is a plain channel section, with web depth 93 mm, flange width 67 mm, and gage 1.2 mm. The middle stud is a lipped channel section, with web depth 90 mm, flange width 60 mm, lip length 12 mm, and gage 1.2 mm.

Three basic types of frame are tested: Type A is a frame without strap bracing, Type B is a frame with X strap bracing, and Type C is a frame with double X bracing.

For Frame A, there are 2 sub types: one has no bracing at all (A-1) and the other has board bracings (A-2), with two different bracing boards used, namely, oriental strand board (OSB) and cement particle board (CPB).

For Frame B are used 60x1.0 mm steel straps for X bracing. B-1 is braced on two sides whereas B-2 is braced only on one side.

For Frame C, with double X bracing, are used 60x1.2 mm steel straps on two sides.

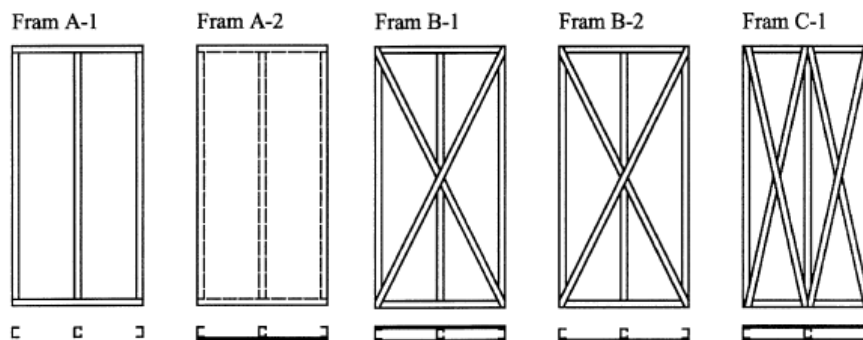


Figure 2.19 Frame bracing configurations.

The frame is placed on an horizontal basement, and there is also a top supporting system, clamped to the basement. This test set-up scheme has been designed to ensure that the deformation of the frame is confined to the horizontal plane, with minimal vertical movement. The racking load is applied to the frame by a mechanical jack via a loading block.

For the test procedure of the shear tests of cold-formed wall panel were used two loading methods based on BS: EN 594: 1996.

The first is a 1-step loading, in which the load is applied continuously till frame failure occurs. The second is a 3-step loading, in which the test is divided into 3 load steps: stabilizing step, stiffness step, and strength step. If two frames are identical, one will be tested according to the 1-step loading procedure to obtain the maximum load, and the other according to the 3-step loading.

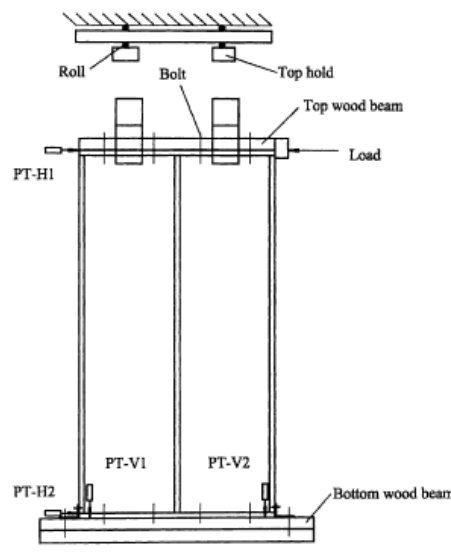


Figure 2.20 Test set-up.

2.8.3 Results and conclusions

Generally speaking, when the lateral deflection increased to about 30 mm, the lateral load of all braced frames (except for Frame B-2 braced with 1-side X straps) reached the damage load or maximum load, approximately 10 kN. In comparison, at the same lateral deflection, Frame A-1 without any bracing could only carry about 0.4 kN racking load. In other words, the frame itself can only contribute about 4% to the total racking resistance of a braced frame.

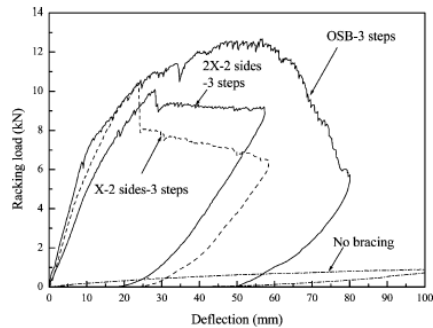


Figure 2.21 Racking load vs deflection curves of the tested frames.

The average damage load for Frame A-2 braced with OSB and CPB is 10.15 kN and 9.85 kN, respectively. After damage has occurred, the load continues to increase with increasing deflection, very slowly, and the load versus deflection curve becomes strongly nonlinear and unstable.

Amongst the 6 different frames tested, those braced with CPB and OSB have the best performance, with a maximum load of 13.1 kN and 12.7 kN, respectively, about 30% higher than the corresponding damage load. Three typical failure modes were observed during the test, namely, board damage failure, overall buckling of the track, and bracing rivet failure. For Frame A-2 braced with boards, all failures (cracks or permanent damage) occurred on the boards around screw connections. It appears that the board property dominates this failure mode. For Frame B-1 braced with 2-side X straps, there were two possible failure modes: overall buckling of the left track or strap rivet failure.

Table 2.5 Racking test results.

Frame type	Bracing type	Loading steps	Racking stiffness (kN/mm)	Damage load (kN)	Maximum load (kN)	Failure mode
A-1	No bracing	1			0.093	Plastic def. corners
A-2	OSB-1 side	1		10.0	16.0	Screws
A-2	OSB-1 side	3	0.526	10.3	12.7	Screws
A-2	CPB-1 side	1		9.8	11.6	Screws
A-2	CPB-1 side	3	0.603	9.9	14.6	Screws
B-1	1X-2 side	1		10.7	10.7	Top-left rivets
B-1	1X-2 side	3	0.534	10.3	10.3	Left track
B-2	1X-1 side	1		5.2	5.2	Bottom-right rivets
C-1	2X-2 side	1		10.7	10.7	Left track
C-1	2X-2 side	3	0.464	10.1	10.1	Left track

At the end of the study, the following conclusions can be drawn:

- a frame without any bracing has a racking strength less than 5% of that of the same frame with bracing;
- the racking strength of a frame braced with thin flat steel straps (except 1-side X bracing) is nearly the same as that of a frame braced with the more expensive and heavier CPB or OSB boards;
- for frames braced with boards, failure occurs on the board near screw connections. If the board thickness increases or screw spacing decreases, it is possible to increase the racking strength;
- strap width has relatively small influence on racking resistance, but affects frame stiffness significantly. The lateral deflection of the frame decreases dramatically with increasing strap width;
- the performance of a frame under racking depends on several key factors, including individual member section design, bracing method, connection method, and strap size. All these aspects need to be carefully examined if the racking performance of the frame is to be optimized.

2.9 AL KHARAT AND ROGERS (2005)

Details about the experimental tests on cold-formed steel strap braced walls developed by M. Al-Kharat and C.A. Rogers at the Department of Civil Engineering and Applied Mechanics of Montreal (Canada) are exposed below (Al Kharat and Rogers, 2006). In this study the inelastic performance of sixteen $2.44\text{ m} \times 2.44\text{ m}$ cold-formed steel strap braced walls was evaluated experimentally.

2.9.1 Objectives of the research program

The aim of this research project was to evaluate the inelastic lateral load carrying performance of typical light gauge steel frame-strap braced wall configurations which are not designed following a strict seismic capacity based design philosophy.

The main objectives were to determine the ductility of common strap braced walls by means of physical testing and to assess the inelastic performance with respect to the ASCE7-05 R-value of 4.0.

Three typical wall configurations were tested; light, medium and heavy in the context of cold-formed steel. The investigation involved the assembly testing of representative strap braced walls under lateral in-plane loading. A total of sixteen $2.44 \text{ m} \times 2.44 \text{ m}$ walls with standard non-seismic details were tested using monotonic and reversed cyclic loading protocols.

A comparison of the failure mode, ductility, shear strength and shear stiffness characteristics of the strap walls was made.

2.9.2 Experimental tests

The test program involved sixteen strap braced stud wall specimens ($2.44 \text{ m} \times 2.44 \text{ m}$). Experimental tests were carried out using a test frame designed specifically for in-plane shear loading.

The predicted factored lateral in-plane resistance of the three wall configurations in a wind loading situation was approximately 20 kN (light), 40 kN (medium) and 75 kN (heavy), respectively.

The walls were braced with diagonal flat straps installed in an X configuration on both sides.

Chord stud members were composed of double C-section shapes stitch welded front-to-front, while the remainder of the single interior C-section studs were placed at a nominal spacing of 406 mm.

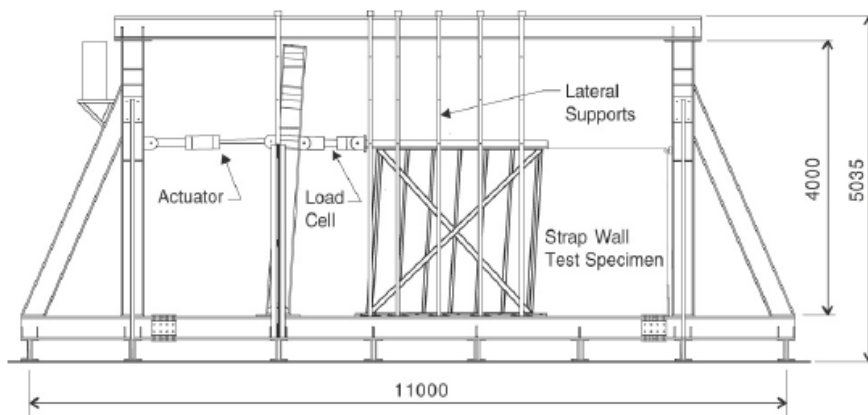


Figure 2.22 Testing frame with displaced strap braced wall.

The light walls were constructed of straps connected directly to the stud framing whereas the medium and heavy walls comprised of straps that were fillet welded to the gusset plates.

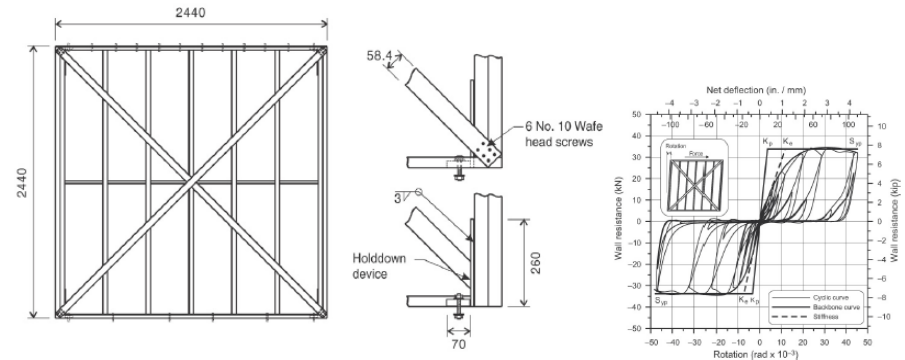


Figure 2.23 Light strap braced wall.

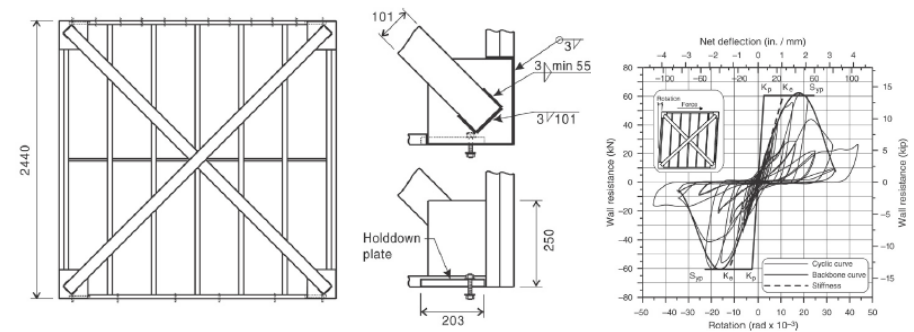


Figure 2.24 Medium strap braced wall.

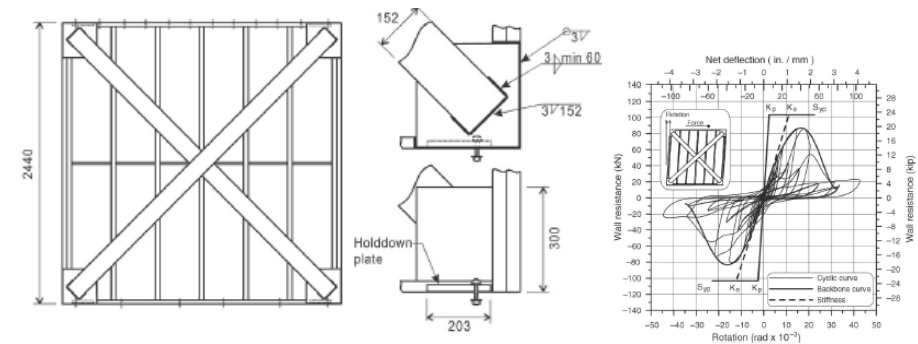


Figure 2.25 Heavy strap braced wall.

The load path for the light walls traced from the straps to the chord studs and then directly to the holddowns. In contrast, flat plate holddowns were placed within the upper and lower tracks at the four corner locations of the medium and heavy walls.

The holddown plates for the medium and heavy walls were attached to the loading beam and reaction frame by means of threaded rods. No direct connection was made from these holddown plates to either the braces, gusset plates or the chord studs.

The testing frame was equipped with a ± 125 mm stroke 250 kN dynamic actuator. Displacement controlled monotonic and reversed cyclic protocols were used in testing. The testing frame incorporated external beams to prevent out-of-plane buckling of the wall specimen, such that only lateral in-plane displacement would take place. The monotonic loading procedure consisted of a steady rate of displacement (2.5 mm/min) starting from the zero load position. The CUREE ordinary ground motions reversed cyclic loading protocol run at 0.5 Hz, was chosen for the testing of the strap braced walls.

2.9.3 Results and conclusions

The performance of CFS walls was affected by the hold-down detail, which in many cases did not allow the test specimens to reach or maintain a yield capacity and severely diminished the overall system ductility.

In particular, the overall performance of the tested walls under lateral loading was not governed by the yielding of the straps, as indicated by the strain gauge measurements that were taken. Rather, failure of or extensive damage to the tracks, chord studs, gusset plates, holddown threaded rods and straps (due to net section fracture) was often observed depending on the wall configuration being tested. These undesirable modes of failure prevented the straps from maintaining their yield load, or from yielding altogether. Thus the ductility and energy absorption ability of the SFRS was reduced in comparison to what could theoretically be expected given the material properties of the strap braces and what inherently would be assumed when a seismic response modification coefficient of $R = 4.0$ is selected in design.

2.10 KIM ET AL. (2006)

Details about the experimental tests on CF full-scale two-story one-bay structure developed by T.W. Kim, J. Wilcoskib, D.A. Foutchc and M.S. Leed at the Construction Engineering Research Laboratory of the Engineer Research and Development Center, Illinois (USA) are showed below (Kim et al., 2006).

2.10.1 Objectives of the research program

Although several static cyclic tests of individual shear panels have been conducted by several investigators, no dynamic tests have previously been conducted. So, the lack of information on the dynamic behavior CFS led to the shaketable tests performed in this research program.

2.10.2 Experimental tests

The CFS specimen was assembled on the ERDC-CERL shaketable, tri-axial Earthquake and Shock Simulator (TESS). The specimen was full-scale, consisting of two framing lines with two-story CFS shear panels. This specimen was shaken with horizontal-uniaxial motions in the plane of the diagonal straps.

The specimen consisted of two identical two-story, one-bay wide frames, which were separated from each other by 3.9 m on center in the out-of-plane direction. The width of the shear panel in center-line distance was 2.8m, and the story height was 3.0 m as a clear distance between slabs. The columns at the exterior edges of the frame were constructed from three channels, of which the size measures 51 mm×152mm×2.6 mm.

These columns were welded to steel anchors and bolted to the slab through top and bottom tracks. A heavy reinforced concrete slab diaphragm was installed at the top of each floor level.

The ground motion selected for the test was one of those suggested by SAC recommendations. This was the SE 32 accelerogram that has the same spectral response acceleration as the design response spectrum, an SDS of 1.5g, around the fundamental period of the test specimen.

The maximum displacement of the accelerogram exceeded the displacement limit of the TESS in this direction, so the accelerogram had to be high-pass filtered at 1 s to bring the maximum displacement down to within the limit.



Figure 2.26 Specimen tested on shaketable.

In the low-level tests, three different levels (2%, 5%, and 8%) of the SE 32 accelerogram were applied to the test specimen. The full-level test means that 100% of the SE 32 was applied. The 2% and 5% level tests were conducted to check if all of the data channels were recording properly, and to provide a preliminary estimate of the test levels that would begin to cause a non-linear response based on diagonal strap strains. The 8% and 100% tests had peak ground accelerations of 0.064g and 0.80g, respectively. The 100% test caused significant yielding in the straps along their entire length and yielding of the columns near the anchors. The response showed severe non-linear behavior of the straps.

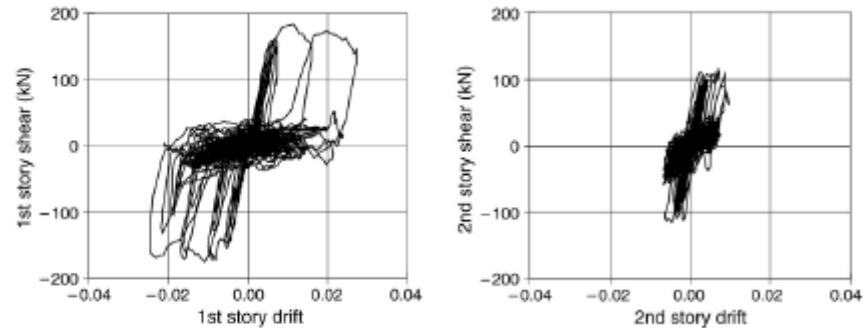


Figure 2.27 Shear vs drift in 100% test.

2.10.3 Results and conclusions

The fundamental period of the specimen was checked, because it is a major parameter in an elastic dynamic analysis. This fundamental period was determined using random vibration tests. Then, the behaviors of straps, columns, and anchors were also studied using results from the 8% (elastic) and 100% (inelastic) tests. Finally, the displacement history, which is related to drift, was investigated, because it is a major parameter used in performance-based earthquake engineering. The hysteretic behavior of the structure was investigated as well, because it can clearly show the nonlinear behavior of structures, especially energy dissipation and ductility capacities.

During the large amplitude tests, the cross-bracing straps showed very ductile but highly pinched hysteresis behavior. The columns that were fixed at the top and bottom provided limited strength, stiffness, and energy dissipation because of local buckling of the thin-walled members.

The following observations and conclusions were made:

- the dynamic tests confirmed what cyclic tests have shown that the thin steel straps used as cross-bracing in CFS buildings are very tough and ductile members;
- the built-up CFS columns also performed very well even after local buckling occurred. Local buckling and flexural strength are well predicted using standard equations;
- the contribution of the columns to the shear capacity of the structure was small but dependable throughout the earthquake simulation. The columns also provided energy dissipation during

regions of the earthquake response where the braces provided no strength or stiffness;

- the CFS building structure was shown to be a very effective and dependable structural system for resisting seismic loads. However, this good behavior is expected only if the brace is prevented from fracture due to improperly designed welded or screwed connections to the columns.

2.11 CASAFont ET AL. (2007)

Details about the experimental tests on CF X-braced frames developed by M. Casafont, A. Arnedo, F. Roure, A. Rodríguez-Ferran at the Universitat Politècnica de Catalunya in Barcelona (Spain) are summarized below (Casafont et al., 2007). The investigation was performed in the context of the European research project “Seismic Design of Light-Gauge Steel Framed Buildings”.

2.11.1 Objectives of the research program

An experimental campaign on CF x-braced frames was performed. The experimental campaign has two main objectives: the first is to gain knowledge about the behaviour of joints in order to establish criteria for their seismic design and the second is to obtain experimental data to calibrate a numerical model also developed in the project.

When x-bracings are used, connections should be designed such that they are strong enough to allow the development of the dissipative action of the bracings, i.e., the strength of connections should be higher than the yielding load of diagonal straps.

For this reason, the research program was basically oriented on the investigation of connections in x-braced frames.

The tests were performed on parts of the frames: strap-gusset joints and lower and upper corner joints.

In the last phase of the experimental campaign, verification tests are performed on two identical full x-braced frames, which are designed according to the achieved design recommendations, to check if these recommendations are really effective.

2.11.2 Experimental tests

For the scope of this chapter, here are reported the tests on x-braced shear frames only.

Tests are performed on two identical shear frames whose height is about four times shorter than the height of a conventional frame. This reduced model is used because it will allow one to record the hysteretic response of the x-braced frames, avoiding any problem related to premature buckling of studs. The main components of the shear panels are two tracks, two studs and four diagonal straps. Tracks and studs are composed of U100 and C100 profiles. The diagonal bracings are two straps of 65mm width and 0.8mm thickness. Diagonals are connected to studs and tracks through 210x140mm gusset plates whose thickness is 1.5 mm. f, 6.3mm self-drilling screws are used to connect all the components of the frame.

To ensure the dissipative yielding of the straps occurs before failure:

- Diagonal straps are thin and narrow. On the contrary, the cold-formed profiles chosen for tracks and studs have high load-bearing capacity.
- The steel grade of the diagonal straps is lower than the steel grade of the other members of the frame. Furthermore, a steel of low grade and ductile is used in straps, thus giving them more dissipation capacity.
- Only one row of screws is used to connect the straps to the gussets. This results in high net cross-section area, which also increases the dissipation capacity of the strap. The row contains nine screws, so that the strength of the connection is governed by the NSF mode, and the bearing failure is avoided.
- Anchor bolt connections without eccentricity are used, so that all the dissipative yielding takes place in the straps and premature failure of the corner joints is avoided.

For the test procedure a 100kN hydraulic cylinder is used to apply a cyclic horizontal force. Tests are displacement-controlled.

There are five loading cycles with an increasing value of displacement amplitude that ranges from 715 to 775 mm.

The displacement law is chosen so that yielding of the diagonal straps occurs from the first cycle of the test. The maximum displacement is limited to the maximum allowable displacement amplitude of the

hydraulic cylinder, 160 mm. The loading rate is constant for all the cycles: 0.2 mm/s.

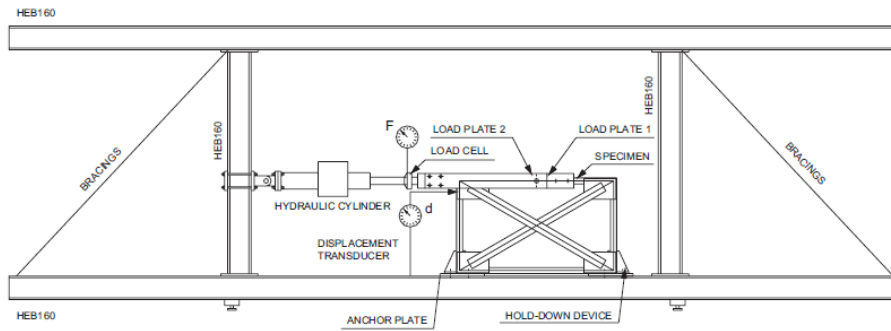


Figure 2.28 Test set-up.

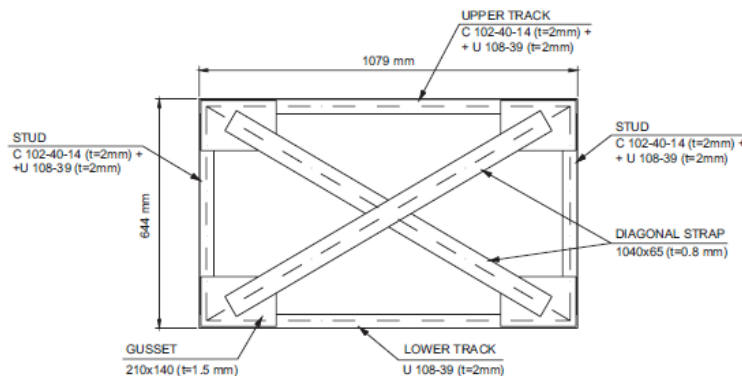


Figure 2.29 Shear frame tested.

2.11.3 Results and conclusions

Just from the beginning, there is the flexural buckling of the compressed straps. There is also yielding of the straps in the first cycle, as it was planned, and some local buckling phenomena.

In view of the results obtained, it is believed that the shear frames tested show satisfactory performance, because all the failure modes observed in the previous phases of the experimental campaign have been avoided.

However, it should also be pointed out that local damage occurred in joints as a consequence of their semi-rigid nature.

The force-displacement curves obtained in the tests show pinching and slackness, as it is usual for x-braced frames.

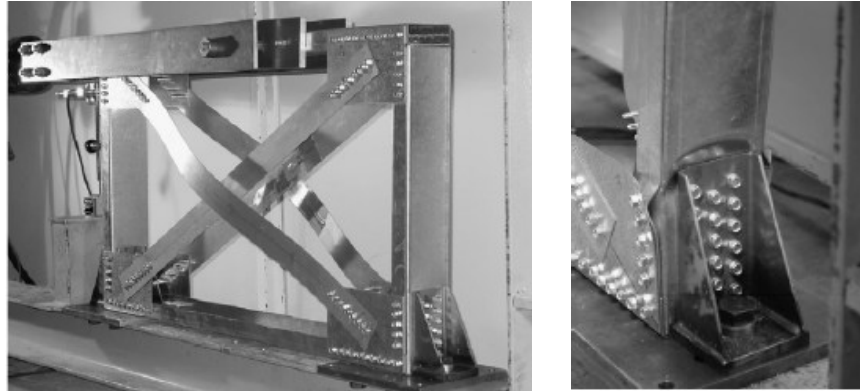


Figure 2.30 Test specimens after loading.

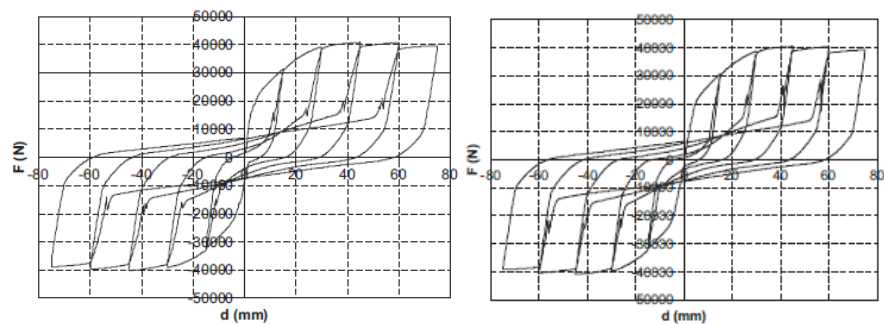


Figure 2.31 Test results: force-displacement curves.

The behaviour of the frame is symmetric all through the test. There is a small stiffness degradation as the number of cycles increases, which affects loading branches at a higher degree than unloading branches. There is also a small strength degradation.

Finally, it should be noted that a small, but sudden, fall in the force-displacement curves is observed in the loading branches of every cycle. This fall is caused by a small dynamic phenomenon that occurs when gussets go from their buckled configuration to the tensioned one.

In conclusion, the testing campaign shows that properly designed x-braced frames are a very effective means of dissipating seismic energy in a controlled manner.

2.12 VELCHEV, COMEAU AND ROGERS (2008)

Details about the experimental tests on CF X-braced wall developed by K. Velchev, G. Comeau, N. Balh and C.A. Rogers at the Jamieson Structures Laboratory of the Department of Civil Engineering & Applied Mechanics of Mc Gill University of Montreal (Canada) are exposed below (Velchev et al., 2008).

2.12.1 Objectives of the research program

The aim of this research project was to evaluate the inelastic lateral load carrying performance of weld and screw-connected strap braced walls that are designed following the capacity-based approach, required for the design of limited ductility walls, as described in AISI S213.

2.12.2 Experimental tests

A total of thirty screw-connected single-storey wall specimens 2.44 m x 2.44 m in size were designed according to the capacity design philosophy required by AISI S213 and then subjected to monotonic and reversed cyclic loading protocols. Three factored lateral load levels were used in design; 20 kN (light), 40 kN (medium) and 75 kN (heavy).

All but two specimens were constructed with diagonal cross bracing on both sides of the wall. Ten wall specimens were fabricated with fuse (reduced width) braces.

During testing lateral load and displacement, strain in the braces, as well as the slip and uplift at the base of the wall were recorded. These measurements were used to calculate the wall resistance, stiffness, ductility and energy dissipation.

Also, R_d and R_o values based on the test data were computed and compared with those listed in AISI S213 for type LD walls.

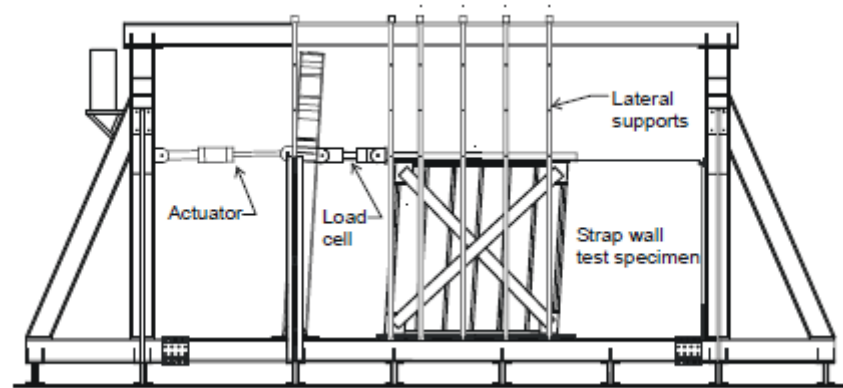


Figure 2.32 Testing frame with test specimen.

The testing frame was equipped with a 250 kN dynamic actuator with a stroke of ± 125 mm. Displacement controlled monotonic and reversed cyclic CUREE (Consortium of Universities for Research in Earthquake Engineering) protocols were used in testing. The testing frame incorporates external beams to prevent out-of-plane displacement of the wall specimen, such that only lateral in-plane displacement takes place.

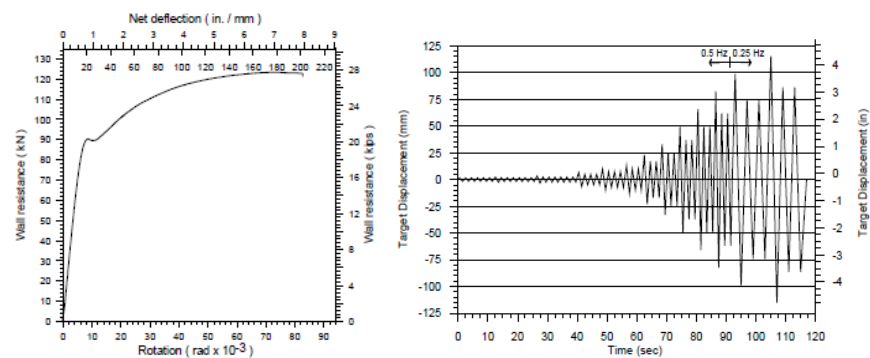


Figure 2.33 Monotonic and cyclic loading protocols.

2.12.3 Results and conclusions

The desirable behaviour of all strap braced walls is gross-cross section yielding of the braces. This would likely be followed by strain hardening, and in some cases net section fracture of a strap at high storey drift, far beyond that which would be anticipated during a seismic event.

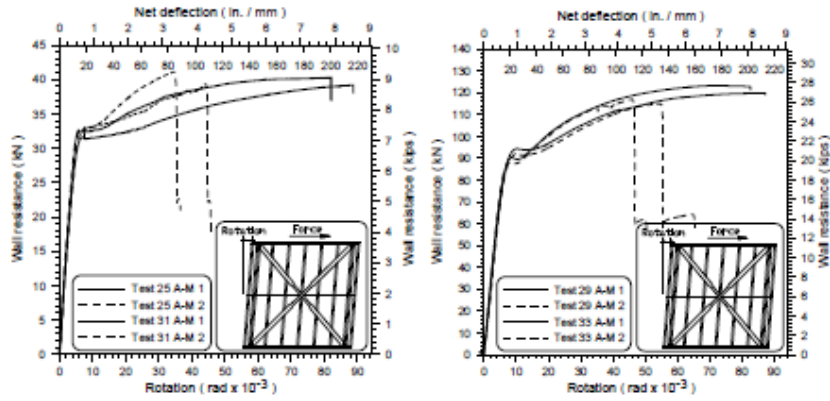


Figure 2.34 Monotonic resistance of light and heavy braced walls.

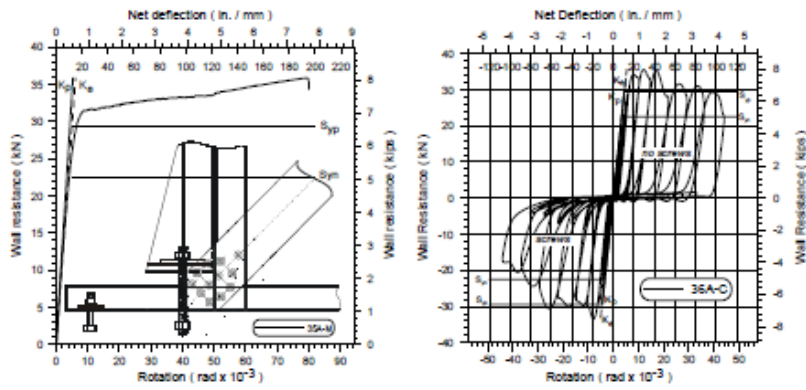


Figure 2.35 Cyclic response of light braced walls.

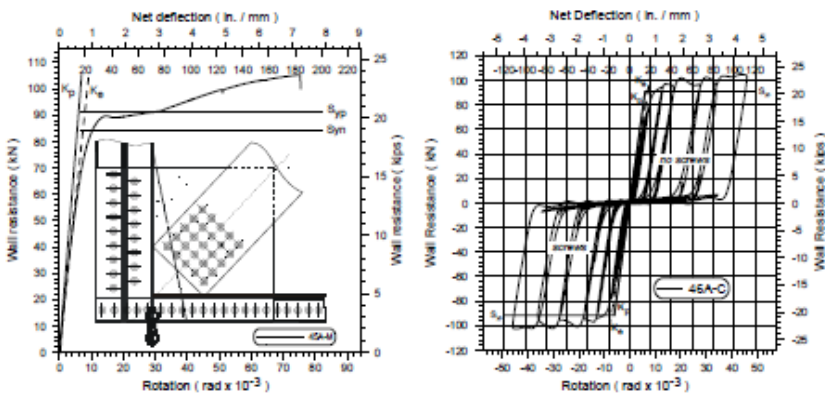


Figure 2.36 Cyclic response of heavy braced walls.

To achieve this ductile response and to allow for a stable and reliable hysteretic energy-dissipation mechanism, braces were designed to reach and maintain their yield capacity while undergoing large inelastic deformations over expected lateral displacement of the test wall. All remaining elements in the SFRS (brace connections, gusset plates, chord studs, tracks, anchor rods, holddowns and shear anchors) were detailed to be able to carry the probable capacity of the brace.

The performance of most of the test specimens subjected to monotonic and cyclic lateral loading was governed by the yielding of the straps, and even at a lateral drift of 8% for the monotonic and 4.5% for the cyclic tests net cross-section fracture was not observed. Significant increase of the wall resistance due to strain hardening of the braces was observed above 1.2%, 1.6% and 2.5% drift for test specimens with short fuse, long fuse and regular braces, respectively. Also, an elastic bending and distortional buckling of the chord studs was observed likely due to the large drift reached at the end of all monotonic tests.

2.13 MOGHIMI AND RONAGH (2009)

Details about the experimental tests on full scale CF X-braced wall developed by H. Moghimi and H.R. Ronagh at the Structural Engineering Laboratory of the Department of Civil Engineering of the University of Queensland (Australia) are analyzed below (Moghimi and Ronagh, 2009).

2.13.1 Objectives of the research program

The experimental program was designed to provide information on the failure modes of walls braced with different types of strap braces and to study the effects of various parameters on the vertical and lateral performance of CFS shear panels subjected to cyclic loads.

While conventional strap bracing and conventional connections to studs and top track were used, the following effects were studied:

- the effect of vertical load on the lateral response,
- the effect of non-structural gypsum board on lateral performance of a strap-braced wall system with and without vertical load,

- the effect of double-sided bracing,
- the effect of doubling the chords.

2.13.2 Experimental tests

The program consisted of 20 full-scale specimens to evaluate the performance of five different strap-braced. All of the frame components, i.e. top and bottom tracks, noggings and studs, were identical C channels of 90 x 36 x 0.55, connected together by one rivet at each flange. For this section, and under axial loading, the half wavelength of local buckling is less than 50 mm, for distortional buckling is between 50 and 850 mm, and for overall (flexural-torsional) buckling is greater than 900 mm. In specimens using gypsum board as cladding, two 10 mm thick sheets of 2400 x 1200 mm size were placed horizontally and connected to one side of all frame members by self-tapping screws at 150 mm intervals. Each back-to-back double section was constructed by connecting the web of two sections by screws at 150 mm centers. Bracing was implemented by means of 30 x 0.84 mm² straps connected to one or both sides of the frame. Five different bracing schemes were examined, as well as one unbraced wall clad with two horizontally-laid gypsum boards on one side.

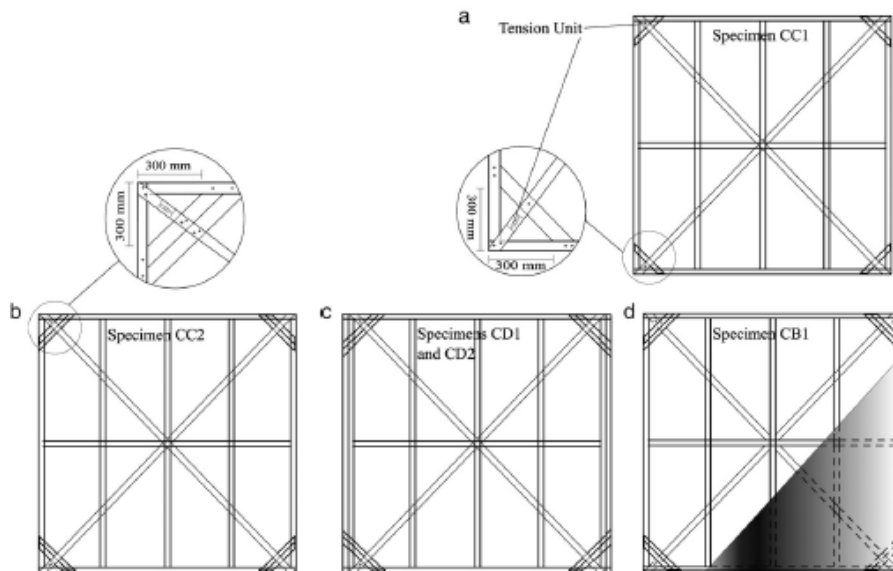


Figure 2.37 Example of specimen types.

The second scheme takes advantage of four brackets placed at the four corners of the wall. The strength, stiffness and ductility of this system depend mostly on the brackets' shape and size and to a lesser extent on the chords. The effect of bracket members, the effect of chords, the influence of the presence of two side straps and concurrent vertical, the effect of gypsum board in conjunction with bracket members load were investigated.

Finally, for the sake of completeness, the lateral performance of a wall panel strap-braced with gusset plates at four corners was investigated.

Experiments were conducted using a displacement control regime, measuring the shear capacity of the wall at every load interval via a load cell. The testing rig was set up to allow the application of concurrent vertical load and lateral cyclic displacement.



Each specimen was fixed to the base beam by means of five M16 high-strength bolts in the vicinity of middle and chords. Between a bolt head and the base beam and a nut surface and the track, two glossed 50x50 mm² washers were placed to increase the contact surface and friction, and to reduce the slip possibility between the bottom track and the base beam. A similar arrangement was implemented to connect the top track to the loading beam. Moreover, to reduce the possibility of overturning and to provide a proper load path from the strap to the wall supports, four hold-down angles were placed near the top and bottom tracks.

Cyclic loading methodology followed Method B of ASTM E2126-05 standard, which was originally developed for ISO (International Organization for Standardization) standard 16670. The loading velocity was 3 min/cycle or about 0.8 mm/s.

The above mentioned standard stipulates that the amplitude of cyclic displacements has to be selected based on fractions of monotonic ultimate displacement. Since each specimen has its own ultimate displacement, the loading regime would vary for different specimen types. To make possible the comparison of different types of strap-braced walls it has been used identical cyclic amplitudes for different walls.

For the specimens under concurrent vertical and horizontal load, special care was exercised to maintain the vertical load constant as the wall was loaded cyclically in the horizontal direction.

2.13.3 Results and conclusions

The response of strap type I is unacceptable. The benefit of non-structural gypsum board cladding on the lateral performance of strap-braced wall panels is evident in the response of walls AB1 and CB1, and can even be seen in strap type I. However, the benefits are mostly on the lateral resistance capacity and ductility, and the stiffness is not influenced significantly.

Strap types II, III and V exhibit the best performance and are fairly similar to each other, but type V (solid strap) provides a stiffer response especially for small displacements. Also the response of strap type IV is acceptable, although it is more flexible in comparison with other types such as II, III and especially V, and needs more lateral displacement to develop full plasticity in the strap. Even when the response is adjusted

for the inclination angle, the system is less efficient than other system. Tests showed that a high deformation and strength demand applies to wall corners type III, but the system presents a good lateral performance provided that the chord members are double back-to-back studs and tracks are strong enough to connect these two studs properly. The envelope graphs show that most wall panels yield around 0.5% to 0.6% inter-story drift. Only the brace type IV, which is not post-tensioned, required larger displacements to yield.

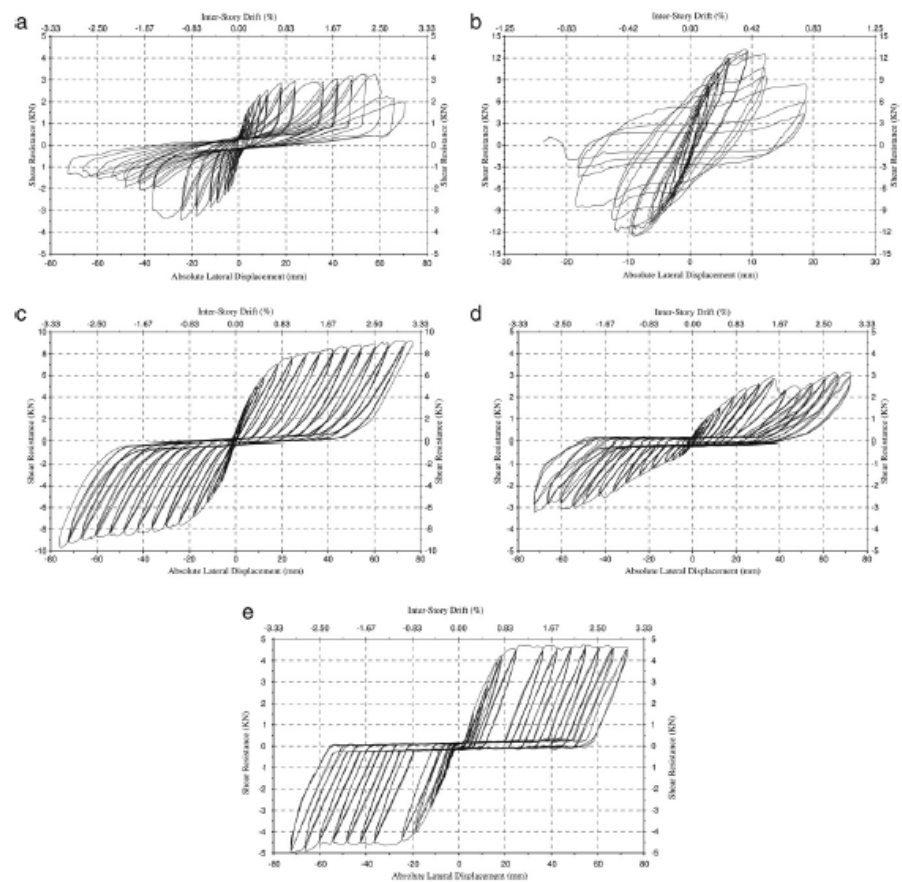


Figure 2.39 Force-displacement response.

3 CFS STRUCTURES IN SEISMIC CODES

In this chapter the main prescriptions about lateral design of CFS structures are critically analyzed and in particular the principles and the prescriptions of the American code AISI S213-07/s1-09 are considered.

3.1 AISI S213-07/S1-09

There are no prescriptions in the Italian Code for seismic design of CFS structures. At the moment, the only document that provides prescriptions for the lateral design of this structural typology is the AISI S213-07 "North American Standard for Cold Formed Steel Framing - Lateral Design" developed by the American Iron and Steel Institute Committee on Framing Standards.

In fact, this standard was written to address the design of lateral force resisting systems to resist wind and seismic forces in a wide range of buildings constructed with cold-formed steel framing. The standard is intended for adoption and use in United States, Canada and Mexico.

With the aim to present accurate, reliable and useful information on cold-formed steel framing design and installation, the Committee collected the contribution of many researchers and engineers. Specific references to the works that contributed to the body of knowledge on the subject are included in the Commentary of the Standard.

The Standard provides an integrated treatment of Allowable Strength Design (ASD), Load and Resistance Factor Design (LRFD), and Limit States Design (LSD). This is accomplished by including the appropriate resistance factors for use with LRFD and LSD, and the appropriate factors of safety for use with ASD. It should be noted that LSD is limited to Canada and LRFD and ASD are limited to Mexico and United States. To be able to compare this Standard with European and Italian codes, the attention was focused on the prescription for Canada, and in particular for diagonal strap bracings.

The AISI standard is divided into 4 main parts:

A: General, B: General design requirements, C: Walls, D: Diaphragms.

In the next paragraphs will be analyzed and discussed the first 3 parts, and will be neglected part D. Concerning part C, the attention will be focused on seismic requirements (C1, C5) and diagonal strap bracings (C4), neglecting C2 and C3 (shear walls with sheathing panels).

3.1.1 Part A: General

Part A of AISI S213-07 provides general information about Capacity Based Design, that is defined as a method for designing a seismic force resisting system (SFRS) in which specific elements or mechanisms are designed to dissipate energy, and all other elements are sufficiently strong for this energy dissipation to be achieved. Moreover, elements and connections in the horizontal and vertical load paths are designed to resist the seismic loads, and diaphragms and collector elements are capable of transmitting the loads developed at each level to the vertical SFRS and then to the foundations, always maintaining the structural integrity.

In this part there are also defined the force modification factors related to ductility, R_d , and related to overstrength, R_o , for seismic loads, for each structural typology of CFS structures considered in the code.

Details were presented and discussed in the next paragraphs when the attention is focused on the behaviour factor.

3.1.2 Part B: General Design Requirements

Part B of AISI S213-07 provides general design requirements for CFS structures subjected to lateral loads. This part of the Standard underlines that the design and detailing of SFRS shall be in accordance with AISI S100, AISI S200 and the limitations in the applicable building code (NBCC for Canada).

The shear resistance of diagonal strap bracing is permitted to be calculated by principles of mechanics. The nominal strength so calculated defines the maximum resistance that the diagonal strap bracing is capable of developing, on the other hand, the available strength shall be computed based on the wind and seismic force requirements in the applicable building code.

The Commentary to the Standard clarifies that the development of design values for other systems or configurations not included in the

standard is permitted in accordance with rational engineering procedures and principles of mechanics.

In seismic design, loads are modified to account for system or element or component ductility (inelastic behaviour), redundancy and overstrength. As a result, the lateral resisting element must meet some minimum performance requirements. In light of this, where design values are determined by calculation, these values must be scaled to existing values. Boundary members, chords and connections shall be proportioned to transmit the induced forces and the probable seismic resistance of the diagonal strap bracing following a capacity based design approach. Since in wind design, design loads are not reduced, the basic lateral resisting element need only to be designed for the design loads. However, because seismic loads are reduced, to develop the anticipated performance, it is desirable to focus damage (inelastic behaviour) in the lateral element. Depending on the seismic risk level, the component transferring load to or from the lateral element should be capable of resisting the nominal strength of the element or some amplified seismic load. The amplified seismic load is essentially an estimation of the nominal strength that the lateral element is capable of developing.

3.1.3 Part C: Walls

Part C of AISI S213-07 is about walls and is subdivided into:

C1: General, in which are listed the basic seismic requirements;

C2 and C3: Type I and Type II shear walls, in which are defined and analyzed shear walls designed according to the principles of 'sheathing braced design' (cfr. Par. 2.2 of this dissertation), SFRS specifically detailed assuming that the sheathing connections act as the energy dissipating elements;

C 4: Diagonal Strap Bracing, in which are defined and analyzed diagonal strap braced walls designed according to the principles of 'all steel design' (cfr. Par. 2.2 of this dissertation), SFRS specifically detailed so that all members of the bracing system are subjected primarily to axial forces, assuming the braces act as the energy dissipating element (gross section yielding);

C5: Special Seismic Requirements, in which are exposed special seismic requirements for each typology.

It can be recognized two main subjects in part C: the seismic requirements for elastic design approach and the seismic requirements for dissipative design approach.

For the aims of this thesis, the attention is focused on general (C1) and special (C5) seismic requirements and diagonal strap bracings (C4).

Concerning diagonal strap bracings, the standard AISI S213 provides some requirements on their installation: the tension-only diagonal strap bracing is expected to be installed taut, to avoid lateral displacements without increase of resistance. The slenderness ratio of the diagonal strap bracing member shall be permitted to exceed 200.

Concerning the aspect ratio of walls, the standard AISI S213 suggest some limitations. Based on recent research studies (Comeau and Rogers, 2008) it can be demonstrated that 1:1 and 2:1 aspect ratio walls allow the development of the desired ductile wall performance (yielding of braces) according to the capacity design procedures and material requirements of this standard. Instead, the aspect ratio of 4:1 is not recommended, because this walls are not able to maintain their yield capacity, and in some cases they are not able to reach the predicted yield capacity as determined using the brace strength, even if the walls with this aspect ratio were observed to be significantly more flexible than other. So, in case of walls with aspect ratio of 4:1, is required a rational analysis that includes joint flexibility and end moments in combination with the axial compression force, in the design of chord studs.

3.2 DISCUSSION AND COMPARISONS

Seismic requirements provided by the AISI S213 will be analyzed in the following, considerations and comparisons with Italian code (NTC 08) were made, focusing the attention on the behaviour factor, the diagonal brace verifications and the overstrength of fragile elements.

3.2.1 Behaviour Factor

Considering the linear static approach to seismic design, the dissipative structural behaviour, that buildings usually perform in case of severe seismic loads, is considered in an indirect way, through the so-called "behaviour factor" (R), that reduces the seismic design forces as a

function of the expected levels of overstrength and ductility of the structure.

Part A of AISI S213 defines the behaviour factor as a function of ductility related force modification factor, R_d , and overstrength related force modification factor, R_o , see equation (1), that are listed in Table A4-1 of the standard (fig. 3.1) for each SFRS and for each design approach (elastic or dissipative).

$$R = R_d \cdot R_o \quad (3.1)$$

In which:

R_d = Ductility-related force modification factor reflecting the capability of a structure to dissipate energy through inelastic behaviour (to be used with NBCC);

R_o = Overstrength-related force modification factor accounting for the dependable portion of reserve strength in a structure (to be used with NBCC).

Table A4-1
Canada
Design Coefficients and Factors for Seismic Force Resisting Systems in Canada

Type of Seismic Force Resisting System	R_d	R_o	Building Height (m) Limitations ¹				
			Cases Where $I_E F_a S_a(0.2)$				Cases Where $I_E F_y S_a(1.0)$
			< 0.2	≥ 0.2 to < 0.35	≥ 0.35 to ≤ 0.75	> 0.75	> 0.3
Shear Walls ²							
Screw connected shear walls: wood-based structural panel	2.5	1.7	20	20	20	20	20
Screw connected shear walls: wood based structural and gypsum panels in combination	1.5	1.7	20	20	20	20	20
Diagonal Strap Braced (Concentric) Walls ³							
Limited ductility braced wall ⁴	1.9	1.3	20	20	20	20	20
Conventional construction ⁵	1.2	1.3	15	15	NP	NP	NP
Other Cold-Formed Steel SFRS(s) Not Listed Above	1.0	1.0	15	15	NP	NP	NP

Figure 3.1 Table A4-1 of AISI S213.

In Fig. 3.1 are highlighted the values for diagonal strap braced walls in case of elastic (conventional construction) and dissipative (limited ductility braced walls) design approaches.

Moreover, in the same Table are listed building height limitations as a function of short (0.2) and long (1.0) period spectral acceleration (S_a), adjusted for the site class and the earthquake importance factor.

$S_a(0.2)$ = 5% damped spectral response acceleration for a period of 0.2 s for the reference ground condition Site Class C as defined in NBCC;

$S_a(1.0)$ = 5% damped spectral response acceleration for a period of 1.0 s for the reference ground condition Site Class C as defined in NBCC.

R_d and R_o values are also recommended for diagonal strap braced walls using the NBCC. In case where the braces are able to reach and maintain their yield strength in the inelastic range of behaviour, ductility and overstrength reach levels associated with those of a limited ductility (LD) concentrically braced frame (CBF) (Al-Kharat and Rogers, 2006).

Al-Kharat and Rogers showed through experimental tests that the R values used for conventional constructions (CC) could also be applied for CFS structures not designed with capacity design approach. The use of diagonal strap bracings designed with CC R values is limited to areas of low seismicity and the height limit has been reduced.

In 2008 findings of a research project at Mc Gill University on the inelastic performance of welded (Comeau and Rogers, 2008) and screw connected (Velchev and Rogers, 2008) strap braced walls demonstrated that the R_d , R_o and height limits values listed in Table A4-1 of AISI S213 were appropriate.

It have to be noticed that only the most common structural systems are identified and have assigned values of R_d and R_o . In an SFRS not specifically identified in Table A4-1 $R_d = R_o = 1.0$ must be used for design. This requirement (Part A of AISI S213) is based on the assumption that systems that are not described should be designed conservatively, because their ductility and overstrength capacity have not yet been demonstrated.

The first part of Part C of AISI S213 provides the field of application of seismic requirements:

- the design shall comply with provisions for elastic design (C1 - C4) when in diagonal strap braced walls $R_d * R_o \leq 1.625$.
- the design shall comply also with additional provisions for dissipative design (C5) when in diagonal strap braced walls $R_d * R_o > 1.625$. In this case height restrictions of Table A4-1 shall apply.

In both cases height restrictions of Table A4-1 shall apply.

For diagonal strap braced walls a designer has the option to choose an $R_d * R_o = 1.625$ for systems with a higher $R_d * R_o$ to determine the seismic load and thereby avoid the special detailing in Section C5. For this case the height limitations for Conventional Constructions in Table A4-1 would apply. In the Commentary to the standard it is underlined that the value of $R_d * R_o \leq 1.625$ for diagonal strap bracing was chosen to ensure that the system remains essentially elastic.

So we can notice the inconsistency of Part A and Part C in the definition of R values for elastic design.

In the Italian Code (NTC 08) the behaviour factor (q) is defined depending on the limit state considered, and so according to the design approach considered.

For elastic design approach $q = 1$, instead for dissipative design approach q is defined as a function of structural typology, the design approach and taking into account the non-linear behaviour of the material.

$$q = q_0 \cdot K_R \quad (3.2)$$

In which:

q_0 = is the maximum value of the behaviour factor, depending on the expected ductility level, the structural typology and the α_u/α_1 ratio (ratio between the value of the seismic action for which the structure becomes labile, and the value of the seismic action for which the first element reach the plasticization);

K_R = is a reducing factor depending on the regularity in elevation of the structure, is equal to 1 if the structure is regular and 0.8 if the structure is not regular in elevation;

α_u/α_1 = is defined for structures regular in plan for each structural typology.

In Table 7.5 II of NTC 08 (fig. 3.2) are listed the maximum values of the behavior factor for each structural typology for dissipative design.

Tabella 7.5.II – Limiti superiori dei valori di q_0 per le diverse tipologie strutturali e le diverse classi di duttilità.

TIPOLOGIA STRUTTURALE	q_0	
	CD "B"	CD "A"
a) Strutture intelaiate	4	$5\alpha_u/\alpha_t$
c) Strutture con controventi eccentrici		
b1) Controventi concentrici a diagonale tesa attiva	4	4
b2) Controventi concentrici a V	2	2,5
d) Strutture a mensola o a pendolo inverso	2	$2\alpha_u/\alpha_t$
e) Strutture intelaiate con controventi concentrici	4	$4\alpha_u/\alpha_t$
f) Strutture intelaiate con tamponature in muratura	2	2

Figure 3.2 Table 7.5 II of NTC 08.

Cold Formed Steel structures are not considered among the possible structural typologies in the Italian Code NTC 08, so the appropriate behavior factor is $q = 1$. The elastic design approach have to be used to reach a ductile behavior.

3.2.2 Diagonal Brace Verifications

Part C5 of AISI S213 underlines that in areas where the expected demand from seismic event is high, it is desirable that the lateral resisting elements develop its full range of behaviour before failure, so that the performance of all components related to the overall response of the lateral system become significant. For the diagonal strap braced wall typology, the ductile failure mechanism is assured by yielding of the diagonal strap brace.

To ensure gross cross section yielding of the diagonal strap bracing member, AISI S213 requires that the expected yield strength ($A_g R_y F_y$) not exceed the expected tensile strength ($A_n R_t F_u$) of the diagonal strap bracing member.

$$A_g \cdot R_y \cdot F_y \leq A_n \cdot R_t \cdot F_u \quad (3.3)$$

In which:

A_g = gross cross section area; R_y = factor for expected yield strength;

A_n = net cross section area; R_t = factor for tensile strength;

F_y = nominal value of yield strength;

F_u = nominal value of ultimate tensile strength.

When $A_g R_y F_y$ exceeds $A_n R_t F_u$ a material with a larger ratio F_u to F_y could be selected or the diagonal strap member could be modified to reduce the ratio A_g to A_n . It is not considered acceptable to just assume a lower F_y in the calculations.

The factors for expected yield strength and tensile strength of the diagonal strap bracing member, R_y and R_t , were based on similar values published for hot-rolled structural steel materials, results of studies on galvanized sheet steel by a sheet steel producer and engineering judgement.

R_y and R_t can be determined in accordance with an approved test method, but in absence of verified physical properties measured in accordance with approved test methods, the R_y and R_t values in Table C5-1 of AISI S213 shall be used. In either case R_y shall not be less than 1.1.

Table C5-1
 R_y and R_t Values for Diagonal Strap Bracing Members

Yield Strength	R_y	R_t
33 ksi [230 MPa]	1.5	1.2
37 ksi [255 MPa]	1.4	1.1
40 ksi [275 MPa]	1.3	1.1
50 ksi [340 MPa]	1.1	1.1

Figure 3.3 Table C5-1 of AISI S213.

The Italian code NTC 08 provides verifications for dissipative elements in tension, that are similar to the equation (3.3) for x-braced structures in hot rolled structural steel. NTC 08 provides that design plastic strength of the diagonal cross section have to be less than ultimate design strength of the net cross section in correspondence of the fasteners holes.

$$N_{pl,Rd} \leq N_{u,Rd} \quad (3.4)$$

in which:

$$N_{pl,Rd} = \frac{A \cdot f_{yk}}{\gamma_{M0}} \quad (3.5)$$

$$N_{u,Rd} = \frac{0.9 \cdot A_{net} \cdot f_{tk}}{\gamma_{M2}} \quad (3.6)$$

So the following equation have to be satisfied (par. 7.5.3.2 of NTC 08):

$$\frac{A_{res}}{A} \geq 1.1 \cdot \frac{\gamma_{M2}}{\gamma_{M0}} \cdot \frac{f_{yk}}{f_{tk}} \quad (3.7)$$

In which:

A = gross cross section area;

A_{res} = net cross section area;

γ_{M0} = safety factor for member resistance (gross cross section);

γ_{M2} = safety factor for member resistance (net section with fasteners);

f_{yk} = nominal value of yield strength;

f_{tk} = nominal value of ultimate tensile strength.

A numerical comparison were made between the verifications provided by the two codes considering different steel grades for both cold formed and hot rolled steel.

So, for direct comparison, equation (3.3) can be written as:

$$\frac{A_n}{A_g} \geq \frac{R_y}{R_t} \cdot \frac{F_y}{F_u} \quad (3.8)$$

Table 3.1 Comparison for Cold Formed Steel grades.

Steel grade	R_y/R_t	$1.1 \gamma_{M2}/\gamma_{M0}$
S220GD+Z 33 ksi (230 MPa)	1.25	1.3
S250GD+Z 37 ksi (255 MPa)	1.27	
S280GD+Z 40 ksi (275 MPa)	1.18	
S350GD+Z 50 ksi (340 MPa)	1.00	

Table 3.2 Comparison for Hot Rolled Steel grades.

Steel grade	R_y/R_t	$1.1 \gamma_{M2}/\gamma_{M0}$
S 235 33 ksi (230 MPa)	1.25	1.3
S 275 40 ksi (275 MPa)	1.18	
S 355 50 ksi (340 MPa)	1.00	

From the numerical comparison, some considerations can be made. First of all it can be noted that R_y/R_t changes as a function of the steel grade, and, on the contrary, $1.1 \gamma_{M2}/\gamma_{M0}$ is a constant value equal to 1.3. Moreover, the different values of R_y/R_t are always less than 1.3, so we can say that the NTC 08 is more conservative than AISI S213.

In AISI S213 there is also another condition to be satisfied, that is not present in the Italian code NTC 08.

Capacity based design calculations demonstrated that the gross cross section yielding failure mode occur prior to the net section fracture, if the diagonal strap bracing member satisfies this equation:

$$(R_t \cdot F_u)/(R_y \cdot F_y) \geq 1.2 \quad (3.9)$$

Also in this case, numerical comparison were made, considering different steel grades for both cold formed and hot rolled steel.

Table 3.3 Comparison for Cold Formed Steel grades.

Steel grade	$R_t \cdot F_u$	$R_y \cdot F_y$	$(R_t \cdot F_u)/(R_y \cdot F_y)$
S220GD+Z 33 ksi (230 MPa)	360	330	1.09
S250GD+Z 37 ksi (255 MPa)	363	350	1.04
S280GD+Z 40 ksi (275 MPa)	396	364	1.09
S350GD+Z 50 ksi (340 MPa)	462	385	1.20

Table 3.4 Comparison for Hot Rolled Steel grades.

Steel grade	$R_t \cdot F_u$	$R_y \cdot F_y$	$(R_t \cdot F_u)/(R_y \cdot F_y)$
S 235 33 ksi (230 MPa)	432	352.5	1.23
S 275 40 ksi (275 MPa)	473	357.5	1.32
S 355 50 ksi (340 MPa)	561	390.5	1.44

It can be noted from the numerical comparisons, that the equation (3.9) is satisfied for all steel grades of hot rolled structural steel, on the contrary, for cold formed steel grades, only S350GD+Z satisfies the equation.

For increasing material resistance, the relation is ruled by the ratio R_t/R_y , because the difference between R_t and R_y decrease, and in particular for steel S355 (hot rolled) and S350GD+Z (cold formed), $R_t = R_y = 1.1$.

3.2.3 Overstrength Factor

In the case where the braces of the wall are able to reach and maintain their yield strength in the inelastic range of behaviour (yielding take place along the length of the braces without failure of any other SFRS element), the capacity based design approach is applied to all SFRS elements, that are selected based on the probable yield capacity of the brace.

In particular, to develop a desirable response, AISI S213 requires that components transferring loads to and from the diagonal strap bracing member shall have the nominal strength to resist the expected yield strength ($A_g R_y F_y$) of the diagonal strap bracing member or, if lower, the expected overstrength (seismic loads calculated with $R_d R_o = 1$) of the diagonal strap bracing member.

So the following equation shall be satisfied:

$$H_{j,d} \geq A_g \cdot R_y \cdot F_y \quad (3.10)$$

in which:

A_g = gross cross section area;

F_y = nominal value of yield strength.

The Italian code NTC 08, for x-braced structures in hot rolled structural steel, provides equivalent prescriptions for connections in dissipative zones, and in particular they shall have an adequate overstrength to permit the plasticization of the connected parts.

So the following equation shall be satisfied:

$$R_{j,d} \geq \gamma_{Rd} \cdot 1.1 \cdot R_{pl,Rd} = R_{U,Rd} \quad (3.11)$$

in which:

$R_{j,d}$ = connection design strength;

$R_{pl,Rd}$ = member strength, see equation (3.5).

So the two equations (3.10) and (3.11) can be compared by the overstrength factors R_y and $1.1 \gamma_{Rd} / \gamma_{M0}$.

γ_{Rd} is the overstrength factor defined in NTC 08 for different hot rolled steel grades.

A numerical comparison was made between this two overstrength factors, considering different steel grades for both cold formed and hot rolled steel.

Table 3.5 Comparison for Cold Formed Steel grades.

Steel grade	γ_{Rd}	γ_{M0}	$1.1 \gamma_{Rd}/\gamma_{M0}$	R_y
S220GD+Z 33 ksi (230 MPa)	1.2	1.05	1.3	1.5
S250GD+Z 37 ksi (255 MPa)	1.15	1.05	1.2	1.4
S280GD+Z 40 ksi (275 MPa)	1.15	1.05	1.2	1.3
S350GD+Z 50 ksi (340 MPa)	1.1	1.05	1.2	1.1

Table 3.6 Comparison for Hot Rolled Steel grades.

Steel grade	γ_{Rd}	γ_{M0}	$1.1 \gamma_{Rd}/\gamma_{M0}$	R_y
S 235 33 ksi (230 MPa)	1.2	1.05	1.3	1.5
S 275 40 ksi (275 MPa)	1.15	1.05	1.2	1.3
S 355 50 ksi (340 MPa)	1.1	1.05	1.2	1.1

It can be noted from the numerical comparisons, that the factor $1.1\gamma_{Rd}/\gamma_{M0}$ is variable from 1.3 (lower steel strength) to 1.2 (higher steel strength) and R_y is variable from 1.5 (lower steel strength) to 1.1 (higher steel strength), both overstrength parameters are decreasing with material resistance increasing.

Only for steel S355 (hot rolled) and S350GD+Z (cold formed) the Italian code NTC 08 is more conservative than AISI S213.

4 PLANNING OF THE EXPERIMENTAL ACTIVITY

In this chapter there is the description of the planning of the experimental campaign and in particular the basic assumptions in terms of loads and strategies for elastic design and dissipative design of diagonal strap braced walls.

4.1 BASIC ASSUMPTIONS AND DESIGN ACTIONS

With the aim to assess a large number of different cases, three residential buildings with different storeys numbers are considered as case studies (Fig. 4.1), and in particular:

- one storey building (3 m height);
- two storeys building (6 m height);
- three storeys building (9 m height).

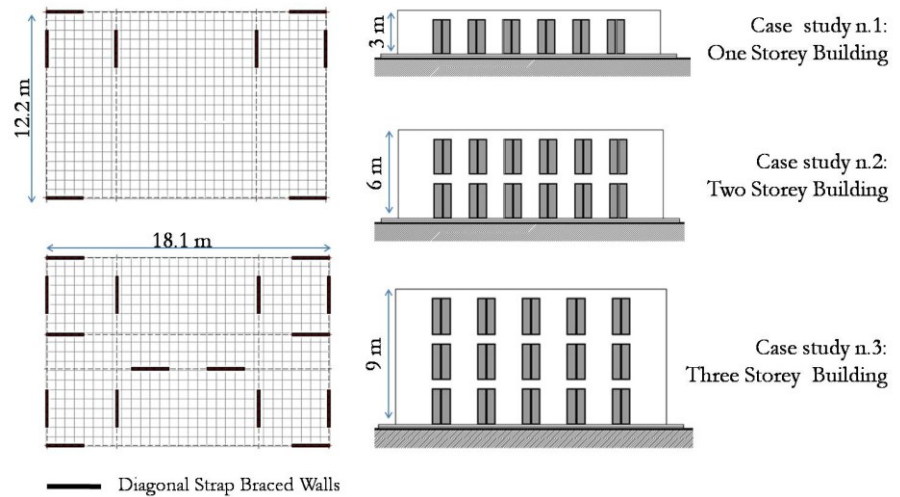


Figure 4.1 Case studies: residential buildings.

In Table 4.1 are listed the geometrical dimensions of the case studies buildings.

Table 4.1 Geometrical characteristics of case studies buildings.

Dimension	unit	Value
Plan dimensions	m	12.20 x 18.10
Plan area	m ²	220.00
Interstorey height	m	2.70
Diagonal strap braced wall	m	2.40 x 2.70

The structural design of these buildings was carried out in accordance with the Italian Code “Norme Tecniche per le Costruzioni, 2008” (NTC08) and for details not considered in this code, in accordance with Eurocode 3 (EC3-1-3).

The three residential buildings were designed considering two different geographical locations: Roma and Potenza (IT), that are representative of seismic and snow loads respectively medium-low and medium-high. Details on the two zones are presented in Table 4.2.

Table 4.2 Geographical characteristics.

City	Seismic zone	Soil	Altitude (m)	Snow load
Roma	3	C	20	medium-low
Potenza	1	C	892	medium-high

Diagonal strap braced walls have been designed based on the following loads: dead loads, variable loads, seismic loads.

4.1.1 Definition of dead loads

The dead loads were computed taking into account a range of values (kN/m²) for structural and non-structural elements, considering light or heavy configurations of floors, internal and external walls.

In particular, for the floor, this range of values for the components was considered:

- flooring (0.10 ÷ 0.20 kN/m²);
- slab (0.40 ÷ 1.10 kN/m²);
- corrugated sheet (0.05 ÷ 0.10 kN/m²);
- ceiling (0.05 ÷ 0.10 kN/m²).

And for walls this range of values for the components was considered:

- structural profiles ($0.03 \div 0.10 \text{ kN/m}^2$);
- insulating panel ($0.02 \div 0.20 \text{ kN/m}^2$);
- internal/external sheathing ($0.05 \div 0.20 \text{ kN/m}^2$);
- internal/external cladding ($0.10 \div 0.25 \text{ kN/m}^2$).

So the minimum and maximum values of dead loads can be listed in the following Table.

Table 4.3 Dead loads.

element	Roma		Potenza	
	min	max	min	max
floor (kN/m^2)	0.60	1.50	0.60	1.50
external walls (kN/m^2)	0.30	1.00	0.30	1.00
internal walls (kN/m^2)	0.70	0.70	0.70	0.70

4.1.2 Definition of variable actions

For the design of the three residential buildings, the variable actions that have been considered are:

- accidental actions: loads due to intended use of the building,
- snow loads.

In Table 3.1 II of NTC 08 are listed the loads due to the different intended uses of the building, that in this case, for Cat. A, residential buildings, is 2.00 kN/m^2 .

The snow load is different for the two different geographical locations (Roma and Potenza), and can be calculated through the expression:

$$q_s = \mu_i \cdot q_{sk} \cdot C_E \cdot C_t \quad (4.1)$$

In which:

q_s = snow load on the roof [kN/m^2];

μ_i = snow load shape coefficient, defined in § 3.4.5 of NTC 08;

q_{sk} = characteristic value of snow load on the ground at the relevant site expressed in [kN/m^2], given in § 3.4.2 of NTC 08 for a return period of 50 years;

C_E = exposure coefficient, given in § 3.4.3 of NTC 08;

C_t = thermal coefficient, given in § 3.4.4 of NTC 08.

In particular, the snow load on the ground is expressed as a function of local climate and exposure conditions, so for the considered cities, it is:

$$\begin{aligned} q_{sk} &= 0.60 \text{ kN/m}^2 & \text{for } a_s \leq 200 \text{ m} \\ q_{sk} &= 0.51 [1 + (a_s/481)^2] \text{ kN/m}^2 & \text{for } a_s > 200 \text{ m} \end{aligned}$$

where a_s is the site altitude above the sea level.

So the values of accidental and snow loads can be listed in the following Table.

Table 4.4 Variable actions.

Load	Roma	Potenza
accidental loads (kN/m ²)	2.00	2.00
snow load (kN/m ²)	0.48	1.81

4.1.3 Definition of seismic actions

For the design of the three residential buildings, the seismic actions that have been considered are computed according to NTC 08.

The design seismic actions are defined starting from the value of “base seismic hazard” referred to the geographical position of the construction site. In Table 4.5 the principal parameters that are necessary to calculate the seismic action for the Life Safety limit state are defined.

Table 4.5 Parameters for the definition of seismic action.

	medium-low seismicity level	medium-high seismicity level
a_g (g)	0.110	0.202
F_0	2.682	2.446
T_c^* (s)	0.306	0.363
S_S	1.500	1.403
S_T	1.000	1.000

Where:

a_g = design ground acceleration on type A ground;

F_0 = maximum value of the amplification factor for the horizontal ground acceleration response spectrum;

T_c^* = value defining the beginning of the constant velocity range of the response spectrum;

S_s = stratigraphic soil factor

S_T = topographic soil factor

The case studies buildings are regular in plan and in elevation, so the static equivalent analysis can be applied.

The fundamental period of the building can be estimated with the expression:

$$T_1 = C_1 \cdot H^{\frac{3}{4}} \quad (4.2)$$

Where:

H = height of the building, measured from the foundation soil (m);

C_1 = 0.085 for moment resisting steel frames, 0.075 for r.c. frames, 0.050 for all other structures.

The value of the seismic action (F_h) is calculated on the basis of the spectral acceleration in correspondence of the period T_1 and the distribution along the structure is derived from the principal vibration mode of the structure. The seismic force for each mass of the building has to be evaluated by the following expression:

$$F_i = \frac{F_h \cdot z_i \cdot W_i}{\sum_j z_j \cdot W_j} \quad (4.3)$$

where:

$$F_h = \frac{S_d(T_1) \cdot W \cdot \lambda}{g} \quad (4.4)$$

z = height of the masses from the foundation;

W = seismic weight.

In Figure 4.2 details on the definition of the seismic action are showed.

With reference to a seismic action with an overcoming probability in the reference period (P_{VR}) of 10% in 50 years, it was performed an elastic and a dissipative design. In particular for dissipative design it was assumed a behaviour factor equal to 2.5, as given in AISI S213-07.

Case study	City	Se (T) [g] [SLV]	W _{min} [kN]	W _{max} [kN]	F _{h,min} [kN]	F _{h,max} [kN]	z [m]	F _{i,min} [kN]	F _{i,max} [kN]
Case 1: one storey building	Roma	0.544	364	618	198	336	3	200	339
	Potenza	0.868			316	537	3	318	541
Case 2: two storeys building	Roma	0.544	829	1394	451	759	3	150	253
					6	301	506		
	Potenza	0.868			720	1210	3	240	403
					6	480	807		
Case 3: three storeys building	Roma	0.544	1294	2171	598	1004	3	100	167
					6	199	335		
					9	299	502		
	Potenza	0.868			955	1602	3	159	267
					6	318	534		
					9	478	801		

n° walls	Behaviour factor (q)	H _d [kN]
4	2.5*	20
4	1	50

SEISMIC ACTION MEDIUM-LOW
for each wall

SEISMIC ACTION MEDIUM-HIGH
for each wall

n° walls	Behaviour factor (q)	H _d [kN]
8	2.5*	80

* Behaviour factor q = 2,5 (AISI S213)

Figure 4.2 Definition of the seismic actions.

According to this design assumptions, three different kind of diagonal strap braced walls were designed to be tested.

The first wall configuration (elastic light wall, WLE) is representative of the case study n.1, the one-storey building, in a medium-low seismicity level zone with an elastic design approach.

The second wall configuration (dissipative light wall, WLD) is representative of the case study n.1, the one-storey building, in a medium-low seismicity level zone with a dissipative design approach.

The third wall configuration (dissipative heavy wall, WHD) is representative of the case study n.3, the three storeys building, in a medium-high seismicity level zone with a dissipative design approach.

The three configurations of diagonal strap braced walls and their design assumptions are illustrated and summarized in Figure 4.3.

In the figure, H_d is the value of design seismic action for each single wall.

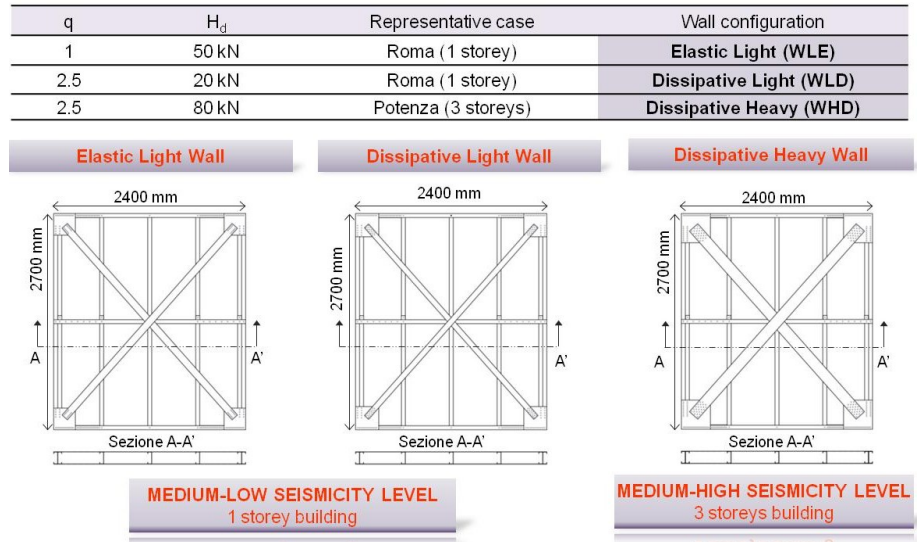


Figure 4.3 Diagonal strap braced walls configurations.

4.2 DESIGN OF DIAGONAL STRAP BRACED CFS WALLS

In all the configurations, diagonal strap braced walls are 2400 mm wide and 2700 mm high.

The design lateral resistance of the walls were computed as the smallest value among the resistances associated with all the possible failure modes.

Being H_c the design lateral resistance of the wall, it can be written as:

$$H_c = \min(H_{c,s}; H_{c,t}; H_{c,a}; H_{c,d}; H_{c,c}) \quad (4.5)$$

in which:

$H_{c,s}$ = lateral resistance for collapse of studs;

$H_{c,t}$ = lateral resistance for collapse of tracks;

$H_{c,a}$ = lateral resistance for collapse of frame to foundations anchors;

$H_{c,d}$ = lateral resistance for collapse of diagonal strap braces in tension;

$H_{c,c}$ = lateral resistance for collapse of frame to diagonals anchors.

The collapse of metal frame for lateral loads is generally due to the buckling caused by compression of chord studs or tracks, so $H_{c,s}$ and $H_{c,t}$ can be calculated with the expressions:

$$H_{c,s} = \frac{N_{s,Rd}}{h} \cdot L \quad (4.6)$$

$$H_{c,t} = N_{t,Rd} \quad (4.7)$$

in which $N_{s,Rd}$ e $N_{t,Rd}$ are the resistances in compression of studs and tracks.

For frame to foundations anchors, the possible collapse mechanisms are due to shear or tension. Usually, the collapse is managed by the tension force in the connection between the chord stud in tension and the bottom track. In any case, $H_{c,a}$ can be calculated with the expression:

$$H_{c,a} = \min \left(n_a \cdot V_{a,Rd}; \frac{N_{a,Rd}}{h} \cdot L \right) \quad (4.8)$$

where the first term is the shear resistance of the anchors and the second term is the overturning resistance due to tension collapse of the anchors:

n_a = number of shear anchors;

$V_{a,Rd}$ = design shear resistance of each anchor;

$N_{a,Rd}$ = design resistance in tension of the anchor.

The lateral resistance of the wall due to the collapse mechanism managed by collapse of diagonal in tension, $H_{c,d}$, can be calculated as the minimum value between the resistance in tension of the gross area section and the resistance in tension of the net area section at the ends:

$$N_{t,Rd} = \frac{A_d \cdot f_{yk}}{\gamma_{M0}} \quad (4.9)$$

$$F_{n,Rd} = \frac{A_{net} \cdot f_{tk}}{\gamma_{M2}} \quad (4.10)$$

where:

A_{net} = net area of cross section in correspondence of fasteners holes;

f_{yk} = yield strength of steel;
 f_{tk} = ultimate strength of steel;
 γ_{M0} = partial factor for resistance of members;
 γ_{M2} = partial factor for resistance of connections.

The lateral resistance of the wall due to the collapse mechanism managed by collapse of diagonal to frame connections, $H_{c,c}$ can be calculated taking into account the shear collapse mechanism based on the use of self-drilling screws, so by the expression:

$$H_{c,c} = n_d \cdot n_s \cdot \min(F_{b,Rd}; F_{V,Rd}) \cos \alpha \quad (4.11)$$

where:

$F_{b,Rd}$ = resistance to bearing of the plate;
 $F_{V,Rd}$ = shear resistance of screws;
 that are both referred to a single screw and can be calculated as:

$$F_{b,Rd} = \frac{\alpha \cdot d \cdot t \cdot f_{tk}}{\gamma_{M2}} \quad (4.12)$$

$$F_{V,Rd} = \frac{F_{V,k}}{\gamma_{M2}} \quad (4.13)$$

where:

t = minimum thickness of the plate;
 d = diameter of screw;
 α = coefficient depending on the diameter of the screws and the thickness of the connected plates;
 $F_{V,k}$ = the shear resistance of the screws.

In the following Figure the different components of the lateral resistance of the wall are shown.

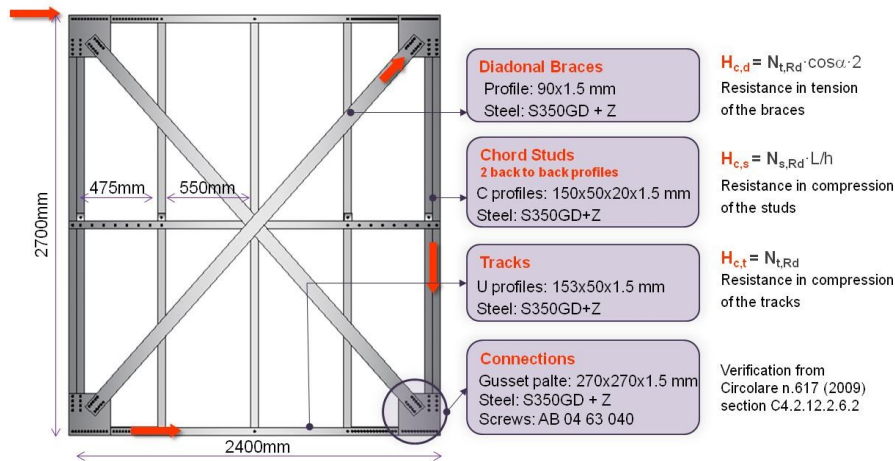


Figure 4.4 Lateral resistance of the wall and its components.

4.2.1 Design of the Elastic Light Wall

In the design of the Elastic Light Wall (WLE), it was applied an elastic design approach, in which the dimension of each element is designed with reference to the design seismic action, not considering any dissipative design approach.

The design values of the lateral resistances associated with each possible collapse mechanism are listed in the following table.

Table 4.6 Lateral resistances for the Elastic Light Wall.

Lateral Resistance due to collapse mechanism of:	H_c [kN]	$H_c/H_{c,min}$
Diagonal Strap Brace	58.20	1.15
Studs	132.70	2.63
Tracks	105.23	2.09
Diagonal connections		
bearing of plate	63.36	1.25
net area in tension	50.45	1.00
Stud connections		
bearing of plate	67.71	1.34
net area in tension	236.69	4.69
Track connections		
bearing of plate	70.36	1.39
net area in tension	187.10	3.71
Gusset Plate	84.60	1.68
$H_{c,min}$	50.45	

It can be noted that the collapse mechanism associated with the design minimum lateral resistance is due to diagonal brace in tension in the section weakened by fastener holes. Figure 4.5 shows the WLE details.

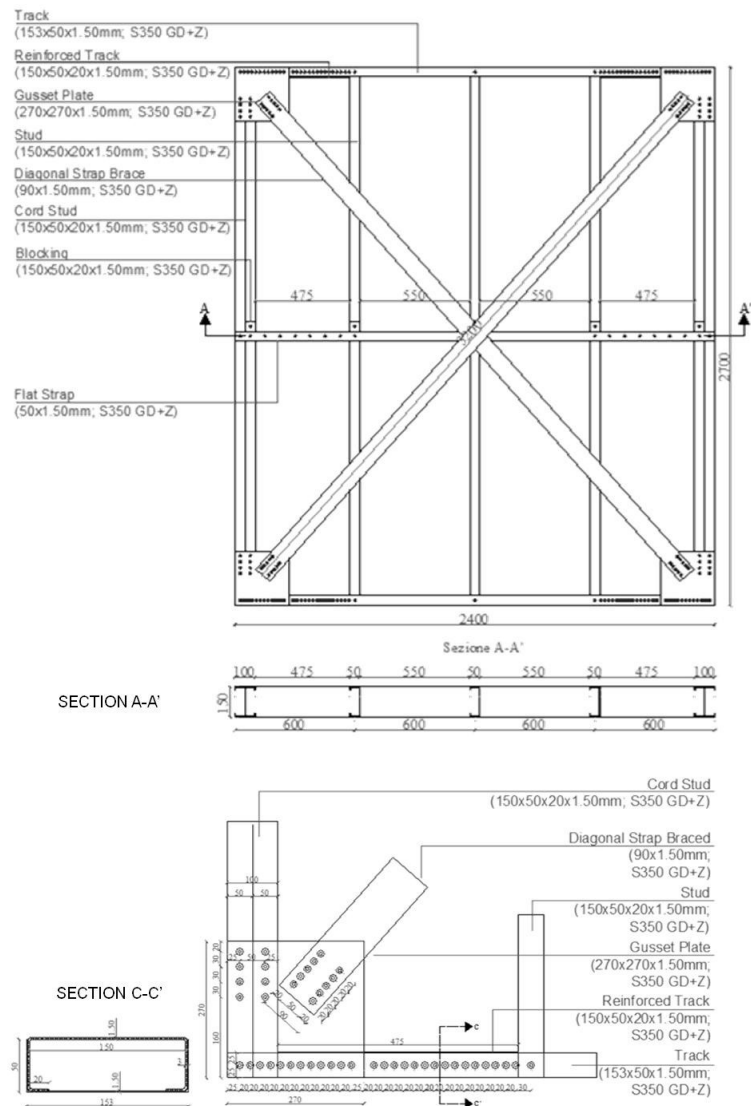


Figure 4.5 Elastic Light Wall.

4.2.2 Design of the Dissipative Walls

In the design of the Dissipative Light Wall (WLD) and Dissipative Heavy Wall (WHD) there were applied the capacity design principles to ensure a dissipative behaviour of the walls.

In this case, the dissipative design approach is applied by making possible the development of the most ductile collapse mechanism, that is the yielding of diagonals in tension. The behaviour factor 'q' used for the seismic action is 2.5, as suggested for this seismic typology by seismic code AISI S213.

To avoid the collapse mechanism due to the net area of diagonals in the connections, it was verified the fulfilment of the expression:

$$\frac{A_{res}}{A} \geq 1.1 \cdot \frac{\gamma_{M2}}{\gamma_{M0}} \cdot \frac{f_{yk}}{f_{tk}} \quad (4.14)$$

that is the condition presented in par. 7.5.3.2 of NTC 08, formerly showed in par. 3.2.2 of this dissertation exp. (3.7), equivalent to the (3.3) of the same 3.2.2 of this dissertation, that refers to AISI S213.

For the fulfillment of this expression, in the design of dissipative walls it was given particular attention in the definition of details for the connections and the choice of different material properties for diagonal braces. Indeed, for diagonal braces was used steel S235 and for all other elements S350GD+Z.

Moreover, to guarantee the overstrength of other elements, and so prevent the other possible collapse mechanisms, all the dissipative elements were dimensioned to be able to satisfy the relation:

$$H_{j,Rd} \geq 1.1 \cdot \gamma_{Rd} \cdot H_{d,Rd} \quad (4.15)$$

that is the condition presented in par. 7.5.3.3 of NTC 08, referring to the connections of dissipative parts, formerly showed in par. 3.2.3 of this dissertation in generic form, with the expression (3.11), equivalent, but more conservative, to the (3.10) of the same 3.2.3 of this dissertation, that refers to AISI S213.

In expression (4.15) the terms are referred specifically to the resistance of the CFS wall and in particular:

$H_{j,Rd}$ = design value of lateral resistance of the wall associated to a generic non-dissipative collapse mechanism;
 $H_{d,Rd}$ = design value of lateral resistance of the wall associated to the dissipative collapse mechanism (yielding of brace in tension);
 γ_{Rd} = overstrength factor defined in NTC 08 for different hot rolled steel grades.

It can be also noted that EN 1993-1-3 provides further relations to be verified, that are not present in NTC 08. In the case that the connection have to be able to provide a certain deformation capacity, an adequate overstrength must be provided to the parts developing a fragile collapse mechanism, so that the following expressions must be satisfied:

$$F_{v,Rd} \geq 1.2 \cdot F_{b,Rd} \quad (4.16)$$

$$\Sigma F_{v,Rd} \geq 1.2 \cdot F_{n,Rd} \quad (4.17)$$

in which:

$F_{b,Rd}$ = bearing resistance of plate;

$F_{v,Rd}$ = shear resistance of screw;

$F_{n,Rd}$ = net area resistance of brace in tension.

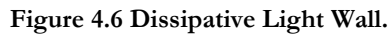
The design values of the lateral resistances associated with each possible collapse mechanism for WLD and WHD are listed in Tables 4.7 and 4.8. Figures 4.6 and 4.7 show respectively the WLD and WHD details.

Table 4.7 Lateral resistances for the Dissipative Light Wall.

Lateral Resistance due to collapse mechanism of:	H_c [kN]	$H_c/H_{c,min}$	$H_c/H_{j,Rd}$
Diagonal Strap Brace	40.80	1.00	
Studs	132.70		2.46
Tracks	105.23		1.95
Diagonal connections			
bearing of plate	70.27		1.30
net area in tension	45.30	1.11	
Stud connections			
bearing of plate	73.88		1.37
net area in tension	239.31		4.44
Track connections			
bearing of plate	74.80		1.39
net area in tension	188.57		3.50
Gusset Plate	127.20		2.36
$H_{c,min}$	40.80		
$H_{j,Rd}$	53.86		

Table 4.8 Lateral resistances for the Dissipative Heavy Wall.

Lateral Resistance due to collapse mechanism of:	H_c [kN]	$H_c/H_{c,min}$	$H_c/H_{j,Rd}$
Diagonal Strap Brace	81.60	1.00	
Studs	336.86		3.13
Tracks	308.55		2.86
Diagonal connections			
bearing of plate	132.91		1.23
net area in tension	90.83	1.11	
Stud connections			
bearing of plate	148.16		1.38
net area in tension	469.26		4.36
Track connections			
bearing of plate	145.85		1.35
net area in tension	373.36		3.47
Gusset Plate	160.97		1.49
$H_{c,min}$	81.60		
$H_{j,Rd}$	108.00		



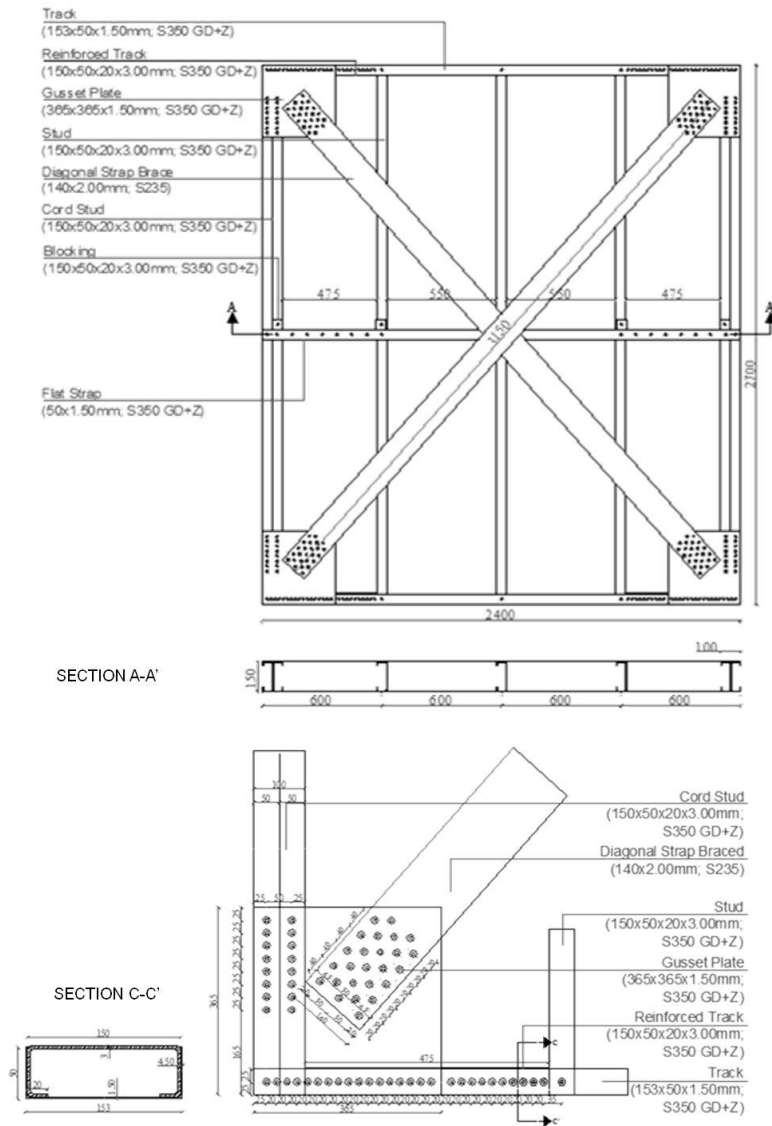


Figure 4.7 Dissipative Heavy Wall.

4.2.3 Evaluation of stiffness of the walls

To define theoretically the lateral displacement (d) at the top of the wall subjected to a horizontal load (H), it must be taken into account the contributions due to: diagonals in tension (d_d), anchorages between frame and foundations (d_a) and connections between frame and diagonal braces (d_c):

$$d = d_a + d_d + d_c \quad (4.18)$$

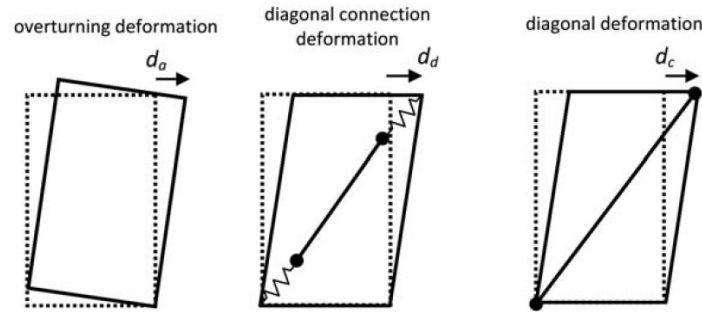


Figure 4.8 Contributions to deformations of a diagonal braced wall.

This expression is valid in the case in which the horizontal relative displacement between the wall and the foundations are completely prevented, that is what generally occurs in real cases.

The calculation of the contributions d_a , d_d and d_c can be obtained theoretically. In particular, the lateral displacement due to the anchors in tension can be calculated through the following expression:

$$d_a = \frac{h^2}{k_a \cdot L^2} \cdot H \quad (4.19)$$

in which:

H = horizontal load;

h = height of the wall;

L = length of the wall;

k_a = extensional stiffness of an anchor in tension.

The extensional stiffness k_a was assumed equal to 30kN/mm for the elastic light wall (WLE) and dissipative light wall (WLD), and 60kN/mm for the dissipative heavy wall (WHD).

The displacement produced by the axial deformability of the diagonals in tension may be obtained by the following expression:

$$d_d = \frac{L}{n_d \cdot E \cdot A_d \cdot \cos^2 \alpha_d} \cdot H \quad (4.20)$$

in which:

n_d = number of diagonals in tension;

A_d = diagonal cross section area;

α_d = inclination of the diagonal to the horizontal line;

E = steel Young's modulus.

And finally, the contribution due to the deformability of the connections between diagonals and frame can be obtained with the following expression:

$$d_c = \frac{2}{n_d \cdot n_s \cdot k_s \cdot \cos^2 \alpha_d} \cdot H \quad (4.21)$$

in which:

n_s = number of screws in the single connection;

k_s = shear stiffness of a single connection (screw).

The shear stiffness of the screws is usually evaluated by means of experimental tests. In this case, k_s is assumed equal to 1.775kN/mm on the basis of experimental data by Rogers and Velchev (2008).



Figure 4.9 Shear tests on connections (Velchev, 2008).

After the calculation of the displacement, it can be possible to evaluate the stiffness of the walls by means of the following expression:

$$k_d = \frac{1}{d} \quad (4.22)$$

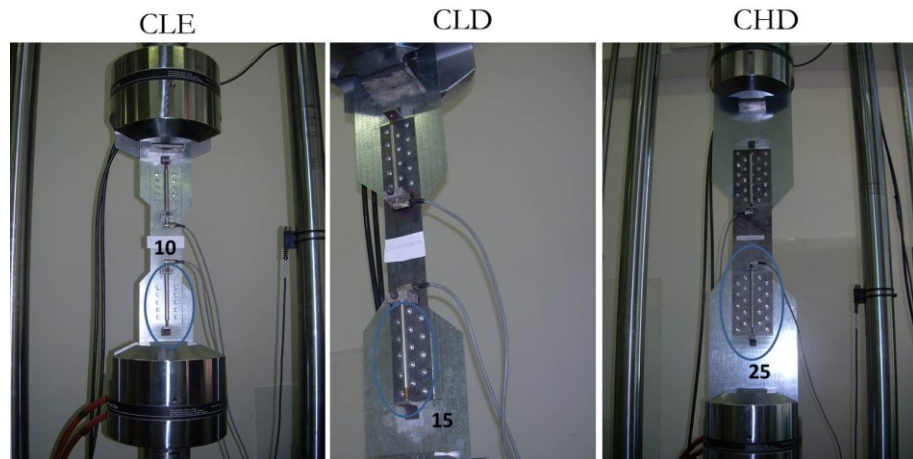


Figure 4.10 Types of tested frame to diagonal connections.

The obtained results, derived from the calculation of displacement and stiffness for the walls designed for the experimental tests, are shown in the following table.

Table 4.9 Displacement and stiffness of designed walls.

	d_a	d_d	d_c	d	k_d
	[mm]	[mm]	[mm]	[mm]	[kN/mm]
Elastic Light Wall (WLE)	0.0435	0.1232	0.1276	0.2943	3.40
Dissipative Light Wall (WLD)	0.0435	0.1140	0.0851	0.2426	4.12
Dissipative Heavy Wall (WHD)	0.0435	0.0541	0.0511	0.1486	6.73

In the following figures the contributions in terms of stiffness of all the elements of the wall are showed.

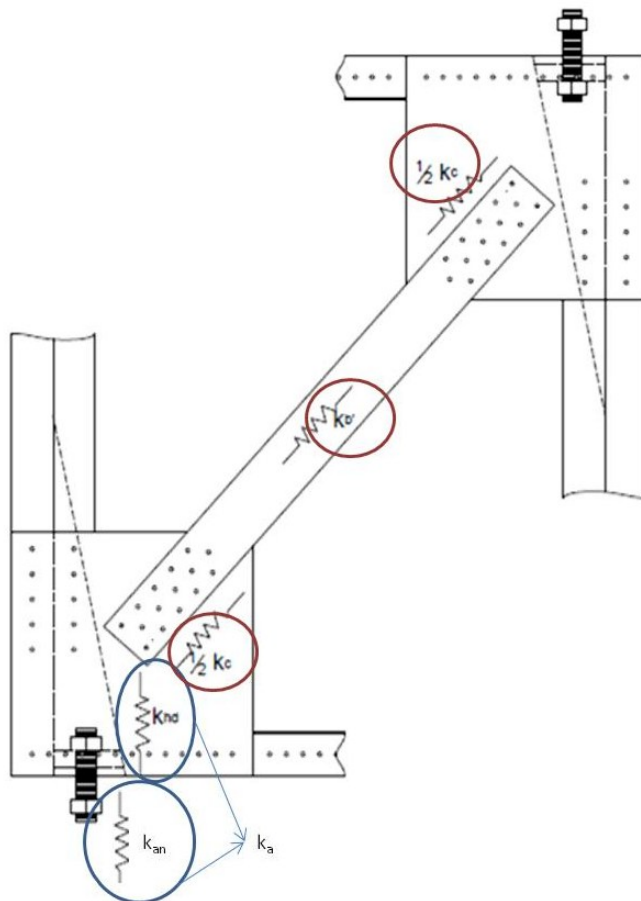


Figure 4.11 Contributions in terms of stiffness.

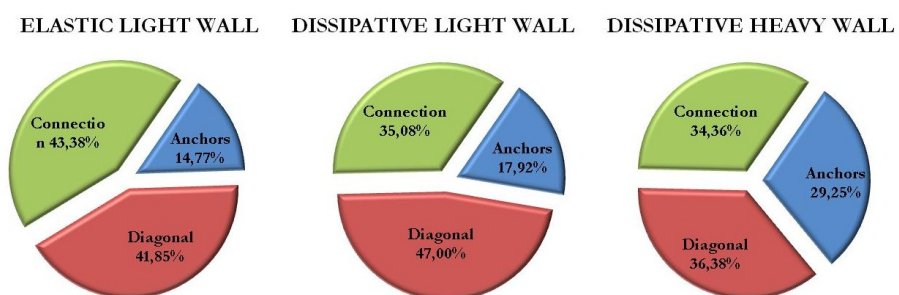


Figure 4.12 Percentage values of stiffness contributions.

5 EXPERIMENTAL ACTIVITY

In this chapter the results of a wide experimental campaign carried out in the framework of the research project ReLUIIS-DPC 2010-2013 were discussed. The experimental tests have been performed at the Dist Laboratory (Department of Structures for Engineering and Architecture, Naples), of the University of Naples Federico II.

5.1 GENERAL

In the context of ReLUIIS-DPC project, AT-2 “Innovations in codes and technologies for seismic engineering”, Line 2.1 “Seismic design of new constructions”, Task 2.1.2 “Steel structures”, the Research Unit n.3 UNINA-ARCH is involved in the issue of “CFS structures and members”.

The research activities of this Research Unit are focused on the study of the seismic behaviour of CFS diagonal strap braced walls. To this end, the experimental program consists of full-scale experimental tests on walls to investigate the global behaviour and small-scale experimental tests on materials, simple mechanical joints and connections to investigate the influence of the local behaviour on the global seismic behaviour. The final scope of the experimental campaign is to provide appropriate design criteria for CFS structures to be introduced in Italian seismic code.

For each of the three CFS walls configurations (WLE, WLD, WHD) previously illustrated in Chapter 4, two monotonic tests and two cyclic tests were performed. In addition, 28 shear tests on diagonal connections and 8 shear tests on simple mechanical joints adopted for these connections were provided. In the end, 17 tensile tests on materials were performed.

In order to assess the effects of the "strain-rate", both the tests on connections and on materials were performed with two different rates: 0.05mm/s and 50mm/s.

In Table 5.1 the experimental program is presented, with details of the tests already carried out and the tests that must be still done.

Table 5.1 Experimental tests program.

Material	S350-1.5			S235-2.0				S350-1.5			
n. tests	3a	3b		2a	3b			3a	3b		
Joints	SLE			SLD				SHD			
n. tests	3b			3b				2b			
Connections	CLE			CLD				CHD			
Config.	1		1	2	3	4	1	2	3	4	
n. tests	3a	3b	3a	3b	2b	2b	2b	1a	3b	2b	2b
Walls	WLE			WLD				WHD			
n. mon tests	2			2				2			
n. cyc tests	2			1 + 1*				2*			

*: test to be done; b: test rate 0.05 mm/s; a: test rate 50 mm/s.

5.2 TESTS ON MATERIALS

The tensile tests on materials were performed on all steel types and thicknesses used for the structural profiles of the walls:

- Steel S235, thickness 2.0 mm (S235-2.0);
- Steel S350GD+Z, thickness 1.5 mm (S350-1.5);
- Steel S350GD+Z, thickness 3.0 mm (S350-3.0).

For each type and thickness of steel were performed 6 tests, including 3 at low speed (0.05 mm/s) and 3 at high-speed (50 mm/s).

The following figure shows the number of tests carried out for each type of specimen.

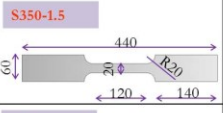
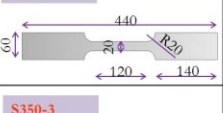
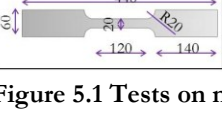
Specimen [mm]	Wall	Steel	Thickness [mm]	Displacement rate [mm/s]	n. of tests
 S350-1.5	WLE WLD (frame)	S350GD+Z	1.5	0.05	3
				50	3
 S235-2	WLD (bracing) WHD (bracing)	S235	2.00	0.05	3
				50	2
 S350-3	WHD (frame)	S350GD+Z	3.00	0.05	3
				50	3

Figure 5.1 Tests on materials.

5.2.1 Description of specimens and testing system

The specimens are in accordance to the European Standard EN-10002-1: 2001 (Annex B), replaced by EN ISO 6892-1:2009 (Annex B) "Metallic materials - Tensile testing - Part 1: Method of test at room temperature". In particular, in Appendix B, "Types of test pieces to be used for thin products: sheets, strips and flats between 1 mm and 3 mm thick" are provided requirements on the shape and size of the specimens, as shown in the following figure.

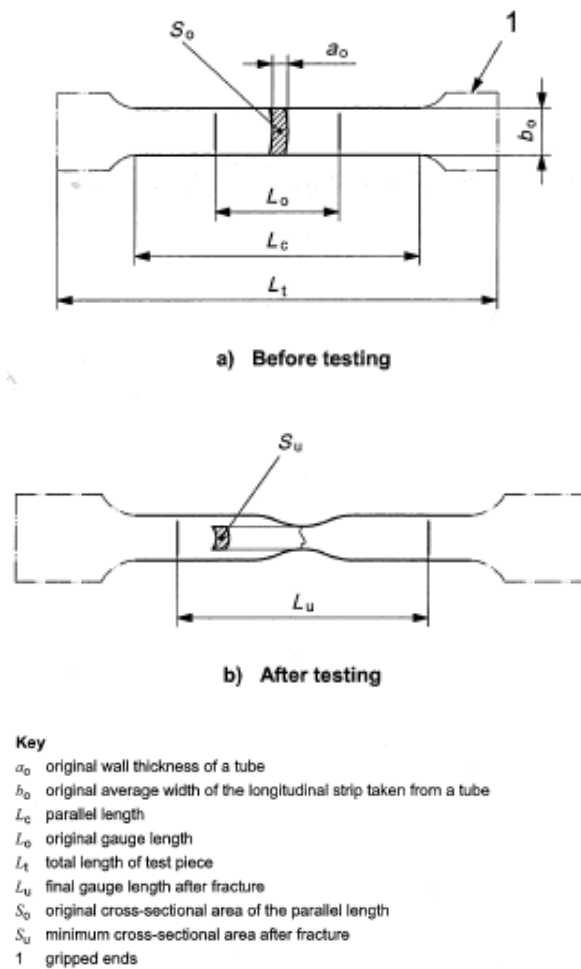


Figure 5.2 Shape and size of specimens (EN ISO 6892-1 - Annex B).

Generally, the specimen has gripped ends which are wider than the parallel length. The parallel length L_C shall be connected to the ends by means of transition curves with a radius of at least 20 mm. The width of these ends should be greater than $1.2 b_0$, where b_0 is the original width. The parallel length shall be:

$$L_C = L_0 + 2b_0 \quad (5.1)$$

where L_0 is the original gauge length.

The cross section of the specimen can be circular, square or rectangular. The initial cross section area S_0 shall be calculated on the basis of the measured dimensions of the specimen during the tests.

In EN ISO 6892-1:2009 Annex B are prescribed three different non-proportional specimen geometries.

Table B.1 — Dimensions of test pieces

Dimensions in millimetres

Test piece type	Width b_0	Original gauge length L_0	Parallel length L_C		Free length between the grips for parallel sided test piece
			Minimum	Recommended	
1	$12,5 \pm 1$	50	57	75	87,5
2	20 ± 1	80	90	120	140
3	25 ± 1	50 ^a	60 ^a	—	Not defined

^a The ratio L_0/b_0 and L_C/b_0 of a type 3 test piece in comparison to one of types 1 and 2 is very low. As a result the properties, especially the elongation after fracture (absolute value and scatter range), measured with this test piece will be different from the other test piece types.

Figure 5.3 Dimension of specimen (EN ISO 6892-1 - Annex B).

For this experimental activity the specimens used were referred to the second type in table B.1 of EN ISO 6892-1:2009 Annex B.

The specific dimensions of specimens are showed in Fig. 5.4.

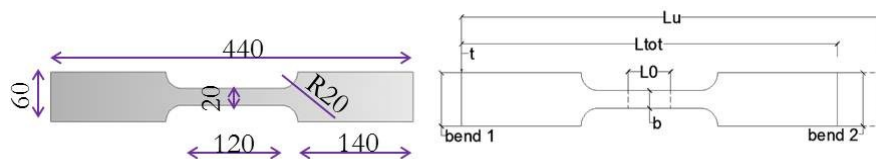


Figure 5.4 Dimension of tested specimen.

Tensile tests on materials were performed to determine the engineering stress-strain response of the material, for each of the tested profiles, with

the universal testing machine MTS 810 series (Fig.5.5) at the laboratory of the DIST. The deformations are read by means of strain gauges positioned near the original gauge length L_0 .

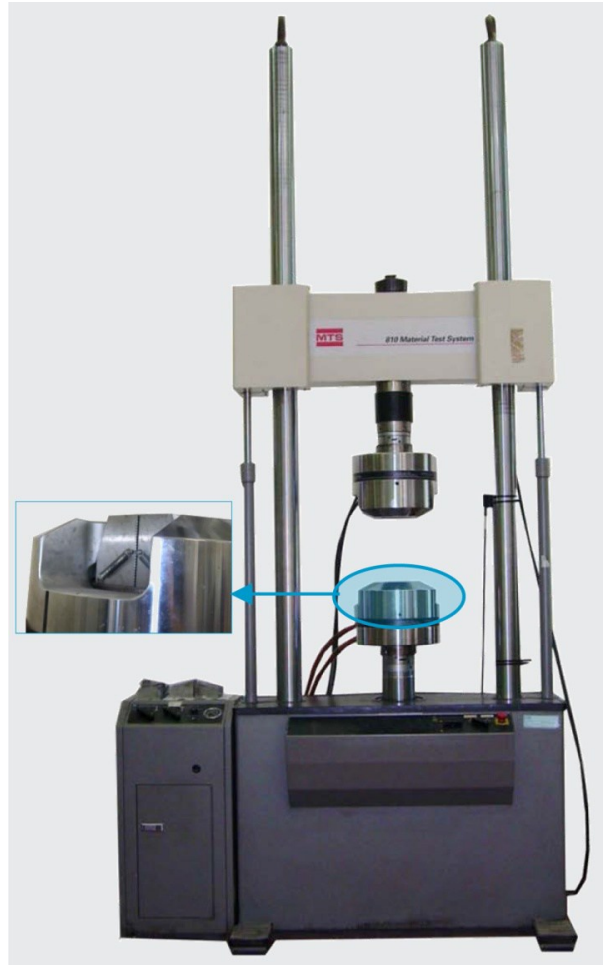


Figure 5.5 Universal testing machine MTS 810 series.

5.2.2 Test results and discussion

The test results are illustrated in terms of stress-strain (σ - ϵ) in Fig. 5.6.

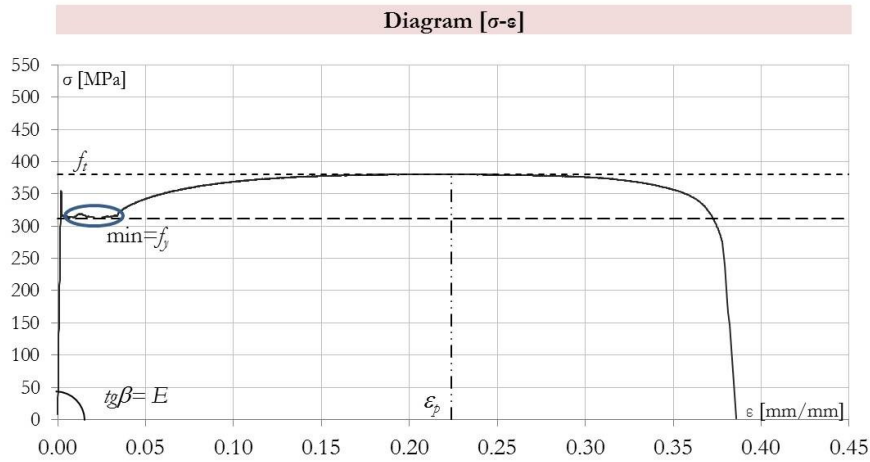


Figure 5.6 Material test results in terms of σ - ϵ .

$$\sigma = F/A \quad (5.2)$$

σ is the stress parameter, where F is the force applied by the MTS machine;

ϵ is the strain parameter;

f_t is the maximum stress observed during the test;

ϵ_p is the strain corresponding to f_t ;

f_y is the yield stress of the material, corresponding to the lowest value of the stress when the yielding occurs;

E is the Young's modulus or modulus of elasticity.

Table 5.2 Material test results.

Specimen	f_{ym} [MPa]	f_{tm} [MPa]	E [MPa]	ϵ_p [%]	f_{ym} [MPa]	f_{tm} [MPa]	E [MPa]	ϵ_p [%]
	$v = 0.05 \text{ mm/s}$				$v = 50 \text{ mm/s}$			
S235-2.0	301.6	366.4	198560.13	0.21	322.6	389.3	198494.99	0.16
S350-1.5	355.4	408.9	211544.27	0.21	379.9	430.3	185395.09	0.24
S350-3.0	364.3	425.1	201264.56	0.18	387.4	454.2	206411.47	0.15

A summary of the results is provided in Table 5.2, where for each type of test are reported the average values of the yield strength ($f_{y,m}$) and ultimate strength ($f_{t,m}$), the Young's modulus E , and the maximum strains for both test rates. In Appendix A of this dissertation "Tests on materials and components" a specific datasheet is given for each test.

For steel S235 the experimental values show an increase of the yield strength and ultimate strength respectively of 22% and 10% compared to the nominal values ($f_y = 235$ MPa and $f_t = 360$ MPa).

For steel S350GD+Z, in case of the specimen with 1.5 mm thickness, there is an increase of 2% of the yield strength ($f_y = 350$ MPa) and a reduction of 3% of the ultimate strength ($f_t = 420$ MPa), while in the case of the specimen with 3.0 mm thickness, both the yield strength and ultimate strength showed an increase respectively of 4% and 1%.

From the comparison of the obtained values for both test rates, it can be noted a moderate influence of the "strain-rate" effect, and in particular the increase of yield and ultimate strength between 5% and 7% and a reduction of the maximum deformation of 33% and 18% respectively for the 2 mm thickness S235 steel and 3 mm thickness S350 steel and an increase of 7.6% for 1.5 mm thickness S350 steel, with the increasing of test rate (Fig. 5.7).

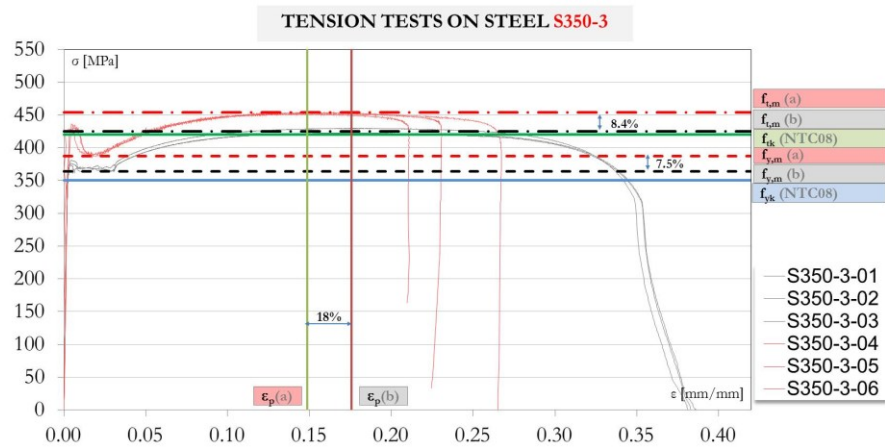


Figure 5.7 Influence of test rate on stress-strain values.

5.3 TESTS ON COMPONENTS: SIMPLE JOINTS

The shear tests were performed on all types of simple mechanical joints used in the walls for diagonal to gusset plate connections. A complete description of the geometrical properties, materials, screws and number of tests performed for each specimens is provided in Fig. 5.8.

For simple joints were performed only low-rate tests (0.05 mm/s).

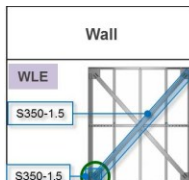
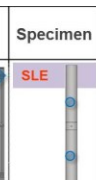


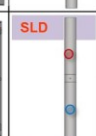

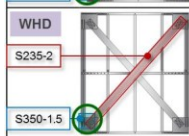
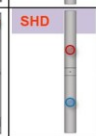


Wall	Specimen	Steel	Thickness [mm]	Screw	Displacement rate [mm/s]	n. Test	
	SLE	S350GD+Z	1.5	 Tecfi AB 04 63 040 Diameter = 6.3 mm	0.05	3	
	SLD	S235	2.0	 Tecfi CI 01 48 016 Diameter = 4.8 mm	0.05	3	
	SHD	S235	2.0	 Tecfi AB 04 63 040 Diameter = 6.3 mm	0.05	2	
		S350GD+Z	1.5				

Figure 5.8 Specimens properties for tests on mechanical joints.

5.3.1 Description of specimens and testing system

The test specimens are obtained by connecting two steel plates through a single screw. The specimens were designed according to the provisions of ECCS "The testing of connections with mechanical fasteners in steel sheeting and sections" that defines the position of the single screw in the specimens.

In the case of use of screws with a diameter $d \leq 6.5\text{mm}$, this provisions requires that (Fig. 5.9):

- the width of the connected plates must be $w = 60\text{ mm}$;
- the original gauge length must be $L_0 = 150\text{mm}$;
- the distance, in the direction of the load, from the center of the screw to the adjacent edge must be $e_1 = 20\text{mm}$.

In addition, the provisions permit the use of only one LVDT for the measurement of small displacements, provided that that the transducer is positioned on the central axis of the specimen.

In Figure 5.9 are shown the provisions of ECCS and the tested specimen sizes. Also in this case the testing machine is the MTS 810 series of the DIST laboratory.

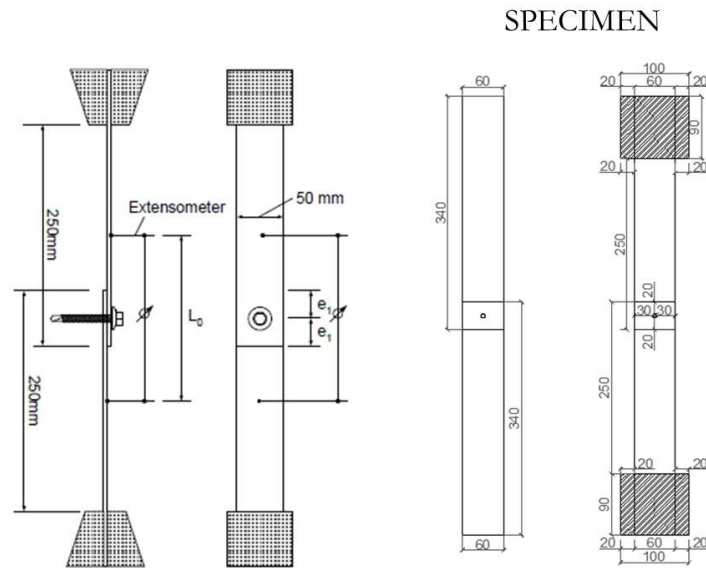


Table 3.1: Specimen dimensions

Fastener diameter d [mm]	Specimen [mm]			
	w	L_0	e_1	p_1
$\leq 6,5$	60	150	30	60
$> 6,5$	$10 \cdot d$	$20 \cdot d + 30$	$5 \cdot d$	$10 \cdot d$
Tolerance	± 2	± 6	± 1	± 1

Figure 5.9 Specimens for tests on mechanical joints.

5.3.2 Test results and discussion

Table 5.3 shows the results obtained for each type of simple mechanical joint in terms of average ultimate strength ($F_{t,m}$), average stiffness ($k_{e,m}$) and collapse mechanism, and the force-displacement curves are shown in Fig. 5.10. In this case the evaluation of the stiffness was made considering the first significant linear portion of the response curve. Table 5.3 contains also the results of the theoretical prediction: for the

three types of joint specimens the joint resistance is associated to the one associated to the bearing failure. In Appendix A of this dissertation "Tests on materials and components" a specific datasheet is given for each test.

Table 5.3 Joint test results.

Specimen		$F_{t,m}$ [kN]	$k_{e,m}$ [kN/mm]	Collapse Mechanism
SLE	exp	7.6	3.5	TI + P
	theor	6.8	-	B
SLD	exp	6.5	3.4	SH
	theor	5.2	-	B
SHD	exp	8.9	4.6	TI + P
	theor	5.8	-	B

TI: screw tilting; P: screw pull-out; B: bearing of plate; SH: shear of fastener.



Figure 5.10 Collapse mechanisms for tests on mechanical joints.

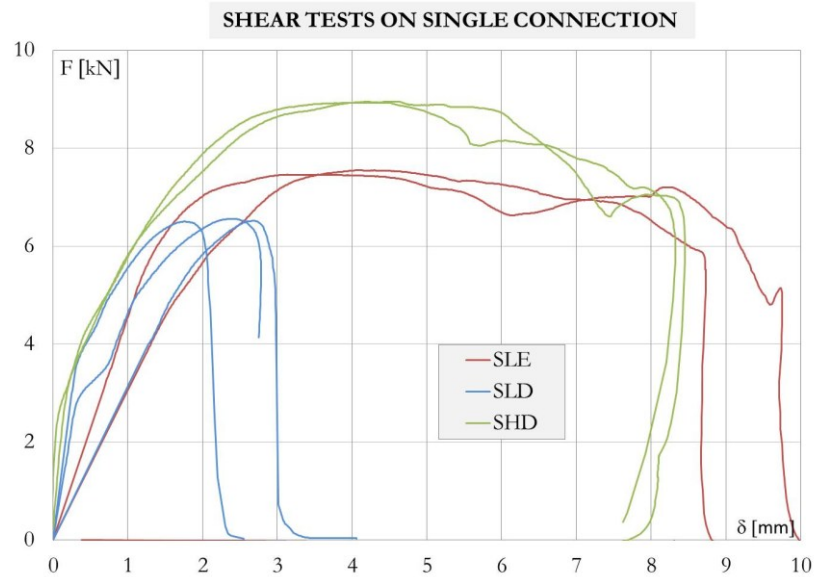


Figure 5.11 Comparison of curves for tests on mechanical joints.

5.3.3 Comparison and concluding remarks

From the analysis of the experimental responses it can be derived that in terms of strength and deformation capacity of the best response is obtained for the joint SHD.

Even SLE specimens are characterized by a good deformation capacity, but with a lower resistance with respect to SHD.

SLD joints exhibit a lower resistance and a very limited deformation capacity.

These differences can be explained considering the different collapse mechanisms observed in the three joint types: tilting and bearing for specimens SHD and SLE, shear failure of the screw for specimens SLD.

5.4 TESTS ON COMPONENTS: CONNECTIONS

5.4.1 Description of specimens and testing system

The shear tests were performed on all types of diagonal to gusset plate connections used in the walls.

The specimens were designed according to the provisions of Eurocode 3 Part 1-3 (UNI ENV 1993-1-3) in which are provided details on the position of the screws in terms of distances from edges and mutual distances.

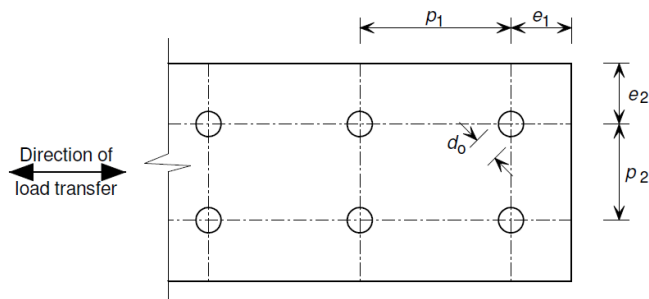


Figure 5.12 Connections distances in EC3 Part 1-3.

Table 8.2 of Eurocode 3 Part 1-3 provides the validity range of the values in the figure that are:

- $e_1 \geq 3d$;
- $e_2 \geq 1.5d$;
- $p_1 \geq 3d$;
- $p_2 \geq 3d$;
- with $3.0 \text{ mm} \leq d \leq 8.0 \text{ mm}$.

Where:

- e_1 = the end distance from the centre of the fastener to the adjacent end of the connected part in the direction of load transfer;
- e_2 = the edge distance from the centre of the fastener to the adjacent edge of the connected part in the direction perpendicular to the direction of load transfer;
- p_1 = the spacing centre-to-centre of fasteners in the direction of load transfer;
- p_2 = the spacing centre-to-centre of fasteners in the direction perpendicular to the direction of load transfer;

d = the nominal diameter of the fastener.

The connections of the dissipative walls have been designed so that the expression (3.7) of this dissertation is satisfied.

$$\frac{A_{res}}{A} \geq 1.1 \cdot \frac{\gamma_{M2}}{\gamma_{M0}} \cdot \frac{f_{yk}}{f_{tk}} \quad (5.3)$$

The connection of the dissipative walls were designed so as to prevent the collapse of net area of the section, that is a fragile collapse mechanism.

In addition, a complementary experimental study were conducted, with the aim to investigate the influence of different geometrical arrangement of the screws. To this end, three additional configurations of specimens have been defined, each one corresponding to a different section weakened by holes.

In particular, the following configurations were defined:

- Configuration n.1: $A_{n1} < A_{n2}$ with staggered spaced screws;
- Configuration n.2: $A_{n1} < A_{n2}$ with aligned screws;
- Configuration n.3: $A_{n1} = A_{n2}$ with staggered spaced screws;
- Configuration n.4: $A_{n1} > A_{n2}$ with staggered spaced screws.

where:

A_{n1} = minimum net area obtained by considering the cross sections perpendicular to the axis of the diagonal;

A_{n2} = minimum net area obtained by considering the cross sections obtained from a broken line (see Fig. 5.13 and 5.14).

In Fig. 5.13 and Fig. 5.14 the tested configurations are shown.

Also for connections, as for materials and for simple joints, the testing machine is the MTS 810 series of the DIST laboratory.

Two LVDT have been used because the specimen is characterized by two connections. For each configuration both low speed (0.05 mm/s) and high-speed (50 mm/s) rate tests were carried out. A complete description of screws configurations, materials and number of tests performed for each specimens is provided in Fig. 5.15.

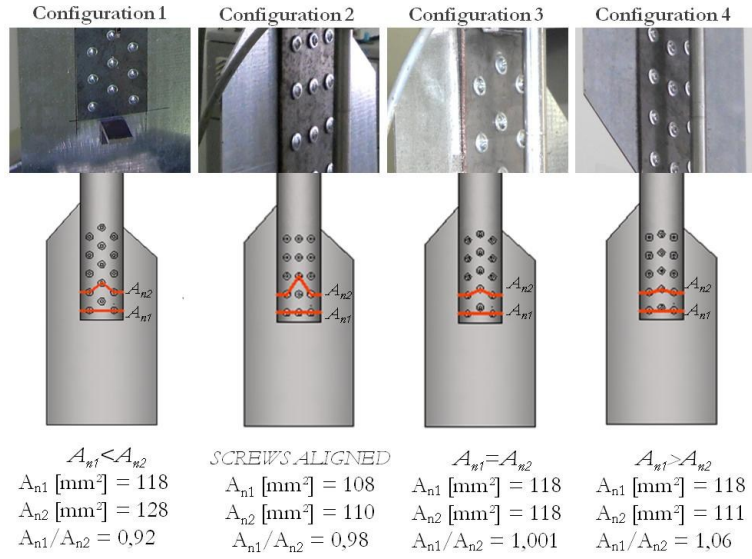


Figure 5.13 Tested configurations of connections for WLD.

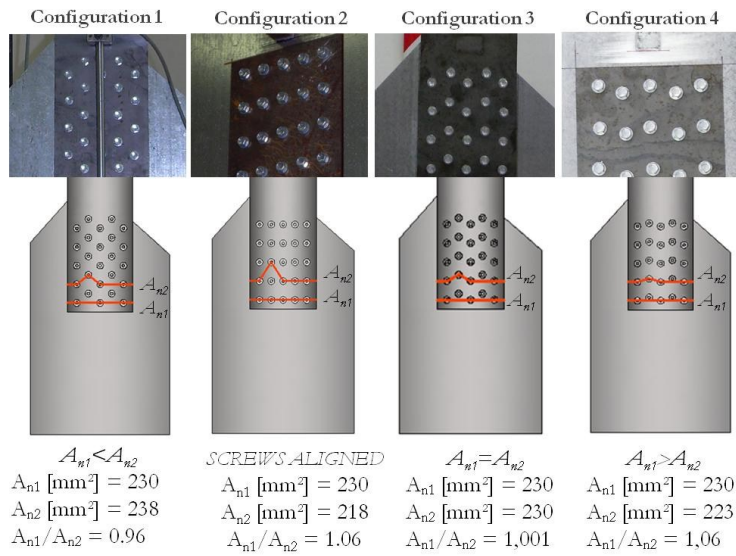


Figure 5.14 Tested configurations of connections for WHD.


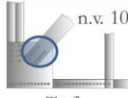





Wall	Connections	Configuration	Steel grade	Displacement rate [mm/s]	n. Tests
WLE 	 Tecfi AB 04 63 040		S350GD+Z 1.5 mm	0.05	3
				50	3
WLD 	 Tecfi CI 01 48 016	1	S235 2.0 mm	0.05	3
		2		50	3
		3	S350GD+Z 1.5 mm	0.05	2
		4		0.05	2
WHD 	 Tecfi AB 04 63 040	1	S235 2.0 mm	0.05	3
		2		50	1
		3	S350GD+Z 1.5 mm	0.05	2
		4		0.05	2

Figure 5.15 Specimens properties for tests on connections.

5.4.2 Test results and discussion

Table 5.4 shows the results obtained for each type of connection in terms of average ultimate strength ($F_{t,m}$), average stiffness ($k_{e,m}$) and observed collapse mechanism.

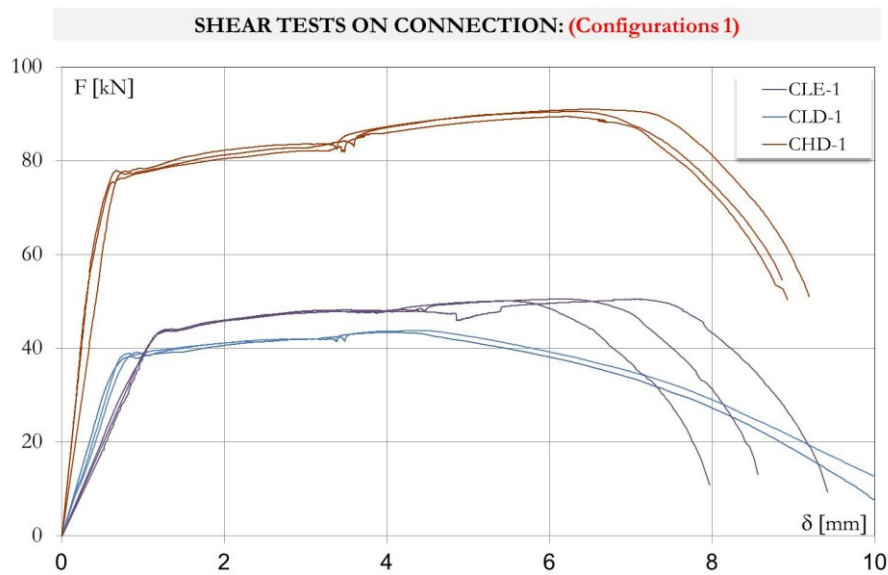
The table also provides the collapse mechanism of the theoretical prediction determined starting from the mechanical properties measured in the tests on materials. In Appendix A of this dissertation "Tests on materials and components" a specific datasheet is given for each test.

From the comparison of the response curves of the tests on connections representative of the real wall configuration (configuration n.1), it can be noted that the best response in terms of strength and stiffness was exhibited by the connection specimens CHD-1, while the connection specimens CLD-1 and CLE-1 show a lower resistance and a lower stiffness (Fig. 5.15). All the three types of specimens are characterized by a good deformation capacity.

Table 5.4 Connection test results.

Specimen		v [mm/s]	$F_{t,m}$ [kN]	$k_{e,m}$ [kN/mm]	$k_{e,m}/n$ [kN/mm]	Collapse Mechanism
CLE-1	exp	0.05	50.4	38.3	3.8	TI + NA
		50.0	54.9	-	-	TI + NA
	theor		46.2	-	-	NA
CLD-1	exp	0.05	43.8	63.1	4.2	TI + NA
		50.0	47.9	-	-	TI + NA
	theor		43.0	-	-	NA
CLD-2	exp	0.05	44.2	59.1	3.9	TI + NA
CLD-3	exp	0.05	44.4	56.5	3.8	TI + NA
CLD-4	exp	0.05	43.6	61.8	4.1	TI + NA
CHD-1	exp	0.05	90.3	166.4	6.6	TI + NA
		50.0	95.1	-	-	TI + NA
	theor		87.0	-	-	AN
CHD-2	exp	0.05	84.4	134.7	5.4	TI + NA
CHD-3	exp	0.05	84.9	113.71	4.5	TI + NA
CHD-4	exp	0.05	84.4	178.59	7.1	TI + NA

n: screw number; TI: screw tilting; NA: net area collapse.

**Figure 5.16 Comparison of the response curves for configuration n.1.**

From the analysis of the experimental response for the different geometric configuration of the screws, it can be noted that there are

significant variations of resistance ($\leq 7\%$) and stiffness ($\leq 22\%$), and that configurations n.1 have the greater deformation capacity. Fig. 5.17 shows the experimental results of the test for CLD and CHD specimens.

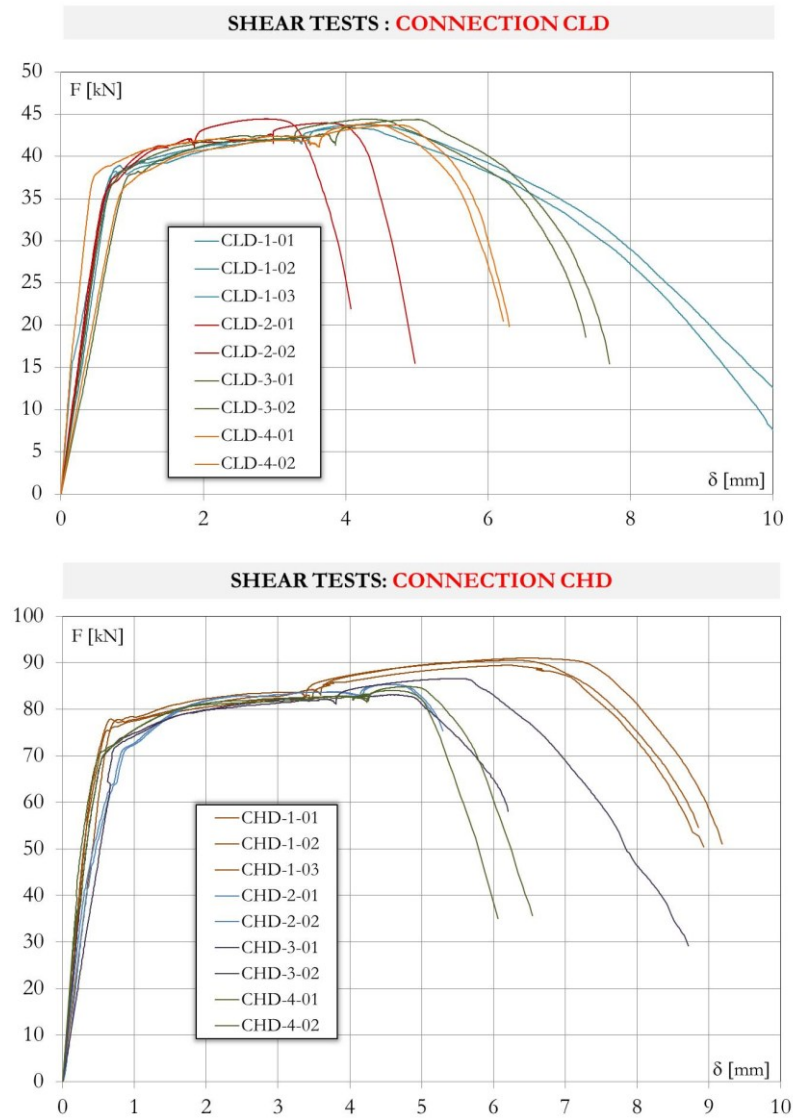


Figure 5.17 Comparison of the response curves for CLD and CHD.

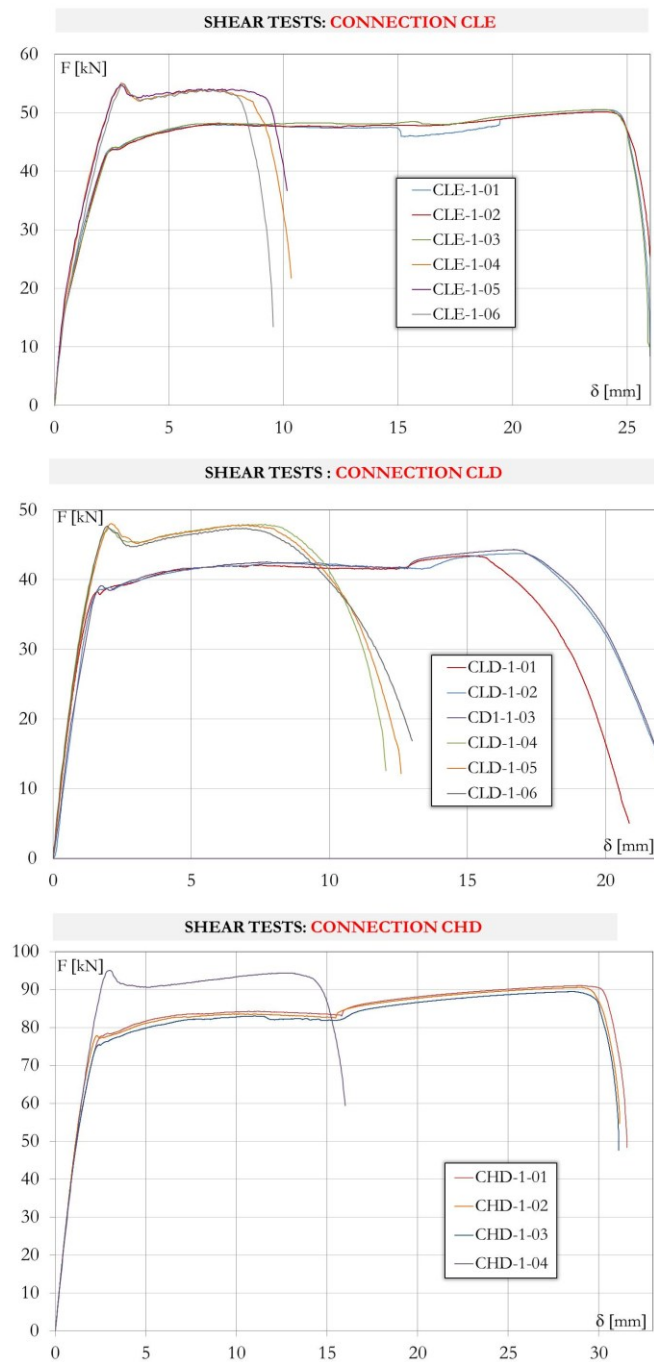


Figure 5.18 Comparison of the response curves in terms of test rate.

The "strain-rate" effects can be analyzed through the examination of Fig.5.18, which presents the experimental curves of the connection configuration n.1 for all the wall types, obtained for the two different test rates (low speed = 0.05 mm/s and high-speed = 50 mm/s).

The experimental evidence, confirmed also in the other connection tests (configurations n.2-3-4), shows that increasing the test rate there is an increase of resistance from 5% to 8%, a significant reduction of the deformation capacity and a slight increase in stiffness.

5.4.3 Comparison and concluding remarks

The connection specimens of the dissipative walls have been designed so that the collapse of the gross area section of the connection plate occurs before than the collapse of the net area section of the brace, satisfying the expression (3.7) of this dissertation.

The theoretical predictions about the collapse mechanism shows, in some cases, that the expression (3.7) that is the same of (5.3), on the basis of the results of the tests on materials, is not satisfied.

In the end, the experimental evidence demonstrates that the theoretical prediction is not in line with the design values, due to the uncertainty of the material response. This consideration can be made because the experimental evidence (Fig.5.19) showed that the collapse mechanism obtained is always the collapse of the net area.

For CLD connections, only for the configuration n.2, the theoretical prediction is in line with the collapse mechanism actually observed, while for CHD connections, this correspondence between theoretical prediction and experimental evidence occurs for both configuration n. 1 and n.2.

In all the other cases, the theoretical prediction is not the real observed collapse mechanism. This problem occurs because the expression (3.7) or (5.3) was recognized to be calibrated for stress values that slightly exceed the yield strength, but in case of large deformations, due to the hardening of the material, the stress values have a large increase, resulting in the net area collapse, as observed.

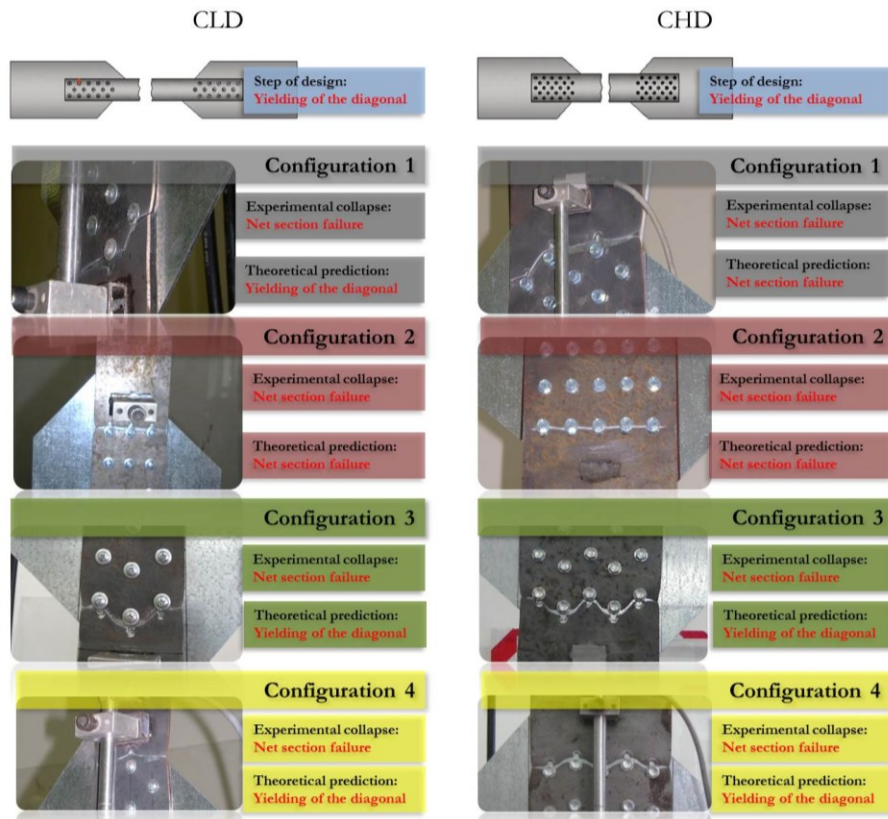


Figure 5.19 Experimental vs theoretical collapse mechanisms.

5.5 TESTS ON WALLS

The core of the research activities for the study of the seismic behaviour of CFS diagonal strap braced walls has been the full-scale experimental tests on walls to investigate the global behaviour under seismic actions.

For each of the three CFS wall configurations (WLE, WLD, WHD) previously illustrated in Chapter 4, two monotonic tests and two cyclic tests have been planned, so 12 experimental tests.

At the present moment, the experimental program is going to be completed. Three cyclic tests have to be still done, one for each wall configuration.

Fig.5.20 shows the experimental program and in red are highlighted the tests to be done.

Wall	Typology of Test	n. Tests
<div>WLE</div> <div>S350-1.5</div> <div>S350-1.5</div>	Monotonic Tests Loading protocol Displacement rate=0.1mm/s Frequency=10Hz Cyclic Tests Loading protocol (modified CUREE) Displacement rate= 0.5mm/s up to 9.97mm Displacement rate= 2.0mm/s Frequency=10Hz	<div>2</div> <div>1</div> <div>1</div>
<div>WLD</div> <div>S235-2</div> <div>S350-1.5</div>	Monotonic Tests Loading protocol Displacement rate=0.1mm/s Frequency=10Hz Cyclic Tests Loading protocol (modified CUREE) Displacement rate= 0.5mm/s up to 7.36mm Displacement rate= 2.0mm/s Frequency=10Hz	<div>2</div> <div>1</div> <div>1</div>
<div>WHD</div> <div>S235-2</div> <div>S350-1.5</div>	Monotonic Tests Loading protocol Displacement rate=0.1mm/s Frequency=10Hz Cyclic Tests Loading protocol (modified CUREE) Displacement rate=0.5mm/s up to 7.27mm Displacement rate= 2.0mm/s Frequency=10Hz	<div>2</div> <div>1</div> <div>1</div>

Figure 5.20 Experimental tests program on walls.

5.5.1 Test set-up

The testing system used for the full scale experimental tests is illustrated in Fig.5.21.

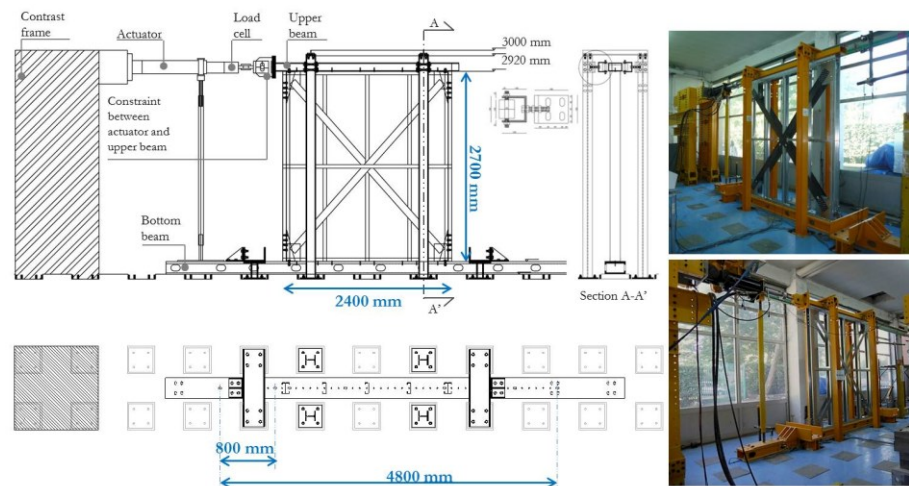


Figure 5.21 Testing system for full-scale tests on CFS walls.

The horizontal action is transmitted to the specimen through an horizontal beam connected to the top track of the wall, and the bottom track of the wall is connected to another beam that is, in turn, connected to the floor slab of the laboratory.

The connection between the wall and the beams are made by means of bolts M8 grade 8.8 distributed along the tracks with a spacing of 300 mm (shear joint) and bolts M24 grade 8.8 positioned in correspondence of the hold-down (tension joint). The loading beam is connected to the actuator by means of a particular joint, that is able to transfer to the wall only the horizontal actions and is restrained against out of plane displacements, using two supporting frames made by HEB 140 profiles, on the top of this frame there are placed some rolling devices that allows the sliding in the plane of the wall during the tests.

The horizontal load is applied by an actuator with a maximum stroke of 500 mm and a maximum load capacity of 500 kN.

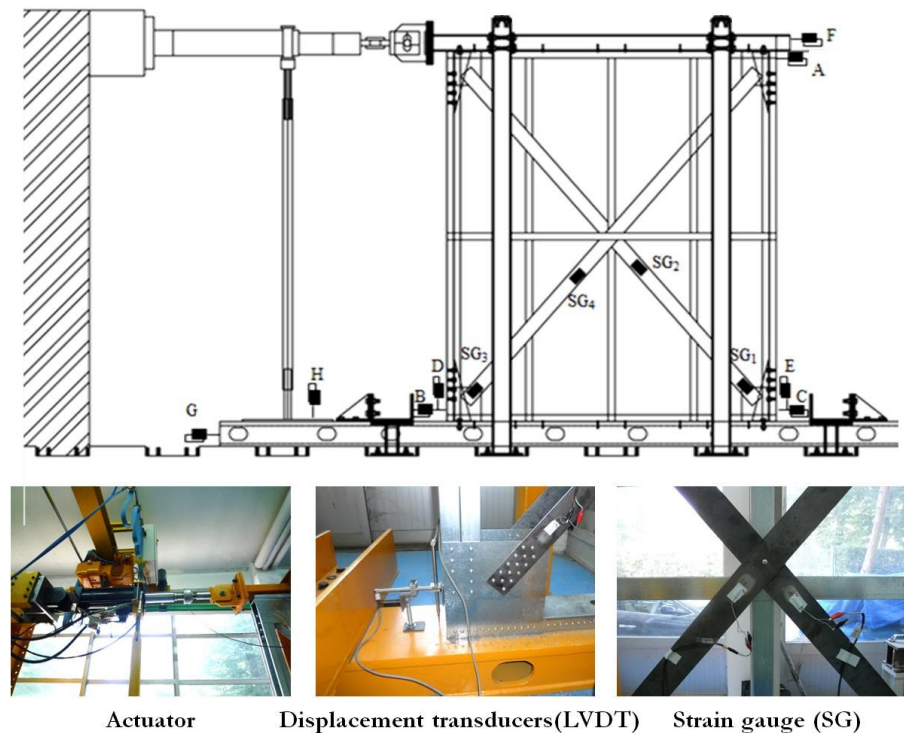


Figure 5.22 Position of measurement devices.

The horizontal displacements were measured using three displacement transducers (LVDT): one positioned on the top (A) and two at the bottom of (B and C). The vertical displacements were measured at the two end sides of the wall, using two LVDT (D and E). The local deformations of the diagonals were measured using two strain gauges (SG) for each diagonal brace, one at the connection (SG 1 and 3) and one in correspondence of the midpoint (SG 2 and 4).

Finally, some other LVDTs were positioned in correspondence of the base beam and the loading beam in order to verify the correct behavior of the testing system.

5.5.2 Monotonic Tests

The monotonic tests were composed of two different phases: the first of pull and the second of push. After each of the two phases there was an unloading phase with the repositioning of the wall in the initial condition (Fig.5.23). The tests were performed with imposed displacements at a constant rate of 0.10 mm/s. The CFS walls were tested until the collapse or until the attainment of the maximum stroke of the actuator (approximately ± 240 mm or 9% of the drift).

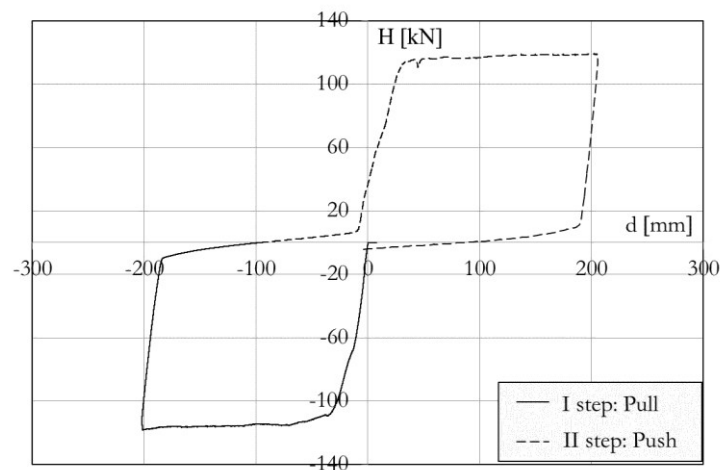


Figure 5.23 Loading protocol for monotonic tests.

A typical response curve of monotonic tests in terms of applied force and displacement measured at the top of the wall is shown in Fig.5.24.

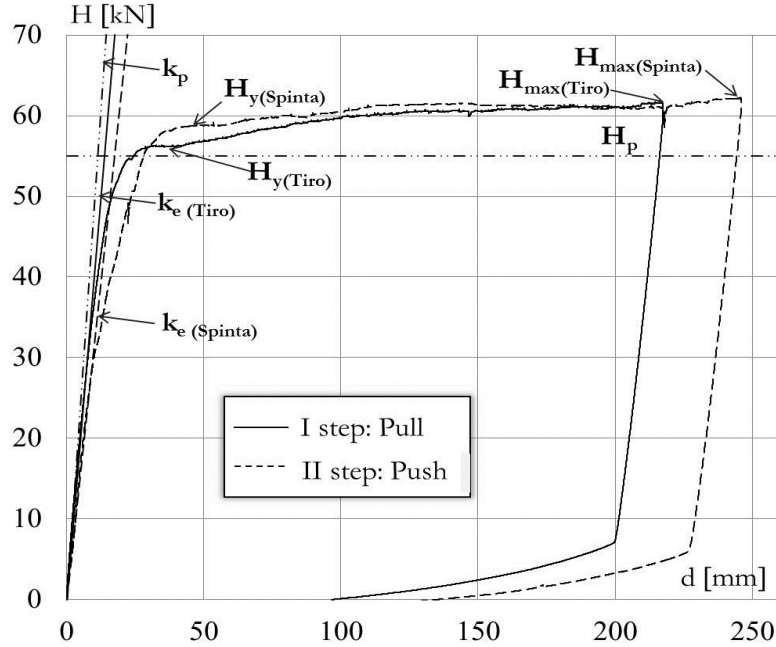


Figure 5.24 Force-displacement response curve for monotonic tests.

The parameters used to assess the structural response are pointed out:

H_y is the yield strength;

H_{max} is the resistance corresponding to the maximum value of the experimental curve;

k_e is the elastic stiffness in correspondence of 40% of the maximum strength.

Following the recommendation of ASTM E2126 the elastic stiffness is given by the following expression:

$$k_e = \frac{H_{0.40}}{d_{0.40}} \quad (5.4)$$

where:

$H_{0.40} = 0.4H_{max}$;

H_{max} = maximum resistance reached by each specimen during testing, regardless of the failure mode;

$d_{0.40}$ = measured displacement at $H_{0.40}$.

The experimental values are then compared with the theoretical prediction of the resistance values of H_p and stiffness k_p determined on the basis of the values of the mechanical properties measured in the tests on the material and on the connections by applying the expression used in Chapter 4.

5.5.2.1 Test results and discussion

The results of the monotonic tests are listed in Table 5.5.

Table 5.5 Results of monotonic tests on walls.

Specimen		H_y [kN]	H_{max} [kN]	K_e [kN/mm]	Collapse Mechanism
WLE-M1	Pull	64.9	66.3	3.5	NA
	Push	65.6	66.6	2.7	NA
	Theor	62.0	61.4	4.4	NA
WLE-M2	Pull	64.1	65.0	4.3	NA
	Push	61.1	63.0	4	NA
	Theor	62.0	61.4	4.4	NA
WLD-M1	Pull	56.7	61.7	4.0	DY
	Push	58.8	62.3	3.2	DY
	Theor	55.0	57.6	4.9	DY
WLD-M2	Pull	56.0	64.2	4.3	DY
	Push	54.5	56.5	3.2	DY
	Theor	55.0	57.6	4.9	DY
WHD-M1	Pull	110.3	116.9	6.2	DY
	Push	107.8	119.3	3.6	DY
	Theor	110.0	115.5	6.6	DY
WHD-M2	Pull	109.5	118.4	5.9	DY
	Push	114.2	119.3	2.8	DY
	Theor	110.0	115.5	6.6	DY

NA: net area collapse; DY: diagonal brace yielding.

It can be observed that the maximum experimental resistance recorded in the two phases of push and pull are almost identical, with differences contained within 3%. Furthermore, the experimental yield strength are in line with the predicted values, with a maximum variation of 9%.

The stiffness in the phase of push shows reduction up to 50%, due to the partial damaging of some elements of the wall during the previous phase of pull. This phenomenon does not occur in the second test on the Elastic Light Wall, indeed the stiffness in the two steps are almost identical (difference of 7%) and are in line with the predicted value.

Monotonic tests on Dissipative Heavy Walls have not been performed on nominally identical walls. During the first test (WHD-M1), both in push and pull phase, there was registered a temporary loss of strength due to local buckling of the tracks in the zones subjected to maximum compression, those adjacent to the reinforced tracks (Fig.5.25 A-C). In order to prevent this local buckling phenomena observed in the first test, in the second wall (WHD-M2) the reinforcement has been extended to the entire length of the tracks (Fig.5.25 B). The experimental response of the reinforced wall demonstrated the effectiveness of the intervention (Fig.5.25 D).

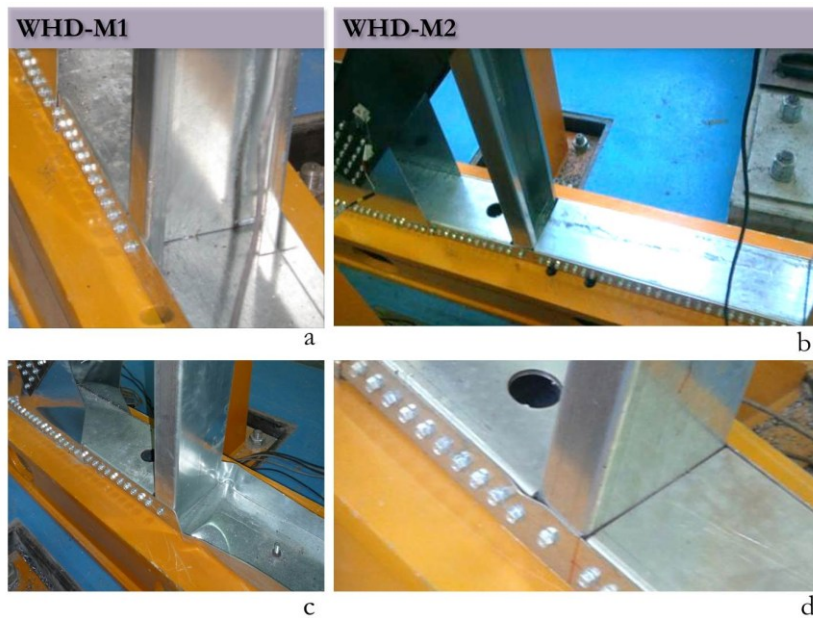


Figure 5.25 Local buckling in the tracks and reinforced tracks.

However, the values of strength and stiffness recorded in the two experimental tests were almost identical (Fig.5.26), with differences of respectively 1% and 3%. This shows how the local buckling, which occurs in the tracks of the first wall, was a transient phenomenon that has affected the global response in a limited manner.

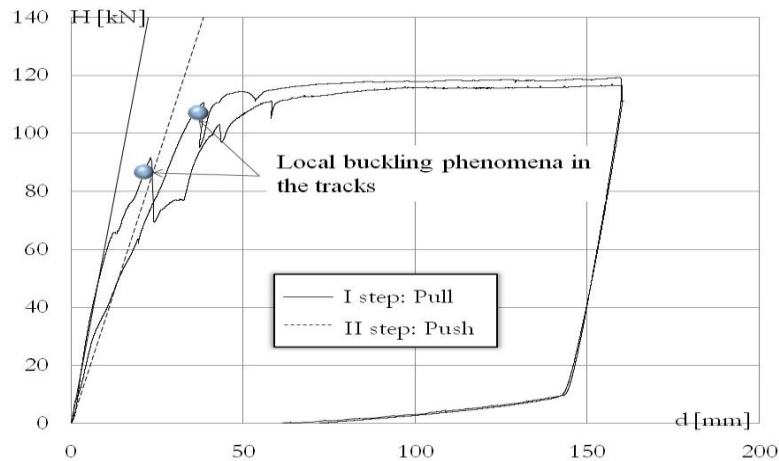


Figure 5.26 Comparison of WHD-M1 and WHD-M2 responses.

5.5.2.2 Comparisons and Concluding Remarks

In the Elastic Light Walls (WLE) the collapse mechanism observed in the two tests is the net area failure of the diagonal brace, that is the same observed in the tests on connections.

In Dissipative Walls (WLD and WHD) the collapse mechanism observed is the yielding of the diagonal without reaching the failure, for the maximum displacements achieved compatibly with the stroke capacity of the actuator. The displacement of the wall is far better than the 2.5% drift, that is considered the limit beyond which the wall lost its load-bearing capacity.

For Dissipative Walls there is no compliance with the collapse mechanism observed in the connections, such phenomenon appears to be explained by the fact that the deformation recorded in the plate are significantly larger than those recorded in the diagonal, and due to the hardening of the material, the stress in the plate is larger than the stress in the diagonal, and so it occurs the failure of the net area.

5.5.3 Cyclic Tests

For cyclic tests was adopted the loading protocol known as CUREE “Consortium of Universities for Research in Earthquake Engineering ordinary ground motions reversed cyclic load protocol” (Krawinkler et al, 2000) designed for wooden walls and adapted to the CFS walls by

Velchev et al (2010). This is a similar procedure to that covered by ASTM E2126 (2005) for the testing of light framed walls containing solid sheathing or metal framing with braces. The CUREE protocol was developed to evaluate the resistance of elements subjected to ordinary (not near-fault) earthquakes with the probability of exceedance of 10% in 50 years. The loading history of the CUREE protocol consists of initiation, primary and trailing cycles. The amplitude of the cycles was defined as a multiple of the reference deformation, defined as:

$$d = 2.667d_y \quad (5.5)$$

where d_y is the displacement at the elastic limit, evaluated from the results of the monotonic tests (AL-Kharat and Rogers, 2005/2007), in which the displacement is measured at the top of the wall, obtained by an identical specimen tested. A typical reversed cyclic displacement protocol is shown in Fig.5.27, while all the cyclic protocol used for each wall specimen are given in Appendix B.

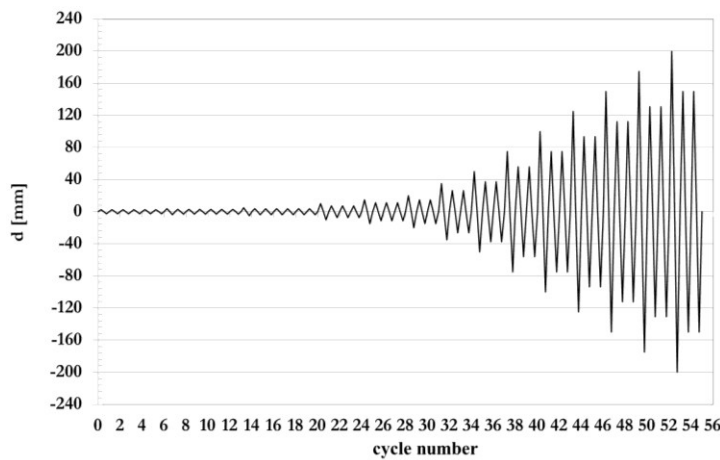


Figure 5.27 Loading protocol for cyclic tests.

Two different test rates were applied: 0.5 mm/s up to 9.97 mm for the Elastic Light Wall (WLE), 7.36 mm for the Dissipative Light Wall (WLD) and 7.27mm for the Dissipative Heavy Wall (WHD), then the test was continued until collapse at a constant speed equal to 2mm/s. This two different test rates were chosen because of the limitations of

the actuator, that was not able to apply so small displacements for test rate of 2 mm/s. The cyclic tests were performed up to a maximum displacement of ± 240 mm defined by the stroke limit of the actuator or until collapse if it occurs before.

The experimental program is going to be completed. Three cyclic tests have to be still done, one for each wall configuration.

A typical response curve of cyclic tests in terms of applied force and displacement measured at the top of the wall is shown in Fig.5.28.

The parameters used to assess the structural response are pointed out:

H_y^+ is the yield strength for push stage;

H_y^- is the yield strength for pull stage;

H_{max}^+ is the resistance corresponding to the maximum value of the experimental curve for push stage;

H_{max}^- is the resistance corresponding to the maximum value of the experimental curve for pull stage;

d_{max}^+ is the displacement corresponding to the collapse for push stage;

d_{max}^- is the displacement corresponding to the collapse for pull stage;

k_e^+ is the elastic stiffness in correspondence of 40% of the maximum strength for push stage;

k_e^- is the secant stiffness in correspondence of 40% of the maximum strength for pull stage.

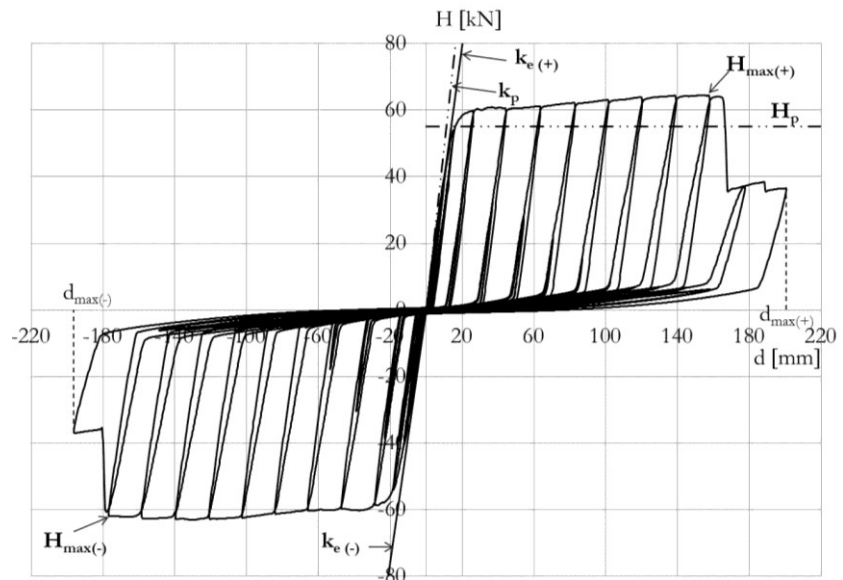


Figure 5.28 Force-displacement response curve for cyclic tests.

5.5.3.1 Test results and discussion

The results of cyclic tests are listed in Table 5.6. It can be noted that the walls exhibit experimental values of resistance and stiffness substantially similar in both load directions, with variations respectively up to 2% and 8%, confirming the symmetric behavior in the two test directions. The cyclic response is characterized by the presence of a marked pinching, which results in a strong crushing of hysteretic loops and, therefore, in a reduction of the dissipating capacity.

Table 5.6 Results of cyclic tests on walls.

Specimen		H_y [kN]	H_{max} [kN]	K_e [kN/mm]	d_{max} [mm]	Collapse Mechanism
WLE-C1	Pull	69.6	70.6	3.7	38.1	NA
	Push	68.9	69.4	3.4	35.7	NA
	Theor	62.0	61.4	4.4	-	NA
WLD-C1	Pull	58.7	63.1	3.8	196.3	NA
	Push	59.8	64.4	4.0	200.6	NA
	Theor	55.0	57.6	4.9	-	DY
WHD-C1	Pull	116.7	124.0	5.7	240.0	NA
	Push	116.0	124.2	7.7	221.0	DY
	Theor	110.0	115.5	6.6	-	DY

NA: net area collapse; DY: diagonal brace yielding.

5.5.3.2 Comparisons and Concluding Remarks

The three cyclic tests carried out showed a collapse mechanism of net area failure of the diagonal (Fig.5.29), which corresponds to the theoretical predictions only for the Elastic Light Walls (WLE).

The test WLE-C1 has been characterized by the failure of all four diagonal braces in correspondence of the central screw placed at half height of the wall which has the function to connect the diagonals to the central stud, in correspondence with the actuator stroke equal to 48.87mm.

The test WLD-C1 has been characterized by the failure of all four diagonal braces in correspondence of the net area of the connection to the gusset plate, in correspondence with the actuator stroke equal to 73.61mm.

The test WHD-C1 has been characterized by the failure of only one diagonal to gusset plate connection, in the pull phase in correspondence of the actuator stroke equal to 218.14mm.

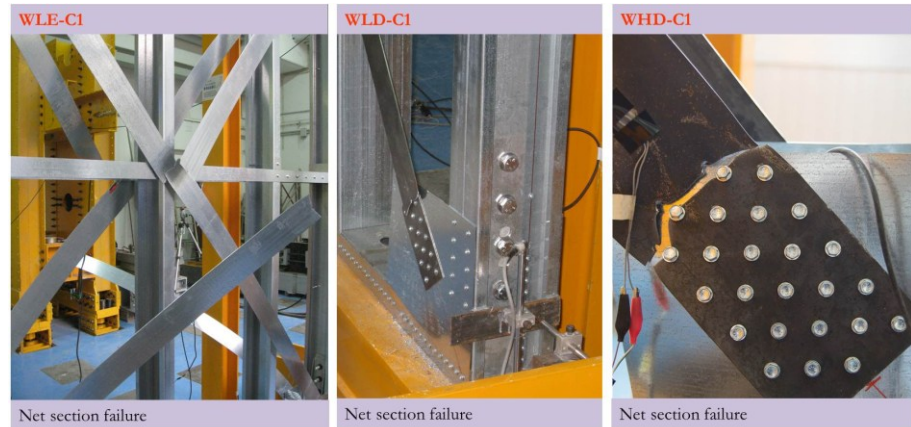


Figure 5.29 Collapse mechanisms for cyclic tests.

5.5.4 Comparison between monotonic and cyclic tests

From a comparison between the results of monotonic tests and cyclic tests it can be noted that there are no substantial differences in terms of resistance and stiffness, with variations respectively up to 13% and 30%. For Elastic Light Wall (WLE) the observed collapse mechanism is the same for the monotonic and cyclic tests and is the net area failure. For the Dissipative Walls (WLD and WHD) the collapse mechanism observed in the monotonic tests is the yielding of the diagonal brace, while in the cyclic tests is the net area failure. This phenomenon is probably due to the loss of resistance that occurs during the cyclic test.

6 DESIGN CRITERIA

In this chapter considerations about design criteria were presented, on the basis of the design assumptions and the experimental test results, in comparison with the prescriptions of national and international seismic codes. The attention is focused (as in Chapter 3) on the behaviour factor, the diagonal brace verifications and the overstrength of fragile elements.

6.1 BEHAVIOUR FACTOR

Part A of AISI S213 defines the behaviour factor (R) as a function of ductility related force modification factor, R_d , and overstrength related force modification factor, R_o , and provides in Table A4-1 the values of these factors for each SFRS and for each design approach (see par.3.2.1 of this dissertation).

For CFS diagonal strap braced walls there are two categories:

- limited ductility braced wall: $R_d = 1.9$; $R_o = 1.3$;
- conventional construction: $R_d = 1.2$; $R_o = 1.3$.

The Italian Code (NTC 08) defines the behaviour factor (q) depending on the design approach considered. For elastic design approach $q = 1$, for dissipative design approach q is defined as a function of structural typology. In Table 7.5 II are listed the maximum values of the behavior factor for each structural typology for dissipative design (see par.3.2.1 of this dissertation).

CFS structures are not considered among the possible steel structural typologies in NTC 08, so the appropriate behavior factor is $q = 1$.

This means that the elastic design approach have to be used to reach a ductile behavior.

In the following, the behaviour factor is evaluated starting from the experimental tests performed.

6.1.1 Evaluation of the behaviour factor of tested walls

In this section, the behaviour factor is evaluated through the expression provided by AISI S213 based on the experimental tests results:

$$R = R_d \cdot R_o \quad (6.1)$$

in which:

R_d = ductility-related seismic force modification factor;

R_o = overstrength-related seismic force modification factor.

The ductility-related force modification factor R_d can be calculated with the expression:

$$R_d = \sqrt{2\mu - 1} \quad (6.2)$$

where μ is the ductility of the tested wall and can be calculated as:

$$\mu = d_{\max} / d_y \quad (6.3)$$

in which:

d_{\max} = maximum lateral displacement of the tested wall;

d_y = yield displacement of tested wall, that can be calculated as:

$$d_y = H_y / k_e \quad (6.4)$$

where H_y is the yield strength, namely the lateral load at which the braces started to yield.

For the cyclic tests:

$$d_y = H_{yp} / k_e \quad (6.5)$$

where H_{yp} is the predicted yield strength, namely the predicted load at which the braces started to yield. It was used this value because it is not possible to determine the yield load from the cyclic test results.

On the other hand, the overstrength-related force modification factor R_o can be calculated with the expression:

$$R_o = R_\Phi \cdot R_{yield} \cdot R_{sh} \quad (6.6)$$

in which:

R_Φ = overstrength due to use of nominal resistances when designing for an extremely rare seismic event;

R_{yield} = overstrength due to minimum specified material strength typically being below the actual strength;

R_{sh} = overstrength due to strain hardening.

In particular R_Φ accounts for the difference between the nominal yield strength and the design yield strength:

$$R_\Phi = 1/\phi \quad (6.7)$$

where Φ is the material resistance factor as defined in the CSA S136 Specification (2007), that is equivalent to $1/\gamma_{M0}$ of the Italian code.

R_{yield} accounts for the difference between the nominal yield strength and the experimental yield strength:

$$R_{yield} = H_y / H_{yd} \quad (6.8)$$

R_{sh} accounts for the strain hardening that was observed during cyclic and monotonic tests:

$$R_{sh} = H_{y4.0\%} / H_y \quad (6.9)$$

where $H_{y4.0\%}$ is the lateral force for an inter-storey drift of 4.0%.

This R_o calculation approach neglected other factors that would further increase the overstrength; i.e. member oversize and development of a collapse mechanism (Velchev and Rogers, 2008).

The calculated values of behaviour factors for monotonic tests on CFS strap braced walls are listed in Table 6.1 and showed in comparison with AISI S213 values in Fig.6.1.

Table 6.1 Behaviour factor for monotonic tests on walls.

specimen	R_d	R_o			q
		R_{ϕ}	R_{yield}	R_{sh}	
WLE-M1	1.74	1.05	1.06	1.02	1.98
WLE-M2	1.74	1.05	1.08	1.01	2.00
WLD-M1	5.42	1.05	1.32	1.06	7.90
WLD-M2	5.95	1.05	1.31	1.08	8.80
WHD-M1	4.09	1.05	1.35	1.05	5.20
WHD-M2	4.57	1.05	1.28	1.05	6.40

For the Elastic Light Walls (WLE) the values of the behaviour factor varies between 1.98 and 2.00 that is a value higher than the one provided by AISI S213 for structures designed with an elastic design approach.

In particular the experimental values of R_d are greater than the one provided by AISI S213, while R_o are smaller.

For Dissipative Walls (WLD and WHD) the values of the behaviour factor varies between 8.80 and 5.20 that is a value higher than the one provided by AISI S213 for structures designed with a dissipative design approach. In particular the experimental values of R_d are greater than the one provided by AISI S213, while R_o are smaller.

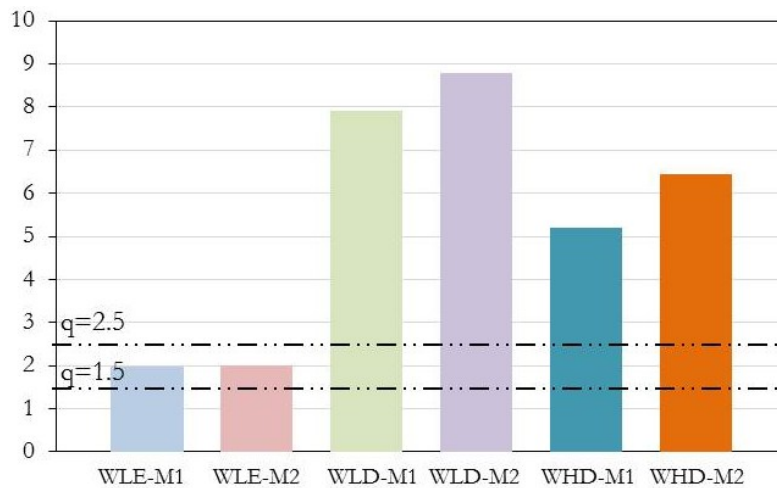


Figure 6.1 Behaviour factor for monotonic tests on walls.

The calculated values of behaviour factors for cyclic tests on CFS strap braced walls are listed in Table 6.2 and showed in comparison with AISI S213 values in Fig.6.1.

Table 6.2 Behaviour factor for cyclic tests on walls.

specimen	R_d	R_o			q
		R_ϕ	R_{yield}	R_{sh}	
WLE-C1	2.25	1.05	1.10	1.01	2.60
WLD-C1	5.09	1.05	1.37	1.05	7.72
WHD-C1	4.87	1.05	1.36	1.03	7.20

For the Elastic Light Walls (WLE) the value of the behaviour factor is 2.60 that is a value higher than the one provided by AISI S213 for structures designed with an elastic design approach.

In particular the experimental value of R_d is greater than the one provided by AISI S213, while R_o is smaller.

For Dissipative Walls (WLD and WHD) the value of the behaviour factor varies between 7.20 and 7.72 that is a value higher than the one provided by AISI S213 for structures designed with a dissipative design approach. In particular the experimental values of R_d are greater than the one provided by AISI S213, while R_o are smaller.

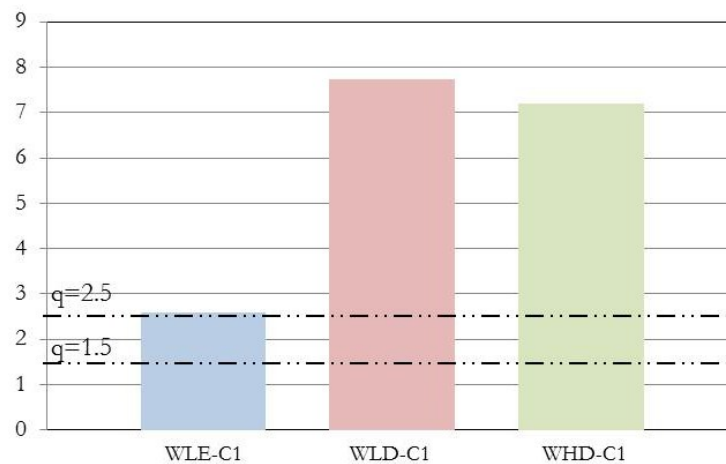


Figure 6.2 Behaviour factor for cyclic tests on walls.

Of course, these values must be validated by non-linear dynamic analysis, but this can be considered a further development of this study.

6.2 DIAGONAL BRACE VERIFICATIONS

Part C5 of AISI S213 provides, for dissipative structures, that the lateral resisting elements develop its full range of behaviour before failure. For the diagonal strap braced wall typology, the ductile failure mechanism is assured by yielding of the diagonal strap brace.

To ensure gross cross section yielding of the diagonal strap bracing member, AISI S213 requires that the expected yield strength ($A_g R_y F_y$) not exceed the expected tensile strength ($A_n R_t F_u$) of the diagonal strap bracing member.

$$A_g \cdot R_y \cdot F_y \leq A_n \cdot R_t \cdot F_u \quad (6.10)$$

The factors for expected yield strength (R_y) and tensile strength (R_t) of the diagonal strap bracing member can be determined in accordance with an approved test method, but in absence of measured physical properties, the values in Table C5-1 of AISI S213 shall be used. In either case R_y shall not be less than 1.1 (see par.3.2.2 of this dissertation).

The Italian code NTC 08 provides verifications for dissipative elements in tension, that are similar to the equation (6.10) for x-braced structures in hot rolled structural steel. NTC 08 provides that design plastic strength of the diagonal cross section have to be less than ultimate design strength of the net cross section in correspondence of the fasteners holes, so that the following equation have to be satisfied (see par.3.2.2 of this dissertation):

$$\frac{A_{res}}{A} \geq 1.1 \cdot \frac{\gamma_{M2}}{\gamma_{M0}} \cdot \frac{f_{yk}}{f_{tk}} \quad (6.11)$$

From a numerical comparison, made in Chapter 3 of this dissertation, between the verifications provided by the two seismic codes, it can be noted that R_y/R_t values are always less than 1.1 $\gamma_{M2}/\gamma_{M0} = 1.3$, so we can say that the NTC 08 is more conservative than AISI S213.

6.2.1 Diagonal brace verifications in the experimental tests

In the design of the Dissipative Walls (WLD and WHD) the capacity design principles were applied to ensure a dissipative behaviour of the walls. So it was promoted the development of the most ductile collapse mechanism, that is the yielding of diagonals in tension. To avoid the collapse mechanism due to the net area of diagonals in the connections, it was verified the fulfilment of the expression (6.11).

For the fulfillment of this condition, in the design of dissipative walls it was given particular attention in the definition of details for the connections and the choice of different material properties for diagonal braces. The connection were designed to fulfill the expression.

In the experimental tests on connections, the theoretical predictions coincides with the collapse mechanism actually observed only in some cases. The following table shows the comparison between the theoretical prediction and the experimental response in the tests on connections.

Table 6.3 Collapse mechanisms for connections.

Specimen	Theoretical prediction	Experimental response
CLD-1	Verified	Not Verified
CLD-2	Not Verified	Not Verified
CLD-3	Verified	Not Verified
CLD-4	Not Verified	Not Verified
CHD-1	Verified	Not Verified
CHD-2	Not Verified	Not Verified
CHD-3	Verified	Not Verified
CHD-4	Verified	Not Verified

Also in the experimental tests on walls, the theoretical predictions coincides with the collapse mechanism actually observed only in some cases. In the monotonic tests, for displacements compatible with the instrumentation capacity, the collapse mechanism observed coincides with yielding of the diagonal, while in the cyclic tests, the collapse mechanism observed was the net area failure, in correspondence of large displacements: for the Dissipative Light Wall (WLD) the failure occurred for a displacement of 162 mm equal to 6% drift; while for Dissipative Heavy Wall (WHD) the failure occurred for a displacement of 198 mm equal to 7% drift. The net area failure in cyclic tests is probably due to the loss of resistance that occurs during the cycles.

The following table shows the comparison between the theoretical prediction and the experimental response in the tests on walls.

Table 6.4 Collapse mechanisms for walls.

Specimen	Theoretical prediction	Experimental response
WLD-M1	Verified	Verified
WLD-M2	Verified	Verified
WHD-M1	Verified	Verified
WHD-M1	Verified	Verified
WLD-C1	Verified	Not Verified
WHD-C1	Verified	Not Verified

6.2.2 Local and global collapse mechanisms

The expression for the verification of the member in tension of the dissipative zones (6.11) was recognized to be calibrated for stress values that slightly exceed the yield strength, but in case of large deformations, due to the hardening of the material, the stress values have a large increase, resulting in the net area collapse, as observed.

For this reason, there is no compliance between the local collapse mechanisms, observed during tests on connections, and global collapse mechanisms, observed during tests on walls.

From the comparison between the tests on connections and the tests on walls, designed with a dissipative design approach, it can be noted that the deformations in the plate of the connection specimen are larger than the deformations in the diagonals of the wall specimen, due to the hardening of the material, so in the tests on connections, the net area failure occurs.

In the following, there is a comparison between the gross area strength and the net area strength alternatively in the connections specimens and the walls specimens (Table 6.5).

To this end, both in the plate for the connections specimens and in the diagonal for the walls specimens, first was defined the deformations as:

$$\varepsilon = \Delta L / L \quad (6.12)$$

then was defined the strength σ , as the average value of the experimental curves of the material S235 (Fig.6.3) and finally, were calculated and

compared the strength in the plate (for the connection) and in the diagonal (for the wall) with the strength in the section weakened by holes.

For:

$$\sigma \cdot A < A_{net} \cdot f_t \quad (6.13)$$

the observed collapse mechanism is the yielding of the diagonal, that is what occurs in tests on walls.

For:

$$\sigma \cdot A > A_{net} \cdot f_t \quad (6.14)$$

the observed collapse mechanism is the net area failure, that is what occurs in tests on connections.

Table 6.5 Local vs global collapse mechanisms.

specimen	ϵ [mm]	σ [Mpa]	$A\sigma$ [kN]	$A_{net}f_t$ [kN]
WLD-M1	0.0490	329	45.20	43.37
CLD	0.0744	346	47.49	43.37
WLD-M2	0.0540	334	45.80	43.37
CLD	0.0744	346	47.49	43.37
WHD-M1	0.0381	317	86.94	86.96
CHD	0.1036	356	97.74	86.96
WHD-M2	0.0490	330	90.51	86.96
CHD	0.1036	356	97.74	86.96
WLD-C1	0.0400	320	43.87	43.37
CLD	0.0744	346	47.49	43.37
WLD-C2	0.0480	329	90.18	86.96
CLD	0.1036	356	97.74	86.96

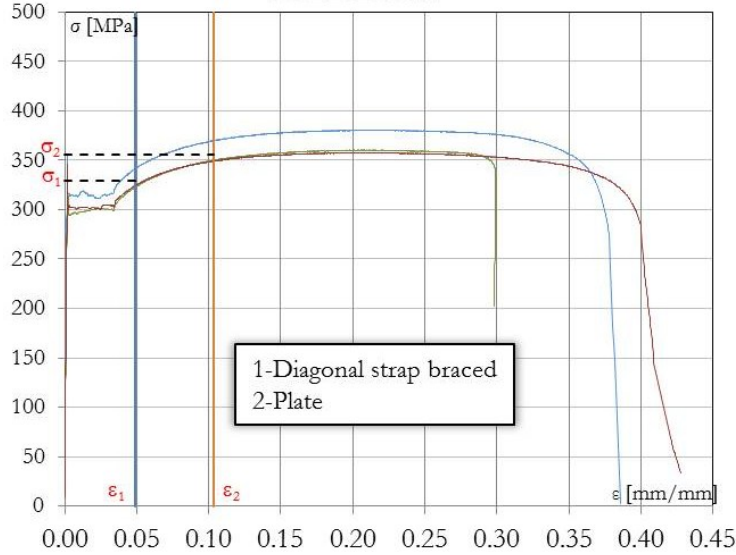


Figure 6.3 Experimental curve for S235.

6.3 OVERSTRENGTH FACTOR

6.3.1 Overstrength of fragile elements

AISI S213 provides prescriptions to apply the capacity design principles to fragile elements, to ensure that the yielding take place along the length of the braces without failure of any other SFRS element.

In particular, to develop a desirable response, AISI S213 requires that components transferring loads to and from the diagonal strap bracing member shall have the nominal strength to resist the expected yield strength ($A_g R_y F_y$) of the diagonal strap bracing member or, if lower, the expected overstrength (seismic loads calculated with $R_d R_o = 1$) of the diagonal strap bracing member (see par.3.2.3 of this dissertation).

So the following equation shall be satisfied:

$$H_{j,d} \geq A_g \cdot R_y \cdot F_y \quad (6.15)$$

The Italian code NTC 08, for x-braced structures in hot rolled structural steel, provides equivalent prescriptions for connections in dissipative

zones, and in particular they shall have an adequate overstrength to permit the plasticization of the connected parts (see par.3.2.3 of this dissertation).

So the following equation shall be satisfied:

$$R_{j,d} \geq \gamma_{Rd} \cdot 1.1 \cdot R_{pl,Rd} = R_{U,Rd} \quad (6.16)$$

So the two equations (6.16) and (6.17) were compared in Chapter 3 through the overstrength factors R_y and $1.1 \gamma_{Rd}/\gamma_{M0}$.

It can be noted from the numerical comparisons, that the factor $1.1\gamma_{Rd}/\gamma_{M0}$ is variable from 1.3 (lower steel strength) to 1.2 (higher steel strength) and R_y is variable from 1.5 (lower steel strength) to 1.1 (higher steel strength), both overstrength parameters are decreasing with material resistance increasing. Only for steel S355 (hot rolled) and S350GD+Z (cold formed) the Italian code NTC 08 is more conservative than AISI S213 (see par.3.2.3 of this dissertation).

In the design of the tested CFS walls, the expression (6.16) was applied to the dimensioning of all the non dissipative elements of the wall, and in conclusion, among the observed collapse mechanisms, there are no fragile collapse mechanisms.

6.3.2 Shear failure of screws

It can be also noted that EN 1993-1-3 provides further relations to be verified, that are not present in NTC 08. In the case that the connection have to be able to provide a certain deformation capacity (dissipative connections), an adequate overstrength must be provided to the parts developing a fragile collapse mechanism, so that the following expressions must be satisfied:

$$F_{v,Rd} \geq 1.2 \cdot F_{b,Rd} \quad (6.17)$$

$$\Sigma F_{v,Rd} \geq 1.2 \cdot F_{n,Rd} \quad (6.18)$$

Among the possible collapse mechanism of screw connections (Fig. 6.4) the shear failure of the screw is a fragile collapse mechanism.

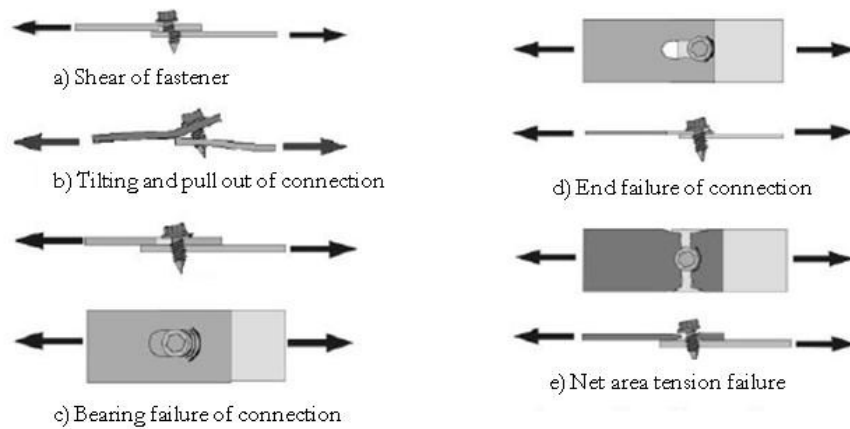


Figure 6.4 Failure modes of connections (ECCS, 2009).

From the analysis of the shear tests on connections and on tests on walls it was never observed a shear failure of screws.

7 CONCLUSIONS

In the last years, the use of Cold Formed Steel (CFS) structures is growing in Europe and in Italy as a valid alternative to traditional structural systems, because of their capacity to combine high performance to a set of structural characteristics such as lightness, rapidity of implementation and the ability to meet high standards of performance in terms of safety, durability and eco-efficiency.

An accurate study of the seismic behaviour of CFS structures is required to be able to compensate for the lack of the Italian seismic code about the requirements for this structural systems. So, the main scope of this dissertation has been to give a contribution to the evaluation of seismic performance of CFS structures and in particular of diagonal strap braced walls. To this end, two main objectives are pursued in this work: the study of the seismic behaviour of diagonal strap braced walls, in terms of global response and the study of local behaviour of connections to understand their influence on the global seismic behaviour of walls.

First of all, a brief introduction on CFS structures is provided and an overview on the main research programs concerning CFS structures is presented, and in particular the attention is focused on the experimental tests performed on CFS strap braced walls that are nowadays available in scientific literature.

In the context of ReLUIIS-DPC project, a wide experimental program was planned and carried out. It consists of full-scale experimental tests on walls to investigate the global behaviour and small-scale experimental tests on materials, simple mechanical joints and connections to investigate the influence of the local behaviour on the global seismic behaviour. In particular 17 tensile tests on materials, 28 shear tests on diagonal connections and 8 shear tests on simple mechanical joints adopted for these connections, 6 monotonic and 6 cyclic (3 to be done) tests on walls were performed. The experimental tests have been performed at the Dist Laboratory (Department of Structures for Engineering and Architecture, Naples), of the University of Naples Federico II. The obtained results demonstrate the ability to pursue, at least for areas with low to medium intensity earthquake, both an elastic

and a dissipative design approach, considering seismic events with 10% probability of exceedance in 50 years.

According to this design assumptions, three different kind of diagonal strap braced walls were designed to be tested: Elastic Light Wall (WLE), Dissipative Light Wall (WLD) and Dissipative Heavy Wall (WHD).

For the elastic design approach, the design of Elastic Heavy Walls (WHE) was neglected, because results less convenient due to over-dimensioned bracing elements and connection details.

In the design of the dissipative walls, to avoid the development of fragile collapse mechanism, it was given particular attention in the definition of details for the connections: staggered spaced screws and different material properties for diagonal braces (S235).

These systems exhibited a satisfactory experimental response in terms of stiffness, strength and deformation capacity, largely confirming the theoretical predictions.

Since the final scope of the whole study, and in particular of the experimental campaign, is to provide appropriate design criteria for diagonal strap braced CFS structures to be proposed for the Italian seismic code, in the last chapter some considerations about design criteria were presented, on the basis of the design assumptions and the experimental test results, in comparison with the prescriptions of national and international seismic codes. The attention is focused on the behaviour factor, the diagonal brace verifications and the overstrength of fragile elements.

With regard to the behaviour factor, both for elastic and dissipative design approach, and both for monotonic and cyclic tests, the values of the behaviour factor, calculated by the test results, with the expression provided by AISI S213, are higher than the one prescribed by AISI S213. In particular the experimental values of R_d are greater than the one provided by AISI S213, while R_o are smaller.

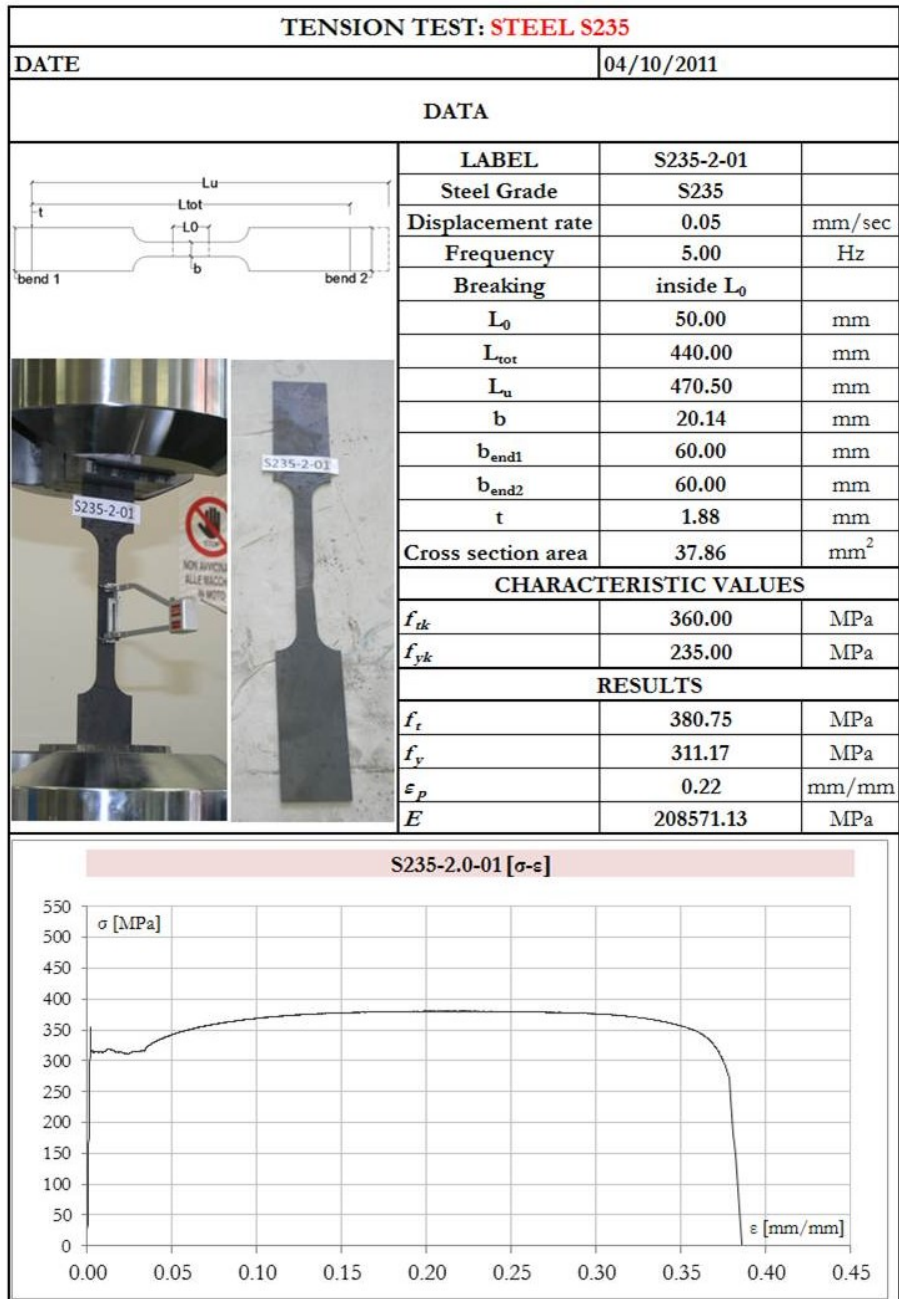
With regard to the diagonal brace verifications, the connection were designed to prevent the net area failure of sections weakened by holes, but in the experimental tests both on connections and on walls, the theoretical predictions coincides with the collapse mechanism actually observed only in some cases. In particular, in monotonic tests, the collapse mechanism observed is with yielding of the diagonal, as predicted, while in the cyclic tests, the collapse mechanism observed was the net area failure, probably due to the loss of resistance that occurs during the cycles.

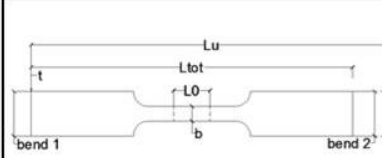


With regard to the overstrength factor, all the considered seismic codes, for dissipative design approach provide prescriptions to apply the capacity design principles to fragile elements, to ensure that the yielding take place along the length of the braces without failure of any other SFRS element. It was observed that, applying the prescriptions of both EN 1993-1-3 and NTC 08, fragile collapse mechanisms were prevented. In conclusion, the presented research, can be considered a first essential step for the characterization of the seismic behaviour of CFS diagonal strap braced structures. As a further development, a theoretical-numerical study (non-linear dynamic analysis), dedicated to the evaluation of seismic demand, will contribute to a complete overview on the seismic performance of the investigated structural typology.

Appendix A:

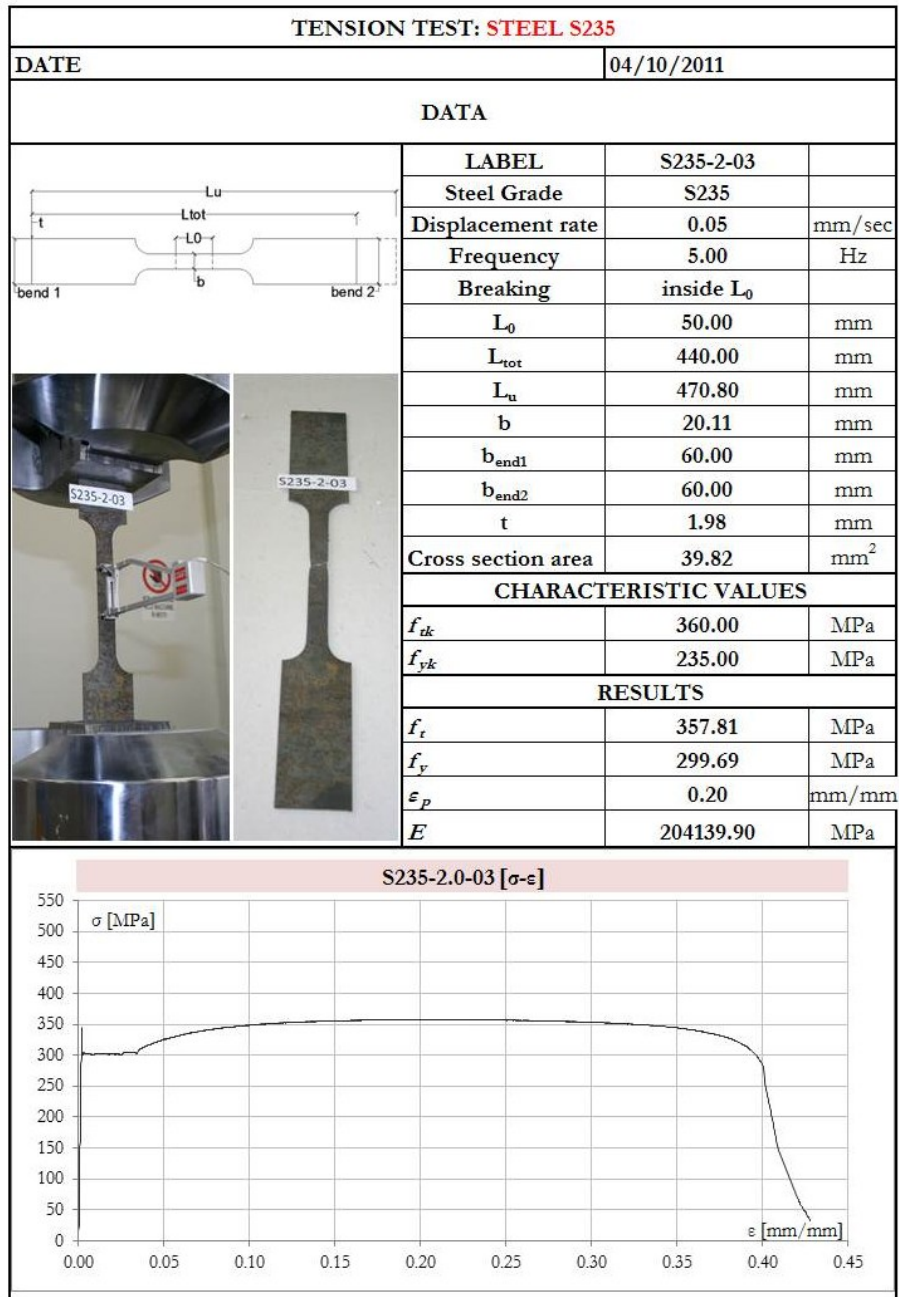
Tests on Materials and Components

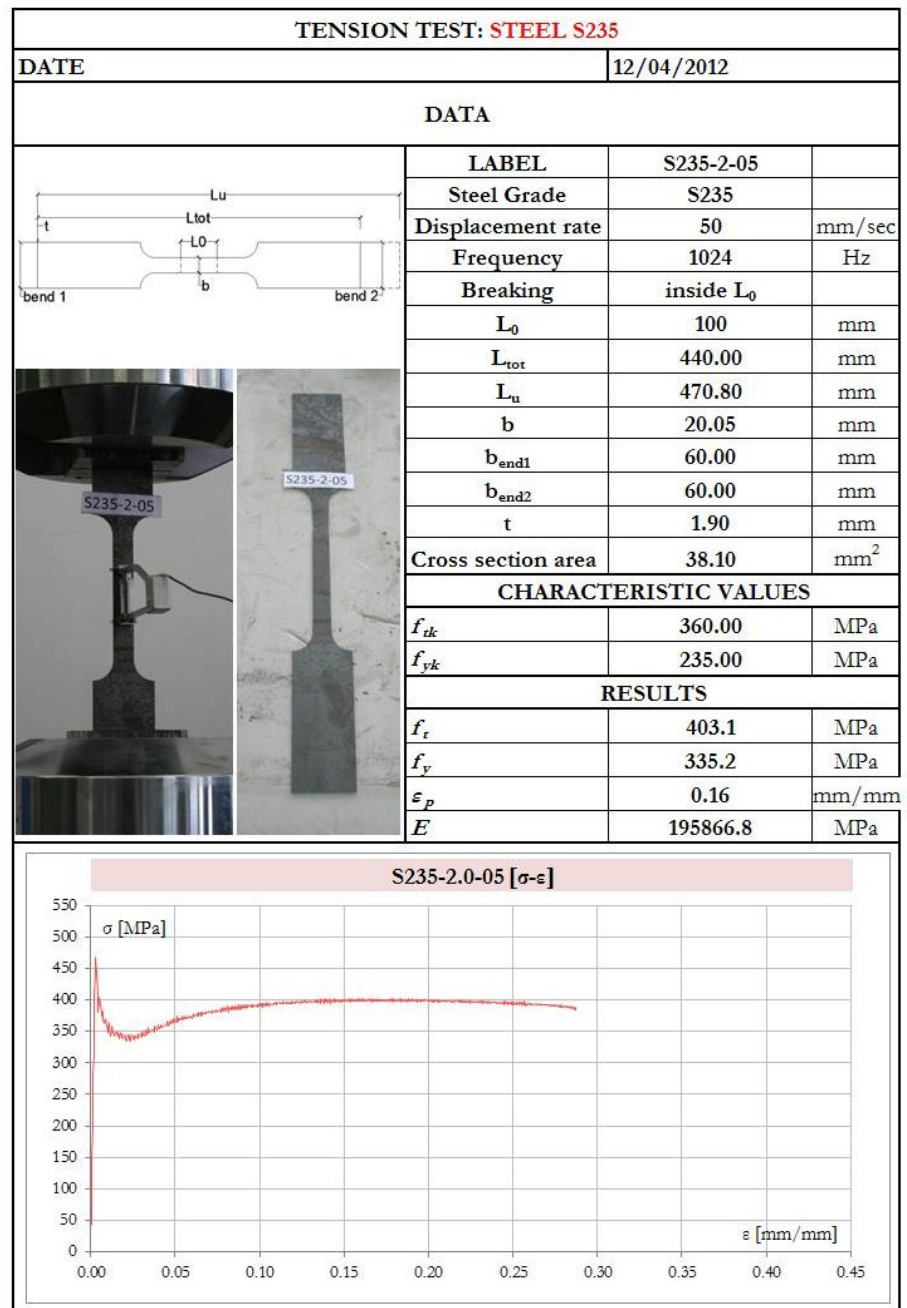
A.1 MATERIAL

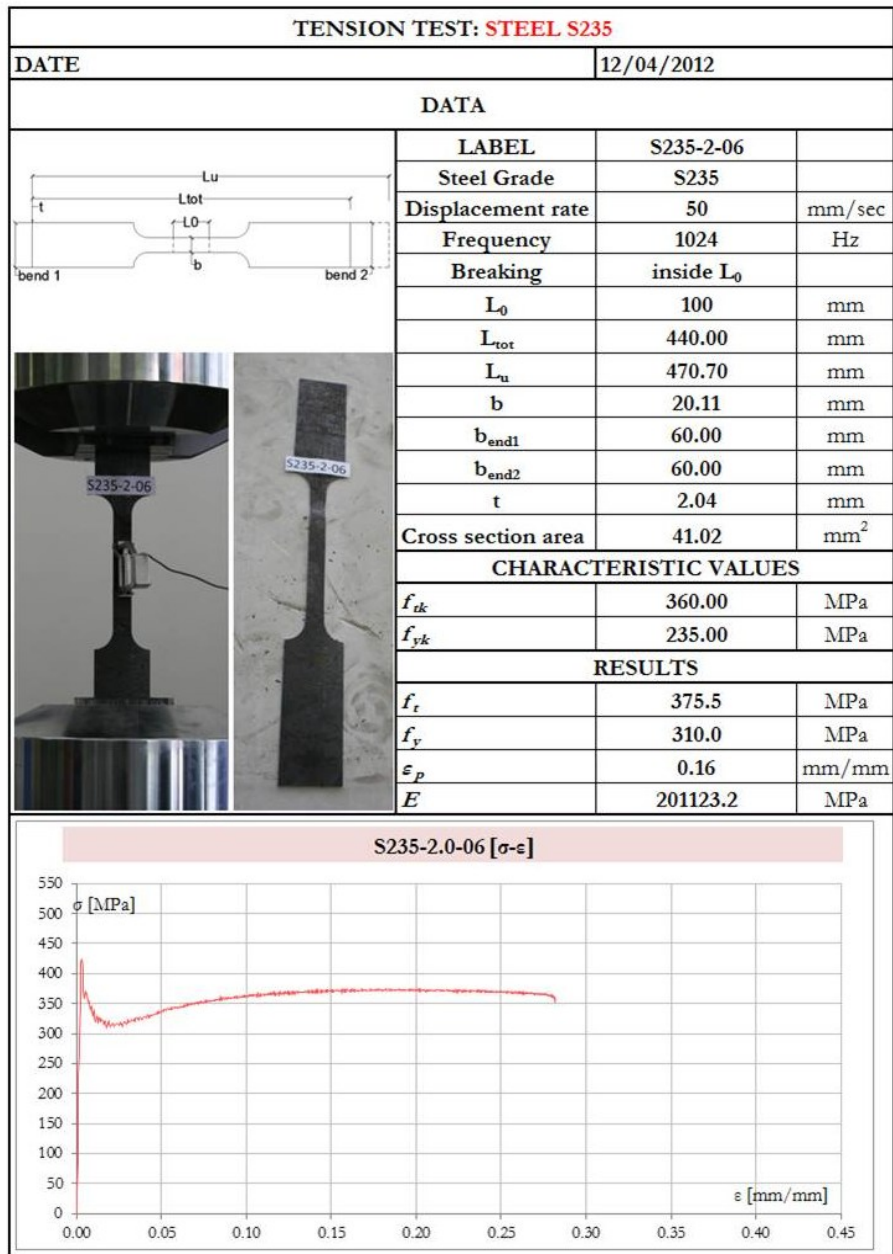


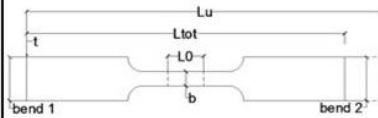


TENSION TEST: STEEL S235			
DATE		04/10/2011	
DATA			
  	LABEL	S235-2-02	
	Steel Grade	S235	
	Displacement rate	0.05	mm/sec
	Frequency	5.00	Hz
	Breaking	outside L_0	
	L_0	50.00	mm
	L_{tot}	440.00	mm
	L_u	470.70	mm
	b	20.00	mm
	b_{end1}	60.00	mm
	b_{end2}	60.00	mm
	t	2.01	mm
	Cross section area	40.20	mm ²
	CHARACTERISTIC VALUES		
	f_{tk}	360.00	MPa
	f_{yk}	235.00	MPa
RESULTS			
f_t	360.48	MPa	
f_y	293.99	MPa	
ε_p	0.21	mm/mm	
E	182969.35	MPa	

S235-2.0-02 [σ - ε]	
σ [MPa]	ε [mm/mm]
550	0.00
500	0.05
450	0.10
400	0.15
350	0.20
300	0.25
250	0.30
200	0.35
150	0.40
100	0.45
50	
0	

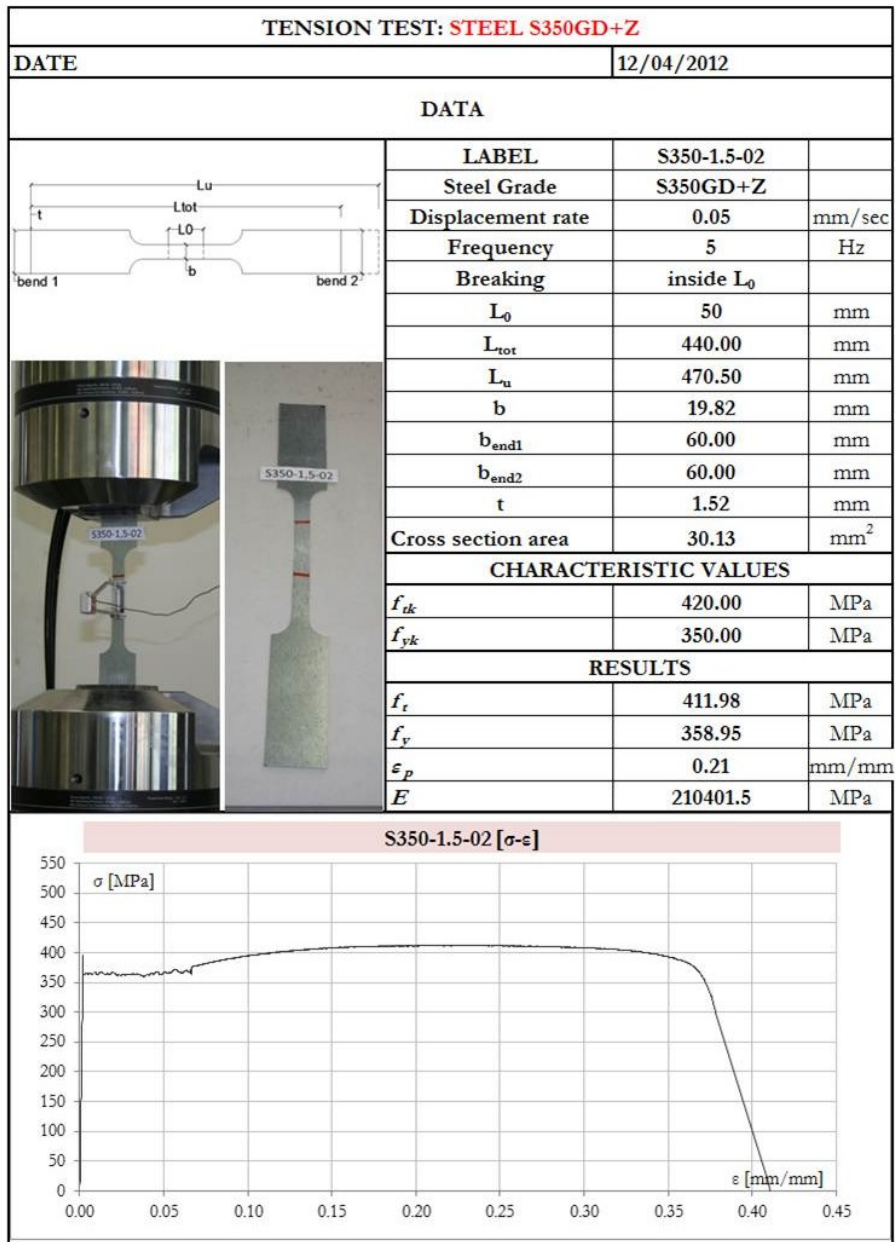


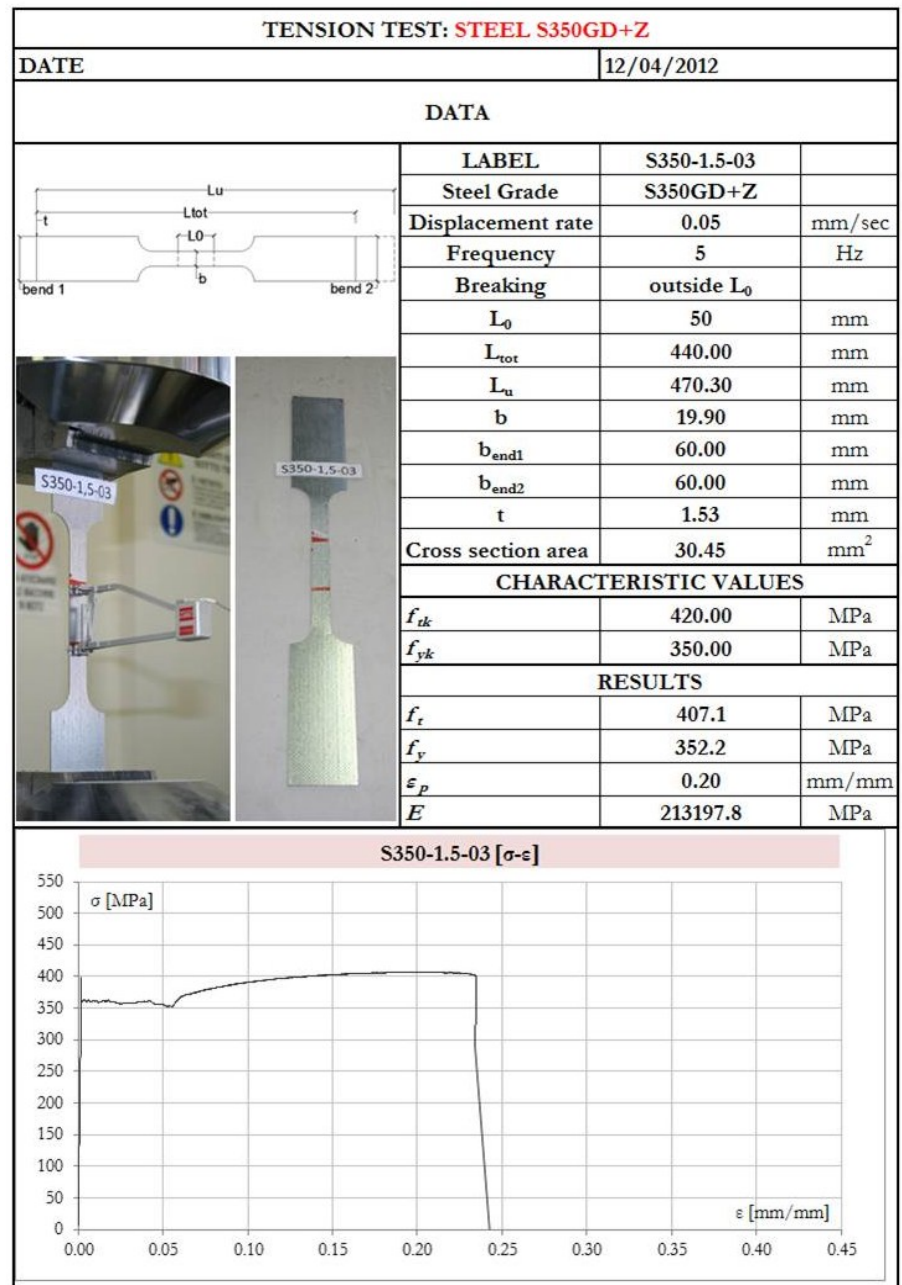


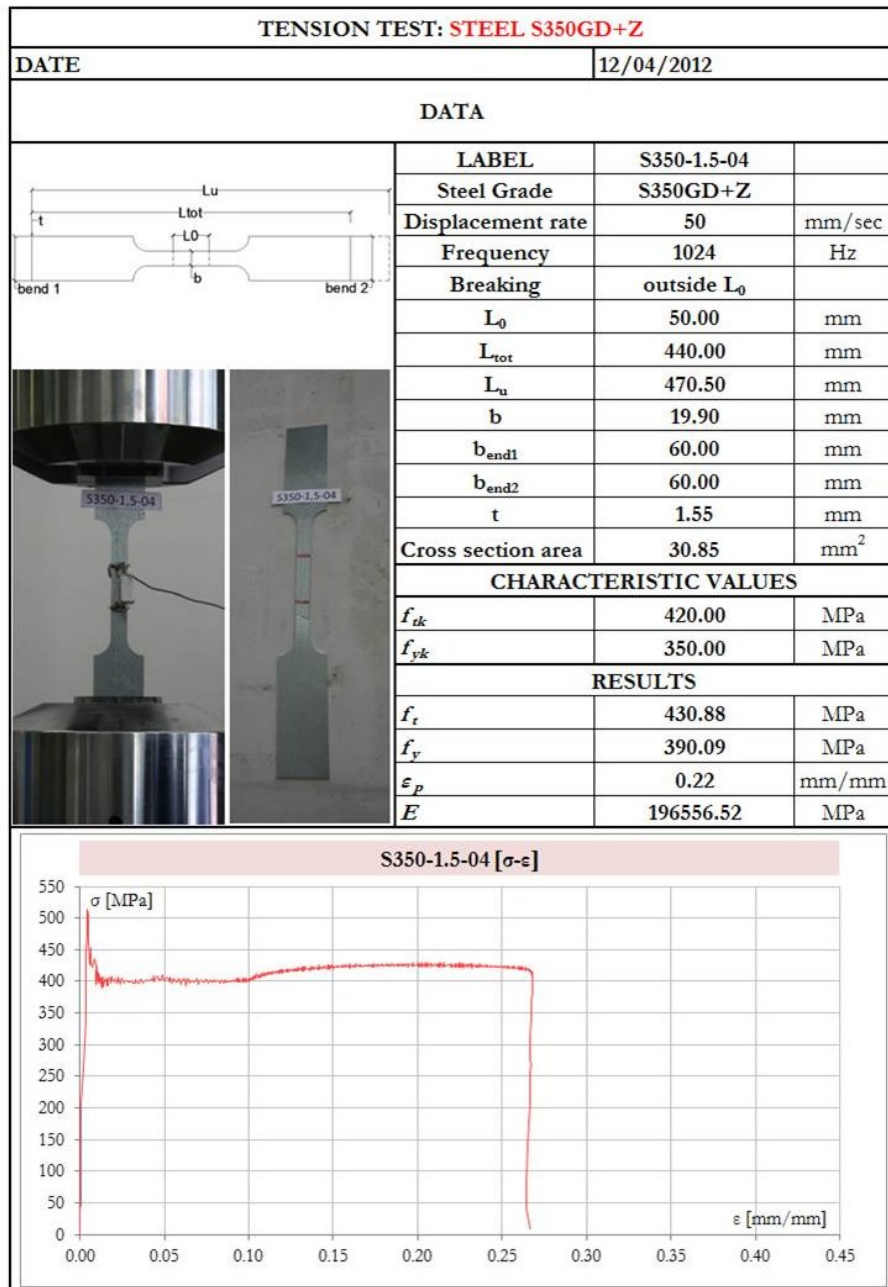


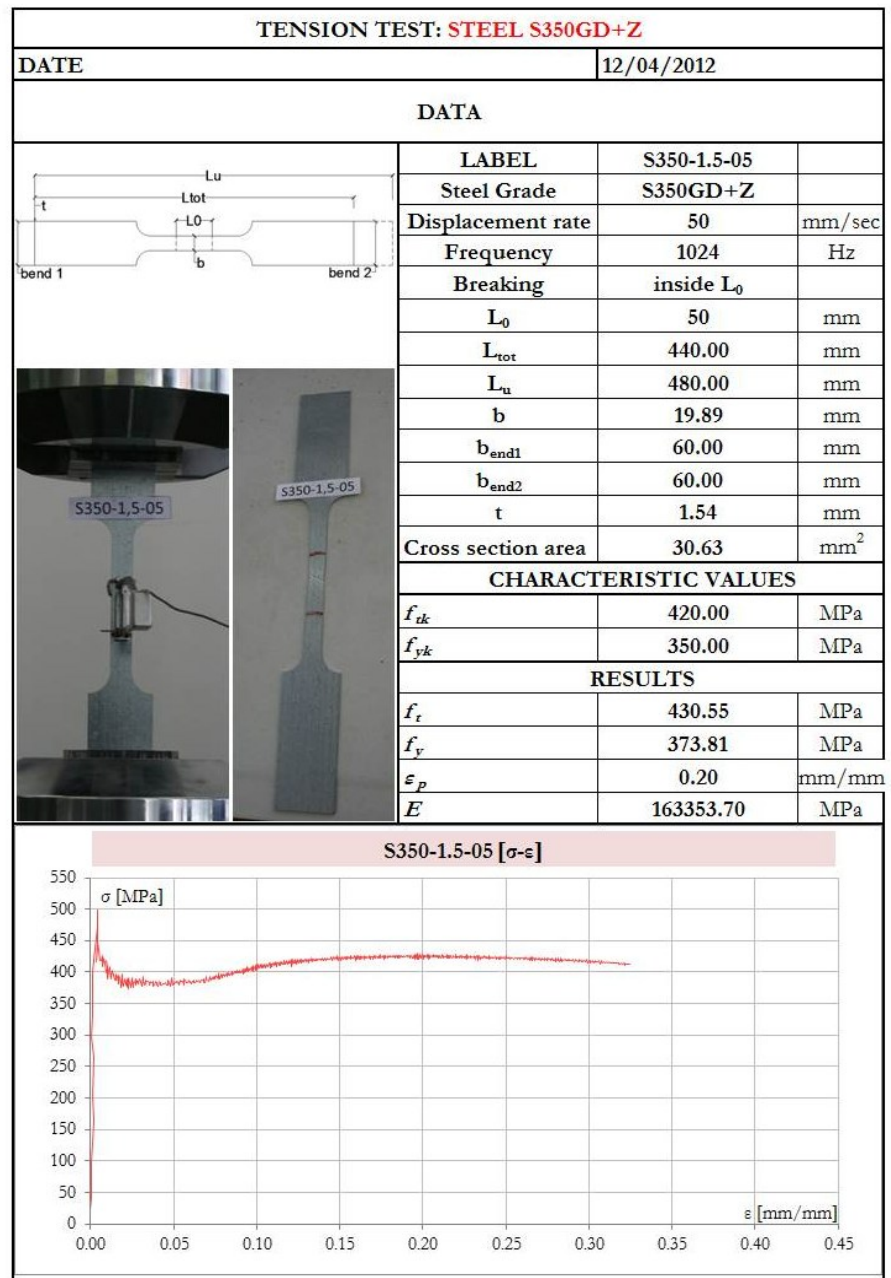
TENSION TEST: STEEL S350GD+Z			
DATE		12/04/2012	
DATA			
  	LABEL	S350-1.5-01	
	Steel Grade	S350GD+Z	
	Displacement rate	0.05	mm/sec
	Frequency	5	Hz
	Breaking	outside L_0	
	L_0	50	mm
	L_{tot}	440.00	mm
	L_u	470.50	mm
	b	19.88	mm
	b_{end1}	60.00	mm
	b_{end2}	60.00	mm
	t	1.54	mm
	Cross section area	30.62	mm ²
	CHARACTERISTIC VALUES		
	f_{tk}	420.00	MPa
	f_{yk}	350.00	MPa
	RESULTS		
f_t	407.61	MPa	
f_y	354.84	MPa	
ϵ_p	0.21	mm/mm	
E	211033.51	MPa	

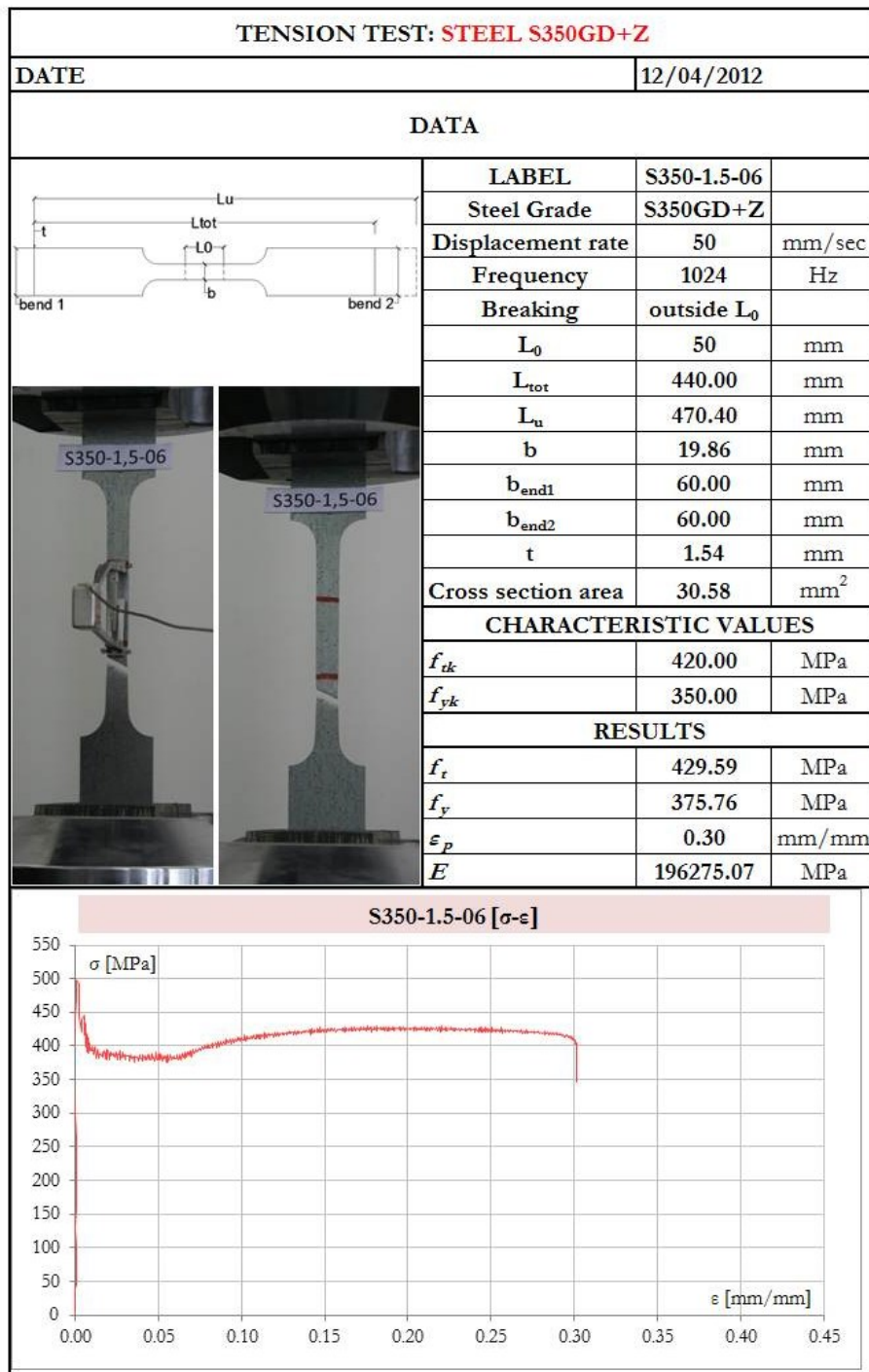
S350-1.5-01 [σ - ϵ]	
σ [MPa]	ϵ [mm/mm]
550	
500	
450	
400	
350	
300	
250	
200	
150	
100	
50	
0	
0.00	0.05
0.05	0.10
0.10	0.15
0.15	0.20
0.20	0.25
0.25	0.30
0.30	0.35
0.35	0.40
0.40	0.45

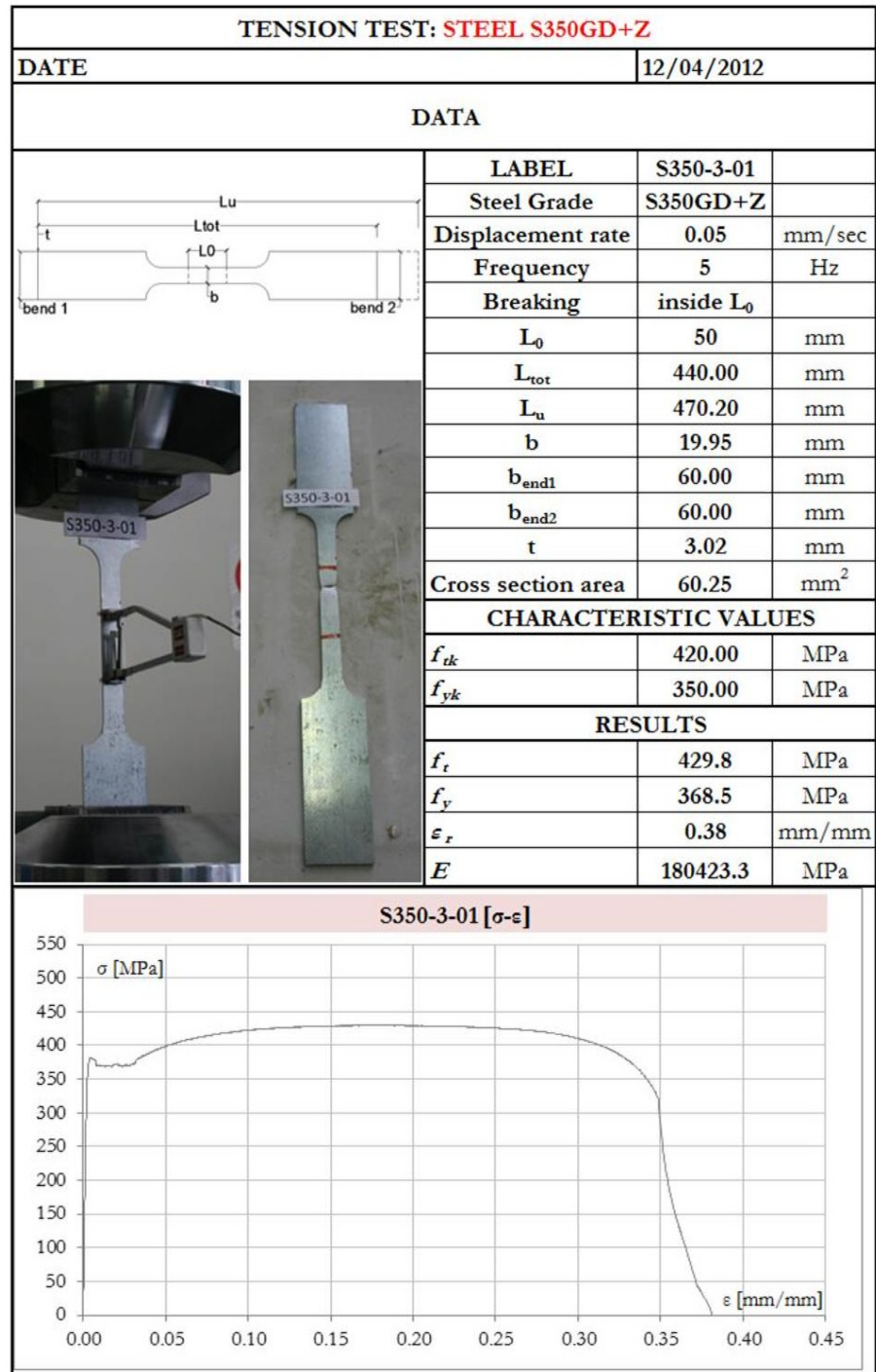


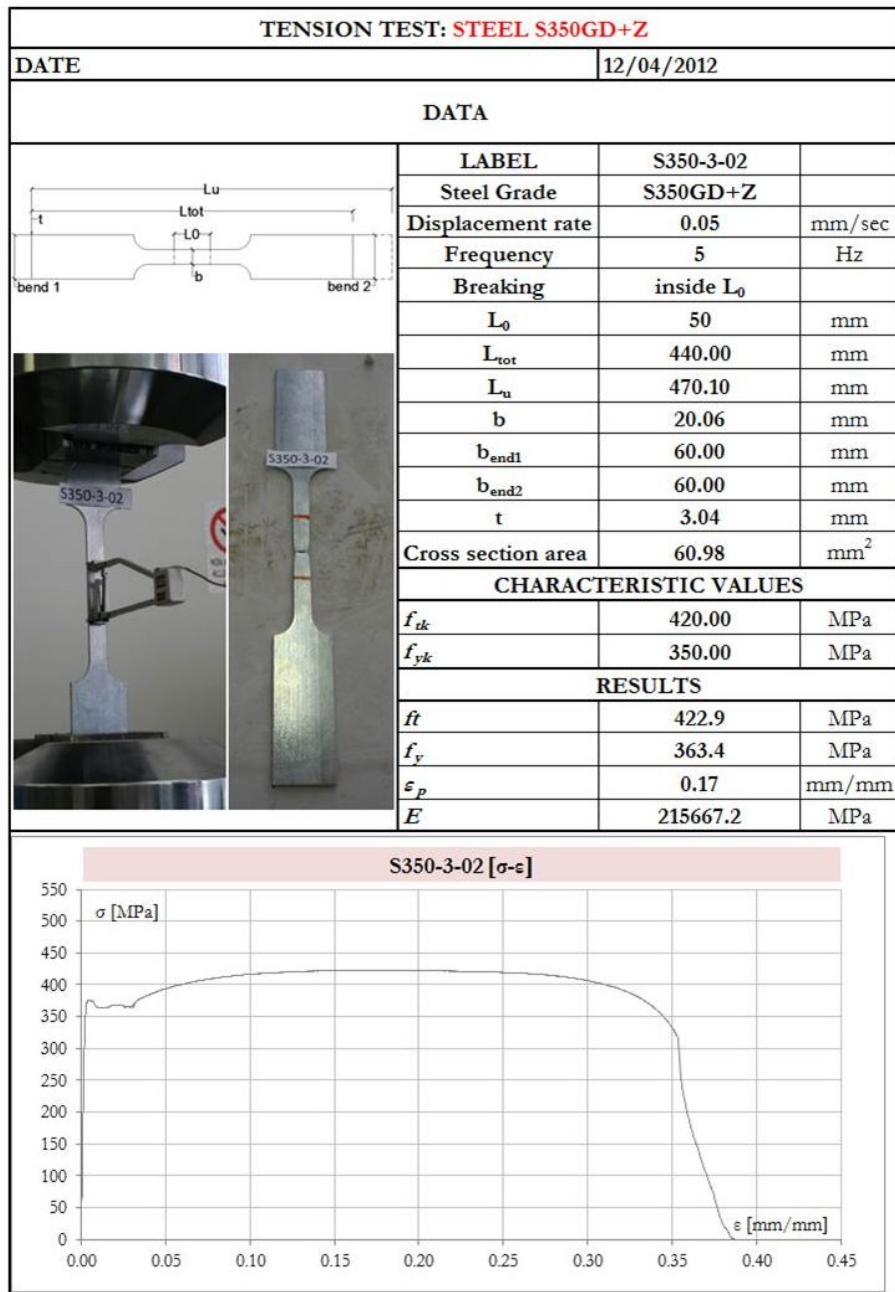


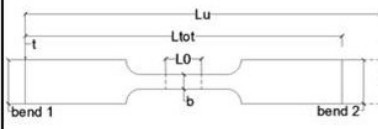






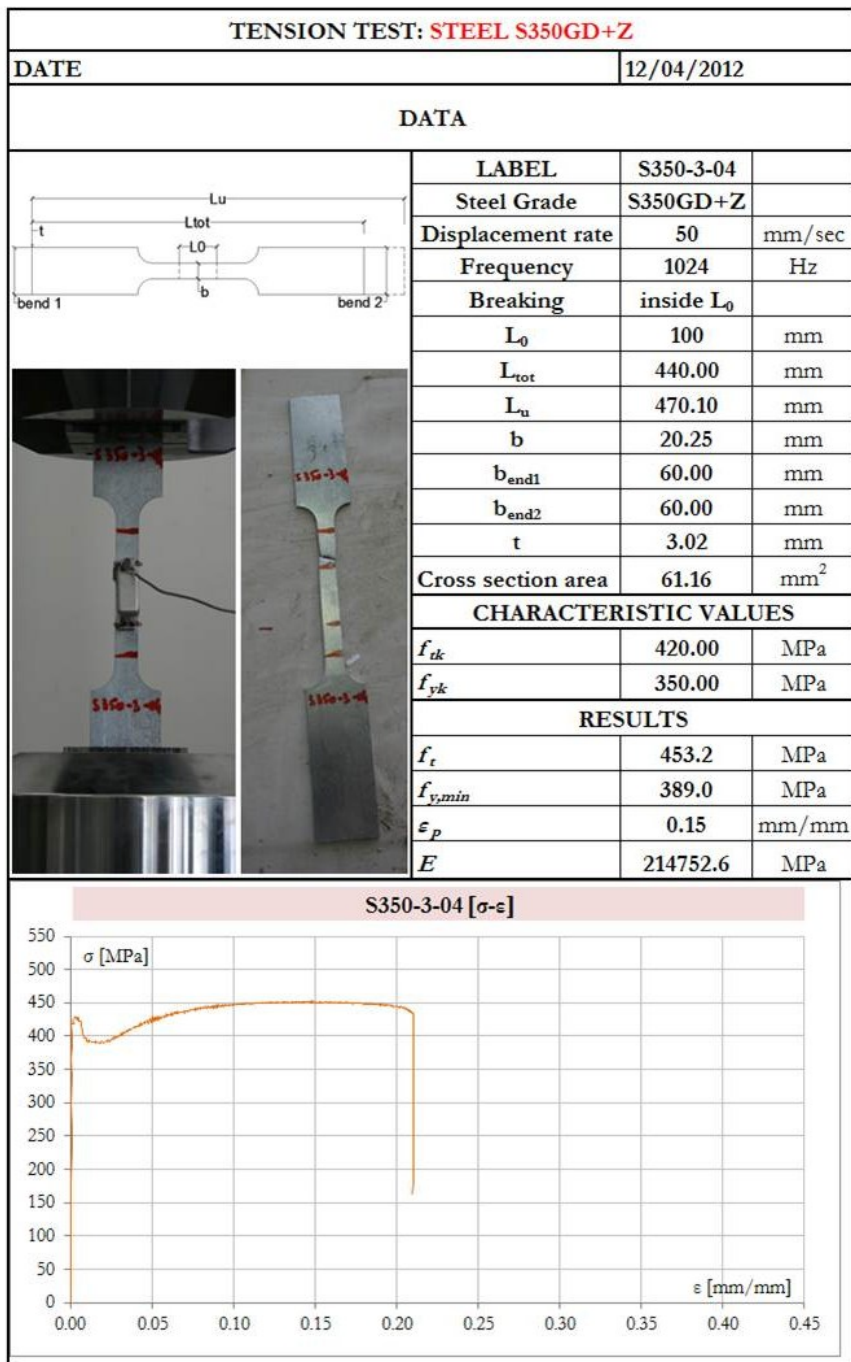


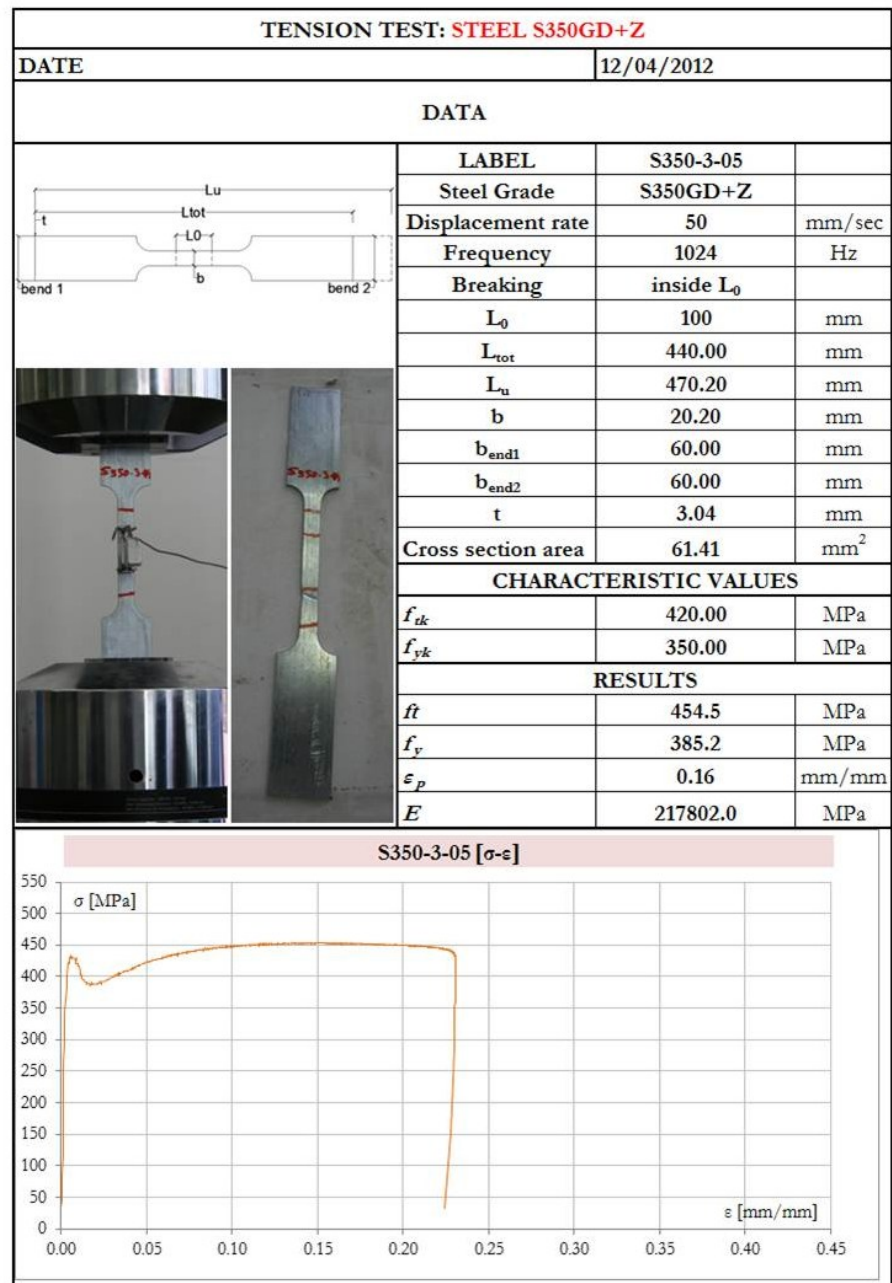


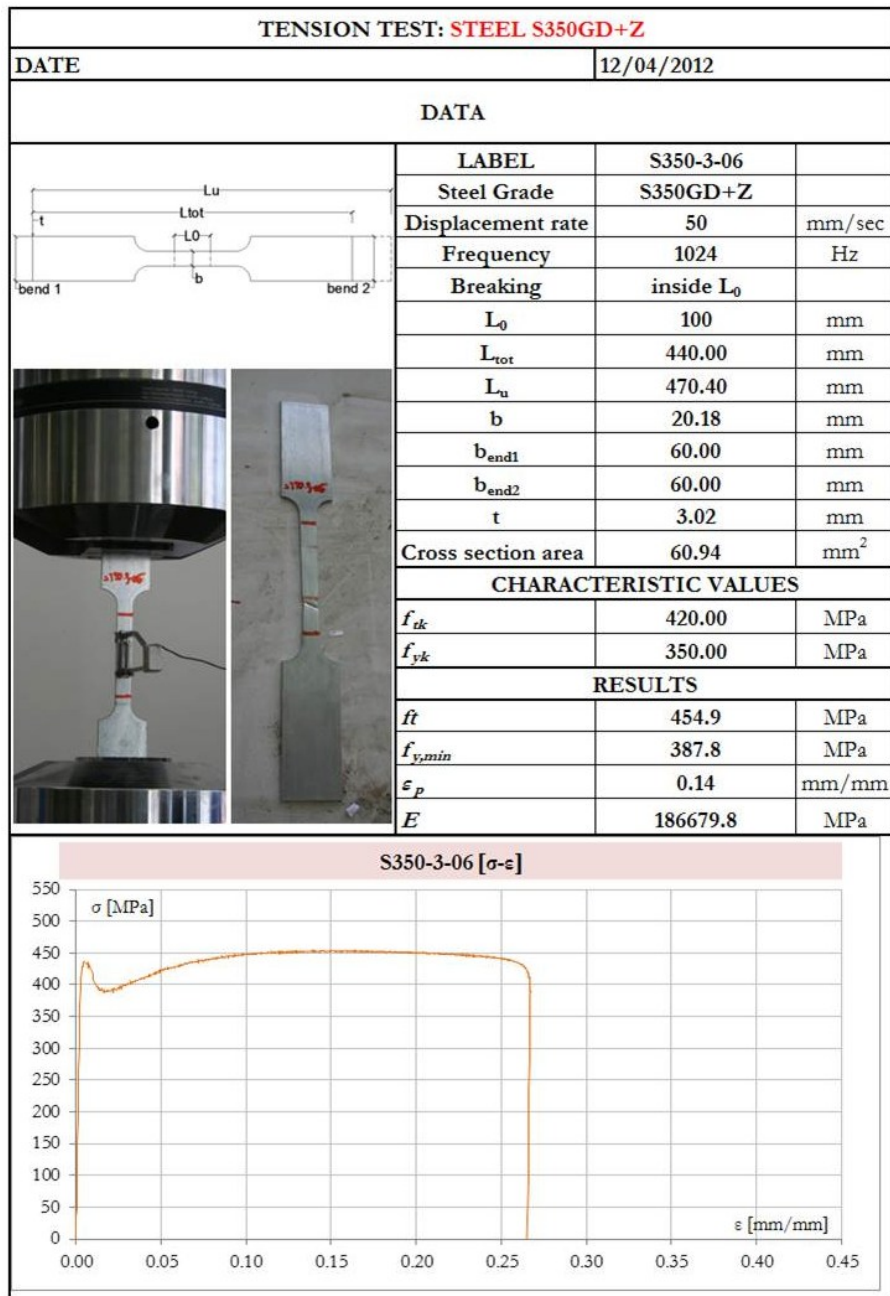


TENSION TEST: STEEL S350GD+Z			
DATE		12/04/2012	
DATA			
  	LABEL	S350-3-03	
	Steel Grade	S350GD+Z	
	Displacement rate	0.05	mm/sec
	Frequency	5	Hz
	Breaking	inside L ₀	
	L ₀	50	mm
	L _{tot}	440.00	mm
	L _u	470.20	mm
	b	19.86	mm
	b _{end1}	60.00	mm
	b _{end2}	60.00	mm
	t	3.08	mm
	Cross section area	61.17	mm ²
	CHARACTERISTIC VALUES		
f _{tk}	420.00	MPa	
f _{yk}	350.00	MPa	
RESULTS			
f _t	422.60	MPa	
f _y	360.9	MPa	
ε _p	0.18	mm/mm	
E	207703.2	MPa	

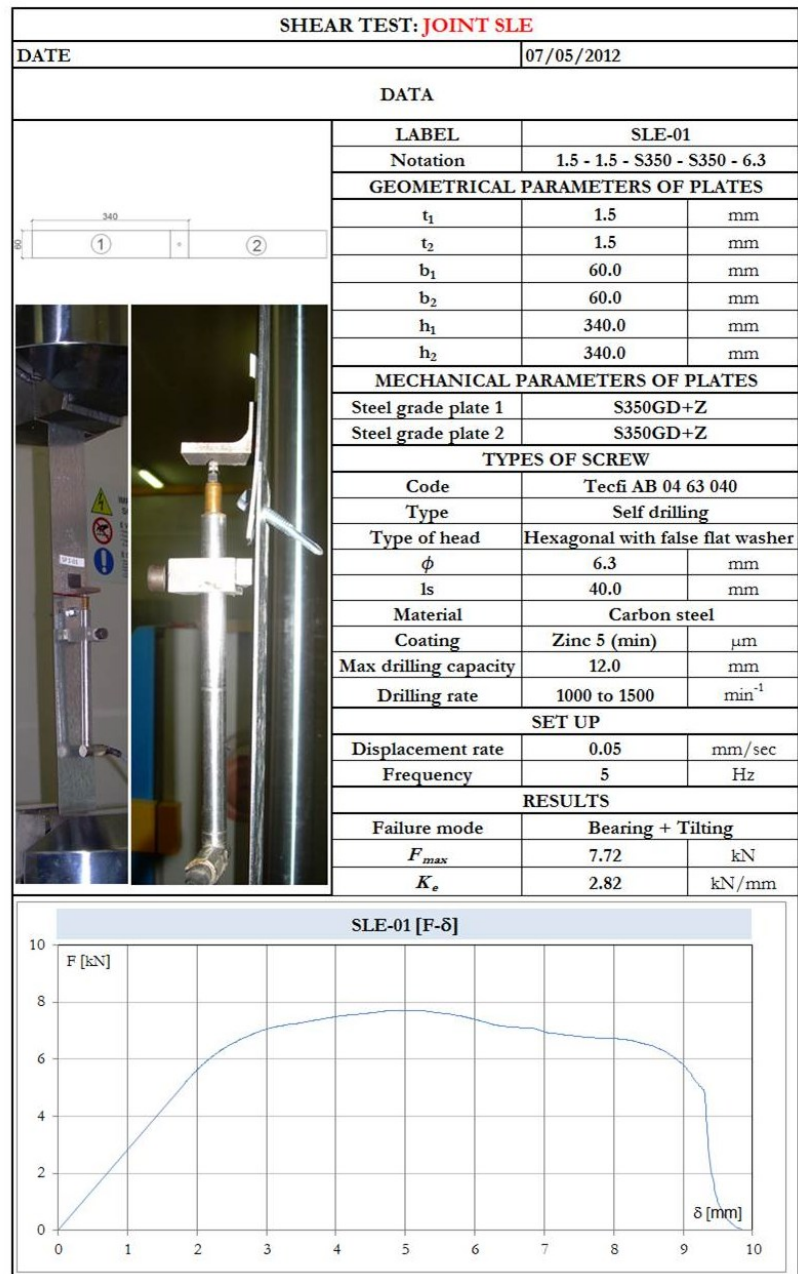
S350-3-03 [σ-ε]	
σ [MPa]	ε [mm/mm]
550	0.00
500	0.05
450	0.10
400	0.15
350	0.20
300	0.25
250	0.30
200	0.35
150	0.40
100	0.45
50	
0	

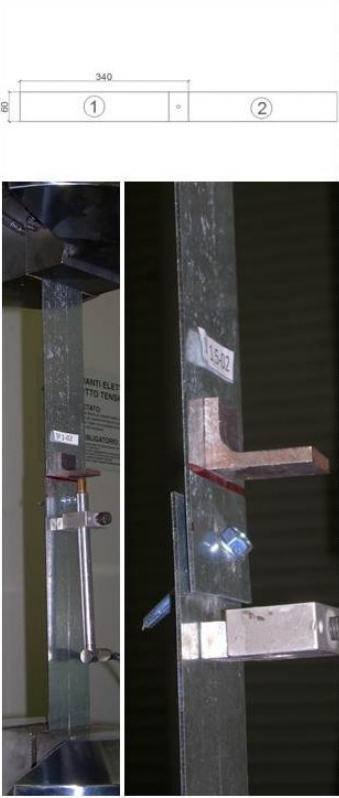
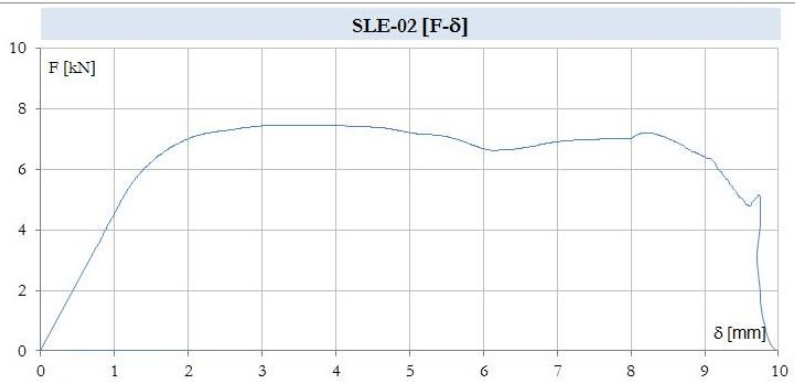





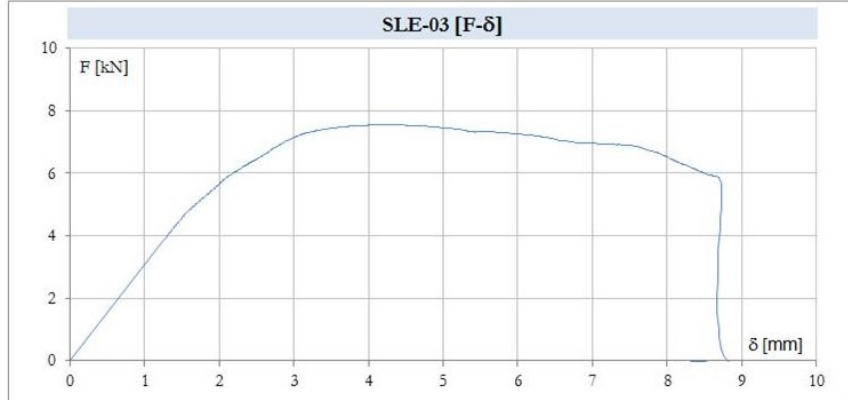


A.2 SIMPLE JOINTS



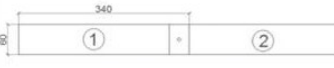


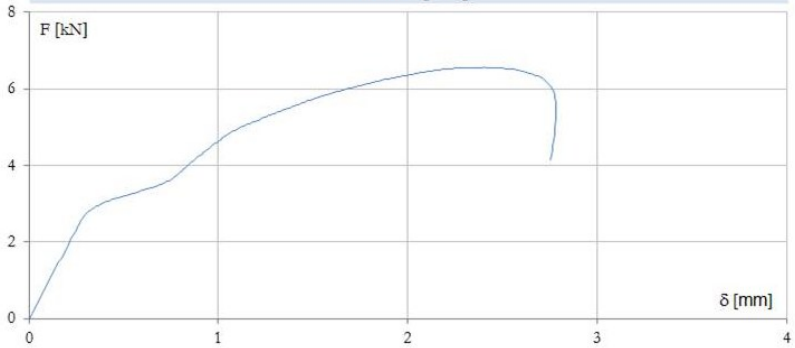
SHEAR TEST: JOINT SLE		
DATE		07/05/2012
DATA		
	LABEL	SLE-02
	Notation	1.5 - 1.5 - S350 - S350 - 6.3
	GEOMETRICAL PARAMETERS OF PLATES	
	t_1	1.5 mm
	t_2	1.5 mm
	b_1	60.0 mm
	b_2	60.0 mm
	h_1	340.0 mm
	h_2	340.0 mm
	MECHANICAL PARAMETERS OF PLATES	
	Steel grade plate 1	S350GD+Z
	Steel grade plate 2	S350GD+Z
	TYPES OF SCREW	
	Code	Tecfi AB 04 63 040
	Type	Self drilling
	Type of head	Hexagonal with false flat washer
	ϕ	6.3 mm
	l_s	40.0 mm
	Material	Carbon steel
	Coating	Zinc 5 (min) μm
	Max drilling capacity	12.0 mm
	Drilling rate	1000 to 1500 min^{-1}
	SET UP	
	Displacement rate	0.05 mm/sec
	Frequency	5 Hz
	RESULTS	
	Failure mode	Bearing + Tilting
	F_t	7.46 kN
	K_e	4.58 kN/mm
		


SHEAR TEST: JOINT SLE			
DATE		07/05/2012	
DATA			
	LABEL	SLE-03	
	Notation	1.5 - 1.5 - S350 - S350 - 6.3	
	GEOMETRICAL PARAMETERS OF PLATES		
	t_1	1.5	mm
	t_2	1.5	mm
	b_1	60.0	mm
	b_2	60.0	mm
	h_1	340.0	mm
	h_2	340.0	mm
	MECHANICAL PARAMETERS OF PLATES		
	Steel grade plate 1	S350GD+Z	
	Steel grade plate 2	S350GD+Z	
	TYPES OF SCREW		
	Code	Tecfi AB 04 63 040	
	Type	Self drilling	
	Type of head	Hexagonal with false flat washer	
	ϕ	6.3	mm
	ls	40.0	mm
	Material	Carbon steel	
	Coating	Zinc 5 (min)	μm
	Max drilling capacity	12.0	mm
	Drilling rate	1000 to 1500	min^{-1}
SET UP			
Displacement rate	0.05	mm/sec	
Frequency	5	Hz	
RESULTS			
Failure mode	Bearing + Tilting		
F_t	7.55	kN	
K_e	3.05	kN/mm	

SLE-03 [F- δ]	
F [kN]	δ [mm]
	


SHEAR TEST: JOINT SLD			
DATE		07/05/2012	
DATA			
	LABEL	SLD-01	
	Notation	1.5 - 2 - S350 - S250 - 4.8	
	GEOMETRICAL PARAMETERS OF PLATES		
	t_1	1.5	mm
	t_2	2.0	mm
	b_1	60.0	mm
	b_2	60.0	mm
	h_1	340.0	mm
	h_2	340.0	mm
	MECHANICAL PARAMETERS OF PLATES		
	Steel grade plate 1	S350GD+Z	
	Steel grade plate 2	S235	
	TYPES OF SCREW		
	Code	Tecfi CI 01 48 016	
	Type	Self drilling	
	Type of head	Cylindrical with false washer and cross type H recess	
	ϕ	4.8	mm
	l_s	16.0	mm
	Material	Carbon steel	
	Coating	Zinc 5 (min)	μm
	SET UP		
	Displacement rate	0.05	mm/sec
	Frequency	5	Hz
	RESULTS		
	Failure mode	Shear	
	F_r	6.50	kN
	K_e	3.23	Kn/mm


SLD-01 [F- δ]	
F [kN]	δ [mm]
8	
6	
4	
2	
0	
0	1
	2
	3
	4

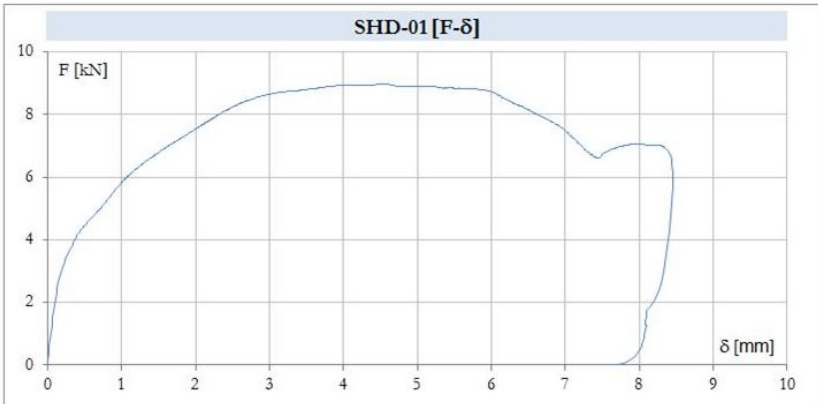
SHEAR TEST: JOINT SLD		
DATE		07/05/2012
DATA		
  	LABEL	SLD-02
	Notation	1.5 - 2 - S350 - S250 - 4.8
	GEOMETRICAL PARAMETERS OF PLATES	
	t_1	1.5 mm
	t_2	2.0 mm
	b_1	60.0 mm
	b_2	60.0 mm
	h_1	340.0 mm
	h_2	340.0 mm
	MECHANICAL PARAMETERS OF PLATES	
	Steel grade plate 1	S350GD+Z
	Steel grade plate 2	S235
TYPES OF SCREW		
Code		Tecfi CI 01 48 016
Type		Self drilling
Type of head		Cylindrical with false washer and cross type H recess
ϕ		4.8 mm
l_s		16.0 mm
Material		Carbon steel
Coating		Zinc 5 (min) μm
SET UP		
Displacement rate		0.05 mm/sec
Frequency		5 Hz
RESULTS		
Failure mode		Shear
F_t		6.56 kN
K_e		3.95 kN/mm
<div>SLD-02 [F-δ]</div> 		

SHEAR TEST: JOINT SLD			
DATE		07/05/2012	
DATA			
	LABEL	SLD-03	
	Notation	1.5 - 2 - S350 - S250 - 4.8	
	GEOMETRICAL PARAMETERS OF PLATES		
	t ₁	1.5	mm
	t ₂	2.0	mm
	b ₁	60.0	mm
	b ₂	60.0	mm
	h ₁	340.0	mm
	h ₂	340.0	mm
	MECHANICAL PARAMETERS OF PLATES		
Steel grade plate 1	S350GD+Z		
Steel grade plate 2	S235		
TYPES OF SCREW			
Code	Tecfi CI 01 48 016		
Type	Self drilling		
Type of head	Cylindrical with false washer and cross type H recess		
φ	4.8	mm	
ls	16.0	mm	
Material	Carbon steel		
Coating	Zinc 5 (min)	μm	
SET UP			
Displacement rate	0.05	mm/sec	
Frequency	5	Hz	
RESULTS			
Failure mode	Shear		
F _t	6.52	kN	
K _e	3.05	kN/mm	

SLD-03 [F-δ]

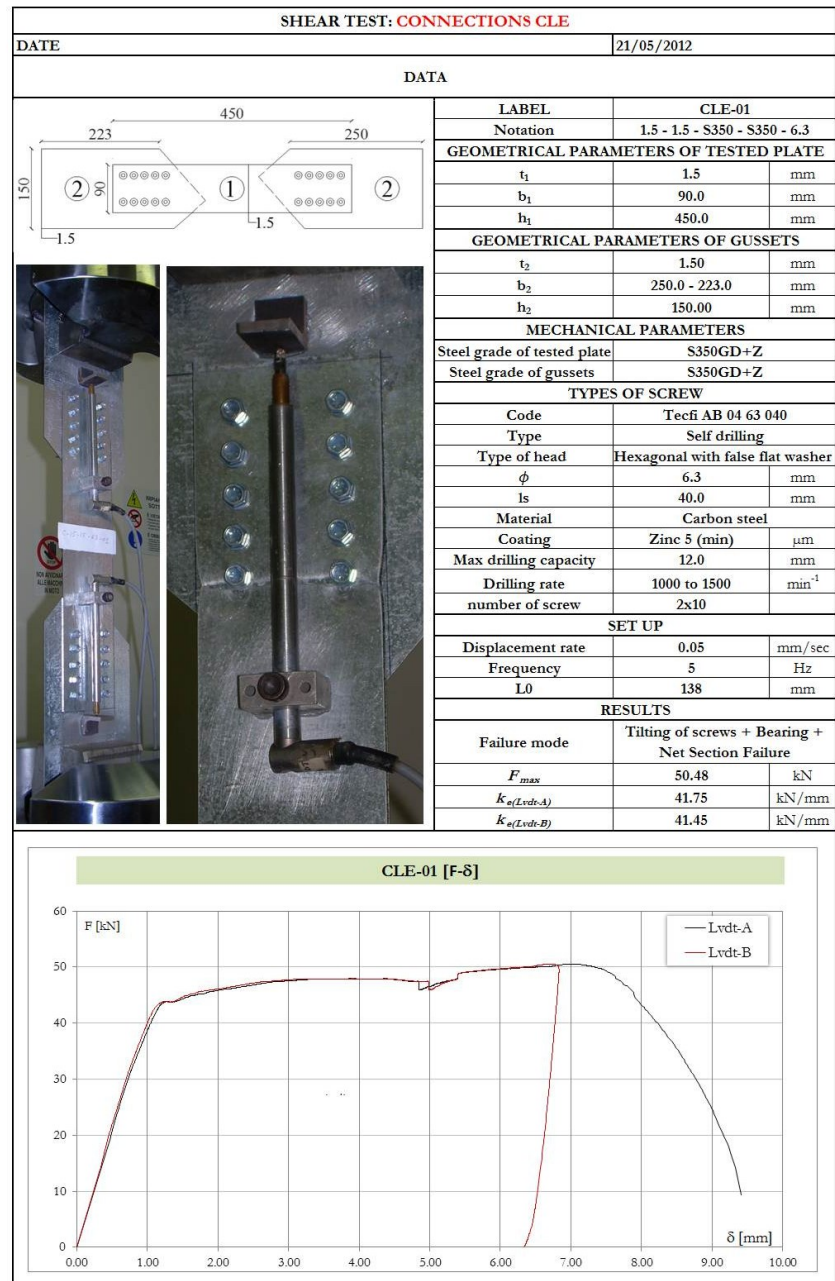


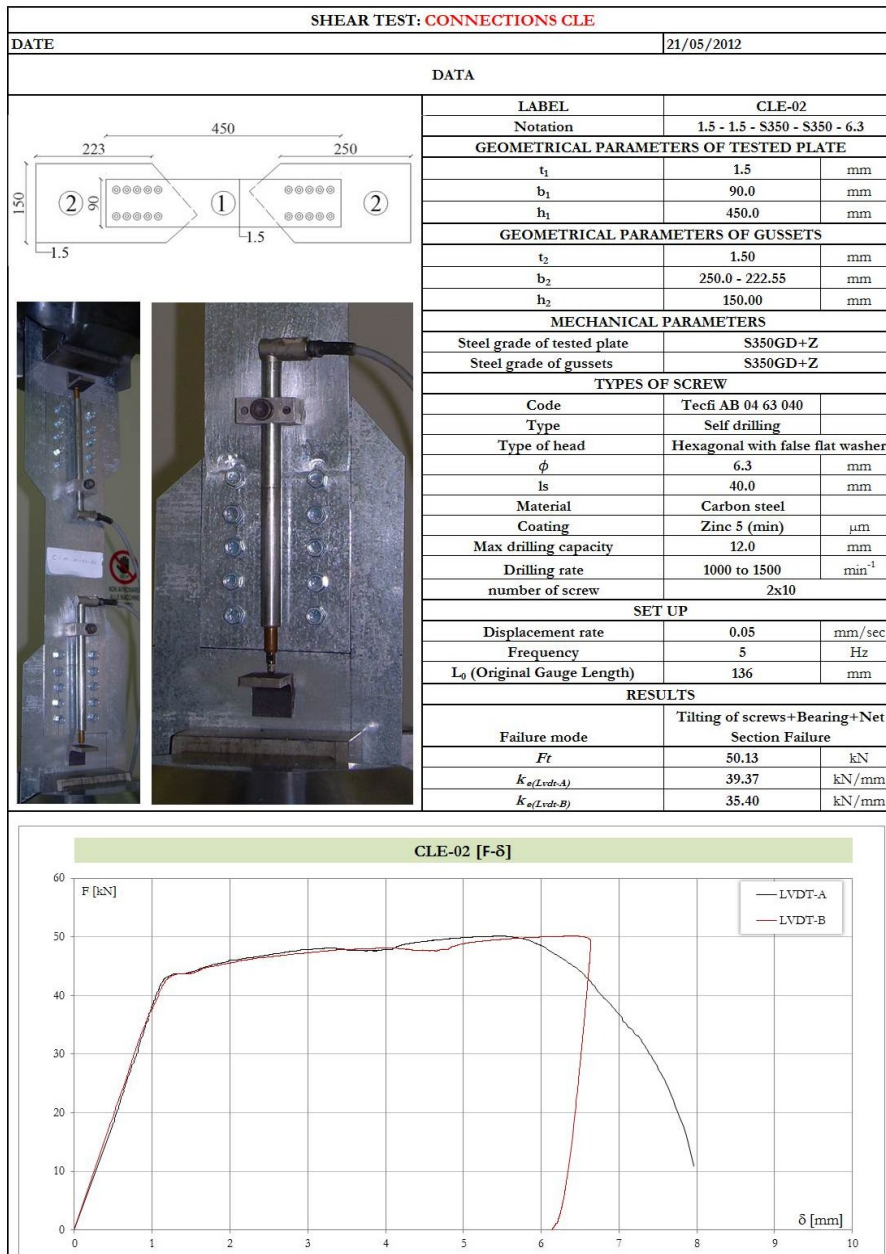
SHEAR TEST: JOINT SHD			
DATE		07/05/2012	
DATA			
	LABEL	SHD-01	
	Notation	1.5 - 2 - S350 - S250 - 6.3	
	GEOMETRICAL PARAMETERS OF PLATES		
	t_1	1.5	mm
	t_2	2.0	mm
	b_1	60.0	mm
	b_2	60.0	mm
	h_1	340.0	mm
	h_2	340.0	mm
	MECHANICAL PARAMETERS OF PLATES		
	Steel grade plate 1	S350GD+Z	
	Steel grade plate 2	S235	
	TYPES OF SCREW		
	Code	Tecfi AB 04 63 040	
	Type	Self drilling	
	Type of head	Hexagonal with false flat washer	
	ϕ	6.3	mm
	ls	40.0	mm
Material	Carbon steel		
Coating	Zinc 5 (min)	μm	
Max drilling capacity	12.0	mm	
Drilling rate	1000 to 1500	min^{-1}	
SET UP			
Displacement rate	0.05	mm/sec	
Frequency	5	Hz	
RESULTS			
Failure mode	Bearing + Tilting		
F_t	8.95	kN	
K_e	3.48	kN/mm	

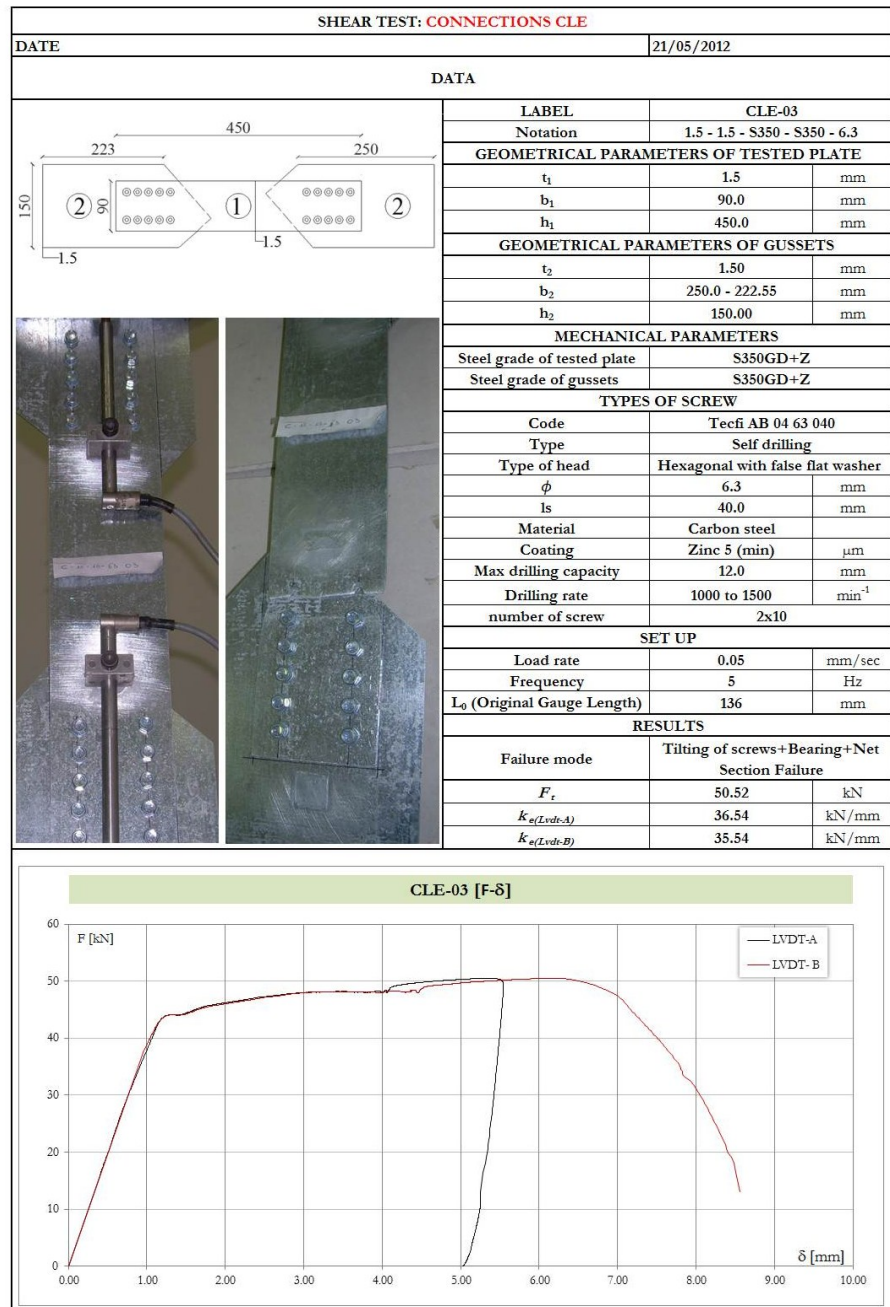
SHD-01 [F- δ]	
F [kN]	
	δ [mm]

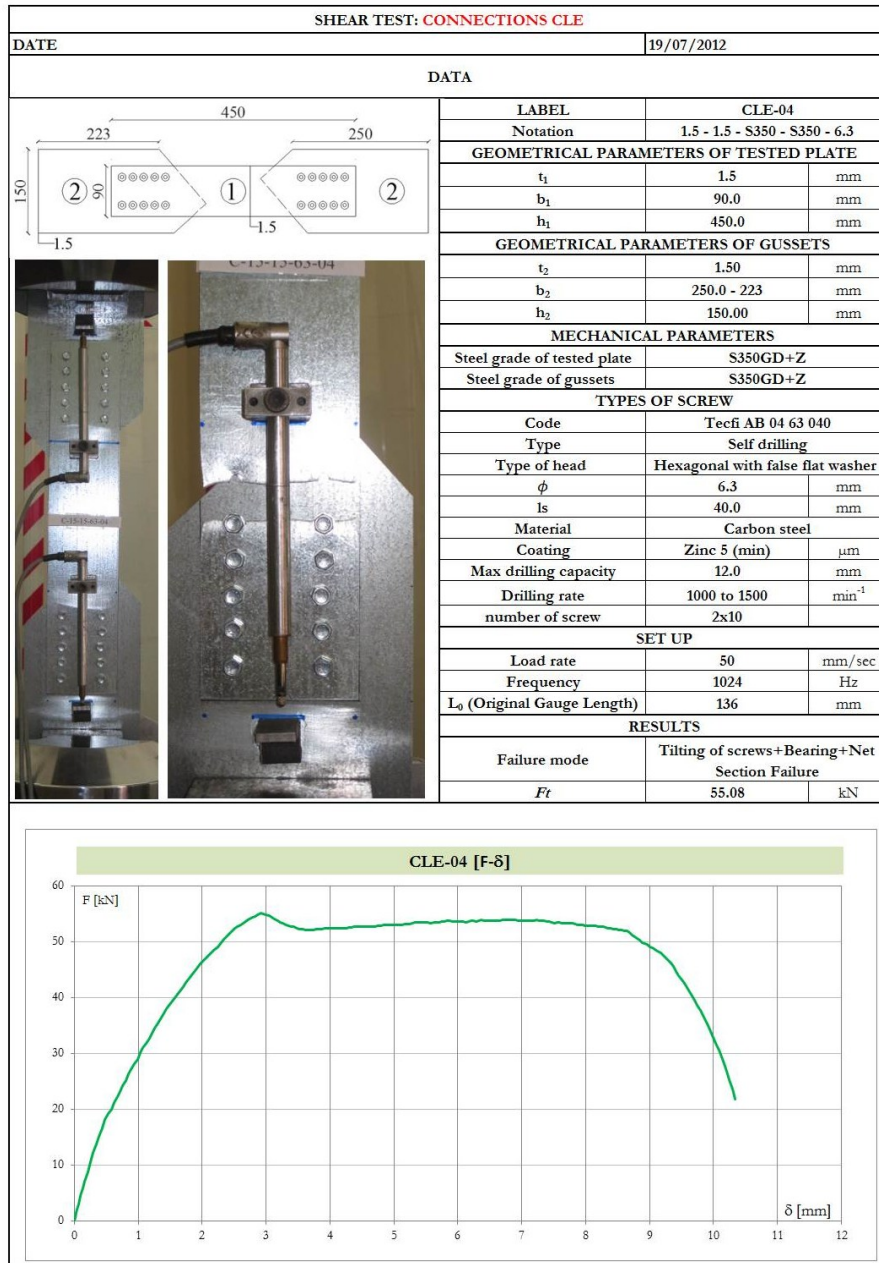


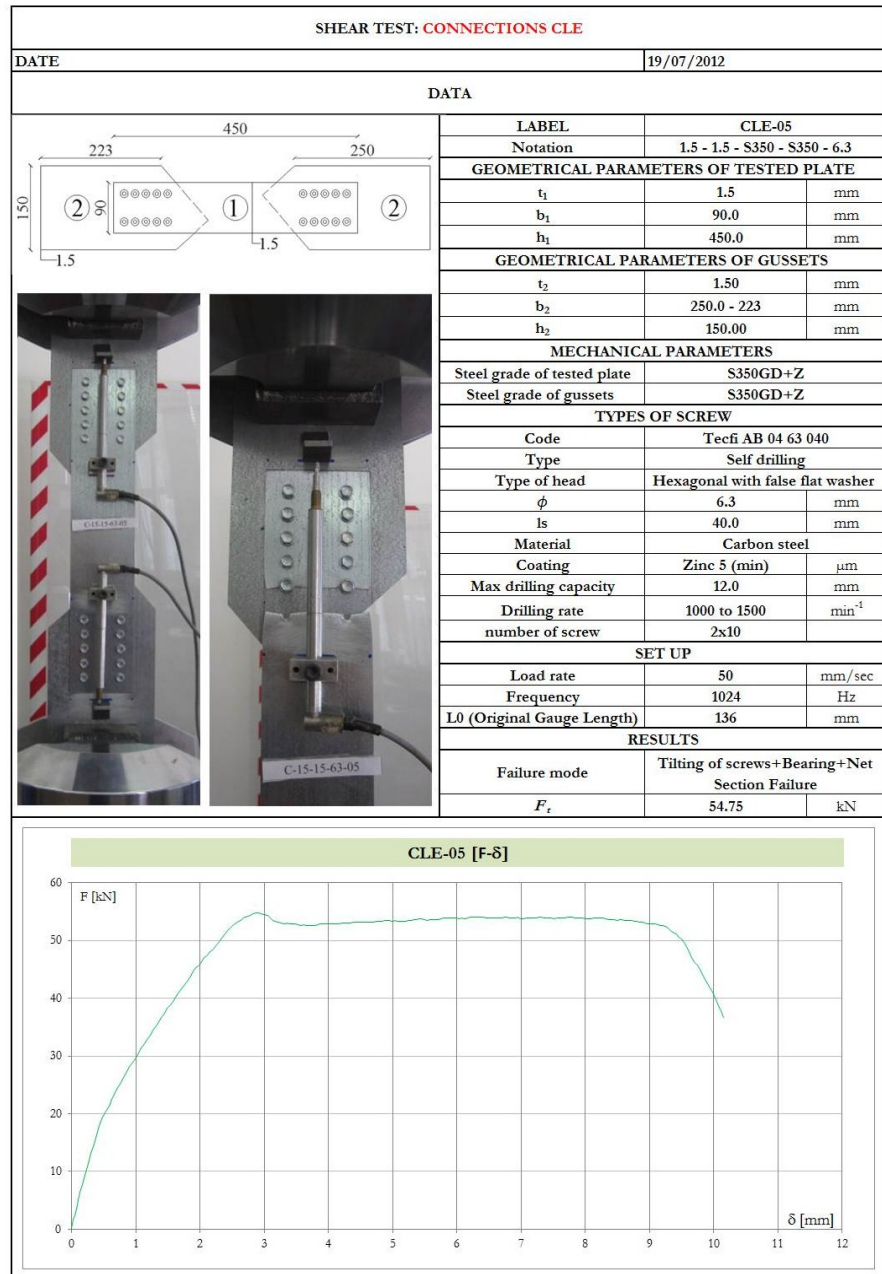
A.3 CONNECTIONS

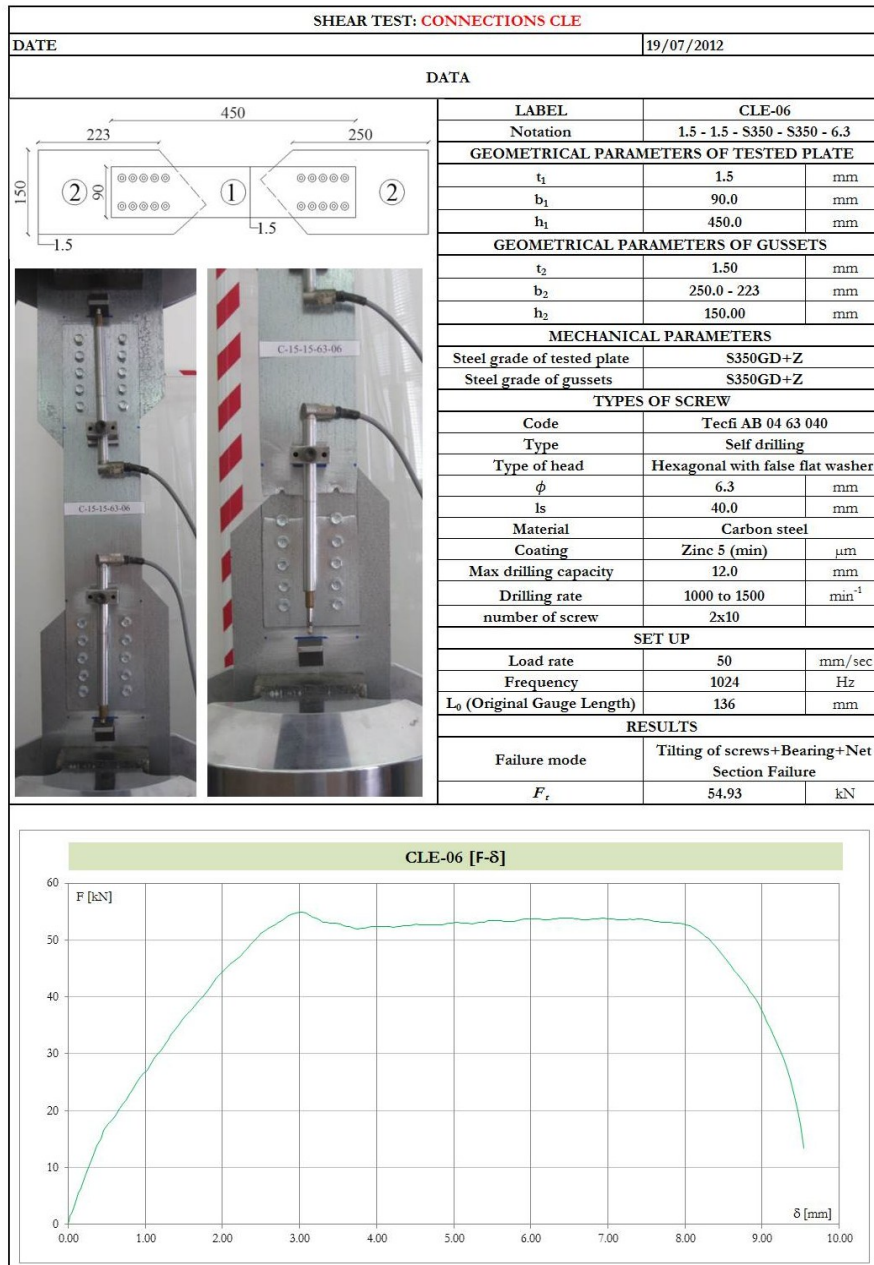


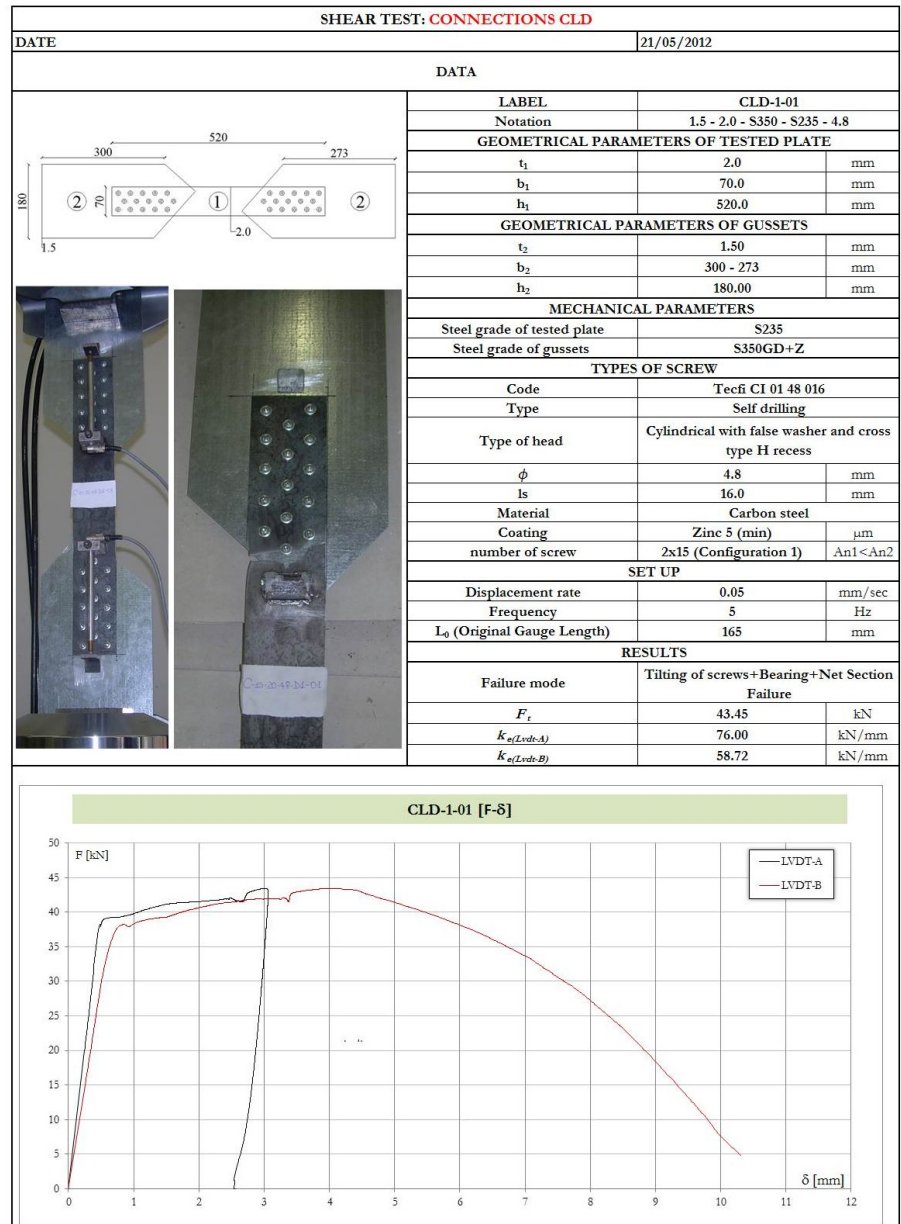


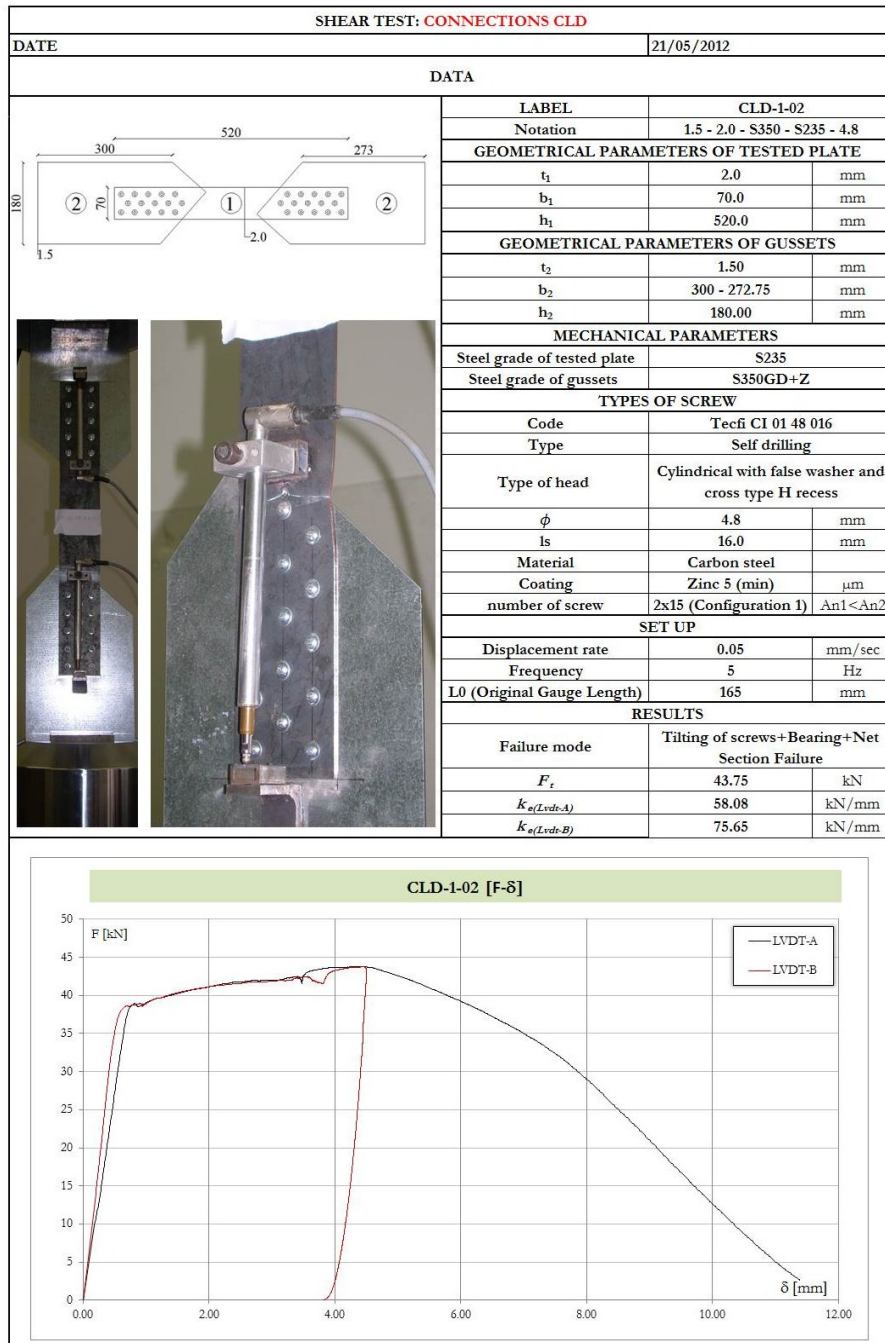


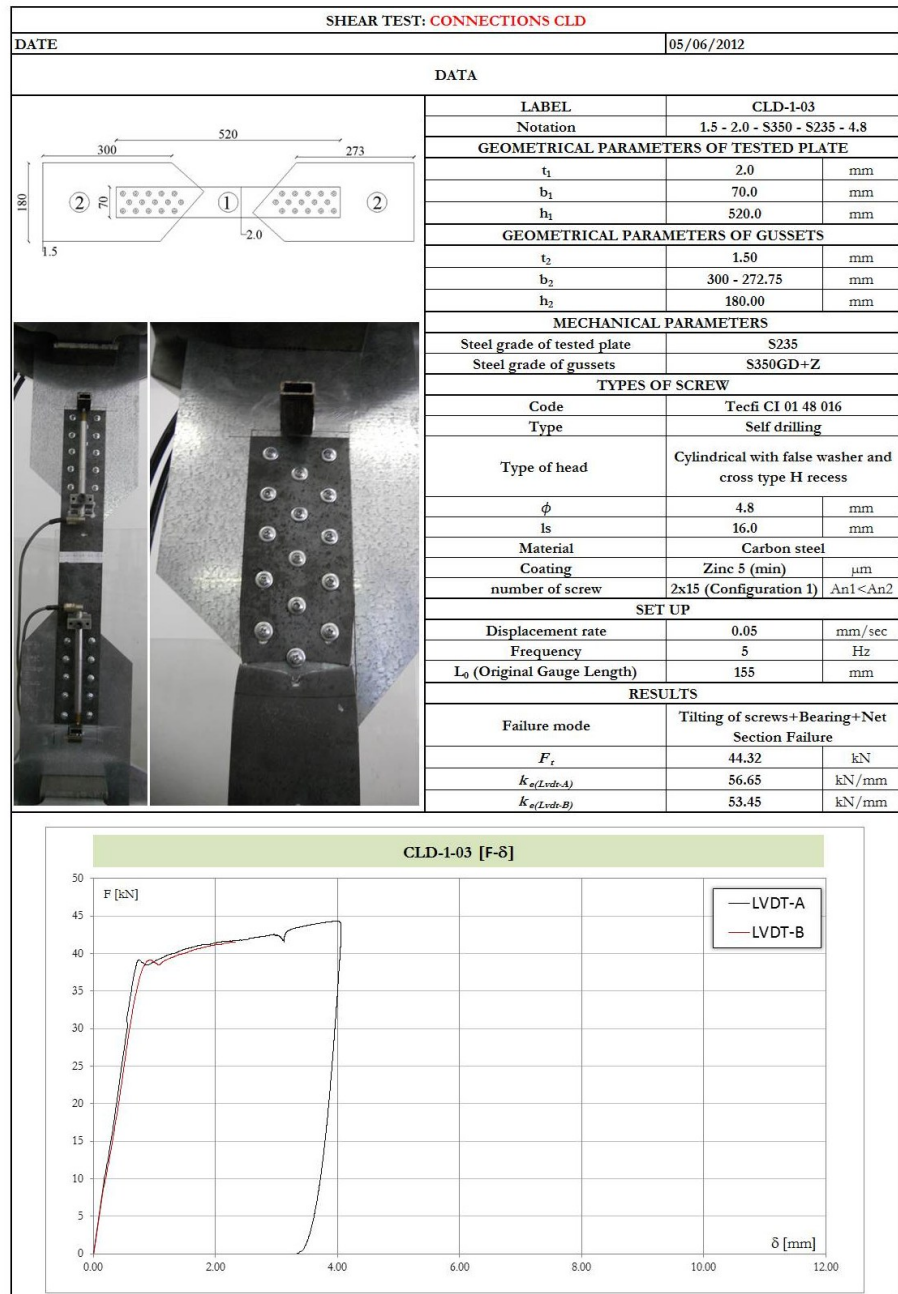


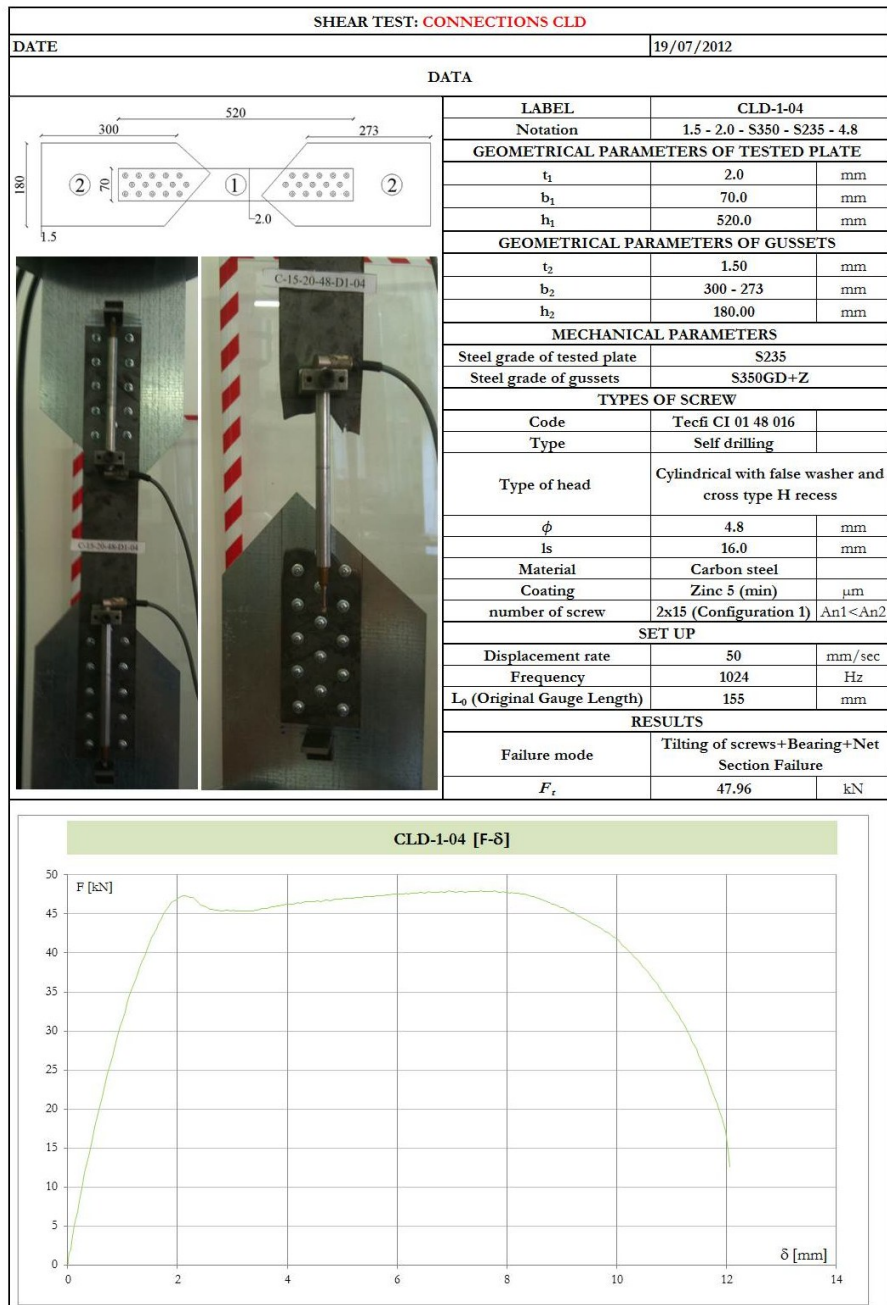


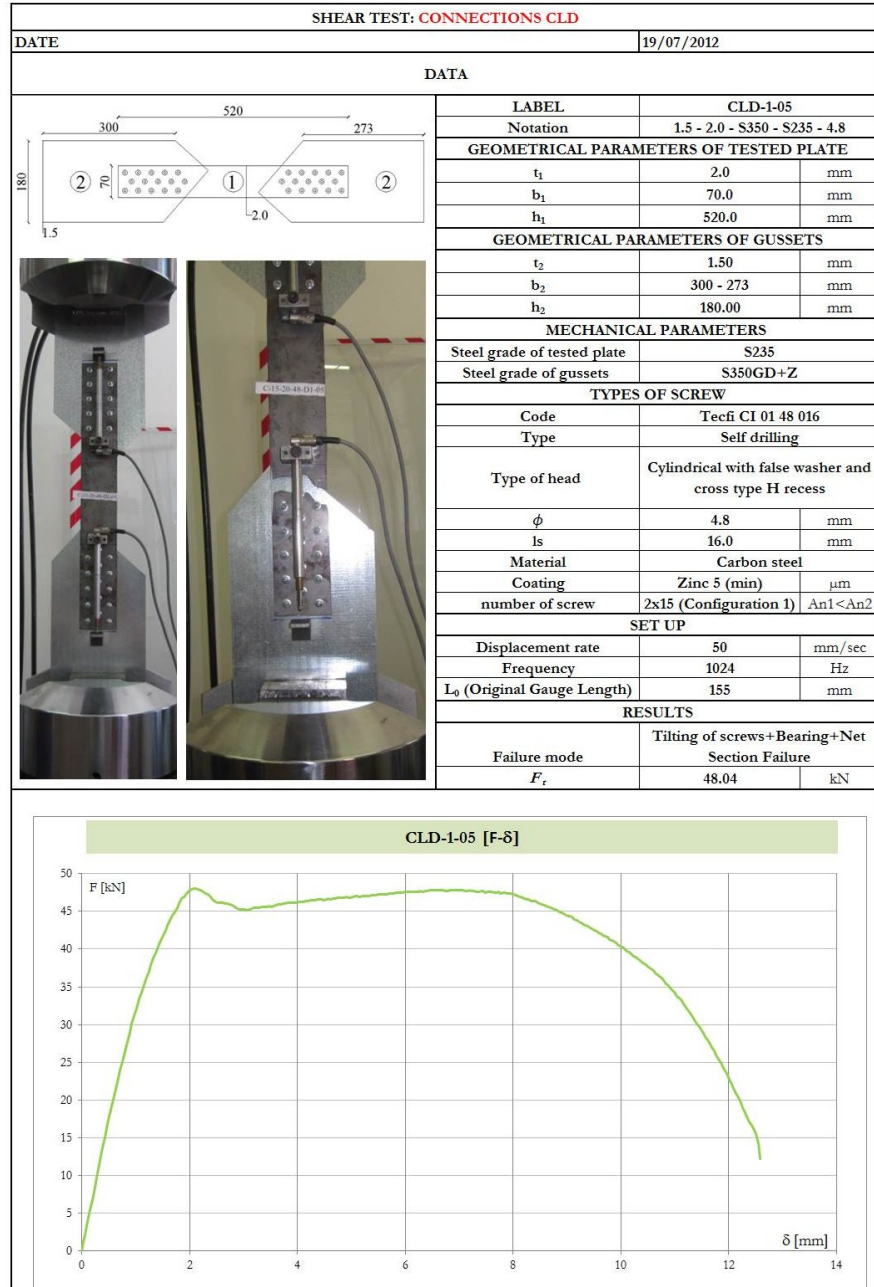


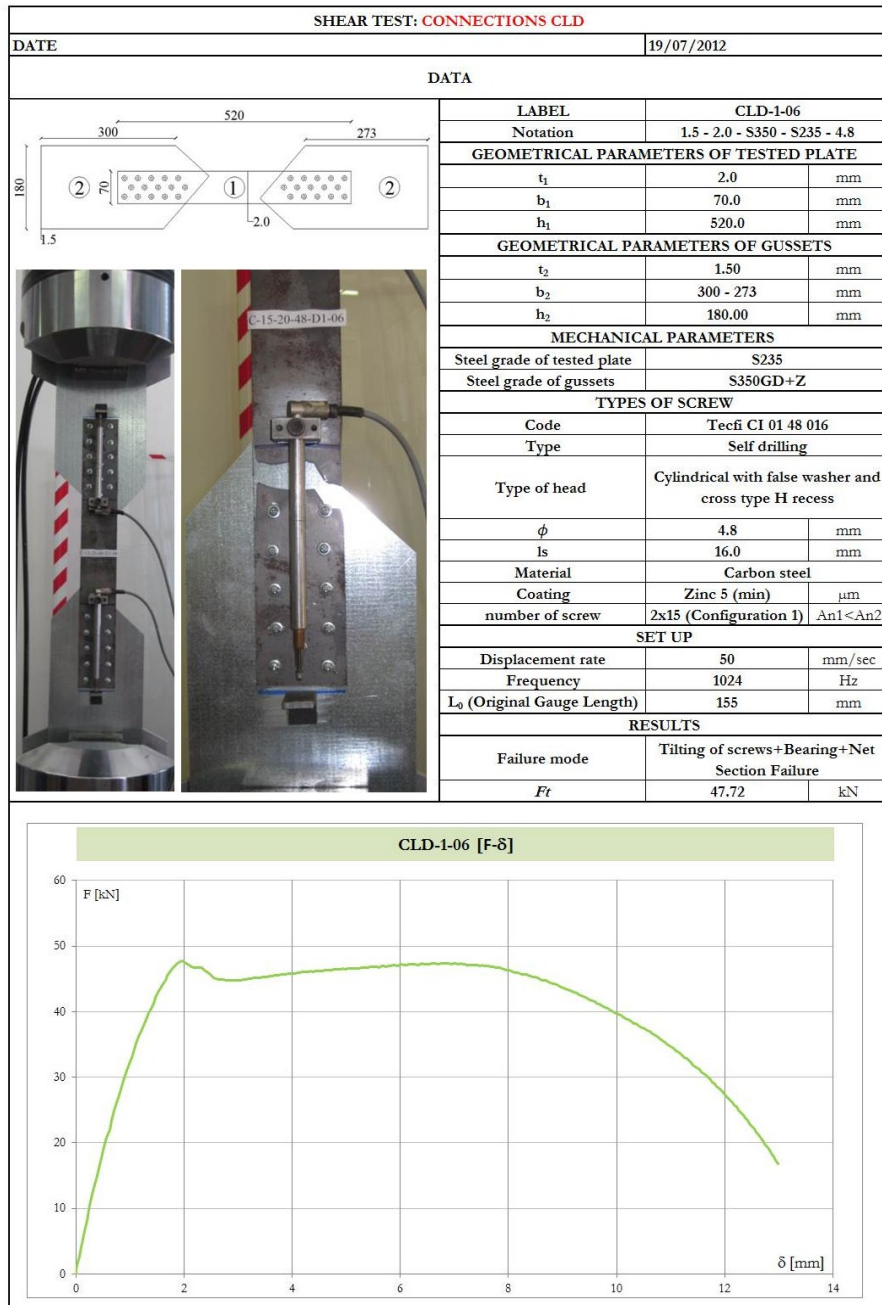


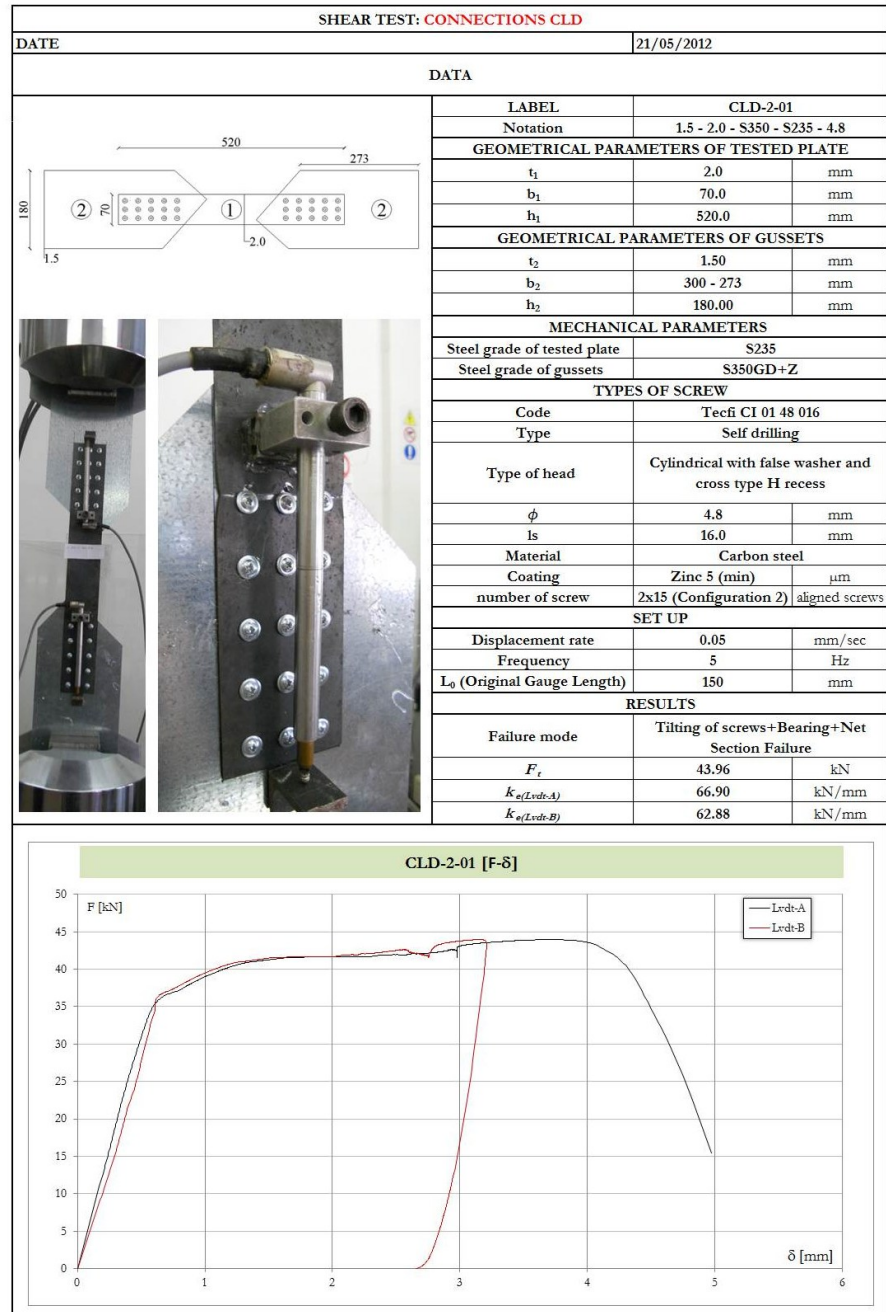


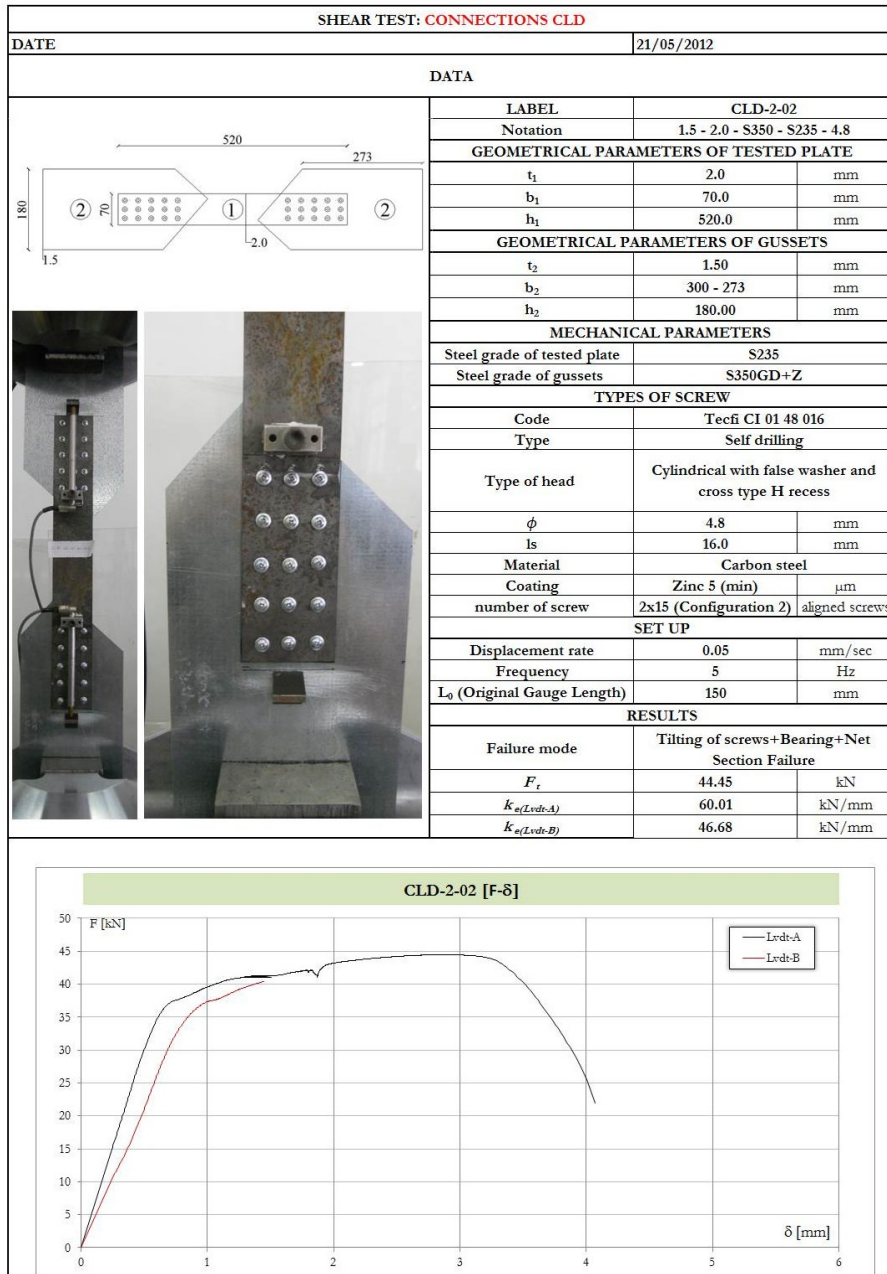


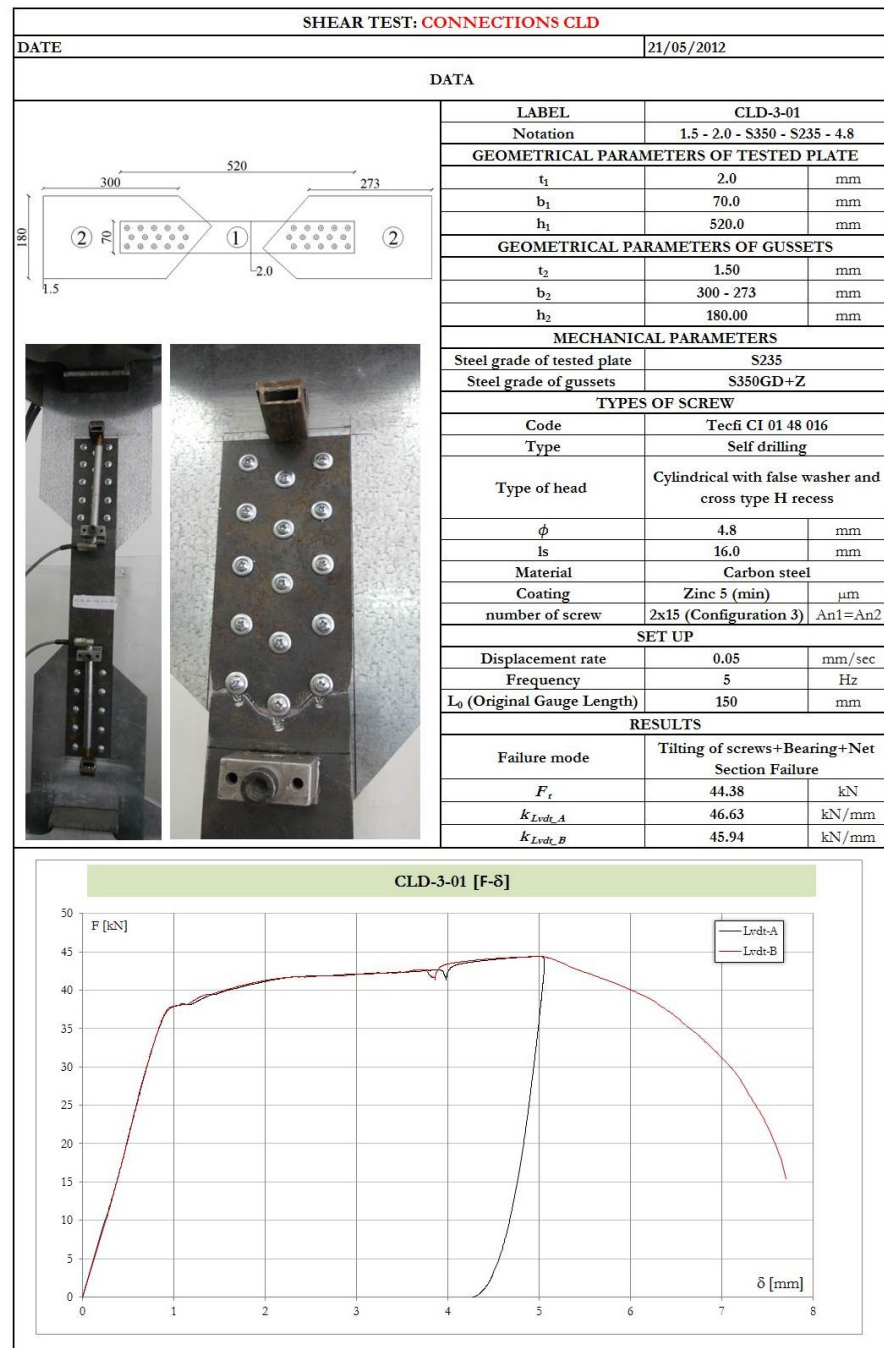


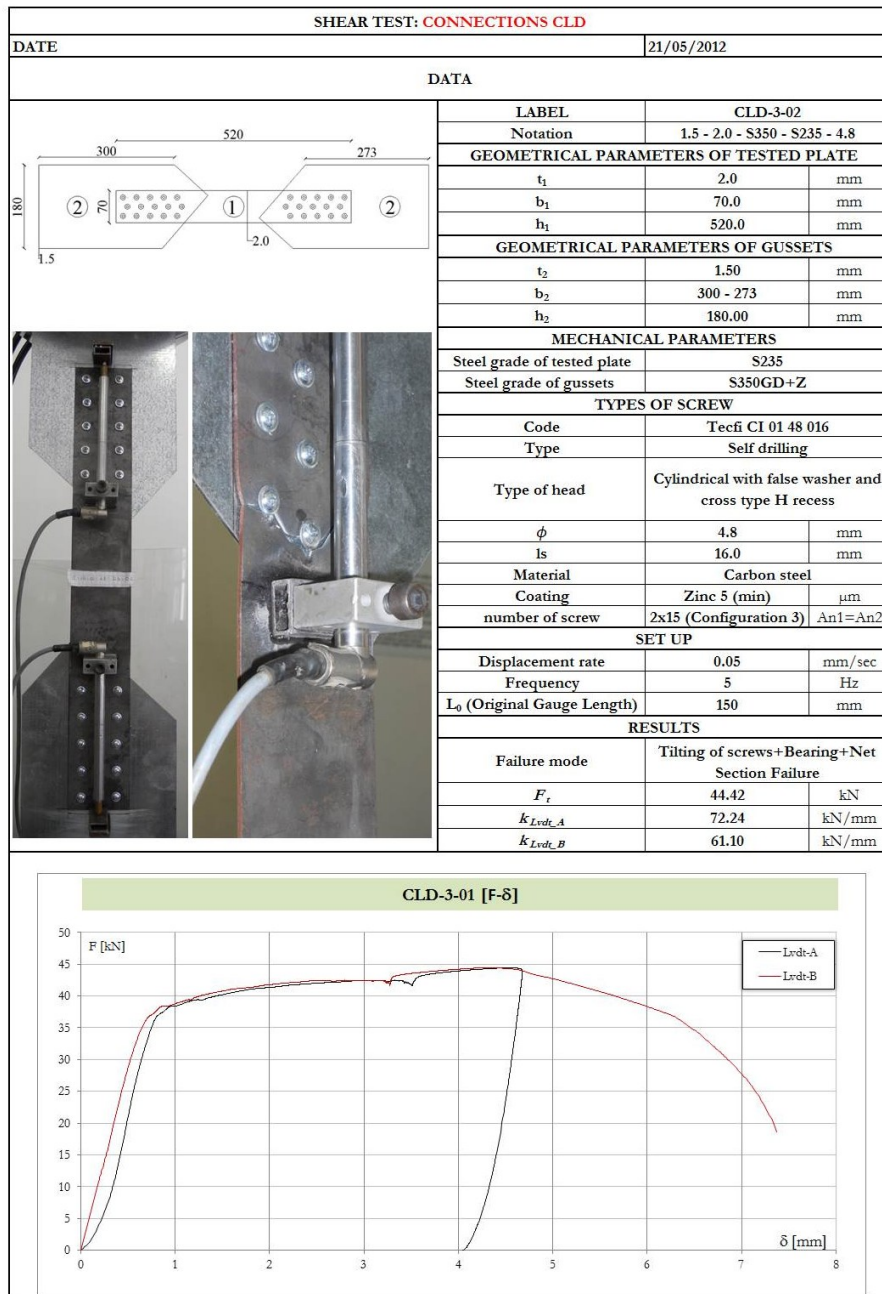


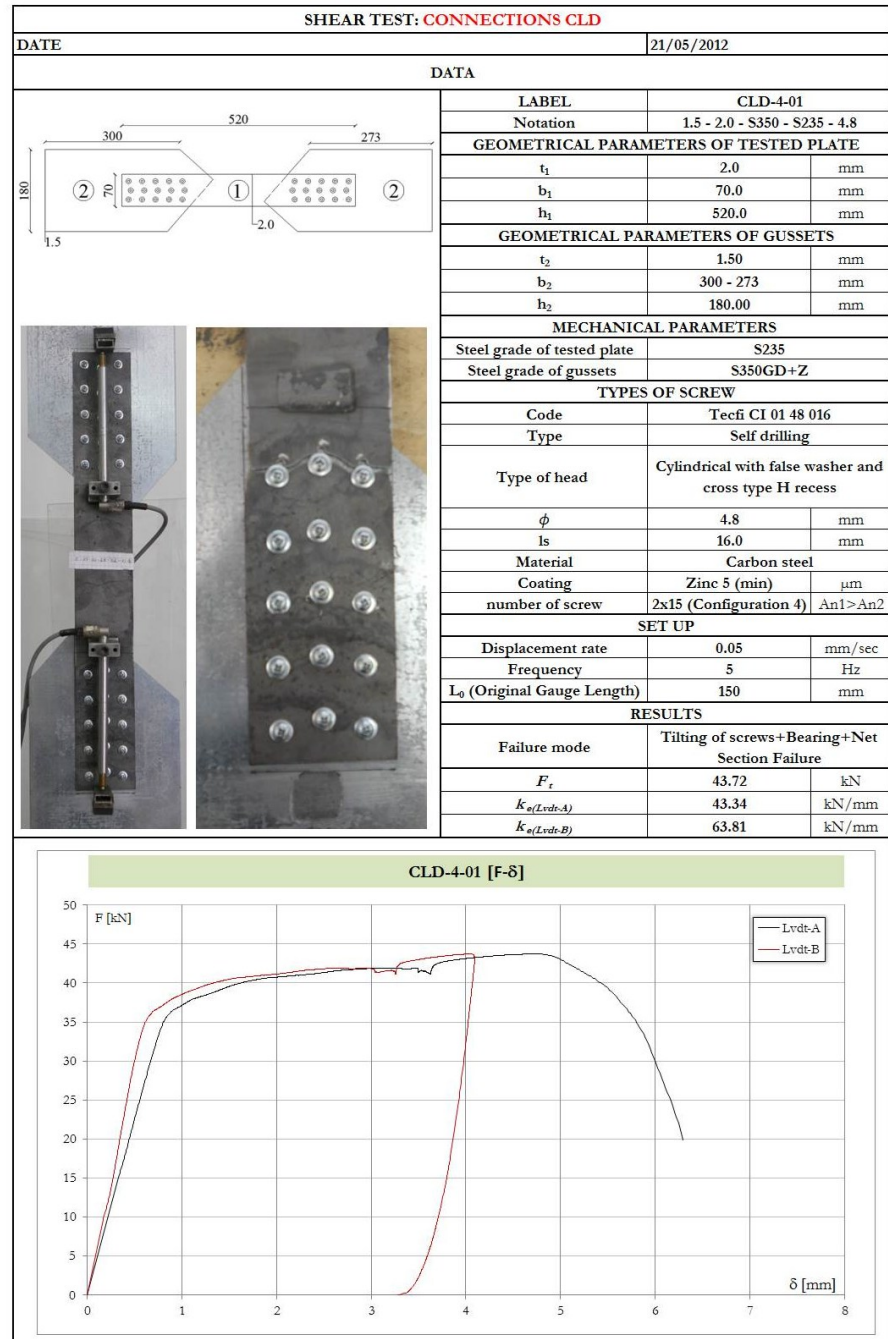


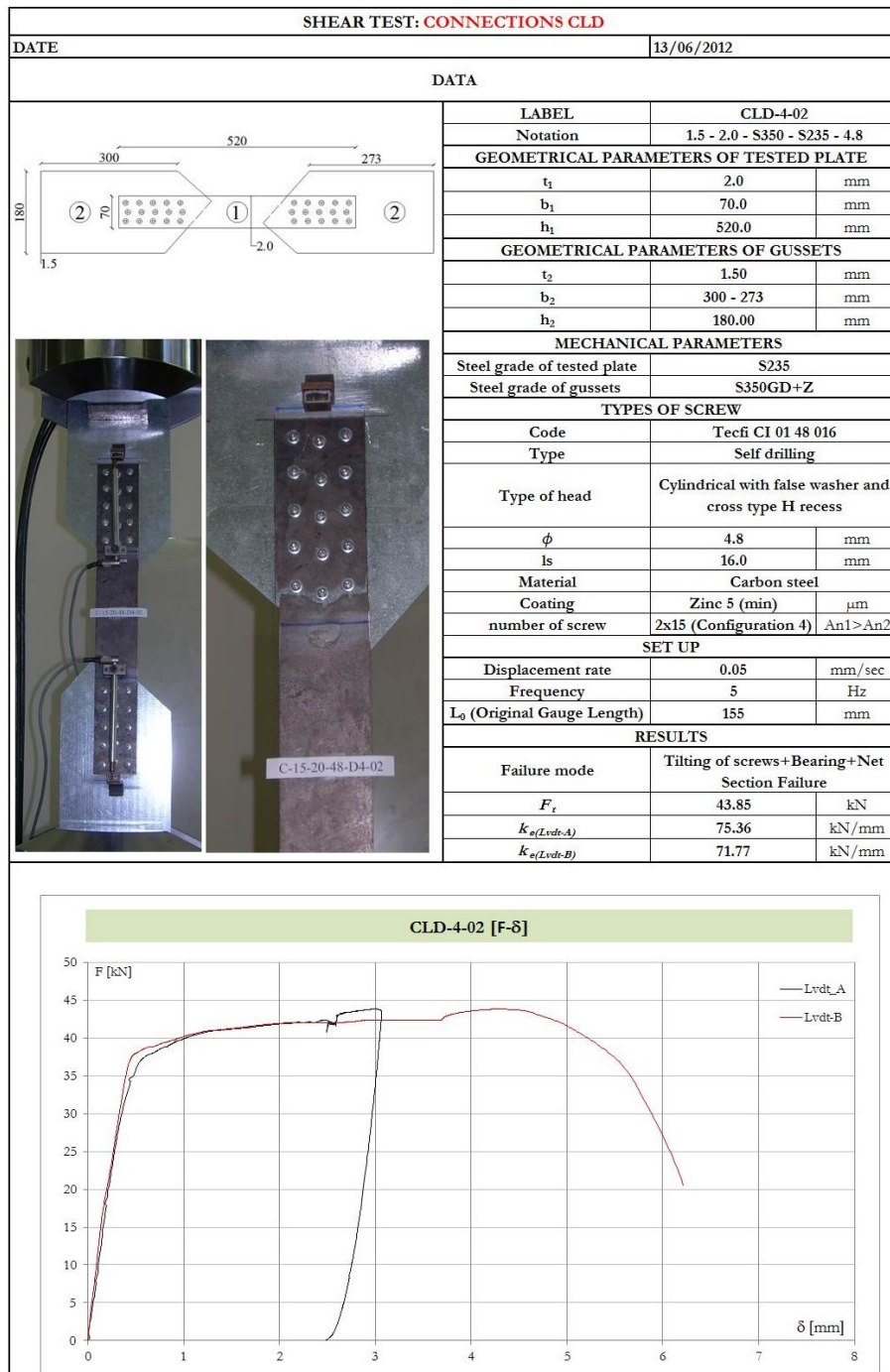


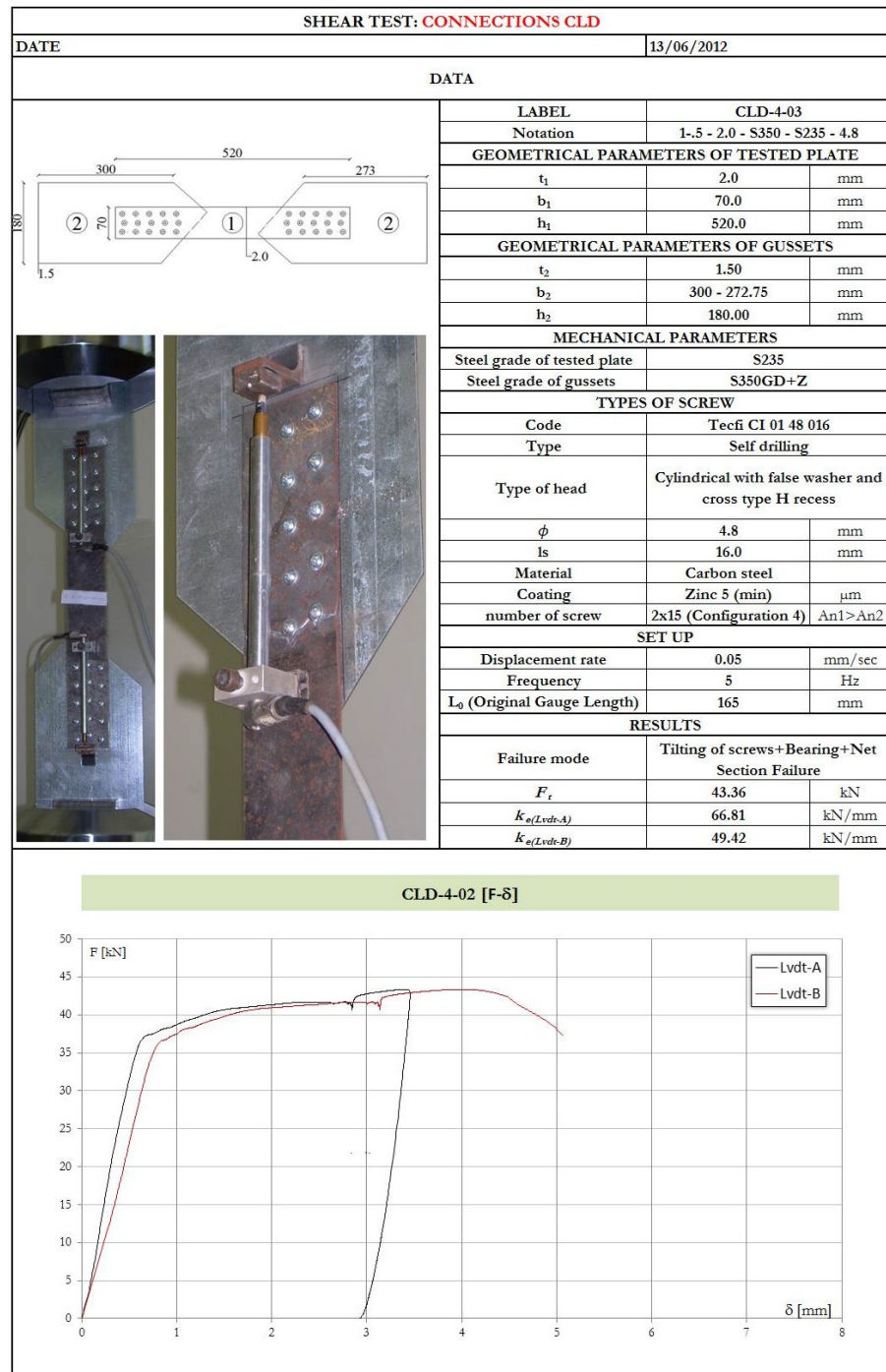


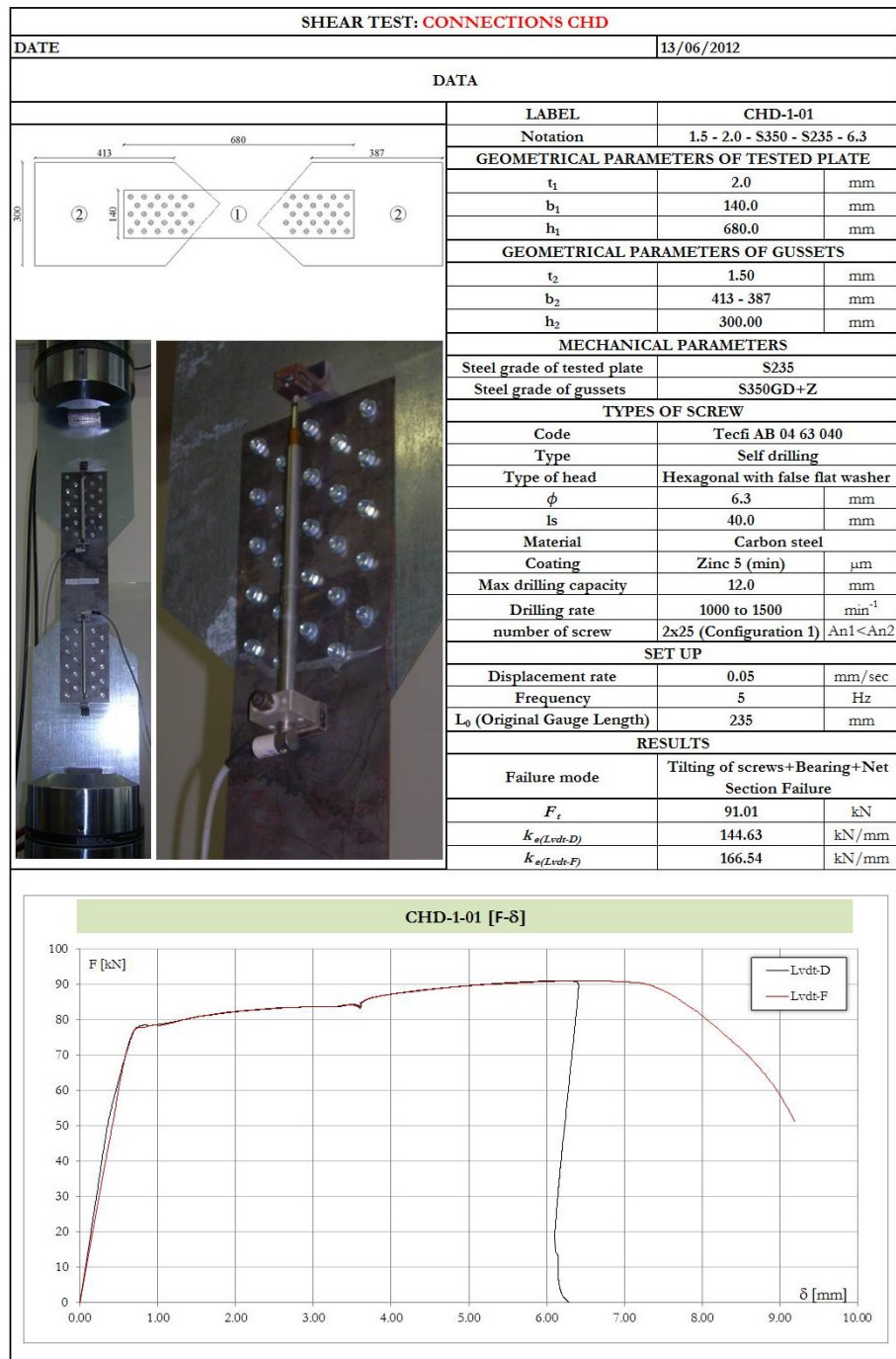












SHEAR TEST: CONNECTIONS CHD

DATE

13/06/2012

DATA

LABEL

CHD-1-02

Notation

1.5 - 2.0 - S350 - S235 - 6.3

GEOMETRICAL PARAMETERS OF TESTED PLATE

t_1	2.0	mm
b_1	140.0	mm
h_1	680.0	mm

GEOMETRICAL PARAMETERS OF GUSSETS

t_2	1.50	mm
b_2	412.61 - 386.99	mm
h_2	300.00	mm

MECHANICAL PARAMETERS

Steel grade of tested plate S235

Steel grade of gussets S350GD+Z

TYPES OF SCREW

Code Tecfi AB 04 63 040

Type Self drilling

Type of head Hexagonal with false flat washer

ϕ 6.3 mm

ls 40.0 mm

Material Carbon steel

Coating Zinc 5 (min) μm

Max drilling capacity 12.0 mm

Drilling rate 1000 to 1500 min^{-1}

number of screw 2x25 (Configuration 1) An1 < An2

SET UP

Displacement rate 0.05 mm/sec

Frequency 5 Hz

L_0 (Original Gauge Length) 235 mm

RESULTS

Failure mode

Tilting of screws+Bearing+Net Section Failure

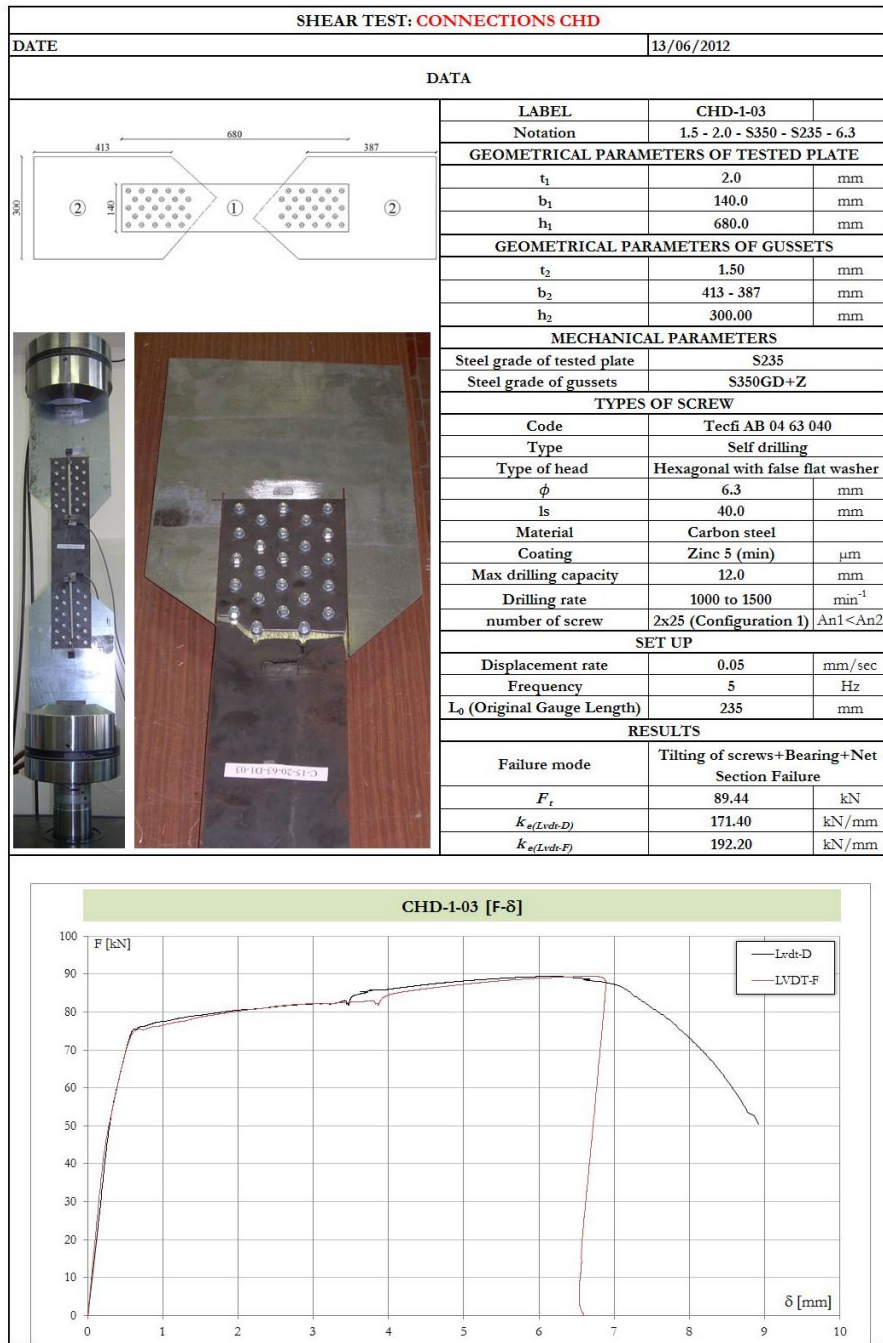
F_t 90.54 kN

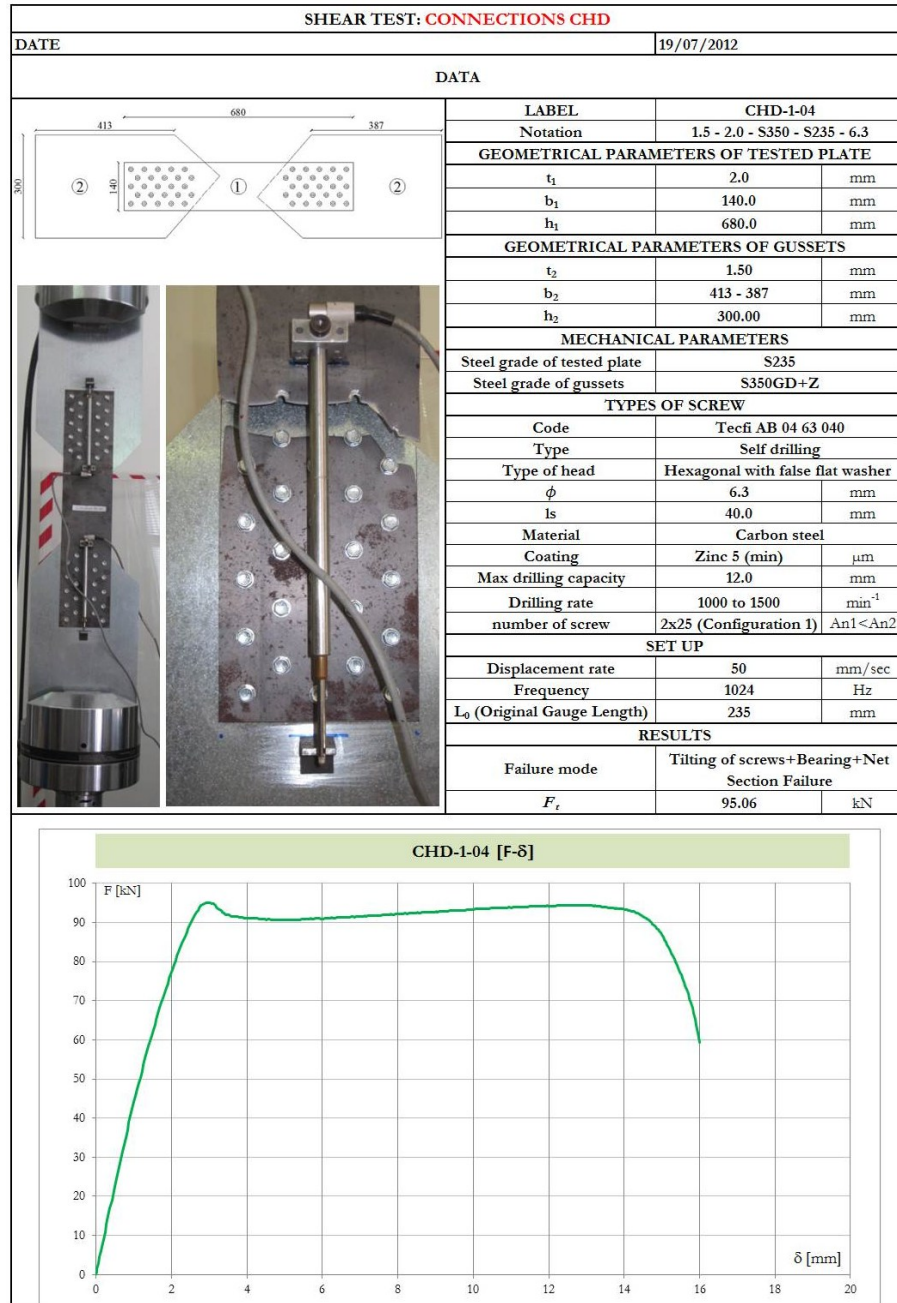
$K_{e(Lvdt-D)}$ 163.73 kN/mm

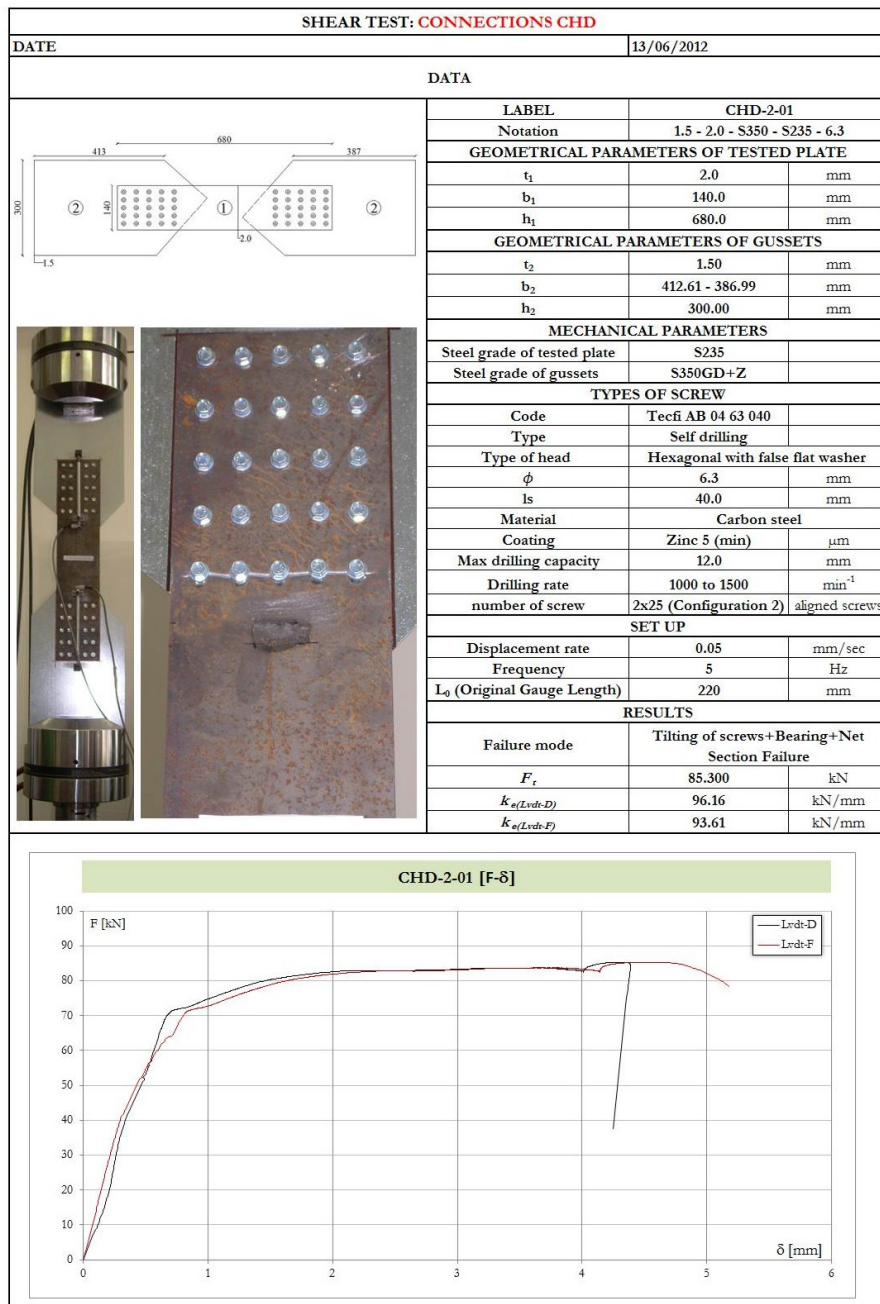
$K_{e(Lvdt-F)}$ 159.66 kN/mm

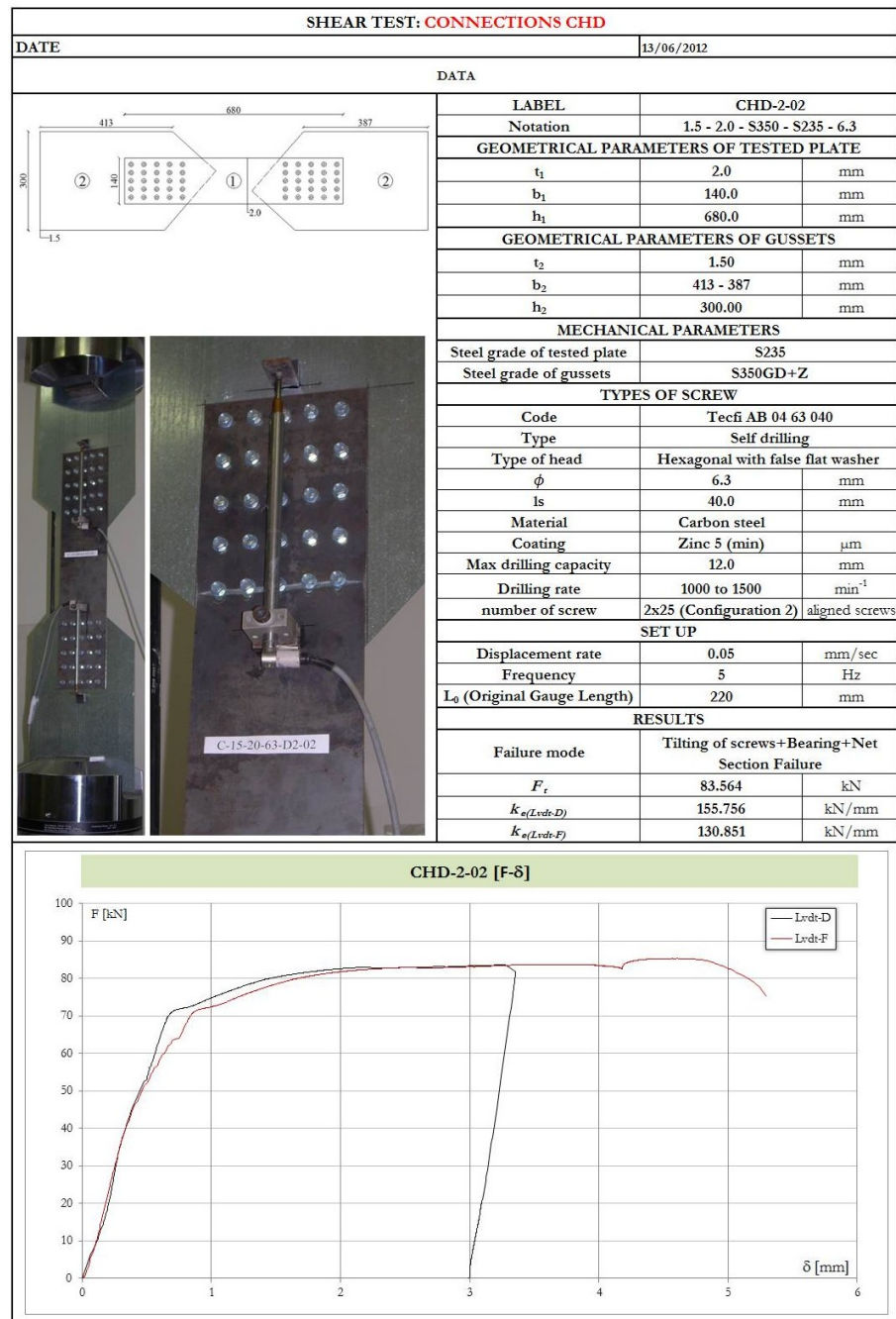
CHD-1-02 [F- δ]

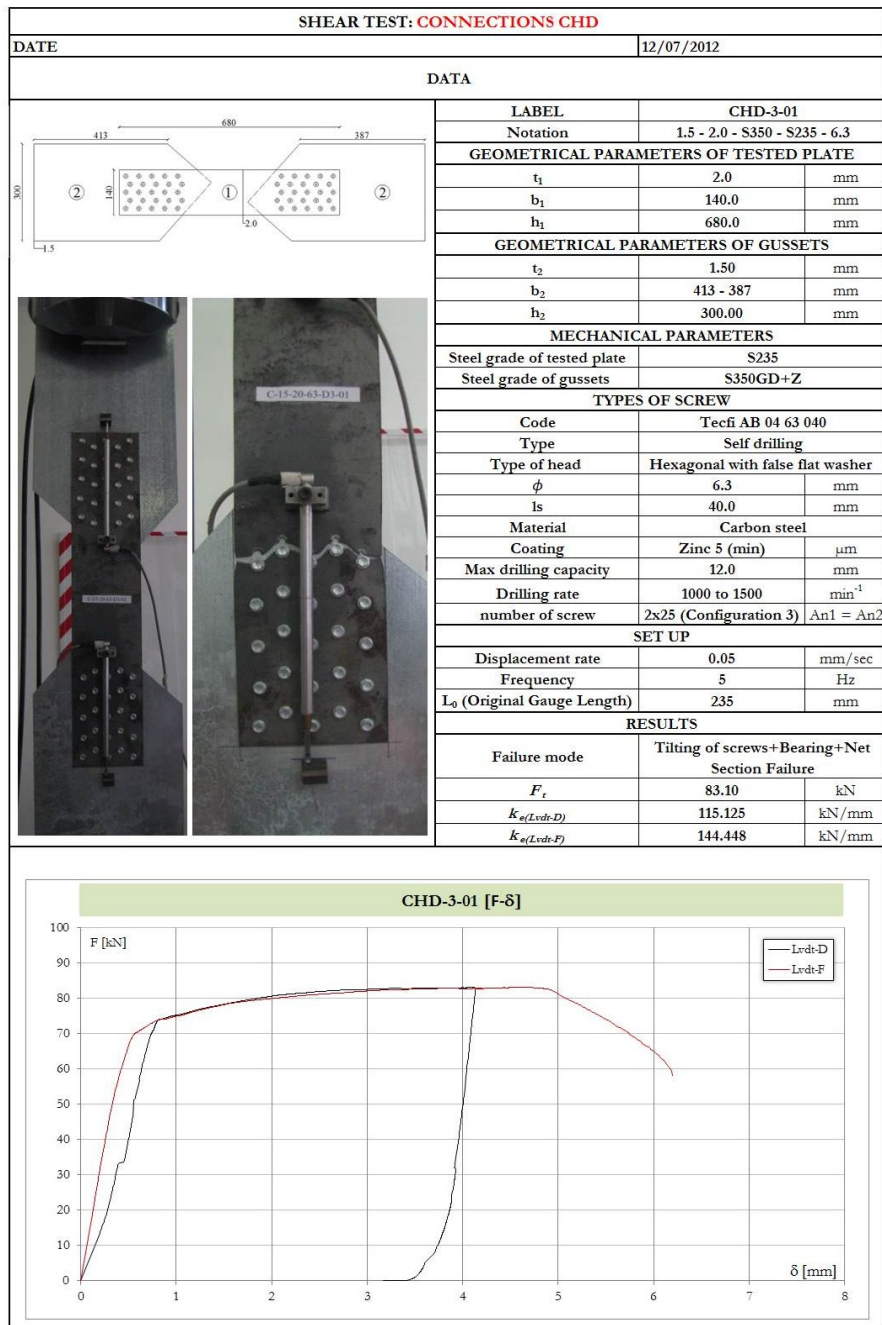
Displacement δ [mm]	Force F [kN] (LVDT-D)	Force F [kN] (Lvdt-F)
0	0	0
0.5	75	75
1.0	78	78
2.0	80	80
3.0	82	82
4.0	85	85
5.0	88	88
6.0	90	90
6.5	90	90
7.0	85	85
8.0	75	75
9.0	55	55

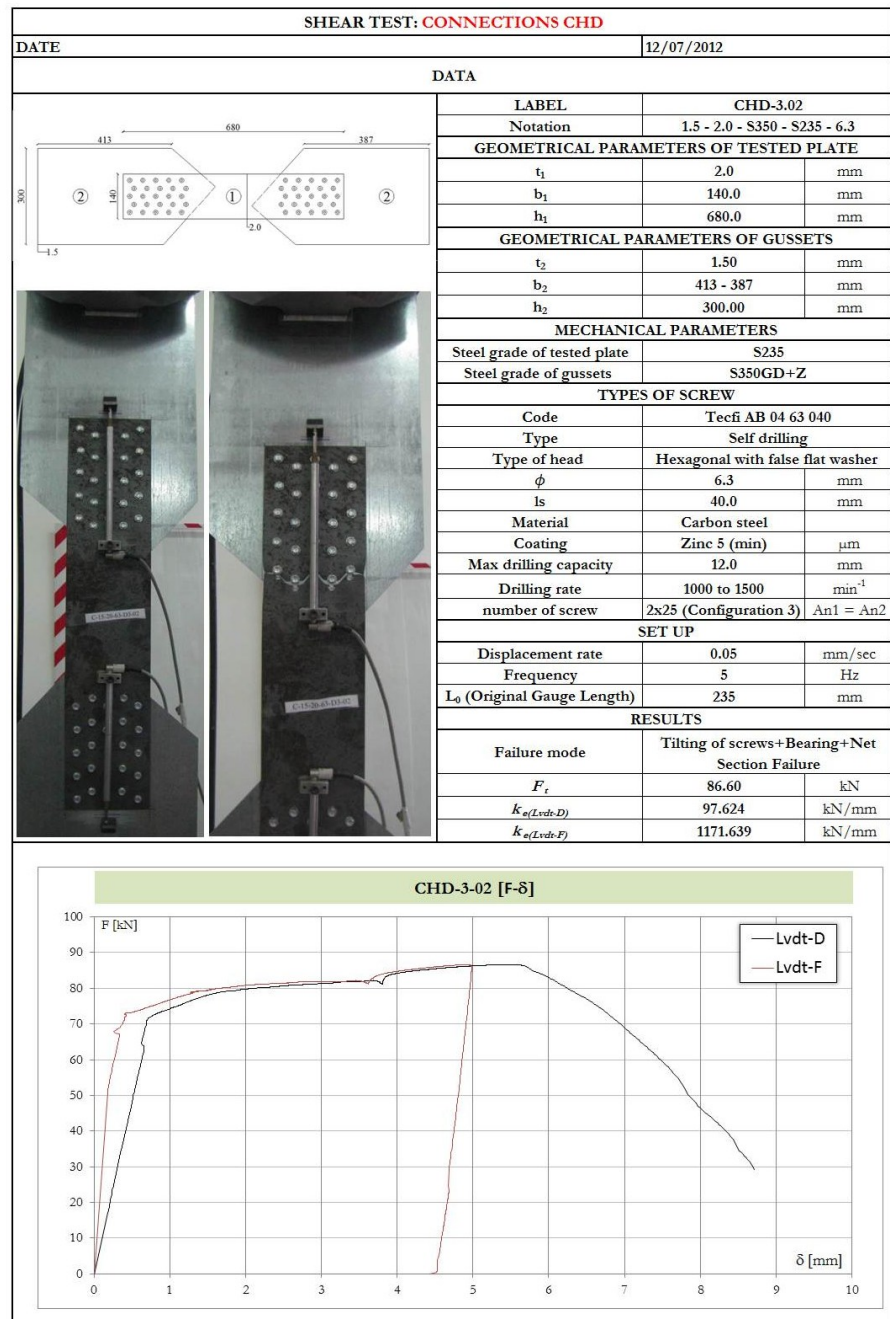


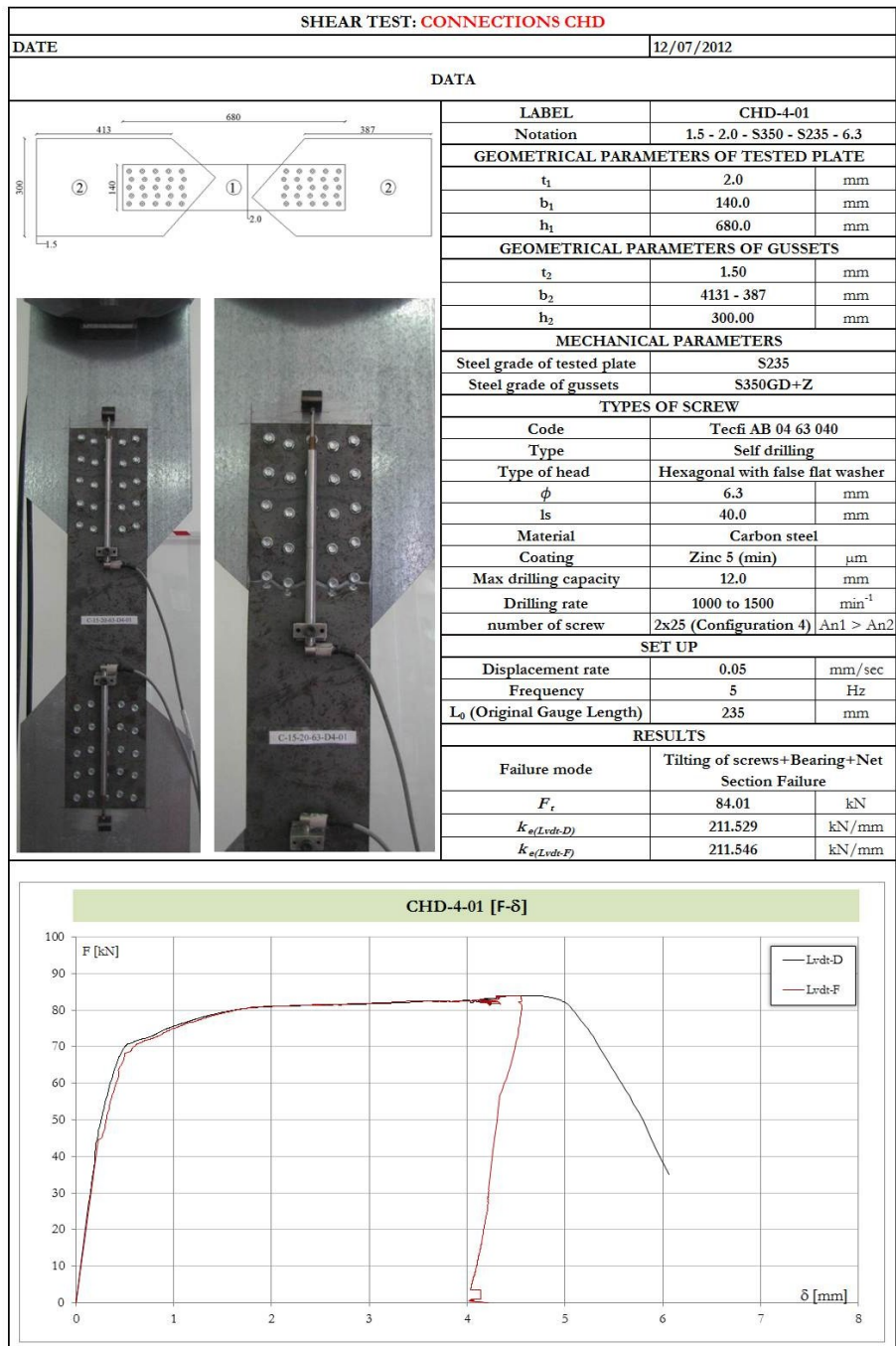


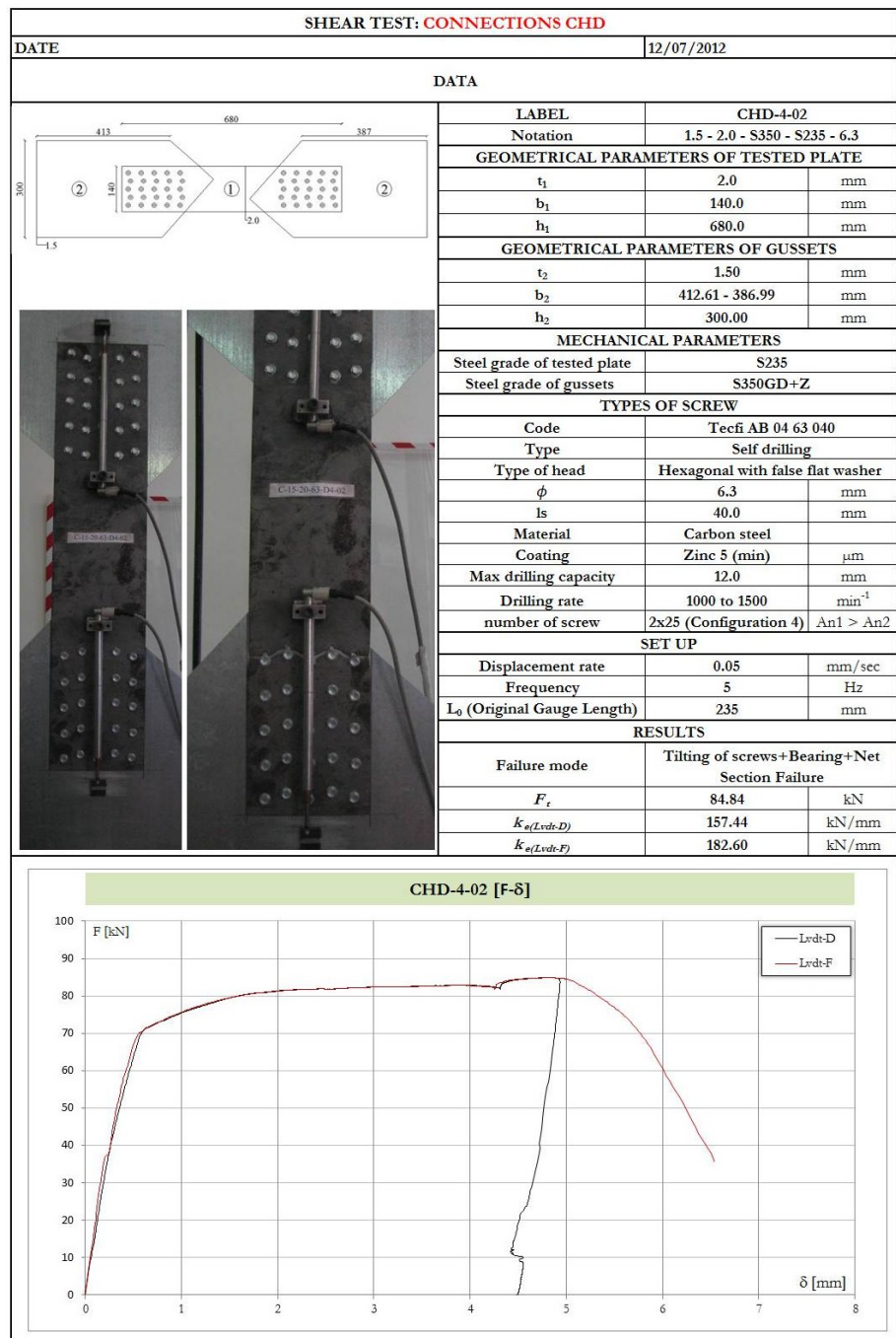






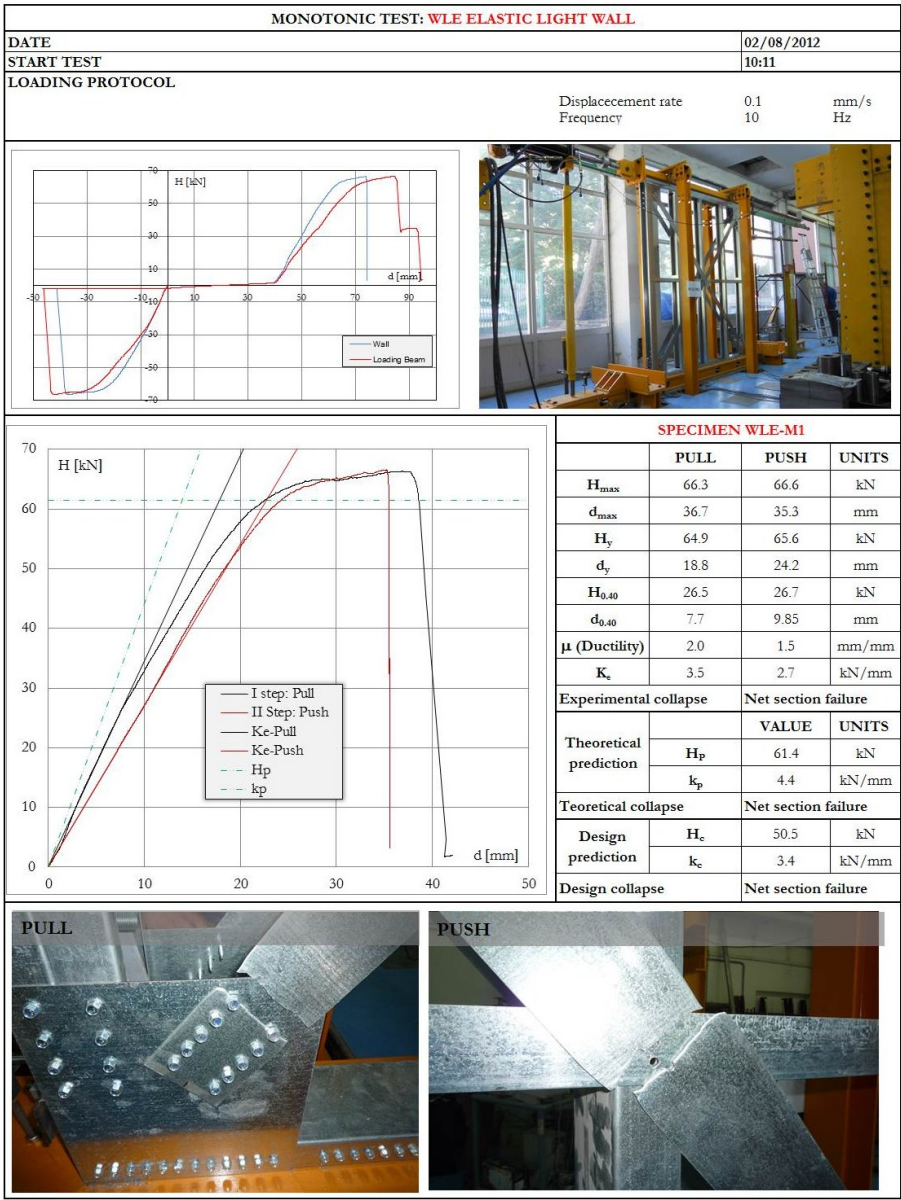


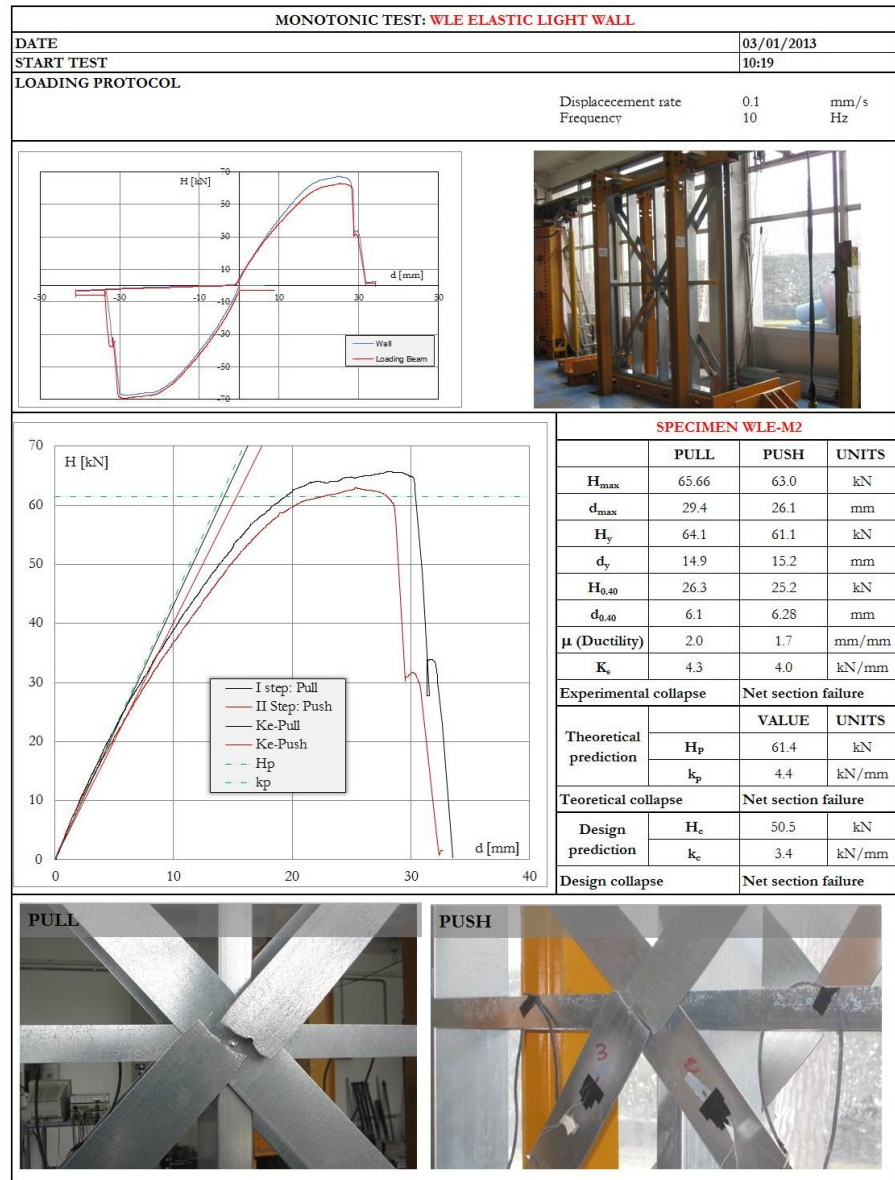


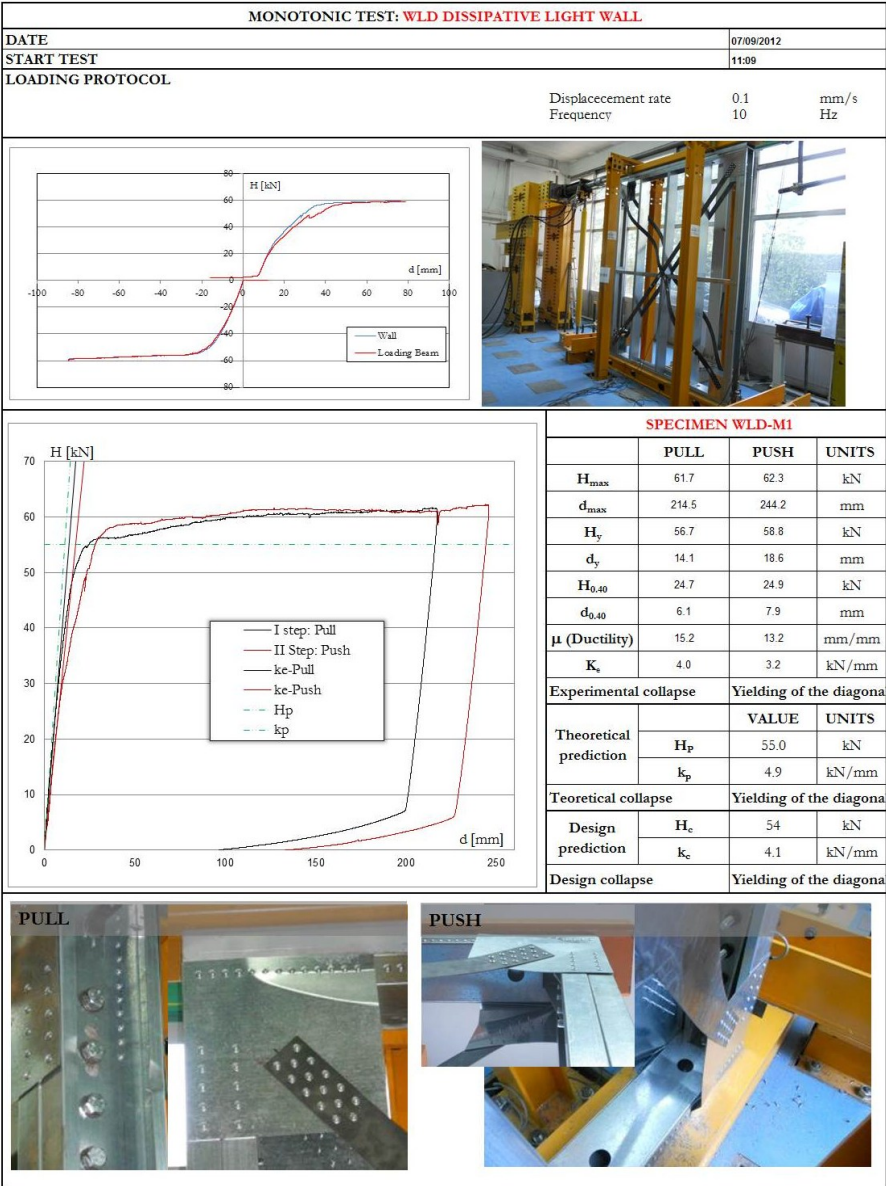


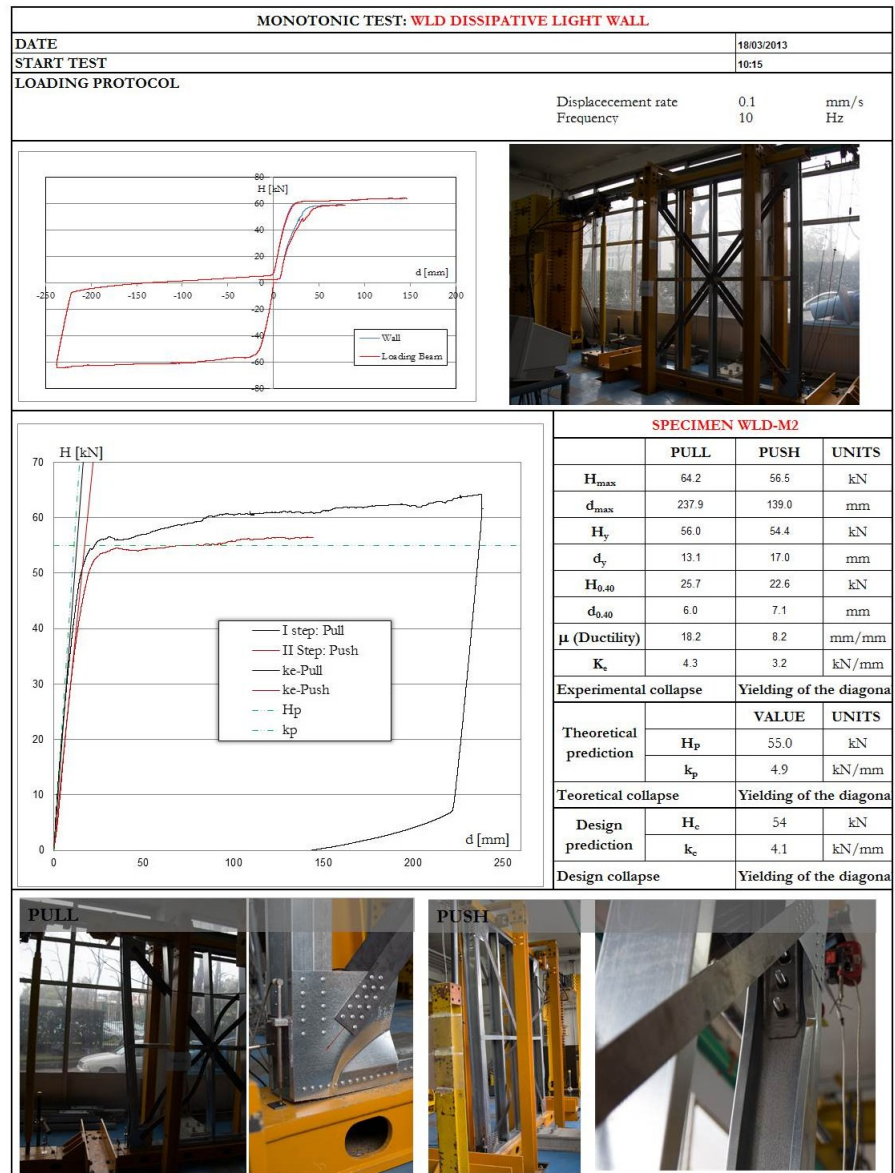
Appendix B: Tests on Walls

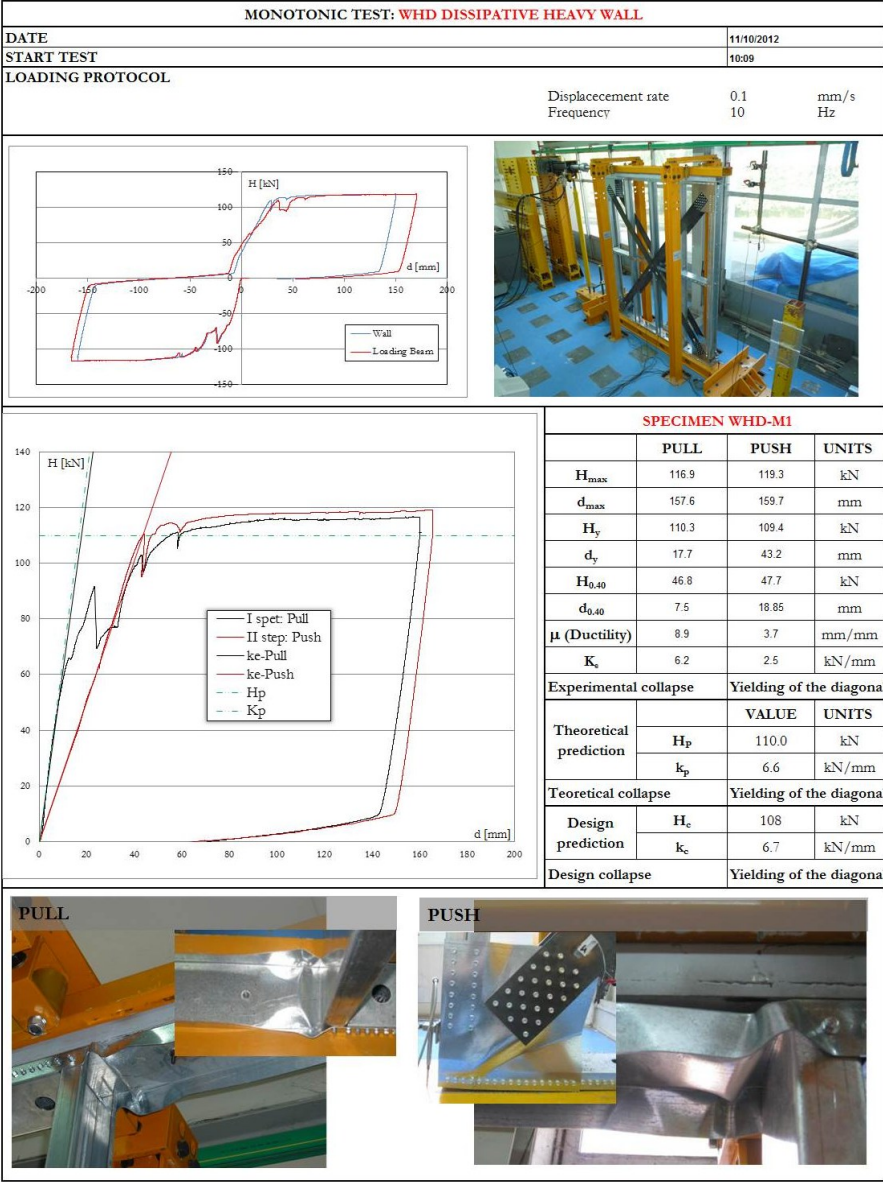
B.1 MONOTONIC TESTS

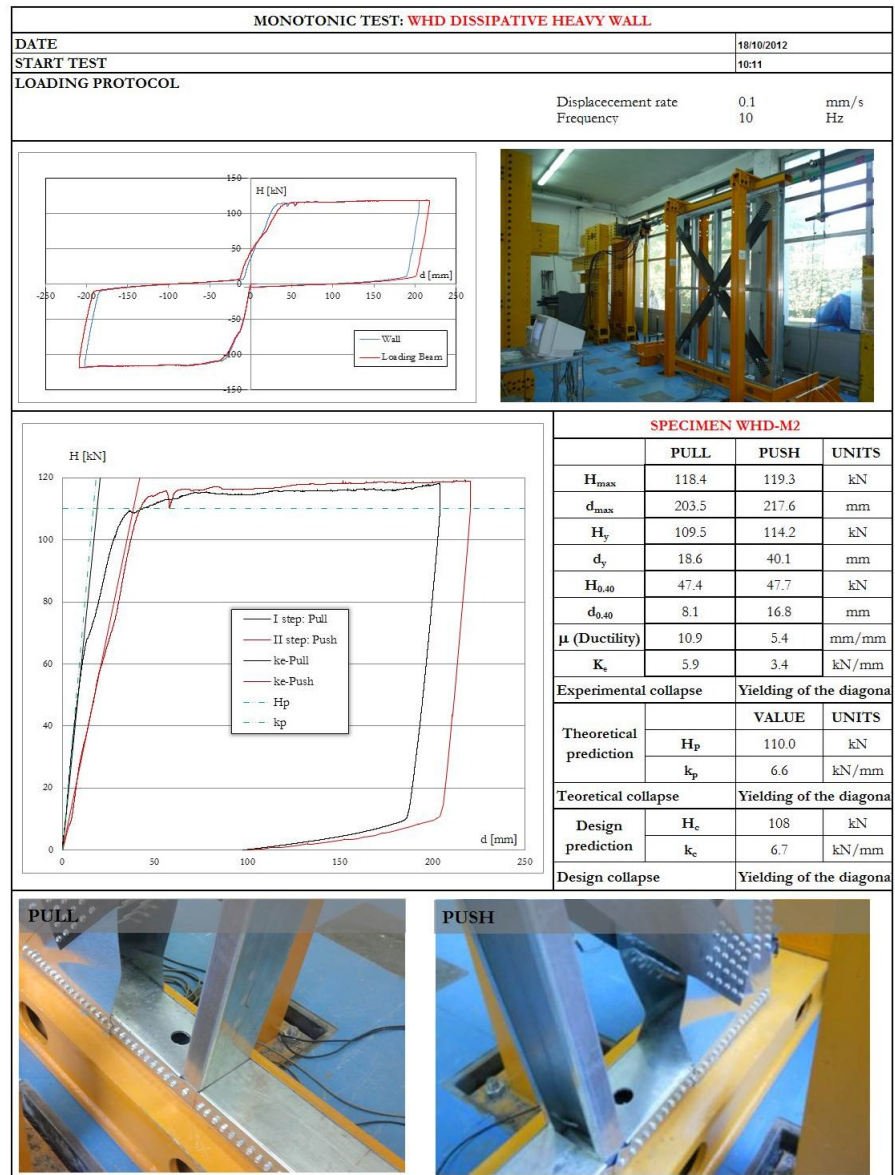




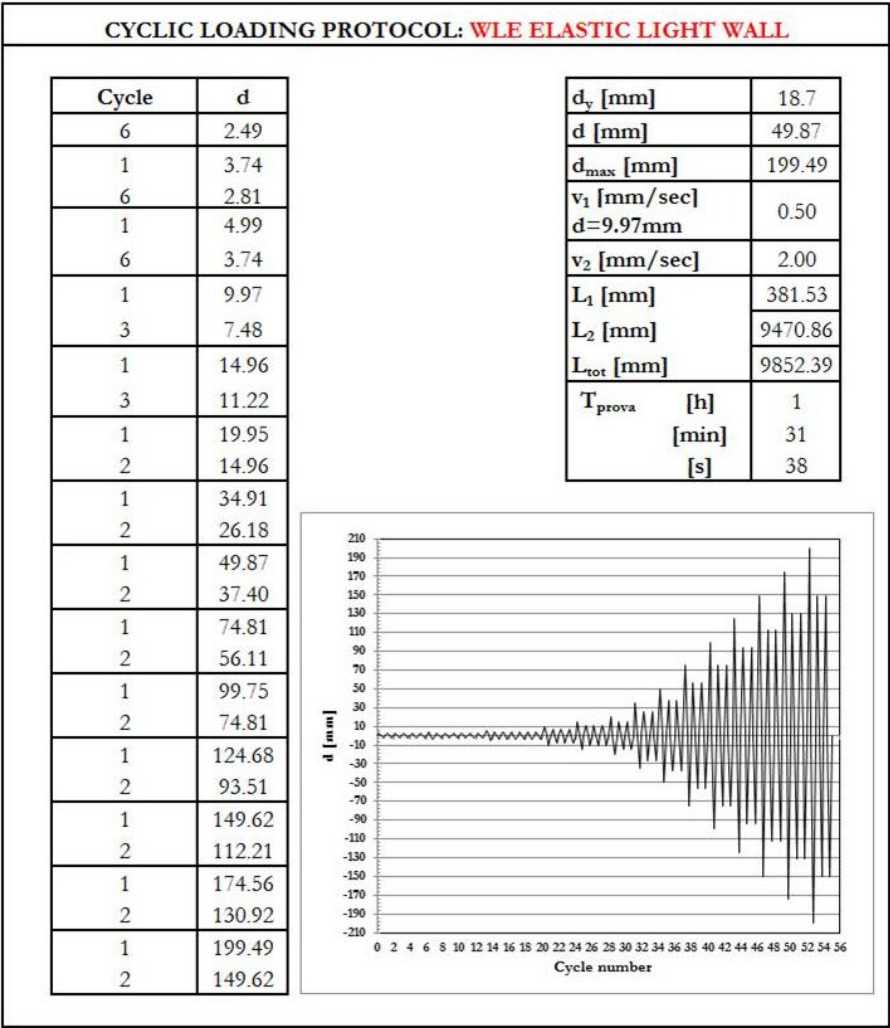








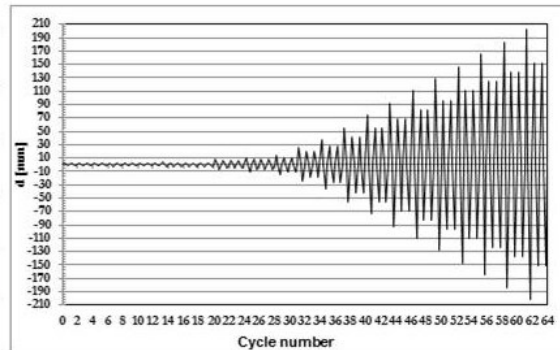
B.2 CYCLIC TESTS

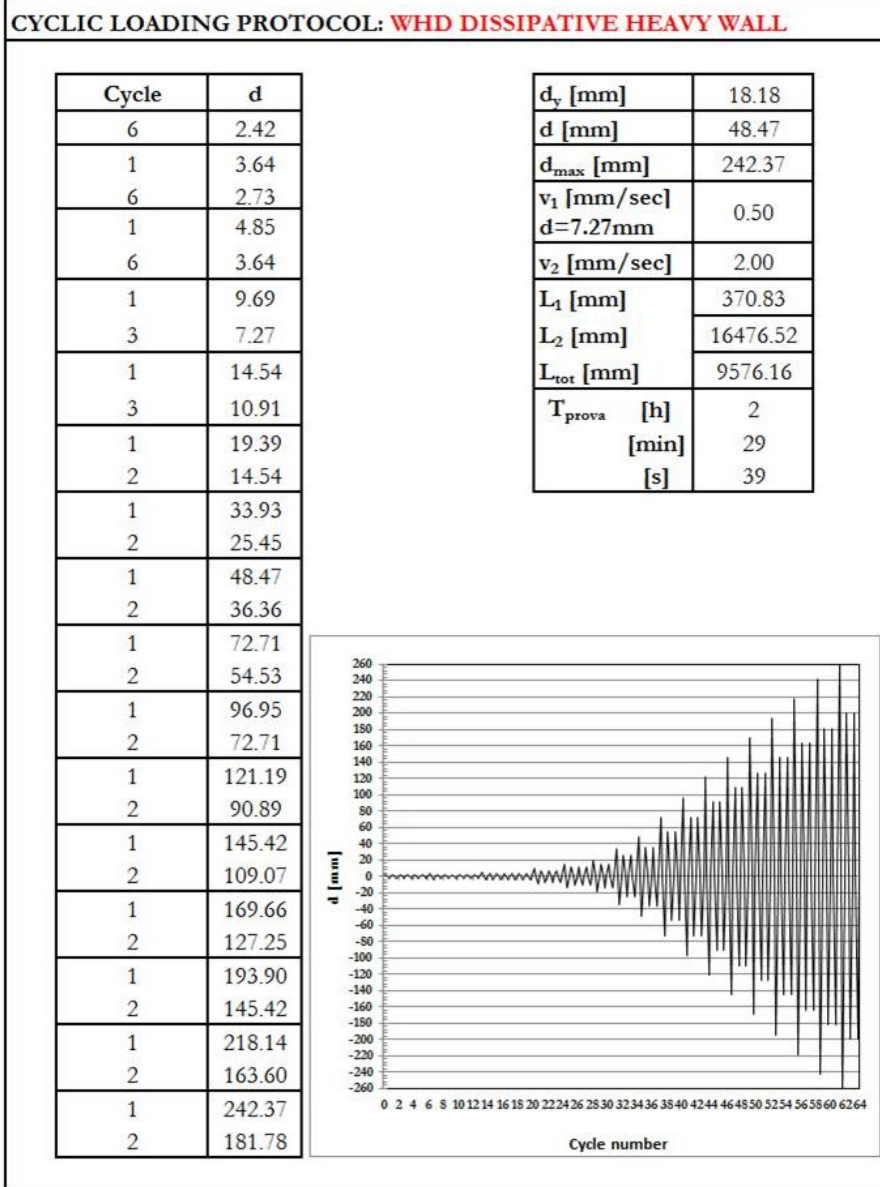


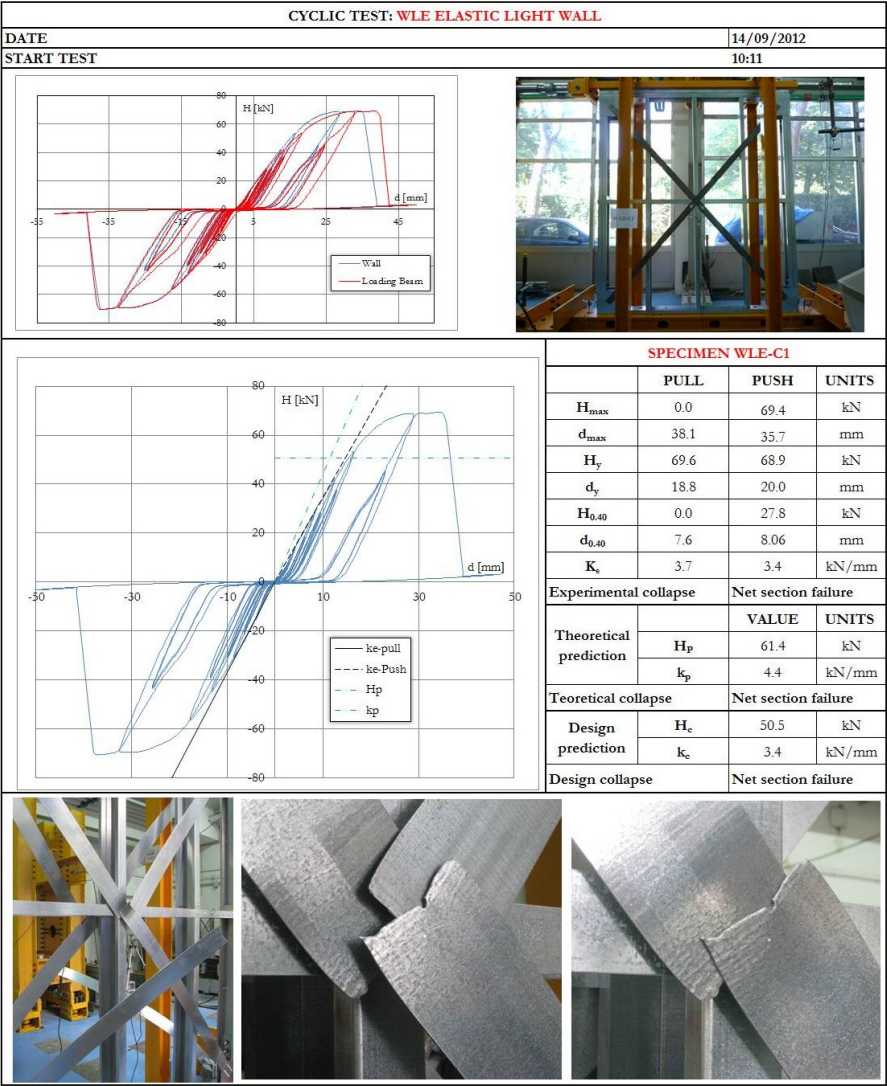
CYCLIC LOADING PROTOCOL: WLD DISSIPATIVE LIGHT WALL

Cycle	d
6	1.84
1	2.76
6	2.07
1	3.68
6	2.76
1	7.36
3	5.52
1	11.04
3	8.28
1	14.72
2	11.04
1	25.76
2	19.32
1	36.80
2	27.60
1	55.21
2	41.41
1	73.61
2	55.21
1	92.01
2	69.01
1	110.41
2	82.81
1	128.82
2	96.61
1	147.22
2	110.41

d_v [mm]	13.8
d [mm]	36.80
d_{max} [mm]	147.22
v_1 [mm/sec] $d=7.36\text{mm}$	0.50
v_2 [mm/sec]	2.00
L_1 [mm]	281.56
L_2 [mm]	12509.88
L_{tot} [mm]	7270.75
T_{prova} [h]	1
[min]	53
[s]	38









References

REFERENCES

- Adham S.A., Avanessian V., Hart G.C., Anderson R.W., Elrnlinger J., Gregory J. (1990). Shear Wall Resistance of Lightgauge Steel Stud Wall Systems. *Earthquake Spectra*, Vol. 6 (No. 1): 1-14.
- AISI. (2009). AISI S213-07/S1-09 North American Standard for Cold-Formed Steel Framing – Lateral Design 2007 Edition with Supplement No. 1. *American Iron and Steel Institute (AISI)*. Washington, DC.
- Al-Kharat M. (2005). Testing of Light Gauge Steel Strap Braced Walls. Phd thesis.
- Al-Kharat M., Rogers C.A. (2006). Inelastic performance of cold-formed steel strap braced walls. *Journal of Constructional Steel Research*.
- ASTM (2005). ASTM E2126. Standard Test Methods for Cyclic (Reversed) Load Test for Shear Resistance of Framed. *American Society for Testing and Materials*, West Conshohocken, PA, USA.
- Walls for Buildings” West Conshohocken, PA, USA.Casafont M., Arnedo A., Rourea F., Rodriguez-Ferran A. (2007). Experimental testing of joints for seismic design of lightweight structures. Part 3: Gussets, corner joints, x-braced frames. *Thin-Walled Structures*, 45, 637-659.
- CEN. (2005). EN 1998-1-1, Eurocode 8, Design of structures for earthquake resistance - Part 1-1: General rules, seismic actions and rules for buildings. *European Committee for Standardization*, Bruxelles.
- CEN. (2006). EN 1993-1-3, Eurocode 3, Design of steel structures - Part 1-3: General rules - Supplementary rules for cold-formed members and sheeting. *European Committee for Standardization*, Bruxelles.
- CEN. (2009). UNI EN ISO 6892-1. Metallic materials Tensile testing: Part 1: Method of test at room temperature. *European Committee for Standardization*.
- Comeau G. (2008). Inelastic Performance of Welded CFS Strap Braced Walls. Phd thesis.
- ECCS TC7 TWG 7.10 (2009). The tesing of connections with Mechanical Fasteners in Steel Sheeting and Sections.
- Fulop L.A., Dubina D. (2004). Performance of wall-stud cold-formed shear panels under monotonic and cyclic loading Part I: Experimental research. *Thin-Walled Structures*, 42, 321–338.
- Gad E.F., Chandler A.M., Duffield C.F., Stark G. (1999). Lateral behavior of plasterboard-clad residential Steel frames. *Journal Of Structural Engineering*, January, 32-39.

- Gad E.F., Duffield C.F., Hutchinson G.L., Mansella D.S., Stark G. (1999). Lateral performance of cold-formed steel-framed domestic structures. *Engineering Structures*, 21, 83-95.
- Ministero delle infrastrutture. (2009). Circ. n. 617 del 02/02/2009, Istruzioni per l'applicazione delle Nuove Norme Tecniche per le Costruzioni.
- Ministero delle infrastrutture. (2008). D.M. 14/01/2008, Norme Tecniche per le Costruzioni.
- Fiorino L., Iuorio O., Macillo V., Landolfo R.. (2012). Performance-based design of sheathed CFS buildings in seismic area. *Thin Walled Structures*, 61, 248-257.
- Fiorino L., Iuorio O., Macillo V., Terracciano M.T., Landolfo R. (2013). Pareti in CFS con Controventi ad X: Caratterizzazione Sperimentale della Risposta Sismica. *Proc. XV Convegno ANIDIS 2013 L'ingegneria sismica in Italia*. June 30 – July 4, Padova. (In press).
- Iuorio O., Fiorino L., Macillo V., Terracciano M.T., Landolfo R.. (2012). The influence of the aspect ratio on the lateral response of sheathed cold formed steel walls. *Proc. 21st International specialty conference Cold-formed steel structures*, October 24-25, St. Louis, Missouri.
- Kim T.W., Wilcoski J., Foutch D. A., Lee M. S. (2006). Shaketable tests of a cold-formed steel shear panel. *Engineering Structures*, 28, 1462-1470.
- Krawinkler H., Parisi F., Ibarra L., Ayoub A., Medina R. (2001). Development of a Testing Protocol for Woodframe Structures, CUREE.
- Landolfo R. (2011). Cold-formed steel structures in seismic area: Research and applications. *Proc. VIII Congresso de Construção Metálica e Mista*, I3-I22. Guimarães, Portugal.
- Landolfo R., Russo Ermolli S., Fiorino L., Iuorio O., D'Acunzi A. (2012). Acciaio e Sostenibilità. Progetto, ricerca e sperimentazione per l'housing in cold-formed steel. *ALINEA editore*.
- Moghim H., Ronagh H.R. (2009). Performance of light-gauge cold-formed steel strap-braced stud walls subjected to cyclic loading. *Engineering Structures*, 31, 69-83.
- Serrette R., Ogunfunmi K. (1996). Shear Resistance Of Gypsum-Sheathed Light-Gauge Steel stud Walls. *Journal Of Structural Engineering*, 383-389.
- Tian Y.S., Wang J., Lu T.J. (2004). Racking strength and stiffness of cold-formed steel wall frames. *Journal of Constructional Steel Research*, 60, 1069-1093.
- Velchev K. (2008). Inelastic Performance of Screw Connected CFS Strap Braced Walls. Phd thesis.
- Velchev K., Comeau G., Balh N., Rogers C.A. (2010). Evaluation of the AISI S213 seismic design procedures through testing of strap braced cold-formed steel walls. *Thin-Walled Structures*, 48, 846–856.